

DISTRIBUTION AGREEMENT

In presenting this thesis or dissertation as a partial fulfillment of the requirements for an advanced degree from Emory University, I hereby grant to Emory University and its agents the non-exclusive license to archive, make accessible, and display my thesis or dissertation in whole or in part in all forms of media, now or hereafter known, including display on the world wide web. I understand that I may select some access restrictions as part of the online submission of this thesis or dissertation. I retain all ownership rights to the copyright of the thesis or dissertation. I also retain the right to use in future works (such as articles or books) all or part of this thesis or dissertation.

Signature:

Shannon L. McNulty

Date

**PHOSPHATIDYLINOSITOL SIGNALING REGULATES
POXVIRAL PATHOGENESIS**

By

**Shannon L. McNulty
Doctor of Philosophy**

**Graduate Division of Biological and Biomedical Sciences
Microbiology and Molecular Genetics**

Daniel Kalman, Ph.D.
Advisor

Victor Faundez, MD, Ph.D.
Committee Member

Eric Hunter, Ph.D.
Committee Member

Aron E. Lukacher, MD, Ph.D.
Committee Member

Samuel Speck, Ph.D.
Committee Member

Accepted:

Lisa A. Tedesco, Ph.D.
Dean of the James T. Laney School of Graduate Studies

Date

**PHOSPHATIDYLINOSITOL SIGNALING REGULATES
POXVIRAL PATHOGENESIS**

By

Shannon L. McNulty
B.S., The College of William and Mary, 2004

Advisor: Daniel Kalman, Ph.D.

An abstract of

A dissertation submitted to the Faculty of the
James T. Laney School of Graduate Studies of Emory University
in partial fulfillment of the requirements for the degree of
Doctor of Philosophy

in

Graduate Division of Biological and Biomedical Sciences
Microbiology and Molecular Genetics

2010

ABSTRACT

PHOSPHATIDYLINOSITOL SIGNALING REGULATES POXVIRAL PATHOGENESIS

By Shannon L. McNulty

Smallpox was declared eradicated from nature in 1980, and mass smallpox vaccinations ceased in ~1978. Therefore, the population is extremely sensitive to the accidental release of Smallpox and to naturally occurring poxviruses, such as Monkeypox. Previous work from our lab identified that inhibitors targeting host Abl-family kinases can improve poxviral survival during a lethal (LD₇₅) murine infection. To identify other host-directed antivirals we screened by plaque assay a focused library of kinase inhibitors for those that caused a reduction in viral growth and identified several compounds that selectively inhibit phosphatidylinositol 3-kinase (PI3K). Using growth curves and electron microscopy in conjunction with inhibitors, we show that PI3Ks additionally regulate morphogenesis at two distinct steps: immature to mature virion (IMV) transition, and IMV envelopment to form intracellular enveloped virions (IEV). Cells derived from animals lacking the p85 regulatory subunit of Type I PI3Ks (p85 $\alpha^{-/-}\beta^{-/-}$) presented phenotypes similar to those observed with PI3K inhibitors. In addition, VV appear to redundantly use PI3Ks, as PI3K inhibitors further reduce plaque size and number in p85 $\alpha^{-/-}\beta^{-/-}$ cells. We extend these observations and demonstrate that Poxviruses regulate not only phosphatidylinositol kinases, but also phosphatidylinositol phosphatases. We found that the phosphoinositide 5'-phosphatase SHIP2 localizes to membranous protrusions formed beneath the virion called, "actin tails." Localization requires phosphotyrosine, Abl- and Src-family tyrosine kinases and N-WASP, but not the Arp2/3 complex nor actin. Cells lacking SHIP2 have normal actin tails, but release more virus. Moreover, viral strains with mutations in release inhibitor A34, release more virus but recruit less SHIP2. Thus, the inhibitory effects of A34 on viral release are mediated by SHIP2. Together, these data suggest that SHIP2 is an intrinsic antiviral factor that regulates dissemination of poxviruses from infected cells. Altogether, these data provide evidence for a novel regulatory mechanism for virion morphogenesis involving phosphatidylinositol dynamics and may represent new therapeutic targets to contain poxviruses.

**PHOSPHATIDYLINOSITOL SIGNALING REGULATES
POXVIRAL PATHOGENESIS**

By

Shannon L. McNulty
B.S., The College of William and Mary, 2004

Advisor: Daniel Kalman, Ph.D.

A dissertation submitted to the Faculty of the
James T. Laney School of Graduate Studies of Emory University
in partial fulfillment of the requirements for the degree of
Doctor of Philosophy
in
Graduate Division of Biological and Biomedical Sciences
Microbiology and Molecular Genetics

2010

TABLE OF CONTENTS

CHAPTER I: INTRODUCTION	1
1.1 History of Smallpox.....	3
1.2 Orthopoxviruses Today.....	7
1.3 Poxviral Structure and Replication.....	8
1.4 Poxviral Pathogenesis.....	11
1.5 Poxviral Treatment.....	14
1.6 Cellular Phosphatidylinositol Signaling.....	15
1.7 Phosphatidylinositol 3-Kinases.....	17
1.8 Phosphatidylinositol 5-Phosphatases.....	19
1.9 Lipid Signaling in Disease.....	20
1.10 Goals of this Dissertation.....	23
Literature Cited.....	24
Figure Legends.....	33
Figures 1-2.....	34-35
CHAPTER II: IDENTIFICATION OF SMALL MOLECULES THAT REDUCE VACCINIA VIRUS REPLICATION AND ACTIN TAIL FORMATION	37
Abstract.....	38
Introduction.....	39
Materials and Methods.....	41
Results.....	44
Discussion.....	45

Literature Cited.....	50
Figure Legends.....	53
Tables 1-16.....	54-68
Figures 1, 2.....	69-70

CHAPTER III: MULTIPLE PHOSPHATIDYLINOSITOL 3-KINASES

REGULATE VACCINIA VIRUS MORPHOGENESIS.....72

Abstract.....	73
---------------	----

Introduction.....	74
-------------------	----

Materials and Methods.....	76
----------------------------	----

Results.....	83
--------------	----

Discussion.....	93
-----------------	----

Literature Cited.....	102
-----------------------	-----

Figure Legends.....	109
---------------------	-----

Table 1.....	120
--------------	-----

Table S1.....	121
---------------	-----

Figures 1-11.....	122-132
-------------------	---------

Figures S1-S13.....	133-145
---------------------	---------

CHAPTER IV: THE HOST PHOSPHOINOSITIDE 5-PHOSPHATASE SHIP2

REGULATES DISSEMINATION OF VACCINIA VIRUS.....147

Summary.....	148
--------------	-----

Introduction.....	149
-------------------	-----

Results.....	151
Discussion	157
Experimental Procedures.....	159
References.....	164
Figure Legends.....	171
Figures 1-5.....	176-180
Figures S1-S4.....	181-184
CHAPTER V: ADDITIONAL OBSERVATIONS.....	186
5.1 Identification of Src- and Abl-family Tyrosine Kinase Substrates Facilitating Vaccinia Virus Actin Tail Motility and Infectious Virion Release.....	187
5.1.1 Introduction.....	187
5.1.2 Results.....	188
5.1.3 Future Directions.....	192
5.2 vps34/15	
5.2.1 Introduction.....	193
5.2.2 Results.....	195
5.2.3 Future Directions.....	198
5.3 Phosphatidylinositol 5-Kinases	
5.3.1 Introduction.....	199
5.3.2 Results.....	200
5.3.3 Future Directions.....	201

5.4 SHIP2 is not recruited to EPEC pedestals, and does <i>not</i> alter pedestal morphology.....	202
Literature Cited.....	206
Figure Legends.....	209
Table 1.....	213-214
Figure 1-14.....	215-228

CHAPTER VI: FUTURE DIRECTIONS AND CONCLUSIONS

6.1 Future Directions.....	230
6.1.1 Phosphatidylinositol 3-Kinases and Vaccinia Virus.....	231
6.1.2 SHIP2 and Vaccinia Virus.....	233
6.2 Conclusions.....	240
Literature Cited.....	242

CHAPTER 1:
INTRODUCTION

Figures 1 and 2 were made by Shannon McNulty.

INTRODUCTION

Poxviruses have long been the scourge of humanity. Variola major, the causative agent of Smallpox, causes mortality in 10-30% of cases and is the only human virus that has been completely eradicated from nature (25). However, despite this eradication, poxviral infections still exist in nature, and with the elimination of mass smallpox vaccinations, the population remains extremely sensitive to other orthopoxviral infections. Furthermore, old stocks of Variola major (and the less infectious form, Variola minor) are stored in repositories at the Centers for Disease Control and Prevention (CDC) in Atlanta, GA, and at the State Center of Virology and Biotechnology (VECTOR), in Kotsovo, Russia (1). The potential for accidental or malicious release of these viruses still exists.

Smallpox was declared eliminated from nature in 1980, and routine vaccinations were halted in the US in 1976 (26, 46), therefore most of the population is sensitive to the naturally occurring or accidentally released poxviruses. There is currently no poxvirus-specific drug, however the CDC does have recommendations for adverse consequences of Smallpox vaccinations or laboratory-acquired infections. These treatments exhibit significant side effects, and stocks may not exist that are capable of covering the entire population. Our lab recently identified an FDA approved compound (Gleevec) that inhibits host molecules used by the virus during viral dissemination (82). During viral dissemination, the virion induces actin polymerization beneath the virion (“actin tail”) and is hypothesized to use this structure to infect neighboring cells. Work by Frischknecht *et al.* and Reeves *et al.* found that host tyrosine kinases are required for tail

formation (30, 82), and Reeves *et al.* found that Gleevec, a host Abl-family kinase inhibitor, could improve survival during a lethal (LD₇₅) vaccinia virus infection (82).

The goal of our lab is to understand host-pathogen interactions. We hypothesize that with this knowledge we can identify novel targets for the development of host-directed antimicrobials. These host-directed compounds should be less likely to engender pathogen resistance than traditional pathogen-directed antimicrobials. In this dissertation I will describe my efforts to identify novel host-directed compounds capable of reducing poxviral replication. Through this approach I found that phosphatidylinositol signaling regulates poxviral pathogenesis – a pathway previously unrecognized as participating in the poxviral lifecycle.

1.1 History of Smallpox

The specific origins of Poxviruses are unknown. Poxviruses can be divided into two families – Chordopoxviruses, those that infect vertebrates, and Entomopoxviruses, those that infect insects. Poxviruses probably evolved and adapted to their host species, just as the host species were speciating themselves. It is hard to speculate when the first human infections started, however, evidence from ancient civilizations hints that smallpox may have existed as early as the Egyptian civilization.

Photographs of the mummified head of Ramses V (1160BC) show lesions thought to be due to smallpox (26, 61). Microscopic examination of skin from the mummy was unsuccessful at confirming the diagnosis and similar vesicular lesions have also been found on another mummy from the Twentieth Dynasty (39). Microscopic examination of

the skin did verify “dome-shaped” vesicles in the middle of the skin, as would be expected for Smallpox (39).

Early reports (~430 BC) from ancient Greek and Roman physicians, such as Thucydides and Galen, provide further evidence that Smallpox existed in antiquity. Both physicians describe large-scale plagues burning through the populace and these outbreaks often coincide with military invasions also occurring at that time (103). Often these descriptions are rather vague, and do little to mention specific symptoms of the disease other than fever and rash. However, during Alexander the Great’s conquests in Asia (~320 BC), the Roman historian Quintus Curtius describes the army is attacked by “a scab attacked the bodies of the soldiers and spread by contagion,” (103). Other cultures besides the Greek and Romans had references to Smallpox infections in their writings. The Jewish philosopher Phil Judaeus described a disease occurring in Exodus as producing pustules (103). In Asia, the physician Ko Hung (291-361AD) described an epidemic which produced, “sores which attack the head, face, and trunk. In short time, these sores spread all over the body. They have the appearance of hot boils containing some white matter,” (103).

The process of inoculating people with Smallpox material, called variolation, is believed to have originated in Asia. Many early accounts from physicians described survivors of the early smallpox plagues as being protected from future outbreaks. The earliest account of Smallpox inoculation was during the tenth century AD, when the eldest son of Chinese Prime Minister Wang Tan died from Smallpox (112). The method involved placing poxy material onto cotton, and placing the cotton in one’s nose. To prevent disastrous outbreaks, inoculators had specific instructions on how to acquire

inoculation material. Early texts describe qualities of the donor, and specific temperature ranges to store the innoculating material (112). Despite the protective effects of variolation, 0.5-2% of people died from the procedure (26). Early texts describe the inoculation process as early as the tenth century AD, however, inoculation did not become widespread until the 16th century, as described in Yu Ch'ang's 1643 book "Miscellaneous Ideas in Medicine" (112).

As the process of variolation spread around Asia, Greece, Turkey and Arabia physicians in England (~1600) were continuing to treat smallpox patients with the "Hot Method" developed earlier by Arabian physicians (106). Patients (or victims) were wrapped in blankets, and placed in an enclosed room near a hot fire. This method was developed to "sweat" the disease out of the individual. In 1660 a "cold" method was developed by physician Thomas Sydenham, which permitted the patient as much fresh air and cool beverages as they could handle (106). Given the wide range in treatment methods, the English eventually separated sick patients into sick, or "pest" houses to prevent the spread of contagion (106).

English ambassadors to Turkey were the first Britons to be inoculated by the new Asian variolation method. This method was publicized by Lady Mary Wortley Montagu, wife of the British ambassador to Turkey (106). Lady Montagu had her children variolated to prevent Smallpox infection, and even had her daughter inoculated in front of members of the London College of Physicians (~1718) (106). These physicians were not completely impressed, however several inoculated their family members, eventually spreading word of this new technique to members of the British royal family and elite members of society (106). In 1722, a spate of high profile deaths resulting from the new

inoculation method reduced the popularity of variolation. Several surgeons wrote to the Royal Society, vocally denouncing variolation as “that dangerous experiment,” (106).

This denunciation was not enough to stop the spread of variolation to the Boston area in the new continent. Six years earlier, a Boston physician-preacher, Cotton Mather, discussed variolation with Dr. John Woodward of the Gresham College in London (128). In this letter Mather relates an earlier conversation (~1706) with his African-born slave, Onesimus, “Enquiring of my Negro-Man Onesimus, who is a pretty Intelligent Fellow, Whether he ever had ye Small-Pox, he answered *Yes* and *No*; and then told me that he had undergone an Operation, which had given him something of ye Small-Pox, and would forever preserve him from it...” (128). While inoculation had spread throughout Africa, it was just beginning to reach the New World.

Approximately 100 years after Lady Montagu introduced variolation into the United States, Edward Jenner published his, “Inquiry into the Causes and Effects of the Variolae Vaccinae.” In a letter to the Royal Society of London he describes his experiments to inoculate various people with what he calls Cowpox (47). However, Jenner also describes his experiments with an unknown, horse disease, called “The Grease,” which when transferred to cow by farm workers became transformed into cowpox (47). Since Vaccinia virus is significantly distinct from cowpox, there exists the possibility that vaccinia virus was derived from The Grease or a combination of cowpox and The Grease. Jenner successfully demonstrated that material from a cowpox blister on the hand of a milkmaid could produce immunity against Smallpox (47). Jenner’s publication was greeted with initial suspicion amongst the medical community, however he was ultimately successful in promoting vaccination over variolation. Jenner was

awarded £30,000 from then English Parliament for his efforts, and in 1840 Parliament passed an act making variolation illegal, and promoting vaccination free of charge (106).

Jenner's plan to inoculate the populace with cowpox proved immensely effective. By the year 1900 vaccination was widespread in industrialized countries, reducing the overall prevalence of Smallpox in these countries, however variolation continued to be used in Africa and Asia (26). Throughout the 19th century the scientific and public health infrastructure developed, allowing for the widescale production of the Smallpox vaccine and by the Second World War smallpox was effectively eliminated in Europe and North America (26). In 1959 the Twelfth World Health Assembly proposed to eliminate Smallpox worldwide, however funding for this enterprise was not gathered until 1967 (26). The Intensified Smallpox Eradication Program was developed by the World Health Organization and existed from 1967 to 1980. The goals of this program were to mass vaccinate at least 80% of the population in all areas, and develop a surveillance system to detect new Smallpox outbreaks (26). Through the dedicated efforts of many countries and individuals mass vaccinations were stopped in 1978, and the disease was declared eradicated from nature in 1980 (26).

1.2 Orthopoxviruses Today

Despite the complete eradication of smallpox from nature, poxviruses still remain a threat to the human population. Smallpox still exists in two repositories: the CDC in Atlanta, and the State Research Center of Virology and Biotechnology (VECTOR) in Russia. With mass vaccinations eliminated in 1978, the population remains extremely sensitive to orthopoxviral infections. Poxviruses still exist in nature and can still infect

humans – these include monkeypox (MPX) and molluscum contagiosum (MCV). In particular, MPX is endemic in Africa (86) and has the potential for spread to humans from squirrels and bushmeat (53, 54, 81, 86, 87), and recent outbreaks in the Sudan have raised the possibility of human-to-human transmission (87). Molluscum contagiosum is a neglected poxviral infection that forms small raised, umbilicated poxes in infected individuals (25). Overall MCV prevalence in North American, European and Greek populations ranges from 1% to 5% to 12% (23, 58). In children MCV is highly contagious and spread by direct contact (32). MCV can also infect adults and immunocompromised individuals and is commonly spread during contact sports, and during sexual activity (32). Efforts to understand the capacity for human-to-human transmission amongst poxviruses have focused how the virus replicates and spreads from cell to cell.

1.3 Poxviral Structure and Replication

Poxviruses are dsDNA viruses that replicate in the cytoplasm. Infection is initiated upon entry of either of two forms of the virus. The first, called the intracellular Mature Virus (“IMV”, and also called the Mature Virion “MV”), consists of a brick-shaped viral core surrounded by one or two lipid bilayers derived from an ER-Golgi intermediate compartment (ERGIC) (38, 88, 90, 109). IMV enter the cell either through direct fusion with the plasma membrane or by internalization and fusion with an endocytic compartment (Figure 1-1) (2, 15, 16). A second infectious form of the virus, called the Extracellular Enveloped Virus (“EEV”, and also called Enveloped Virus “EV”) (105), is released from the cell surface and consists of an IMV enveloped in additional

host-cell derived membranes (Figure 1-10). Entry of the EEV requires disruption of the outer viral membrane either at the plasma membrane, or in endosomes (42, 59, 116).

After delivery of the viral core to the cytoplasm (Figure 1-2), early viral gene transcription and translation (Figure 1-3) initiates replication and morphogenesis.

Morphogenesis is regulated at multiple steps (18), which have been characterized by electron microscopy in conjunction with mutant viruses containing deletions or temperature-sensitive alleles of viral proteins. Morphogenesis ensues approximately four hours after entry with the appearance of viral crescents (21, 51), which consist of semi-spherical membranes containing viral proteins apposed to the viroplasm (Figure 1-4).

The crescent membrane extends to encase viroplasm, forming a spherical immature virions (IV) (Figure 1-5). The transition from IV to IMV (Figure 1-6) depends on several events, including proteolysis of core proteins, such as A3 (P4b), A10 (P4a), and L4 (P25K), and formation of disulfide bonds within nascent viral proteins L1 and E10 (7, 9, 98, 115). IMV formation also depends on the viral kinase F10 (79), core proteins P4a, A10, P4b, A3, P25, and L4 (12), and on redox proteins G4 and E10 (99-101, 126). Mutations in these proteins result in slightly different phenotypic defects, including an inability to form complete crescents, misincorporation of the viroplasm with or without crescent resolution, malformed cores, or incomplete virion maturation.

Once formed, as subset of IMVs traffic along microtubules to a juxta-nuclear region where they are enveloped in host-cell membranes derived from endosomes or from the Golgi apparatus to form IEV (Intracellular Enveloped Virions) (Figure 1-7) (77, 94, 96, 113, 123). The mechanisms controlling envelopment are less well understood, but evidence suggests the involvement of F12, and A36, F13, A33, A34, A56, and B5

(105), which physically associate with or facilitate the localization of other proteins. For example, F13 and A34 have been shown to regulate the cellular trafficking of B5 and its incorporation into the IEV (24, 41). Ultimately, the interaction of these proteins allows the virus to utilize host membranes for envelopment.

Once formed, the IMV and EEV release from the host cell through different mechanisms. IMV are released following lysis of host cells (89), whereas the precursor of EEV traffic along microtubules to the cell periphery (31, 37, 85, 124). Upon fusion with the host cell plasma membrane (Figure 1-8), the doubly enveloped virions stimulate formation of actin-filled membranous protrusions called “tails,” (Figure 1-9) and then disengage from the host cell.

Formation of actin tails occurs by mechanism conserved amongst VV, MPX and VarV (83). EEV recruit host Abl- and Src- family tyrosine kinases (70, 71, 82), which phosphorylate viral protein A36 at residues 112 and 132, thereby facilitating recruitment Nck, Grb2, WIP and N-WASP (30, 77, 95, 125). Interactions with PI(4,5)P₂ in the plasma membrane induce conformational changes in N-WASP, which allow the protein to bind to and activate Arp2/3 complex, a nucleator for actin polymerization (77, 91). The rate of actin tail formation and length appear to be a function of the turnover rate and interactions amongst viral factors and recruited host proteins (22, 125).

While much information is available about the viral and host factors that initiate actin polymerization, much less is known about the viral and host factors that contribute to virion release. Based on mutation experiments, several viral factors including, F12, F13, A33, A34, B5, and A36 have been implicated in viral release (105), although in many cases, such mutations also affect actin tail formation or specific infectivity thereby

precluding unequivocal determination for the role for these proteins in release. Viral strain IHD-J releases larger numbers of EEV compared to viral strain, WR (8). Blasco *et al.* found that replacing the A34 gene from IHD-J into the WR genome (creating strain “WI”) increased EEV release and that a single point mutation within A34_{WR} was sufficient to increase EEV release (8). A34 inhibits virion release, as viral strains deficient in A34 exhibit increased EEV release, but a decrease in specific infectivity (65). Viral release also depends on cell type (66, 76), indicating that host factors also participate in the release process. Reeves *et al.* demonstrated that inhibition/absence of host Abl-family kinases blocks EEV release (82). This data suggests that both Abl-family kinases and A34 regulate virion release, and that Abl-family kinases may promote EEV release through inhibition of viral protein A34.

1.4 Poxviral Pathogenesis

The collective host and viral mechanisms contributing to poxviral pathogenesis and death remain unknown (25). Autopsies of Smallpox patients indicated that no vital organs were destroyed (25) and death is usually the result of disseminated intravascular coagulation, hypotension, and cardiovascular collapse (1). The lack of overt tissue damage indicates that the virus may control the extent of damage, and kill patients by overwhelming the immune response. Histopathological evidence of smallpox infections reveals hallmarks of inflammation, like dilation of blood vessels, swelling of endothelial cells, adhesion of leukocytes and leukocyte infiltration into tissue (111). Such overwhelming immune toxemia is often referred to as the “cytokine storm” and sepsis (111).

Smallpox infections of humans initiate through inhalation of aerosol droplets, or by contamination with infectious material. Patients infected with Smallpox did not have clinical symptoms during the 10-12 day incubation period (26). Early symptoms include headache, fever, nausea, backache, with progression to the characteristic pustular rash, termed “Pox.” Pox typically clustered on the cooler regions of the body, such as the feet, hands and extremities (26). As pustules dry, they umbilicate in the center and the scab grows from this region to cover the entire pox. Only after the patient has sloughed all of the scabs are they noninfectious. A minority of cases develop into Flat or Hemorrhagic pox, where the patient does not develop ordinary Smallpox lesions, but progresses to flat or hemorrhagic lesions (26). Flat and hemorrhagic pox are usually fatal (26). Pregnant women were especially susceptible to hemorrhagic smallpox (26), suggesting that a compromised immune system contributed to disease progression and outcome.

Poxviruses encode many immune evasion genes, and these genes can be separated based on extracellular or intracellular modes of action. To interfere with extracellular immune signaling, poxviruses can produce receptor binding homologues, which can bind the ligand, preventing true ligand-receptor interactions. Examples of host ligands suppressed by viral binding proteins include: IL-18, IFN- γ , IFN- α/β , IL-1 β , TNF and NF κ B (67, 68). Poxviruses also inhibit complement activation by mimicking cellular inhibitors of complement. The smallpox inhibitor of complement enzyme (SPICE) was shown to be 100-fold more specific than that of vaccinia virus at inhibiting human C3b convertase, and 6-fold more potent at inactivating C4b, the complement activator (92). Finally, poxviruses also produce an extracellular serine protease inhibitor “Serpins” (crmA), which inhibit caspase-1, preventing it from cleaving the pro-form of IL-1 β (68).

The overall goal of poxviral extracellular immune modulators is to prevent the trafficking of leukocytes into infected cells already producing cytokines and chemokines. However, poxviruses also have an intracellular mechanism of immune inhibition, which acts to prevent the transduction of these extracellular signals of infection.

Intracellularly, poxviruses can prevent cellular pathogenesis through multiple mechanisms. Stanford *et al.* split these intracellular mechanisms into virotransducers – viral proteins that interfered with the response to infection in the cell, and virostealth proteins – proteins that reduce the likelihood of detection by the immune system (111). Examples of virostealth proteins include those that reduce MHCI, MHCII, and CD4 activation/expression, thus preventing the activation of adaptive immune cells. Rehm *et al.* recently identified that vaccinia virus A35R inhibits MHC class II antigen presentation by localizing to endosomes and reducing the peptide loading of class II MHC (84). Poxviruses can also prevent activation of CD4⁺ T lymphocytes by downregulating the CD4 co-receptor (5, 63). Furthermore, Guerin *et al.* demonstrated that the Myxoma virus LAP protein induces extensive depletion of MHC I molecules, similar to other LAP domain-containing proteins identified in herpesviruses (33).

Virotransducers, viral proteins that interfere with cellular signal transduction, interfere with host cellular signaling to produce an intracellular environment that is beneficial to the virus. Most viral proteins transcribed under early promoters are immune modulators and virotransducers. To keep the cell membrane intact, poxviruses inhibit apoptosis at multiple levels. The crmA protein, expressed extracellularly, can also inhibit intracellular caspase activation (102). At the mitochondria, vaccinia virus protein F1L inhibits cytochrome C release by preventing activation of Bak and Bax (13). To produce

a favorable environment for gene transcription/translation, poxviruses encode two mRNA decapping enzymes (74, 75), and infection redistributes the eukaryotic translation initiation factor 4F to sites of viral replication (122). Through the combination of both intracellular and extracellular immune modulators, poxviruses create a secure environment that allows for efficient spread and replication.

1.5 Poxviral Treatment

Current poxviral treatment methods recommended by the CDC, while effective against the virus, are not without considerable side effects. The current treatment method recommended by the CDC for accidental or serious smallpox vaccine adverse events is Vaccine Immune Globulin (VIG). As a second treatment method, cidofovir may be administered under the FDA-regulated Investigational New Drug Protocol.

Unfortunately, cidofovir treatment itself produces severe side-effects. Cidofovir is a nucleoside analog that exhibits significant renal toxicity (52). To reduce toxicity and extend therapeutic levels, it is administered in combination with IV fluids and probenecid, a renal tubular blocker. Given the significant toxicity associated with cidofovir, and limited resources of VIG, there has been a significant push to identify new poxviral inhibitors, particularly those with fewer side effects.

Since the Anthrax attacks in 2001, new funding sources have developed that have led to the recent development of novel poxviral therapeutics. ST-246, developed by Siga Technologies, targets the viral F13L protein, preventing the virus from leaving the cell (130). While ST-246 has been shown effective at preventing poxviral spread *in vivo* (110, 130), Yang *et al.* demonstrated it was possible to generate escape mutants in F13L

(130). Given the ease to generate escape mutants in tissue culture, it seems possible that similar escape mutants may develop within an infected individual.

To reduce the possibility of generating viral escape mutants resistant to poxviral inhibitors, our lab has developed novel host-directed poxviral therapeutics. Work by Frischknecht *et al.* and Reeves *et al.* demonstrated that host Src- and Abl-family tyrosine kinases are utilized by vaccinia, monkeypox, and variola virus to form actin tails (30, 82, 83). Reeves extended this observation and identified that Abl-family tyrosine kinases are used for viral release and that the host tyrosine kinase inhibitor imatinib mesylate (STI-571, Gleevec), originally developed for the treatment of chronic myelogenous leukemia (CML) and FDA-approved, can reduce the spread of poxviruses in tissue culture, and increases survival during a lethal murine infection.

1.6 Cellular Phosphatidylinositol Signaling

Prior to the work of Mabel R. and Lowell E. Hokin phospholipids were considered inert structural components of cellular membranes (57). They were initially studying acetylcholine-induced stimulation of pancreatic slices and thought that stimulation increased ^{32}P uptake into RNA. However, RNA purified from pancreatic slices was not radioactive, implying that ^{32}P was being incorporated into another molecule. The Hokins found that most of the ^{32}P was incorporated into phosphoinositides and other phospholipids. This incorporation came to be known as “The PI effect” (43).

Subsequent groups working to understand the Hokins’ PI effect broadened the lipid signaling field. Durell and Garland found that changes in the PI effect occurred

downstream of lipid signaling and suggested that lipid signaling may change cellular Ca^{2+} levels (43). Other groups found that cleavage of a specific lipid resulted in two signaling molecules – DAG, and $\text{Ins}(1,4,5)\text{P}_3$ and that $\text{Ins}(1,4,5)\text{P}_3$ modified cellular Ca^{2+} levels. By purifying large quantities of lipids (one group processed more than 100 cow brains!) and determining the phosphate to lipid ratio, $\text{PI}(4,5)\text{P}_2$, the parental molecule of DAG and $\text{Ins}(1,4,5)\text{P}_3$ was discovered. Other groups identified similar polyphosphoinositol lipids, but with a different phosphate:lipid ratio (3:1) (43).

Current research has identified approximately seven different phosphoinositide species, and numerous inositol phosphates, which can be generated by cleaving the phosphoinositide head groups from the fatty acid moiety (35, 114). When conjugated to fatty acids, the inositol head group can only be phosphorylated at the 3, 4, or 5 positions, as phosphorylations on carbons 2 and 6 are likely sterically hindered due to their proximity to carbon 1 on the glycerol moiety. Interestingly, it is currently unknown how the fatty acid tails and the composition of these tails participate in signaling (35).

Phosphoinositides are essential in eukaryotic cells and regulate nuclear processes, cytoskeletal dynamics, signaling and membrane trafficking (60). Various protein domains have been identified which recognize specific phosphorylation patterns on phosphoinositides. For instance, FYVE and PX domains recognize $\text{PI}(3)\text{P}$, whereas the PH of Akt recognizes $\text{PI}(3,4)\text{P}_2$ and $\text{PI}(3,4,5)\text{P}_3$ and the PH domain PLCdelta1 recognizes $\text{PI}(4,5)\text{P}_2$ (20). Expression of many of these phospholipid-recognizing domains alone is sufficient to induce membrane localization. Embedding a signaling molecule into the membranes of various organelles in cells creates a “zipcode,” which helps to localize effector proteins spatially and temporally (60).

1.7 Phosphatidylinositol 3-Kinases

Phosphatidylinositol 3-kinases (PI3Ks) catalyze addition of a phosphate group to the D3 hydroxyl of the inositol ring of phosphatidylinositol (Figure 2A, B, E, F, H) (6, 35, 36), and regulate many cellular processes including growth factor and hormonal signaling, autophagy, nutrient sensing, and endosomal trafficking (3, 27, 36, 121). PI3Ks are encoded by multiple genes and are categorized into three classes based on domain structure and substrate preference (reviewed by (35)). Kinases within each class are controlled by regulatory proteins. These proteins are encoded by multiply spliced genes, which can generate additional signaling complexity. Genes encoding PI3Ks are frequently mutated in human cancers, making this class of enzymes an important pharmaceutical target (48, 55, 56, 93).

The mammalian PI3K family is divided into three different classes based on kinase substrate preference and domain structure. Class I kinases phosphorylate PI(4,5)P₂ into PI(3,4,5)P₃ (Figure 2G, H) and consist of heterodimers of regulatory (p85) and catalytic subunits (p110) (35). Class II kinases have recently been identified, and though not fully characterized, are hypothesized to phosphorylate PI(4)P and PI into PI(3,4)P₂ and PI(3,4,5)P₃, respectively (Figure 2C, E, H). Class II kinases do not exist as heterodimers (35). Their activity may be regulated through membrane binding, as PI3K- α has a PX domain capable of binding lipids (117). The class III kinase phosphorylates PI into PI(3)P (Figure 2A, B) and consists of a heterodimer of regulatory (vps15) and catalytic subunit (vps34) (35). Vps34/15 is the sole PI3K in yeast, and was

originally identified in a screen for mutants defective in Vacuolar Protein Sorting of proteins from the Golgi apparatus to the vacuole (72).

The Type 1a and Type 1b PI3Ks are heterodimers of regulatory and catalytic subunits. The catalytic subunit (p110) consists of 4 genes, and the regulatory subunit (p85) is encoded by 5 genes (35). The regulatory subunits of PI3KR1 can be spliced into three isoforms; altogether mammals may form 15 distinct p85-p110 combinations (117). Furthermore, the stability of the p110 subunit is dependent on the p85 subunit (132). As such, cells deficient in p85 subunits are effectively deficient in Type 1 kinase signaling. The type 1 PI3K primarily interact with cell surface receptors and catalyze the phosphorylation of PI(4,5)P₂ into PI(3,4,5)P₃ (Figure 2G, H). The contribution of different isoforms to cellular signaling is unknown; however, their tissue expression provides insight into regulation of potential cellular pathways. P110 δ and p110 γ are expressed primarily in the hematopoietic system, whereas p110 α and p110 β are expressed ubiquitously (117). Inactivating mutations within the class I PI3Ks *in vivo* produced distinct phenotypes, indicating that isoforms control distinct and non-redundant signaling pathways (117).

The canonical PI3K signaling pathway is the Akt/PKB and mTor pathway, which can be activated by pro-growth signals binding to receptor tyrosine kinases. Following ligand binding, the type 1 PI3K is recruited to the plasma membrane, potentially through interactions of p85-SH2 and phosphotyrosine. Localization of PI3K at the membrane produces PI(3,4,5)P₃, which recruits Akt/PKB and PDK1 to the membrane via their PH domains (40). PDK1 phosphorylates Akt at Thr308 and mTORC2 (a complex of mTOR,

rector, SIN1, and mLST8) phosphorylates Akt on Ser473 (40). These phosphorylations activate Akt, a serine/threonine kinase, and lead to downstream phosphorylation of pro-growth substrates (40). Specifically, Akt activates mTORC1 (raptor and mLST8), and mTORC1 phosphorylates ribosomal kinases S6K1, S6K2, and eukaryotic initiation factor 4E binding proteins 4E-BP1 and 4E-BP2 (40). Phosphorylation of the ribosomal kinases and initiation factor binding proteins stimulates mRNA translation and cell growth (40).

1.8 Phosphatidylinositol 5-Phosphatases

Phosphatidylinositol 5-phosphatases dephosphorylate lipids specifically on the 5th carbon of the inositol headgroup (Figure 2D, F, G, H). This family of proteins consists of ten mammalian and four yeast proteins that share homology at the catalytic domain (73). 5-ptases typically downregulate cellular signaling, however, they can also create new signals by removing the 5' phosphorylation site. Specifically, the SHIP1/2 phosphatases downregulate signaling through receptor tyrosine kinases, such as insulin receptor (45) and FcγRIIB (69). Other 5' phosphatases include: OCRL1, synaptojam 1/2, SKIP, PIPP, and Inpp5e (69). While these proteins have been identified to contain the 5' catalytic domain, their contribution to cellular signaling is still relatively uncharacterized.

SHIP2 and its related isoform SHIP1 are SH2 domain-containing inositol polyphosphate 5-phosphatases (69). Whereas SHIP1 is expressed in hematopoietic cells, SHIP2 is expressed ubiquitously (34, 97). Both isoforms exhibit 5-phosphatase activity and have similar ligand specificity for PI(3,4,5)P₃, PI(4,5)P₂, and PI5P (Figure 2H, G, D), but differ in enzymatic (34, 42, 69, 129) and ligand-binding kinetics (132). Originally identified as a negative regulator of insulin signaling (17), SHIP2 mutations have also

been linked to metabolic disorders, including, type II diabetes (44, 49, 50, 64, 104). In addition, SHIP2 has also been recently implicated in regulating cytoskeletal organization (78, 107, 131). Furthermore, Smith *et al.* recently demonstrated that SHIP2 localizes to actin protrusions, called pedestals, which form beneath enteropathogenic *E. coli* (EPEC), and that reduction of SHIP2 levels causes an aberrant pedestal structure (107).

1.9 Lipid Signaling In Disease

Since lipid signaling controls many aspects of endomembrane trafficking and cellular signaling, it is unsurprising that genetic or pathogenic disruptions can result in disease. Distribution of specific phospholipids maintains organelle identity and microdomains within organelle membranes specify regions of cargo loading, vesicle fusion or fission. Genetic lesions resulting in nonfunctional kinases or phosphatases can alter the lipid “zipcode,” producing dysregulated vesicle trafficking. Likewise, pathogens can inhibit cellular trafficking to create a special pathogen-specific niche within the host cell.

As previously described, pro-growth signaling through receptor tyrosine kinases recruits Type I PI3Ks to the plasma membrane, which produces PI(3,4,5)P₃ and recruits Akt. Mutations within this pathway that result in hypersignaling, or the ability to signal in the absence of pro-growth signals can lead to cancer. Specifically, activating mutations within the p110 α subunit have been found in human tumors (14). Also, mutations within PTEN (phosphatase and tensin homolog), a 3' phosphatase that dephosphorylates PI(3,4,5)P₃ downregulating growth factor signaling, has been associated with cancer predisposition syndromes and sporadic cancers (62)

Disruption of PIK signaling does not always lead to cancer predisposition. Genetic disruptions of lipid phosphatases (MTM1, MTM2, SBF2, OCRL1, and SNJ1) can result in a range of disorders (11). Interestingly, disruptions within molecules that regulate cellular trafficking do not result in the same spectrum of disorders. For instance, these disorders can affect the nervous system (Lowe syndrome and Marie-Carcot-Tooth disease), muscle, eye (fleck corneal dystrophy, and Lowe syndrome), and kidney (Lowe syndrome) (11). Different tissue distribution and kinase/phosphatase preference likely control disease outcome and pathogenesis.

Lipid signaling is an important component of cellular signaling and many intracellular pathogens have evolved to hijack this form of communication for their own nefarious purposes. *Salmonella typhimurium* is a facultative intracellular pathogen that replicates and survives within host cells in a vacuolar niche (SCV) (4). Upon entry several effector proteins are secreted through the type III secretion system; deletion mutations within these proteins prevent efficient intracellular replication. SopB is a bacterially encoded phosphoinositide phosphatase that helps form the SCV (4). During bacterial invasion the SCV acquires rab5, vps34, and LAMP1, but the vesicle does not acidify, nor does it fuse with the lysosome (4). Bakowski *et al.* demonstrated that Δ sopB strains (and phosphatase dead strains) internalize into host cells, but quickly fuse with the lysosome, suggesting that sopB inhibits SCV-lysosome fusion.

Interestingly, *Salmonella* is not the only bacterial strain that has evolved a mechanism of interfering with host lipid signaling to promote bacterial survival. *Mycobacterium tuberculosis* is also internalized into host cells, where it interferes with endosome maturation and establishes a *M.Tb.*-specific vacuole (80). Mycobacteria-

containing endosomes acquire early endosomal markers rab5 and vps34, had delayed eea1 recruitment (28, 29) and failed to fuse with lysosomes (120). Vergne *et al.* demonstrate that lipoarabinomannan from mycobacteria can suppress vps34 activity and also encode a PI3P-specific phosphatase, SapM (118, 119).

Instead of interfering with host lipid signaling to create a virus-specific vacuole, most viruses modify host lipids to inhibit cellular apoptosis (10, 19). Since Akt is a central node that regulates pro-growth signals within a cell most viruses disrupt PI3K-Akt-mTOR signaling (19). PI3K activity was first identified as a complex with the tyrosine kinase Src and polyomavirus Middle T antigen (127). Thus, polyomaviruses activate PI3K, producing activation of Akt, which activates the pro-growth signaling pathway independently of growth factors ultimately resulting in cellular transformation (10). The adenoviridae and herpesviridae also activate the PI3K-Akt-mTOR pathway by activating the mTORC1 and PI3K/mTORC2, respectively (10). Soares *et al.* recently demonstrated that Vaccinia and Cowpox virus induced phosphorylation of Akt at T308 and S473, albeit at different kinetics (108). Likewise, Zaborowska demonstrated that Akt phosphorylation and p70S6K (downstream of PI3K signaling) hyperphosphorylation was increased in VV-infected cells (133). Furthermore, Zaborowska also demonstrated that viral infection could be reduced following PI3K inhibitor treatment, although the exact mechanism was not identified (133). Altogether, these data demonstrate that pathogens have evolved mechanisms of interfering with host lipid signaling. Therefore, therapeutics that are under development to limit dysregulated phosphoinositide signaling in cancer may also exhibit efficacy against intracellular pathogens.

1.10 Goals of this Dissertation

The work described herein describes the identification and contribution of phosphatidylinositol signaling during a poxviral replication. I identified the importance of lipid signaling during a poxviral infection by screening a compound library for those compounds that could inhibit actin tail formation and viral spread. Through this screen I found that phosphatidylinositol 3-kinase inhibitors reduced poxviral replication. Importantly, at the time of this discovery, phosphatidylinositol-modifying enzymes had not previously been described as necessary for poxviral infections. In combination with PI3K inhibitors and PI3K-deficient cell lines I identified that poxviruses use host PI3K during the immature to mature virion transition, and during virion envelopment. Lipid kinases are not the only lipid signaling molecule contributing to viral pathogenesis, I also identified that vaccinia virus requires host lipid phosphatase activity. I found that the host lipid 5' phosphatase, SHIP2, localizes to the top of VV actin tails, and that SHIP2 is a negative regulator of virion release. By defining the host enzymes required by the virus, one may develop specific inhibitors that could prevent or reduce viral spread. Targeting the host enzymes required by the virus may reduce the likelihood of engendering pathogen resistance, and could yield important new drugs capable of treating poxviral infections. Furthermore, acquisition of lipid envelopes from host cell-derived membranes is an important process conserved amongst the enveloped viruses. The possibility exists that other enveloped viruses may also hijack host phosphatidylinositol kinases and phosphatases during replication and spread.

LITERATURE CITED

1. 1999. Assessment of Future Scientific Needs for Live Variola Virus 0-309-06441-4. National Academies Press.
2. **Armstrong, J. A., D. H. Metz, and M. R. Young.** 1973. The mode of entry of vaccinia virus into L cells. *J Gen Virol* **21**:533-7.
3. **Backer, J. M.** 2008. The regulation and function of Class III PI3Ks: novel roles for Vps34. *Biochem J* **410**:1-17.
4. **Bakowski, M. A., V. Braun, G. Y. Lam, T. Yeung, W. Do Heo, T. Meyer, B. B. Finlay, S. Grinstein, and J. H. Brumell.** The phosphoinositide phosphatase SopB manipulates membrane surface charge and trafficking of the Salmonella-containing vacuole. *Cell Host Microbe* **7**:453-62.
5. **Barry, M., S. F. Lee, L. Boshkov, and G. McFadden.** 1995. Myxoma virus induces extensive CD4 downregulation and dissociation of p56lck in infected rabbit CD4+ T lymphocytes. *J Virol* **69**:5243-51.
6. **Berridge, M. J., and R. F. Irvine.** 1989. Inositol phosphates and cell signalling. *Nature* **341**:197-205.
7. **Betakova, T., E. J. Wolffe, and B. Moss.** 1999. Regulation of vaccinia virus morphogenesis: phosphorylation of the A14L and A17L membrane proteins and C-terminal truncation of the A17L protein are dependent on the F10L kinase. *J Virol* **73**:3534-43.
8. **Blasco, R., J. R. Sisler, and B. Moss.** 1993. Dissociation of progeny vaccinia virus from the cell membrane is regulated by a viral envelope glycoprotein: effect of a point mutation in the lectin homology domain of the A34R gene. *J Virol* **67**:3319-25.
9. **Blouch, R. E., C. M. Byrd, and D. E. Hraby.** 2005. Importance of disulphide bonds for vaccinia virus L1R protein function. *Virol J* **2**:91.
10. **Buchkovich, N. J., Y. Yu, C. A. Zampieri, and J. C. Alwine.** 2008. The TORrid affairs of viruses: effects of mammalian DNA viruses on the PI3K-Akt-mTOR signalling pathway. *Nat Rev Microbiol* **6**:266-75.
11. **Bunney, T. D., and M. Katan.** 2010. Phosphoinositide signalling in cancer: beyond PI3K and PTEN. *Nat Rev Cancer* **10**:342-52.
12. **Byrd, C. M., and D. E. Hraby.** 2006. Vaccinia virus proteolysis--a review. *Rev Med Virol* **16**:187-202.
13. **Campbell, S., B. Hazes, M. Kvensakul, P. Colman, and M. Barry.** Vaccinia virus F1L interacts with Bak using highly divergent Bcl-2 homology domains and replaces the function of Mcl-1. *J Biol Chem* **285**:4695-708.
14. **Carnero, A.** The PKB/AKT pathway in cancer. *Curr Pharm Des* **16**:34-44.
15. **Carter, G. C., M. Law, M. Hollinshead, and G. L. Smith.** 2005. Entry of the vaccinia virus intracellular mature virion and its interactions with glycosaminoglycans. *J Gen Virol* **86**:1279-90.
16. **Chang, A., and D. H. Metz.** 1976. Further investigations on the mode of entry of vaccinia virus into cells. *J Gen Virol* **32**:275-82.

17. **Clement, S., U. Krause, F. Desmedt, J. F. Tanti, J. Behrends, X. Pesse, T. Sasaki, J. Penninger, M. Doherty, W. Malaisse, J. E. Dumont, Y. Le Marchand-Brustel, C. Erneux, L. Hue, and S. Schurmans.** 2001. The lipid phosphatase SHIP2 controls insulin sensitivity. *Nature* **409**:92-7.
18. **Condit, R. C., N. Moussatche, and P. Traktman.** 2006. In a nutshell: structure and assembly of the vaccinia virion. *Adv Virus Res* **66**:31-124.
19. **Cooray, S.** 2004. The pivotal role of phosphatidylinositol 3-kinase-Akt signal transduction in virus survival. *J Gen Virol* **85**:1065-76.
20. **Cullen, P. J., G. E. Cozier, G. Banting, and H. Mellor.** 2001. Modular phosphoinositide-binding domains--their role in signalling and membrane trafficking. *Curr Biol* **11**:R882-93.
21. **Dales, S., and E. H. Mosbach.** 1968. Vaccinia as a model for membrane biogenesis. *Virology* **35**:564-83.
22. **Dodding, M. P., and M. Way.** 2009. Nck- and N-WASP-dependent actin-based motility is conserved in divergent vertebrate poxviruses. *Cell Host Microbe* **6**:536-50.
23. **Douglas, J.** 1999. Molluscum Contagiosum, p. 385-9. *In* S. P. Homes KK, Mardh PA, Lerner SM, Stamm WE, Piot P (ed.), *Sexually Transmitted Diseases*, 3rd ed. McGraw Hill, New York.
24. **Earley, A. K., W. M. Chan, and B. M. Ward.** 2008. The vaccinia virus B5 protein requires A34 for efficient intracellular trafficking from the endoplasmic reticulum to the site of wrapping and incorporation into progeny virions. *J Virol* **82**:2161-9.
25. **Fenner, F.** 1996. Poxviruses. *In* D. K. BN Fields, PM Howley (ed.), *Fields Virology*, 3rd ed. Lippincott-Raven Publishers, Philadelphia.
26. **Fenner, F., D. A. Henderson, I. Arita, Z. Jezek, and I. D. Ladnyi.** 1988. *Smallpox and Its Eradication*. World Health Organization, Geneva Switzerland.
27. **Franke, T. F.** 2008. Intracellular signaling by Akt: bound to be specific. *Sci Signal* **1**:pe29.
28. **Fratti, R. A., J. M. Backer, J. Gruenberg, S. Corvera, and V. Deretic.** 2001. Role of phosphatidylinositol 3-kinase and Rab5 effectors in phagosomal biogenesis and mycobacterial phagosome maturation arrest. *J Cell Biol* **154**:631-44.
29. **Fratti, R. A., J. Chua, and V. Deretic.** 2003. Induction of p38 mitogen-activated protein kinase reduces early endosome autoantigen 1 (EEA1) recruitment to phagosomal membranes. *J Biol Chem* **278**:46961-7.
30. **Frischknecht, F., V. Moreau, S. Rottger, S. Gonfloni, I. Reckmann, G. Superti-Furga, and M. Way.** 1999. Actin-based motility of vaccinia virus mimics receptor tyrosine kinase signalling. *Nature* **401**:926-9.
31. **Geada, M. M., I. Galindo, M. M. Lorenzo, B. Perdiguero, and R. Blasco.** 2001. Movements of vaccinia virus intracellular enveloped virions with GFP tagged to the F13L envelope protein. *J Gen Virol* **82**:2747-60.
32. **Gould, D.** 2008. An overview of molluscum contagiosum: a viral skin condition. *Nurs Stand* **22**:45-8.
33. **Guerin, J. L., J. Gelfi, S. Boullier, M. Delverdier, F. A. Bellanger, S. Bertagnoli, I. Drexler, G. Sutter, and F. Messud-Petit.** 2002. Myxoma virus

- leukemia-associated protein is responsible for major histocompatibility complex class I and Fas-CD95 down-regulation and defines scrapins, a new group of surface cellular receptor abductor proteins. *J Virol* **76**:2912-23.
34. **Habib, T., J. A. Hejna, R. E. Moses, and S. J. Decker.** 1998. Growth factors and insulin stimulate tyrosine phosphorylation of the 51C/SHIP2 protein. *J Biol Chem* **273**:18605-9.
 35. **Hawkins, P. T., K. E. Anderson, K. Davidson, and L. R. Stephens.** 2006. Signalling through Class I PI3Ks in mammalian cells. *Biochem Soc Trans* **34**:647-62.
 36. **Hirsch, E., C. Costa, and E. Ciruolo.** 2007. Phosphoinositide 3-kinases as a common platform for multi-hormone signaling. *J Endocrinol* **194**:243-56.
 37. **Hollinshead, M., G. Rodger, H. Van Eijl, M. Law, R. Hollinshead, D. J. Vaux, and G. L. Smith.** 2001. Vaccinia virus utilizes microtubules for movement to the cell surface. *J Cell Biol* **154**:389-402.
 38. **Hollinshead, M., A. Vanderplassen, G. L. Smith, and D. J. Vaux.** 1999. Vaccinia virus intracellular mature virions contain only one lipid membrane. *J Virol* **73**:1503-17.
 39. **Hopkins, D. R.** 1983. *Princes and Peasants*. The University of Chicago Press, Chicago.
 40. **Huang, J., and B. D. Manning.** 2009. A complex interplay between Akt, TSC2 and the two mTOR complexes. *Biochem Soc Trans* **37**:217-22.
 41. **Husain, M., and B. Moss.** 2001. Vaccinia virus F13L protein with a conserved phospholipase catalytic motif induces colocalization of the B5R envelope glycoprotein in post-Golgi vesicles. *J Virol* **75**:7528-42.
 42. **Ichihashi, Y.** 1996. Extracellular enveloped vaccinia virus escapes neutralization. *Virology* **217**:478-85.
 43. **Irvine, R. F.** 2003. 20 years of Ins(1,4,5)P₃, and 40 years before. *Nat Rev Mol Cell Biol* **4**:586-90.
 44. **Ishida, S., A. Funakoshi, K. Miyasaka, H. Shimokata, F. Ando, and S. Takiguchi.** 2006. Association of SH-2 containing inositol 5'-phosphatase 2 gene polymorphisms and hyperglycemia. *Pancreas* **33**:63-7.
 45. **Ishihara, H., T. Sasaoka, H. Hori, T. Wada, H. Hirai, T. Haruta, W. J. Langlois, and M. Kobayashi.** 1999. Molecular cloning of rat SH2-containing inositol phosphatase 2 (SHIP2) and its role in the regulation of insulin signaling. *Biochem Biophys Res Commun* **260**:265-72.
 46. **Jahrling, P. B., E. A. Fritz, and L. E. Hensley.** 2005. Countermeasures to the bioterrorist threat of smallpox. *Curr Mol Med* **5**:817-26.
 47. **Jenner, E.** 1798. *An Inquiry into the Causes and Effects of the Variolae Vaccine*. Sampson Low, London.
 48. **Jiang, B. H., and L. Z. Liu.** 2008. PI3K/PTEN signaling in tumorigenesis and angiogenesis. *Biochim Biophys Acta* **1784**:150-8.
 49. **Kagawa, S., T. Sasaoka, S. Yaguchi, H. Ishihara, H. Tsuneki, S. Murakami, K. Fukui, T. Wada, S. Kobayashi, I. Kimura, and M. Kobayashi.** 2005. Impact of SRC homology 2-containing inositol 5'-phosphatase 2 gene polymorphisms detected in a Japanese population on insulin signaling. *J Clin Endocrinol Metab* **90**:2911-9.

50. **Kaisaki, P. J., M. Delepine, P. Y. Woon, L. Sebag-Montefiore, S. P. Wilder, S. Menzel, N. Vionnet, E. Marion, J. P. Riveline, G. Charpentier, S. Schurmans, J. C. Levy, M. Lathrop, M. Farrall, and D. Gauguier.** 2004. Polymorphisms in type II SH2 domain-containing inositol 5-phosphatase (INPPL1, SHIP2) are associated with physiological abnormalities of the metabolic syndrome. *Diabetes* **53**:1900-4.
51. **Kajioka, R., L. Siminovitch, and S. Dales.** 1964. The Cycle of Multiplication of Vaccinia Virus in Earle's Strain L Cells. Ii. Initiation of DNA Synthesis and Morphogenesis. *Virology* **24**:295-309.
52. **Kazory, A., S. Singapuri, A. Wadhwa, and A. A. Ejaz.** 2007. Simultaneous development of Fanconi syndrome and acute renal failure associated with cidofovir. *J Antimicrob Chemother* **60**:193-4.
53. **Khodakevich, L., Z. Jezek, and D. Messinger.** 1988. Monkeypox virus: ecology and public health significance. *Bull World Health Organ* **66**:747-52.
54. **Khodakevich, L., M. Szczeniowski, D. Manbu ma, Z. Jezek, S. Marennikova, J. Nakano, and D. Messinger.** 1987. The role of squirrels in sustaining monkeypox virus transmission. *Trop Geogr Med* **39**:115-22.
55. **Knight, Z. A., B. Gonzalez, M. E. Feldman, E. R. Zunder, D. D. Goldenberg, O. Williams, R. Loewith, D. Stokoe, A. Balla, B. Toth, T. Balla, W. A. Weiss, R. L. Williams, and K. M. Shokat.** 2006. A pharmacological map of the PI3-K family defines a role for p110alpha in insulin signaling. *Cell* **125**:733-47.
56. **Knight, Z. A., and K. M. Shokat.** 2007. Chemically targeting the PI3K family. *Biochem Soc Trans* **35**:245-9.
57. **Kresge, N., Simoni. R.D., Hill, R.L.** 2005. A Role for Phosphoinositides in Signaling: the Work of Mabel R. Hokin and Lowell E. Hokin. *The Journal of Biological Chemistry* **280**:e27.
58. **Kyriakis, K. P., I. Palamaras, I. Alexoudi, and F. Vrani.** 2010. Molluscum contagiosum detection rates among Greek dermatology outpatients. *Scand J Infect Dis* **42**:719-20.
59. **Law, M., G. C. Carter, K. L. Roberts, M. Hollinshead, and G. L. Smith.** 2006. Ligand-induced and nonfusogenic dissolution of a viral membrane. *Proc Natl Acad Sci U S A* **103**:5989-94.
60. **Lindmo, K., and H. Stenmark.** 2006. Regulation of membrane traffic by phosphoinositide 3-kinases. *J Cell Sci* **119**:605-14.
61. **Lyons, A. S., Petrucelli, II, R. Joseph.** 1978. *Medicine: An Illustrated History.* H. N. Abrams, New York.
62. **Maehama, T.** 2007. PTEN: its deregulation and tumorigenesis. *Biol Pharm Bull* **30**:1624-7.
63. **Mansouri, M., E. Bartee, K. Gouveia, B. T. Hovey Nerenberg, J. Barrett, L. Thomas, G. Thomas, G. McFadden, and K. Fruh.** 2003. The PHD/LAP-domain protein M153R of myxomavirus is a ubiquitin ligase that induces the rapid internalization and lysosomal destruction of CD4. *J Virol* **77**:1427-40.
64. **Marion, E., P. J. Kaisaki, V. Pouillon, C. Gueydan, J. C. Levy, A. Bodson, G. Krzentowski, J. C. Daubresse, J. Mockel, J. Behrends, G. Servais, C. Szpirer, V. Kruys, D. Gauguier, and S. Schurmans.** 2002. The gene INPPL1, encoding

- the lipid phosphatase SHIP2, is a candidate for type 2 diabetes in rat and man. *Diabetes* **51**:2012-7.
65. **McIntosh, A. A., and G. L. Smith.** 1996. Vaccinia virus glycoprotein A34R is required for infectivity of extracellular enveloped virus. *J Virol* **70**:272-81.
 66. **Meiser, A., D. Boulanger, G. Sutter, and J. Krijnse Locker.** 2003. Comparison of virus production in chicken embryo fibroblasts infected with the WR, IHD-J and MVA strains of vaccinia virus: IHD-J is most efficient in trans-Golgi network wrapping and extracellular enveloped virus release. *J Gen Virol* **84**:1383-92.
 67. **Mohamed, M. R., and G. McFadden.** 2009. NFkB inhibitors: strategies from poxviruses. *Cell Cycle* **8**:3125-32.
 68. **Moss, B., and J. L. Shisler.** 2001. Immunology 101 at poxvirus U: immune evasion genes. *Semin Immunol* **13**:59-66.
 69. **Muraille, E., P. Bruhns, X. Pesse, M. Daeron, and C. Erneux.** 2000. The SH2 domain containing inositol 5-phosphatase SHIP2 associates to the immunoreceptor tyrosine-based inhibition motif of Fc gammaRIIB in B cells under negative signaling. *Immunol Lett* **72**:7-15.
 70. **Newsome, T. P., N. Scaplehorn, and M. Way.** 2004. SRC mediates a switch from microtubule- to actin-based motility of vaccinia virus. *Science* **306**:124-9.
 71. **Newsome, T. P., I. Weisswange, F. Frischknecht, and M. Way.** 2006. Abl collaborates with Src family kinases to stimulate actin-based motility of vaccinia virus. *Cell Microbiol* **8**:233-41.
 72. **Odorizzi, G., M. Babst, and S. D. Emr.** 2000. Phosphoinositide signaling and the regulation of membrane trafficking in yeast. *Trends Biochem Sci* **25**:229-35.
 73. **Ooms, L. M., K. A. Horan, P. Rahman, G. Seaton, R. Gurung, D. S. Kethesparan, and C. A. Mitchell.** 2009. The role of the inositol polyphosphate 5-phosphatases in cellular function and human disease. *Biochem J* **419**:29-49.
 74. **Parrish, S., and B. Moss.** 2007. Characterization of a second vaccinia virus mRNA-decapping enzyme conserved in poxviruses. *J Virol* **81**:12973-8.
 75. **Parrish, S., W. Resch, and B. Moss.** 2007. Vaccinia virus D10 protein has mRNA decapping activity, providing a mechanism for control of host and viral gene expression. *Proc Natl Acad Sci U S A* **104**:2139-44.
 76. **Payne, L. G.** 1979. Identification of the vaccinia hemagglutinin polypeptide from a cell system yielding large amounts of extracellular enveloped virus. *J Virol* **31**:147-55.
 77. **Ploubidou, A., V. Moreau, K. Ashman, I. Reckmann, C. Gonzalez, and M. Way.** 2000. Vaccinia virus infection disrupts microtubule organization and centrosome function. *Embo J* **19**:3932-44.
 78. **Prasad, N. K., and S. J. Decker.** 2005. SH2-containing 5'-inositol phosphatase, SHIP2, regulates cytoskeleton organization and ligand-dependent down-regulation of the epidermal growth factor receptor. *J Biol Chem* **280**:13129-36.
 79. **Punjabi, A., and P. Traktman.** 2005. Cell biological and functional characterization of the vaccinia virus F10 kinase: implications for the mechanism of virion morphogenesis. *J Virol* **79**:2171-90.
 80. **Purdy, G. E., R. M. Owens, L. Bennett, D. G. Russell, and B. A. Butcher.** 2005. Kinetics of phosphatidylinositol-3-phosphate acquisition differ between

- IgG bead-containing phagosomes and Mycobacterium tuberculosis-containing phagosomes. *Cell Microbiol* **7**:1627-34.
81. **Reed, K. D., J. W. Melski, M. B. Graham, R. L. Regnery, M. J. Sotir, M. V. Wegner, J. J. Kazmierczak, E. J. Stratman, Y. Li, J. A. Fairley, G. R. Swain, V. A. Olson, E. K. Sargent, S. C. Kehl, M. A. Frace, R. Kline, S. L. Foldy, J. P. Davis, and I. K. Damon.** 2004. The detection of monkeypox in humans in the Western Hemisphere. *N Engl J Med* **350**:342-50.
 82. **Reeves, P. M., B. Bommarius, S. Lebeis, S. McNulty, J. Christensen, A. Swimm, A. Chahroudi, R. Chavan, M. B. Feinberg, D. Veach, W. Bornmann, M. Sherman, and D. Kalman.** 2005. Disabling poxvirus pathogenesis by inhibition of Abl-family tyrosine kinases. *Nat Med* **11**:731-9.
 83. **Reeves, P. M., S. K. Smith, V. A. Olson, S. H. Thorne, W. Bornmann, I. K. Damon, and D. Kalman.** 2011. Variola and monkeypox utilize conserved mechanisms of virion motility and release that depend on Abl- and Src-family tyrosine kinases. *Journal of Virology* **85**.
 84. **Rehm, K. E., R. F. Connor, G. J. Jones, K. Yimbu, and R. L. Roper.** 2010. Vaccinia virus A35R inhibits MHC class II antigen presentation. *Virology* **397**:176-86.
 85. **Rietdorf, J., A. Ploubidou, I. Reckmann, A. Holmstrom, F. Frischknecht, M. Zettl, T. Zimmermann, and M. Way.** 2001. Kinesin-dependent movement on microtubules precedes actin-based motility of vaccinia virus. *Nat Cell Biol* **3**:992-1000.
 86. **Rimoin, A. W., N. Kisalu, B. Kebela-Ilunga, T. Mukaba, L. L. Wright, P. Formenty, N. D. Wolfe, R. L. Shongo, F. Tshioko, E. Okitolonda, J. J. Muyembe, R. W. Ryder, and H. Meyer.** 2007. Endemic human monkeypox, Democratic Republic of Congo, 2001-2004. *Emerg Infect Dis* **13**:934-7.
 87. **Rimoin, A. W., P. M. Mulembakani, S. C. Johnston, J. O. Smith, N. K. Kisalu, T. L. Kinkela, S. Blumberg, H. A. Thomassen, B. L. Pike, J. N. Fair, N. D. Wolfe, R. L. Shongo, B. S. Graham, P. Formenty, E. Okitolonda, L. E. Hensley, H. Meyer, L. L. Wright, and J. J. Muyembe.** 2010. Major increase in human monkeypox incidence 30 years after smallpox vaccination campaigns cease in the Democratic Republic of Congo. *Proc Natl Acad Sci U S A*.
 88. **Risco, C., J. R. Rodriguez, C. Lopez-Iglesias, J. L. Carrascosa, M. Esteban, and D. Rodriguez.** 2002. Endoplasmic reticulum-Golgi intermediate compartment membranes and vimentin filaments participate in vaccinia virus assembly. *J Virol* **76**:1839-55.
 89. **Roberts, K. L., and G. L. Smith.** 2008. Vaccinia virus morphogenesis and dissemination. *Trends Microbiol* **16**:472-9.
 90. **Rodriguez, J. R., C. Risco, J. L. Carrascosa, M. Esteban, and D. Rodriguez.** 1997. Characterization of early stages in vaccinia virus membrane biogenesis: implications of the 21-kilodalton protein and a newly identified 15-kilodalton envelope protein. *J Virol* **71**:1821-33.
 91. **Rohatgi, R., H. Y. Ho, and M. W. Kirschner.** 2000. Mechanism of N-WASP activation by CDC42 and phosphatidylinositol 4, 5-bisphosphate. *J Cell Biol* **150**:1299-310.

92. **Rosengard, A. M., Y. Liu, Z. Nie, and R. Jimenez.** 2002. Variola virus immune evasion design: expression of a highly efficient inhibitor of human complement. *Proc Natl Acad Sci U S A* **99**:8808-13.
93. **Ruckle, T., M. K. Schwarz, and C. Rommel.** 2006. PI3Kgamma inhibition: towards an 'aspirin of the 21st century'? *Nat Rev Drug Discov* **5**:903-18.
94. **Sanderson, C. M., M. Hollinshead, and G. L. Smith.** 2000. The vaccinia virus A27L protein is needed for the microtubule-dependent transport of intracellular mature virus particles. *J Gen Virol* **81**:47-58.
95. **Scaplehorn, N., A. Holmstrom, V. Moreau, F. Frischknecht, I. Reckmann, and M. Way.** 2002. Grb2 and Nck act cooperatively to promote actin-based motility of vaccinia virus. *Curr Biol* **12**:740-5.
96. **Schmelz, M., B. Sodeik, M. Ericsson, E. J. Wolffe, H. Shida, G. Hiller, and G. Griffiths.** 1994. Assembly of vaccinia virus: the second wrapping cisterna is derived from the trans Golgi network. *J Virol* **68**:130-47.
97. **Schurmans, S., R. Carrio, J. Behrends, V. Pouillon, J. Merino, and S. Clement.** 1999. The mouse SHIP2 (Inpp11) gene: complementary DNA, genomic structure, promoter analysis, and gene expression in the embryo and adult mouse. *Genomics* **62**:260-71.
98. **Senkevich, T. G., A. S. Weisberg, and B. Moss.** 2000. Vaccinia virus E10R protein is associated with the membranes of intracellular mature virions and has a role in morphogenesis. *Virology* **278**:244-52.
99. **Senkevich, T. G., C. L. White, E. V. Koonin, and B. Moss.** 2002. Complete pathway for protein disulfide bond formation encoded by poxviruses. *Proc Natl Acad Sci U S A* **99**:6667-72.
100. **Senkevich, T. G., C. L. White, E. V. Koonin, and B. Moss.** 2000. A viral member of the ERV1/ALR protein family participates in a cytoplasmic pathway of disulfide bond formation. *Proc Natl Acad Sci U S A* **97**:12068-73.
101. **Senkevich, T. G., C. L. White, A. Weisberg, J. A. Granek, E. J. Wolffe, E. V. Koonin, and B. Moss.** 2002. Expression of the vaccinia virus A2.5L redox protein is required for virion morphogenesis. *Virology* **300**:296-303.
102. **Shisler, J. L., and B. Moss.** 2001. Immunology 102 at poxvirus U: avoiding apoptosis. *Semin Immunol* **13**:67-72.
103. **Shurkin, J. N.** 1979. *The Invisible Fire: The Story of Mankind's Victory over the Ancient Scourge Smallpox.* G. P. Putnam's Sons, New York.
104. **Sleeman, M. W., K. E. Wortley, K. M. Lai, L. C. Gowen, J. Kintner, W. O. Kline, K. Garcia, T. N. Stitt, G. D. Yancopoulos, S. J. Wiegand, and D. J. Glass.** 2005. Absence of the lipid phosphatase SHIP2 confers resistance to dietary obesity. *Nat Med* **11**:199-205.
105. **Smith, G. L., A. Vanderplassen, and M. Law.** 2002. The formation and function of extracellular enveloped vaccinia virus. *J Gen Virol* **83**:2915-31.
106. **Smith, J. R.** 1987. *The Speckled Monster.* Witley Press, Norfolk, UK.
107. **Smith, K., D. Humphreys, P. J. Hume, and V. Koronakis.** 2010. Enteropathogenic *Escherichia coli* recruits the cellular inositol phosphatase SHIP2 to regulate actin-pedestal formation. *Cell Host Microbe* **7**:13-24.
108. **Soares, J. A., F. G. Leite, L. G. Andrade, A. A. Torres, L. P. De Sousa, L. S. Barcelos, M. M. Teixeira, P. C. Ferreira, E. G. Kroon, T. Souto-Padron, and**

- C. A. Bonjardim.** 2009. Activation of the PI3K/Akt pathway early during vaccinia and cowpox virus infections is required for both host survival and viral replication. *J Virol* **83**:6883-99.
109. **Sodeik, B., R. W. Doms, M. Ericsson, G. Hiller, C. E. Machamer, W. van 't Hof, G. van Meer, B. Moss, and G. Griffiths.** 1993. Assembly of vaccinia virus: role of the intermediate compartment between the endoplasmic reticulum and the Golgi stacks. *J Cell Biol* **121**:521-41.
110. **Stabenow, J., R. M. Buller, J. Schriewer, C. West, J. E. Sagartz, and S. Parker.** A mouse model of lethal infection for evaluating prophylactics and therapeutics against Monkeypox virus. *J Virol* **84**:3909-20.
111. **Stanford, M. M., G. McFadden, G. Karupiah, and G. Chaudhri.** 2007. Immunopathogenesis of poxvirus infections: forecasting the impending storm. *Immunol Cell Biol* **85**:93-102.
112. **Temple, R.** 2006. *The Genius of China: 3,000 Years of Science, Discovery and Invention.* Carlton Publishing Group, London.
113. **Tooze, J., M. Hollinshead, B. Reis, K. Radsak, and H. Kern.** 1993. Progeny vaccinia and human cytomegalovirus particles utilize early endosomal cisternae for their envelopes. *Eur J Cell Biol* **60**:163-78.
114. **Tsui, M. M., and J. D. York.** 2010. Roles of inositol phosphates and inositol pyrophosphates in development, cell signaling and nuclear processes. *Adv Enzyme Regul* **50**:324-37.
115. **Unger, B., and P. Traktman.** 2004. Vaccinia virus morphogenesis: a13 phosphoprotein is required for assembly of mature virions. *J Virol* **78**:8885-901.
116. **Vanderplasschen, A., M. Hollinshead, and G. L. Smith.** 1998. Intracellular and extracellular vaccinia virions enter cells by different mechanisms. *J Gen Virol* **79 (Pt 4)**:877-87.
117. **Vanhaesebroeck, B., J. Guillermet-Guibert, M. Graupera, and B. Bilanges.** 2010. The emerging mechanisms of isoform-specific PI3K signalling. *Nat Rev Mol Cell Biol* **11**:329-41.
118. **Vergne, I., J. Chua, and V. Deretic.** 2003. Tuberculosis toxin blocking phagosome maturation inhibits a novel Ca²⁺/calmodulin-PI3K hVPS34 cascade. *J Exp Med* **198**:653-9.
119. **Vergne, I., J. Chua, H. H. Lee, M. Lucas, J. Belisle, and V. Deretic.** 2005. Mechanism of phagolysosome biogenesis block by viable Mycobacterium tuberculosis. *Proc Natl Acad Sci U S A* **102**:4033-8.
120. **Vergne, I., J. Chua, S. B. Singh, and V. Deretic.** 2004. Cell biology of mycobacterium tuberculosis phagosome. *Annu Rev Cell Dev Biol* **20**:367-94.
121. **Vieira, O. V., R. J. Botelho, L. Rameh, S. M. Brachmann, T. Matsuo, H. W. Davidson, A. Schreiber, J. M. Backer, L. C. Cantley, and S. Grinstein.** 2001. Distinct roles of class I and class III phosphatidylinositol 3-kinases in phagosome formation and maturation. *J Cell Biol* **155**:19-25.
122. **Walsh, D., C. Arias, C. Perez, D. Halladin, M. Escandon, T. Ueda, R. Watanabe-Fukunaga, R. Fukunaga, and I. Mohr.** 2008. Eukaryotic translation initiation factor 4F architectural alterations accompany translation initiation factor redistribution in poxvirus-infected cells. *Mol Cell Biol* **28**:2648-58.

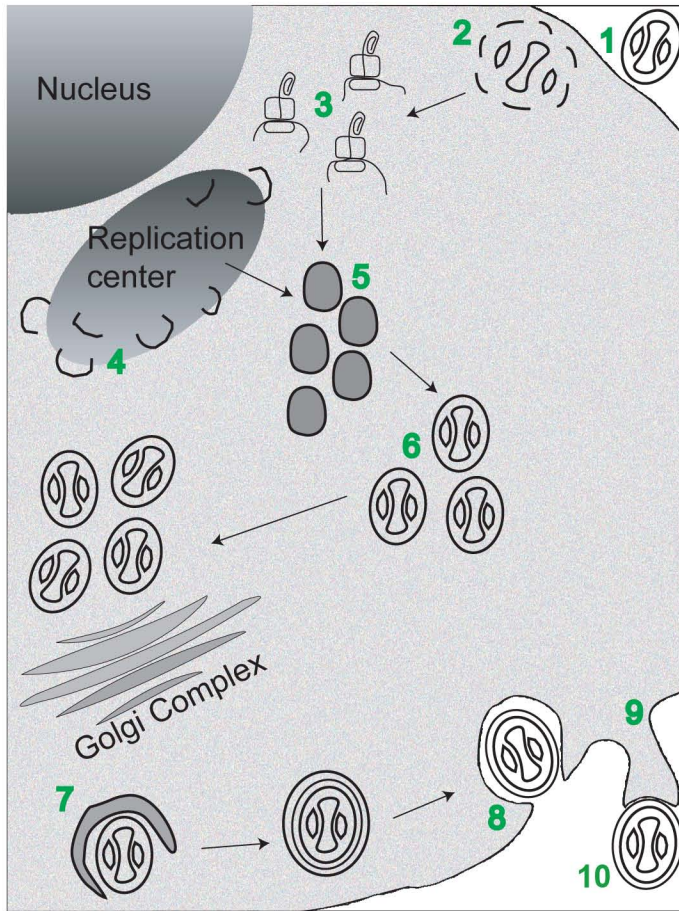
123. **Ward, B. M.** 2005. Visualization and characterization of the intracellular movement of vaccinia virus intracellular mature virions. *J Virol* **79**:4755-63.
124. **Ward, B. M., and B. Moss.** 2001. Vaccinia virus intracellular movement is associated with microtubules and independent of actin tails. *J Virol* **75**:11651-63.
125. **Weisswange, I., T. P. Newsome, S. Schleich, and M. Way.** 2009. The rate of N-WASP exchange limits the extent of ARP2/3-complex-dependent actin-based motility. *Nature* **458**:87-91.
126. **White, C. L., A. S. Weisberg, and B. Moss.** 2000. A glutaredoxin, encoded by the G4L gene of vaccinia virus, is essential for virion morphogenesis. *J Virol* **74**:9175-83.
127. **Whitman, M., C. P. Downes, M. Keeler, T. Keller, and L. Cantley.** 1988. Type I phosphatidylinositol kinase makes a novel inositol phospholipid, phosphatidylinositol-3-phosphate. *Nature* **332**:644-6.
128. **Winslow, O. E.** 1974. *A Destroying Angel: The Conquest of Smallpox in Colonial Boston.* Houghton Mifflin Company, Boston.
129. **Wisniewski, D., A. Strife, S. Swendeman, H. Erdjument-Bromage, S. Geromanos, W. M. Kavanaugh, P. Tempst, and B. Clarkson.** 1999. A novel SH2-containing phosphatidylinositol 3,4,5-trisphosphate 5-phosphatase (SHIP2) is constitutively tyrosine phosphorylated and associated with src homologous and collagen gene (SHC) in chronic myelogenous leukemia progenitor cells. *Blood* **93**:2707-20.
130. **Yang, G., D. C. Pevear, M. H. Davies, M. S. Collett, T. Bailey, S. Rippen, L. Barone, C. Burns, G. Rhodes, S. Tohan, J. W. Huggins, R. O. Baker, R. L. Buller, E. Touchette, K. Waller, J. Schriewer, J. Neyts, E. DeClercq, K. Jones, D. Hruby, and R. Jordan.** 2005. An orally bioavailable antipoxvirus compound (ST-246) inhibits extracellular virus formation and protects mice from lethal orthopoxvirus Challenge. *J Virol* **79**:13139-49.
131. **Yu, J., H. Peng, Q. Ruan, A. Fatima, S. Getsios, and R. M. Lavker.** MicroRNA-205 promotes keratinocyte migration via the lipid phosphatase SHIP2. *FASEB J.*
132. **Yu, J., Y. Zhang, J. McIlroy, T. Rordorf-Nikolic, G. A. Orr, and J. M. Backer.** 1998. Regulation of the p85/p110 phosphatidylinositol 3'-kinase: stabilization and inhibition of the p110alpha catalytic subunit by the p85 regulatory subunit. *Mol Cell Biol* **18**:1379-87.
133. **Zaborowska, I., and D. Walsh.** 2009. PI3K signaling regulates rapamycin-insensitive translation initiation complex formation in Vaccinia Virus-infected cells. *J Virol.*

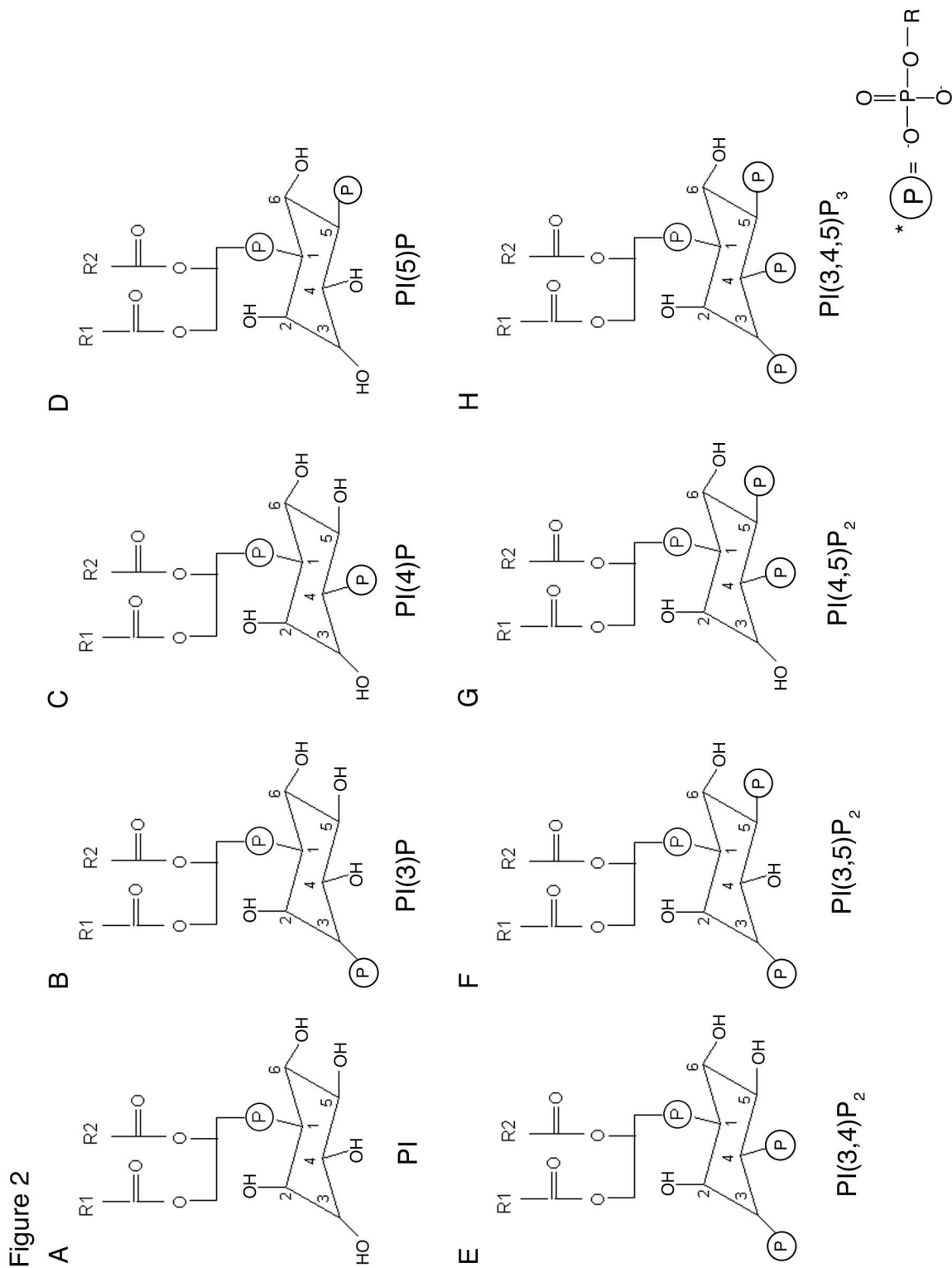
FIGURE LEGENDS

Figure 1: Overview of Poxviral Lifecycle. After VV entry (1) virion uncoating and early protein synthesis occurs (2). These steps are followed by late protein production (3), formation of viral replication centers and viral crescents (4). Crescents envelop viroplasm to form immature virions (IV, 5). The cores of IV condense to form mature virions (IMV, 6). A subset of the IMV traffic to the Golgi Complex where they are enveloped in a host cell derived membrane to form Intracellular Enveloped Virions (IEV) (7). IEV fuse with the plasma membrane, releasing virus to the extracellular milieu, (CEV, 8). CEV form actin tails (9) beneath the virus and ultimately, release to form extracellular enveloped virions (EEV, 10).

Figure 2: Phosphatidylinositol Lipid Species **A)** Phosphatidylinositol. **B)** Phosphatidylinositol 3-Phosphate [PI(3)P]. **C)** Phosphatidylinositol 4-Phosphate [PI(4)P]. **D)** Phosphatidylinositol 5-Phosphate [PI(5)P]. **E)** Phosphatidylinositol 3,4-Bisphosphate [PI(3,4)P₂]. **F)** Phosphatidylinositol 3,4-Bisphosphate [PI(3,5)P₂]. **G)** Phosphatidylinositol 4,5-Bisphosphate [PI(4,5)P₂]. **H)** Phosphatidylinositol 3,4,5-Trisphosphate [PI(3,4,5)P₃].

Figure 1





CHAPTER II: IDENTIFICATION OF SMALL MOLECULES THAT REDUCE VACCINIA VIRUS REPLICATION AND ACTIN TAIL FORMATION

Shannon McNulty¹, William Bornmann², and Daniel Kalman³

¹Microbiology and Molecular Genetics Graduate Program, Emory University School of Medicine, Atlanta, GA.

²MD Anderson Cancer Center, University of Texas, Houston, TX.

³Department of Pathology and Laboratory Medicine, Emory University School of Medicine, Atlanta, GA.

All experiments were conceived by Shannon McNulty and Daniel Kalman. All experiments were performed by Shannon McNulty. Compound library was provided by William Bornman. Tables 1-16 and Figures 1-2 were made by Shannon McNulty.

ABSTRACT

Mass smallpox vaccinations were eliminated in 1978, leaving the populace extremely sensitive naturally occurring poxviruses and the accidental release of Smallpox. Current treatment methods, while effective against the virus, are not without significant side effects. Previous work from our lab identified that inhibition of host tyrosine kinases can induce survival during a lethal (LD_{75}) poxviral infection. Our lab was interested in identifying novel, next-generation tyrosine kinase inhibitors capable of preventing poxviral spread. To accomplish this, a compound library of ~180 compounds was screened by microscopy and plaque assay for a reduction in viral replication and spread. Of the ~180 compounds screened, 53% reduced spread in tissue culture and 43% reduced actin protrusions induced by the virus to spread. Through this approach we identified new small molecule inhibitors of poxviral infections.

INTRODUCTION

Variola, the agent of Smallpox, was declared eradicated from nature in 1980 (8). However, other poxviruses, such as Monkeypox and Molluscum Contagiosum, still pose a potential threat. The problem is compounded because smallpox vaccinations for the general population ceased in 1976, and the population today is exquisitely sensitive to poxvirus infection (8, 14). In particular, monkeypox is endemic in Africa (27) and has the potential for spread to humans from squirrels and bushmeat (17, 18, 23, 27, 28), and recent outbreaks in the Sudan have raised the possibility for human-to-human transmission (28). Furthermore, since poxviruses are resistant to desiccation and can spread through aerosolization (8, 37), the potential exists that poxviruses may be easily weaponized to produce a bioterror agent (14). Therefore, the need exists to produce novel therapeutics which can inhibit the spread of poxviruses.

Current poxviral treatment methods, while effective against the virus, are not without significant side effects. The current treatment method recommended by the CDC for accidental or serious smallpox vaccine adverse events is Vaccine Immune Globulin (VIG). As a second treatment method, cidofovir may be administered under the Investigational New Drug Protocol (FDA regulation). Unfortunately, cidofovir treatment is not without side-effects. As a nucleoside analog, cidofovir exhibits significant renal toxicity (16), and must be administered in combination with IV fluids and probenecid, a renal tubular blocker. Given the significant toxicity associated with cidofovir, and limited resources of VIG, there has been a significant push to identify new poxviral inhibitors, particularly those with fewer side effects.

Since the Anthrax attacks in 2001, new funding sources have developed that have led to the recent development of novel poxviral therapeutics. ST-246, developed by Siga Technologies targets the viral F13L protein, preventing the virus from leaving the cell (39). While ST-246 has been shown effective at preventing poxviral *in vivo* (33, 39), Yang *et al.* demonstrated it was possible to generate escape mutants in F13L (39). Given the ease at which such mutants were generated in tissue culture, and anecdotally in both animals and people, it seems possible that similar escape mutants may also develop within an infected individual treated with this drug.

To reduce the possibility of generating escape viral mutants resistant to poxviral inhibitors, our lab has developed novel host-directed poxviral therapeutics. Work by Frischknecht *et al.* and Reeves *et al.* demonstrated that host Src- and Abl- family tyrosine kinases are utilized by vaccinia, monkeypox and variola virus to form actin tails and spread (10, 24, 25). Reeves *et al.* extended this observation and identified that Abl-family tyrosine kinases are used for viral release. They also showed that the Abl-family kinase inhibitor, imatinib mesylate (STI-571, Gleevec), an FDA-approved drug originally developed for the treatment of chronic myelogenous leukemia (CML), can reduce the spread of poxviruses in tissue culture, and increases survival during an otherwise lethal murine infection (24). Therefore, our lab was interested in exploring the possibility that other tyrosine kinase inhibitors can prevent poxviral spread and, in particular, develop new drug candidates.

To develop novel tyrosine kinase inhibitors Fernandez *et al.* redesigned Gleevec through molecular modeling (9). By modeling the ligand/protein interface they were able to identify the contribution of the hydration shell to drug-protein binding. This approach

was used to generate a library of “second generation” tyrosine kinase inhibitors. We screened this library to identify new molecular structures that reduced vaccinia virus spread, and which, like imatinib may be useful in fighting poxviral infections.

MATERIALS AND METHODS

Cells and Viruses

BSC40 and 3T3 cells (ATCC) were grown in DMEM (Cellgro, MediaTech Inc; Manassas, VA) supplemented with 10%FBS (Atlanta Biologicals; Norcross, GA) and 10 IU/mL Penicillin and 1mg/mL streptomycin (P/S; Cellgro, MediaTech, Inc.; Manassas, VA). Vaccinia virus, strain WR and IHD-J, was grown, propagated and titered on BSC40 cells.

Small Molecule Library

A small molecule library, consisting of 176 unique small molecules was prepared by William Bornmann. Compounds were supplied at 10mM in DMSO. Compounds are grouped into different classes based on shared chemical backbone structure (Table 1). Compounds within the same class share chemical backbone structure, but differ in side group substitutions.

Plaque Assays

BSC40 cells were grown to confluency in 12-well tissue culture dishes. Media was removed and replaced with 500 μ L of 2%FBS/DMEM. 1000PFU of vaccinia virus, strain IHD-J, in 100 μ L volume was added to each well, after one hour media was removed and

replaced with 10%FBS/DMEM. Compounds were diluted 1:10 in 10%FBS/DMEM, and 50 μ L of 1mM compound was added to BSC40 cells, for a final concentration of 100 μ M. Infections proceeded for 72 hours, after which media was removed and plaques were stained with crystal violet solution (0.1% crystal violet and 20% ethanol). Plaque morphology was scored relative to untreated control plaques. Cytopathic effect (CPE) was scored as lighter crystal violet staining and the absence of cells at both the macroscopic and microscopic level. Plaques were scored using the following criteria: Small Plaques, Pinpoint Plaques, No Plaques, Small Plaques with No Comets, Large Comets, More Plaques than Untreated Cells, and Cytopathic Effect (CPE). Compounds that produced small or pinpoint plaques were scored as “Compounds that Reduce Plaque Size” (Table 2). Compounds that produced no plaques were scored as “Compounds that Eliminated Plaques” (Table 3). Compounds that produced large comets or more plaques than untreated cells were scored as “Compounds that Increased Virion Release” (Table 4). Compounds that produced small plaques with no comets were scored as “Compounds that Eliminated Comet Tails” (Table 5). Finally, Compounds that damaged the cell monolayer producing lighted crystal violet staining than untreated cells, or disrupted the number of attached cells were scored as “Compounds that Damaged the Cell Monolayer” (Table 6). Compounds that had no effect on plaque morphology are listed in Table 7.

Microscopy

3T3 cells were grown in 96-well optical bottom plates (Nunc, Thermo Scientific, Rochester, NY), or PDL-collagen coated 12mm glass microscopy slips (Fisher Scientific, Pittsburgh, PA). Cells in 96-well glass bottom dishes were infected with 3.2×10^7

PFU/mL vaccinia virus, strain WR, in 200 μ L of 2%FBS/DMEM for one hour. After one hour media was removed and replaced with 75 μ L of 10% FBS/DMEM. Compounds in 96-well Plate #1 were diluted to 10 μ M in Phenol-free DMEM (Cellgro, MediaTech, Inc; Manassas, VA) and added to cells in 7.5 μ L volume for a final concentration of 1 μ M. Compounds in 96-well Plate #2 were diluted to 100 μ M in Phenol-free DMEM (Cellgro, MediaTech, Inc; Manassas, VA) and added to cells in 7.5 μ L volume for a final concentration of 10 μ M. After a 17 hour infection, cells were washed 2X with PBS, fixed, and stained with DAPI and Phalloidin-594 (Molecular Probes, Invitrogen). Compounds identified as modifying actin tails were retested to confirm their phenotype. BSC40 cells were grown on 12mm glass slips were infected with 1×10^7 PFU/mL B5-gfp vaccinia virus, strain WR. After a one hour adsorption media was removed from cells and replaced with 180 μ L of 10%FBE/DMEM. 20 μ L of compounds were added to cells (Plate #1 final concentration =1 μ M, Plate #2 final concentration = 10 μ M). After 16 hours cells were fixed and stained as described. Compounds that the numbers of actin tails were scored as “Compounds that Reduced/Eliminated Actin Tails” (Table 8). Compounds that reduced the overall length of actin tails were scored as “Compounds that Shortened Actin Tails” (Table 9). Compounds that disrupted overall actin morphology, while still producing tail-like projections were scored as “Compounds that Modified Actin Morphology” (Table 10). Compounds that caused cells to clump, round-up or disrupted nuclei were scored as “Compounds Exhibiting Toxicity by Microscopy” (Table 11). Compounds that did not modify actin morphology are listed in Table 12.

RESULTS

Identification of small molecules that modify vaccinia virus plaque morphology.

To identify compounds that reduce vaccinia virus replication or spread, we screened a library of 180 compounds for those that reduced or changed vaccinia virus plaque size. All compounds were added post-viral adsorption. Many compounds exhibit similar structures, and compounds have been grouped into similar classes based on their shared backbone structure (Table 1). Of the 180 compounds, 44% were scored as modifying plaque morphology (Figure 1). We identified compounds that reduced plaque size (26%, Figure 1A, B and Table 2) or eliminated plaques (8.3%, Table 3). We also identified compounds that increased viral release (5%, Figure 1D and Table 4). Plaques formed by vaccinia virus strain IHD-J consist of a mother plaque closely apposed to an archipelago of smaller plaques. The formation of these “comets” have been attributed to the release of the extracellular enveloped (EEV) form of the virus, as viral mutants unable to form EEV are also unable to form comet tails (3, 11). In our screen, we identified compounds that not only reduced plaque size, but also eliminated comet tails (4%, Table 5 and Figure 1C). Finally, several compounds exhibited toxicity at the concentrations tested, resulting in destruction of the cellular monolayer (9.4%, Table 6) and were not pursued further. Several compounds had no effect on plaque size (Table 7).

Identification of small molecules that modify vaccinia virus actin tail morphology.

In addition to screening the compound library for those compounds that reduced vaccinia virus plaque size, we were also interested in identifying those compounds that modified vaccinia virus actin tails. To do this, compounds were added post-viral

adsorption, thereby eliminating any effects on viral entry. Of the 180 compounds screened, 42% of the compounds modified actin tail morphology (Figure 2). Twenty-five compounds (14%) significantly reduced or eliminated actin tails on infected cells (Table 8 and Figure 2C, D), whereas ten (0.5%, Table 9) compounds reduced actin tail length. Twenty-two compounds (12.2%, Table 10 and Figure 2E) modified cellular actin, making any effect on actin tails difficult to observe. Toxic compounds and those that did not modify actin tails are listed in Tables 11 and 12, respectively.

DISCUSSION

Herein we identify novel, second generation inhibitors of vaccinia virus infections. Notably, the compounds appeared to inhibit poxviral spread through different mechanisms. Based on the plaque assay and microscopy results these drugs can be assigned the following classes: actin tail inhibitors, spread inhibitors, and release accelerators. The drugs and their proposed mechanism of action are explored in greater detail below and summarized in Table 13. Compounds identified as producing a cytotoxic effect at the microscopic or plaque assay levels were eliminated from this classification. We cannot rule out the possibility that these compounds may have activity against poxviruses, but further characterization at lower concentrations that reduce toxicity will be required.

Actin Tail/Replication Inhibitors

Compounds that reduced both plaque size, eliminated comet tails and shortened or eliminated actin tails are similar in biological activity to previously identified Src- and

Abl-family kinase inhibitors (Table 14) (25). Further work will be required to determine whether these compounds inhibit the Src- and Abl-family tyrosine kinases. During vaccinia replication a subset of intracellular mature virions (IMV) traffic to a juxta-nuclear region where they are enveloped in additional host-cell membranes derived from endosomes or from the Golgi apparatus (21, 29, 31, 35, 36). These virions traffic to the plasma membrane, where they fuse and initiate actin polymerization behind the virions (32). Reeves *et al.* demonstrated that a dual Src- and Abl-family kinase inhibitor, dasatinib (BMS-354852), can reduce actin tails and result in small plaques (25). Two compounds (PD-Br and YYB44) in this class have similar structure to an already characterized Src- and Abl-family tyrosine kinase inhibitor, PD166326 (38). These data suggest that compounds classified as actin tail inhibitors may target Src- or Abl-family kinases or other components required for actin tail formation.

An alternative possibility is that these compounds affect the virus at a step prior to actin tail formation. Actin tail formation occurs at the end of the vaccinia replication cycle and can be eliminated if EEV are not produced or released (4, 24). Compounds that prevent EEV wrapping or inhibit the virus prior to EEV formation would thus eliminate tails and produce a small plaque phenotype. For instance, the inhibitor IMCBH prevents EEV wrapping, eliminates actin tails and produces small plaques (12). Additionally, the nucleoside analogue cidofovir slows DNA elongation and inhibits the 3'-5' exonuclease activity of the polymerase (15). The defect in DNA synthesis inhibits DNA encapsidation and virion morphogenesis at a stage upstream of actin tails and producing a small plaque phenotype and eliminating actin tails (15). One compound classified in this group, WBZ-4 was specifically engineered to not inhibit the Abl-family kinases, but does

inhibit c-Kit, PDGFR, CSF1R, and JNK1 (9). Since many viral and host kinases are necessary during the viral lifecycle (1, 22, 26), it remains possible that compounds in this class target not only Src- and Abl-family tyrosine kinases, but also other kinases that affect viral maturation prior to actin tail formation.

Spread Inhibitors

Compounds that reduced both plaque size and comet formation, but did not modify actin tails were classified as spread inhibitors (Table 15). Actin tails formed in the presence of an inhibitory compound suggests that a subset of virions have completed the replication cycle. However, small plaques formed in the presence of the inhibitory compound contradicts the microscopic observations and suggests that actin tails are not contributing to the small plaque phenotype. The presence of mature EEV suggests that two mechanisms could contribute to the small plaque phenotype: 1) the compounds could incompletely reduce replication upstream of actin tails (as outlined above) and allow sporadic EEV breakthrough; or 2) EEV and actin tails are produced, but virions are defective in release, specific infectivity, entry or all of these.

VV entry can occur through fusion at the plasma membrane, or by an macropinocytosis-like endosomal route (2, 5-7, 20). For EEV to enter cells the outer membrane must be disrupted before fusion can occur (13, 19). A large complex of 11 entry/fusion proteins have been identified, however the exact entry mechanism has not been elucidated (30). Mercer *et al.* recently identified that membrane blebbing was involved in productive entry and that blebbing was dependent on PAK1 and rac1 (20). They further identified that entry could be reduced following treatment with tyrosine,

serine-threonine, PI3K, Na⁺/H⁺ exchangers, actin, rac1 and Pak1 inhibitors (20). These data suggest that compounds reducing viral spread, but not actin tails may inhibit either the virion entry complex, or host enzymes required for entry or both.

Alternatively, formation of actin tails and a small comet phenotype could arise following inhibition of EEV release from the host cell. Reeves *et al.* demonstrated that Abl-family kinases are necessary for release of EEV, but not for actin tail formation (24). Since this compound library consisted of “next generation” tyrosine kinase inhibitors, it remains possible that compounds in this group may target the Abl-family kinases, thus preventing viral release and producing a small plaque phenotype.

Release Accelerators

Several molecules in the library appeared to accelerate the spread of the virus in tissue culture and caused larger comets relative to untreated cells (Table 16). While these drugs likely are not useful as therapeutics, they still may be important tools for studying the mechanisms of viral spread and pathogenesis.

In Chapter IV we describe the identification of a host phosphoinositide 5-phosphatase, SHIP2, that inhibits the release of VV. Cells deficient in SHIP2 form larger comets than WT cells. Large comets formed in the presence of inhibitors suggest that SHIP2, or other molecules in the SHIP2 pathway, may be the target of these compounds. Suwa *et al.* recently identified a small molecule inhibitor of SHIP2 (34), suggesting that SHIP2 is “druggable.”. However, Suwa *et al.* was unable or unwilling to share a sample of this inhibitor with us. The contribution of SHIP2 to the viral lifecycle will be described in further detail in Chapter IV.

Herein we identified novel poxviral inhibitors by screening a compound library of “next generation” compounds that reduced poxviral spread. These compounds were identified as having multiple mechanisms of action, which elucidated the contribution of tyrosine kinases to both virion spread and actin tail formation. Surprisingly, the compound library did not consist entirely of tyrosine kinase inhibitors, but included inhibitors to other host enzymes [AS605240 (AS1), AS604850 (AS2), and AS605091 (AS3)]. These enzymes include the phosphatidylinositol 3-kinases, enzymes that modify host cell lipids through the addition of a phosphate group to the D3 position on the inositol headgroup. The contribution of these enzymes to the vaccinia virus lifecycle is explored in further detail in Chapter III.

LITERATURE CITED

1. **Andrade, A. A., P. N. Silva, A. C. Pereira, L. P. De Sousa, P. C. Ferreira, R. T. Gazzinelli, E. G. Kroon, C. Ropert, and C. A. Bonjardim.** 2004. The vaccinia virus-stimulated mitogen-activated protein kinase (MAPK) pathway is required for virus multiplication. *Biochem J* **381**:437-46.
2. **Armstrong, J. A., D. H. Metz, and M. R. Young.** 1973. The mode of entry of vaccinia virus into L cells. *J Gen Virol* **21**:533-7.
3. **Blasco, R., and B. Moss.** 1991. Extracellular vaccinia virus formation and cell-to-cell virus transmission are prevented by deletion of the gene encoding the 37,000-Dalton outer envelope protein. *J Virol* **65**:5910-20.
4. **Blasco, R., J. R. Sisler, and B. Moss.** 1993. Dissociation of progeny vaccinia virus from the cell membrane is regulated by a viral envelope glycoprotein: effect of a point mutation in the lectin homology domain of the A34R gene. *J Virol* **67**:3319-25.
5. **Carter, G. C., M. Law, M. Hollinshead, and G. L. Smith.** 2005. Entry of the vaccinia virus intracellular mature virion and its interactions with glycosaminoglycans. *J Gen Virol* **86**:1279-90.
6. **Chang, A., and D. H. Metz.** 1976. Further investigations on the mode of entry of vaccinia virus into cells. *J Gen Virol* **32**:275-82.
7. **Dales, S.** 1963. The uptake and development of vaccinia virus in strain L cells followed with labeled viral deoxyribonucleic acid. *J Cell Biol* **18**:51-72.
8. **Fenner, F., D. A. Henderson, I. Arita, Z. Jezek, and I. D. Ladnyi.** 1988. *Smallpox and Its Eradication*. World Health Organization, Geneva Switzerland.
9. **Fernandez, A., A. Sanguino, Z. Peng, A. Crespo, E. Ozturk, X. Zhang, S. Wang, W. Bornmann, and G. Lopez-Berestein.** 2007. Rational drug redesign to overcome drug resistance in cancer therapy: imatinib moving target. *Cancer Res* **67**:4028-33.
10. **Frischknecht, F., V. Moreau, S. Rottger, S. Gonfloni, I. Reckmann, G. Superti-Furga, and M. Way.** 1999. Actin-based motility of vaccinia virus mimics receptor tyrosine kinase signalling. *Nature* **401**:926-9.
11. **Herrera, E., M. M. Lorenzo, R. Blasco, and S. N. Isaacs.** 1998. Functional analysis of vaccinia virus B5R protein: essential role in virus envelopment is independent of a large portion of the extracellular domain. *J Virol* **72**:294-302.
12. **Hiller, G., H. Eibl, and K. Weber.** 1981. Characterization of intracellular and extracellular vaccinia virus variants: N1-isonicotinoyl-N2-3-methyl-4-chlorobenzoylhydrazine interferes with cytoplasmic virus dissemination and release. *J Virol* **39**:903-13.
13. **Husain, M., A. S. Weisberg, and B. Moss.** 2007. Resistance of a vaccinia virus A34R deletion mutant to spontaneous rupture of the outer membrane of progeny virions on the surface of infected cells. *Virology* **366**:424-32.
14. **Jahrling, P. B., E. A. Fritz, and L. E. Hensley.** 2005. Countermeasures to the bioterrorist threat of smallpox. *Curr Mol Med* **5**:817-26.

15. **Jesus, D. M., L. T. Costa, D. L. Goncalves, C. A. Achete, M. Attias, N. Moussatche, and C. R. Damaso.** 2009. Cidofovir inhibits genome encapsidation and affects morphogenesis during the replication of vaccinia virus. *J Virol* **83**:11477-90.
16. **Kazory, A., S. Singapuri, A. Wadhwa, and A. A. Ejaz.** 2007. Simultaneous development of Fanconi syndrome and acute renal failure associated with cidofovir. *J Antimicrob Chemother* **60**:193-4.
17. **Khodakevich, L., Z. Jezek, and D. Messinger.** 1988. Monkeypox virus: ecology and public health significance. *Bull World Health Organ* **66**:747-52.
18. **Khodakevich, L., M. Szczeniowski, D. Manbu ma, Z. Jezek, S. Marennikova, J. Nakano, and D. Messinger.** 1987. The role of squirrels in sustaining monkeypox virus transmission. *Trop Geogr Med* **39**:115-22.
19. **Law, M., G. C. Carter, K. L. Roberts, M. Hollinshead, and G. L. Smith.** 2006. Ligand-induced and nonfusogenic dissolution of a viral membrane. *Proc Natl Acad Sci U S A* **103**:5989-94.
20. **Mercer, J., and A. Helenius.** 2008. Vaccinia virus uses macropinocytosis and apoptotic mimicry to enter host cells. *Science* **320**:531-5.
21. **Ploubidou, A., V. Moreau, K. Ashman, I. Reckmann, C. Gonzalez, and M. Way.** 2000. Vaccinia virus infection disrupts microtubule organization and centrosome function. *Embo J* **19**:3932-44.
22. **Punjabi, A., and P. Traktman.** 2005. Cell biological and functional characterization of the vaccinia virus F10 kinase: implications for the mechanism of virion morphogenesis. *J Virol* **79**:2171-90.
23. **Reed, K. D., J. W. Melski, M. B. Graham, R. L. Regnery, M. J. Sotir, M. V. Wegner, J. J. Kazmierczak, E. J. Stratman, Y. Li, J. A. Fairley, G. R. Swain, V. A. Olson, E. K. Sargent, S. C. Kehl, M. A. Frace, R. Kline, S. L. Foldy, J. P. Davis, and I. K. Damon.** 2004. The detection of monkeypox in humans in the Western Hemisphere. *N Engl J Med* **350**:342-50.
24. **Reeves, P. M., B. Bommarius, S. Lebeis, S. McNulty, J. Christensen, A. Swimm, A. Chahroudi, R. Chavan, M. B. Feinberg, D. Veach, W. Bornmann, M. Sherman, and D. Kalman.** 2005. Disabling poxvirus pathogenesis by inhibition of Abl-family tyrosine kinases. *Nat Med* **11**:731-9.
25. **Reeves, P. M., S. K. Smith, V. A. Olson, S. H. Thorne, W. Bornmann, I. K. Damon, and D. Kalman.** 2011. Variola and monkeypox utilize conserved mechanisms of virion motility and release that depend on Abl- and Src-family tyrosine kinases. *Journal of Virology* **85**.
26. **Rempel, R. E., and P. Traktman.** 1992. Vaccinia virus B1 kinase: phenotypic analysis of temperature-sensitive mutants and enzymatic characterization of recombinant proteins. *J Virol* **66**:4413-26.
27. **Rimoin, A. W., N. Kisalu, B. Kebela-Ilunga, T. Mukaba, L. L. Wright, P. Formenty, N. D. Wolfe, R. L. Shongo, F. Tshioko, E. Okitolonda, J. J. Muyembe, R. W. Ryder, and H. Meyer.** 2007. Endemic human monkeypox, Democratic Republic of Congo, 2001-2004. *Emerg Infect Dis* **13**:934-7.
28. **Rimoin, A. W., P. M. Mulembakani, S. C. Johnston, J. O. Smith, N. K. Kisalu, T. L. Kinkela, S. Blumberg, H. A. Thomassen, B. L. Pike, J. N. Fair, N. D. Wolfe, R. L. Shongo, B. S. Graham, P. Formenty, E. Okitolonda, L. E.**

- Hensley, H. Meyer, L. L. Wright, and J. J. Muyembe.** 2010. Major increase in human monkeypox incidence 30 years after smallpox vaccination campaigns cease in the Democratic Republic of Congo. *Proc Natl Acad Sci U S A*.
29. **Sanderson, C. M., M. Hollinshead, and G. L. Smith.** 2000. The vaccinia virus A27L protein is needed for the microtubule-dependent transport of intracellular mature virus particles. *J Gen Virol* **81**:47-58.
30. **Satheshkumar, P. S., and B. Moss.** 2009. Characterization of a newly identified 35-amino-acid component of the vaccinia virus entry/fusion complex conserved in all chordopoxviruses. *J Virol* **83**:12822-32.
31. **Schmelz, M., B. Sodeik, M. Ericsson, E. J. Wolffe, H. Shida, G. Hiller, and G. Griffiths.** 1994. Assembly of vaccinia virus: the second wrapping cisterna is derived from the trans Golgi network. *J Virol* **68**:130-47.
32. **Smith, G. L., A. Vanderplassen, and M. Law.** 2002. The formation and function of extracellular enveloped vaccinia virus. *J Gen Virol* **83**:2915-31.
33. **Stabenow, J., R. M. Buller, J. Schriewer, C. West, J. E. Sagartz, and S. Parker.** A mouse model of lethal infection for evaluating prophylactics and therapeutics against Monkeypox virus. *J Virol* **84**:3909-20.
34. **Suwa, A., T. Yamamoto, A. Sawada, K. Minoura, N. Hosogai, A. Tahara, T. Kurama, T. Shimokawa, and I. Aramori.** 2009. Discovery and functional characterization of a novel small molecule inhibitor of the intracellular phosphatase, SHIP2. *Br J Pharmacol* **158**:879-87.
35. **Tooze, J., M. Hollinshead, B. Reis, K. Radsak, and H. Kern.** 1993. Progeny vaccinia and human cytomegalovirus particles utilize early endosomal cisternae for their envelopes. *Eur J Cell Biol* **60**:163-78.
36. **Ward, B. M.** 2005. Visualization and characterization of the intracellular movement of vaccinia virus intracellular mature virions. *J Virol* **79**:4755-63.
37. **Wehrle, P. F., J. Posch, K. H. Richter, and D. A. Henderson.** 1970. An airborne outbreak of smallpox in a German hospital and its significance with respect to other recent outbreaks in Europe. *Bull World Health Organ* **43**:669-79.
38. **Wolff, N. C., D. R. Veach, W. P. Tong, W. G. Bornmann, B. Clarkson, and R. L. Ilaria, Jr.** 2005. PD166326, a novel tyrosine kinase inhibitor, has greater antileukemic activity than imatinib mesylate in a murine model of chronic myeloid leukemia. *Blood* **105**:3995-4003.
39. **Yang, G., D. C. Pevear, M. H. Davies, M. S. Collett, T. Bailey, S. Rippen, L. Barone, C. Burns, G. Rhodes, S. Tohan, J. W. Huggins, R. O. Baker, R. L. Buller, E. Touchette, K. Waller, J. Schriewer, J. Neyts, E. DeClercq, K. Jones, D. Hruby, and R. Jordan.** 2005. An orally bioavailable antipoxvirus compound (ST-246) inhibits extracellular virus formation and protects mice from lethal orthopoxvirus Challenge. *J Virol* **79**:13139-49.

FIGURE LEGENDS

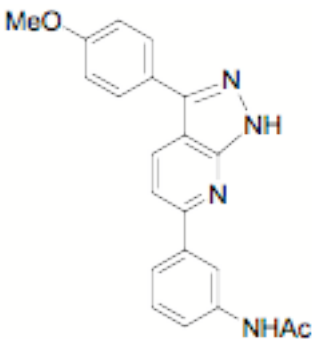
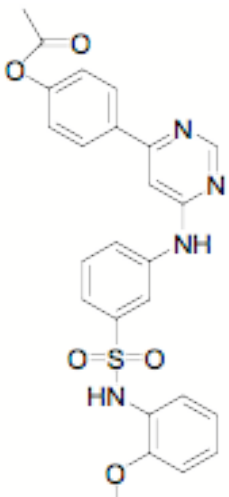
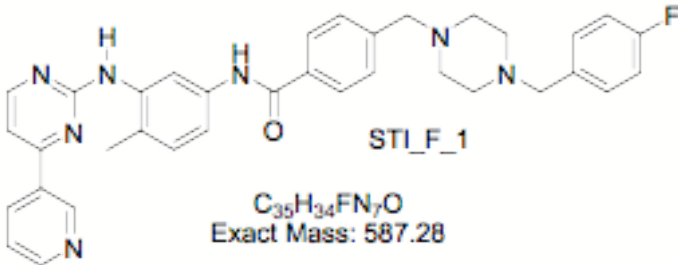
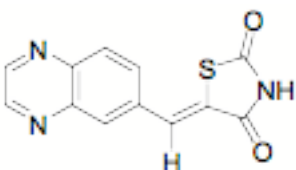
Figure 1: Compounds that modified plaque size relative to untreated controls.

Compounds were added to monolayers 1 hour post viral adsorption. Cells were stained with crystal violet after a 48 hour infection. **A)** No treatment controls. **B)** Compounds that reduced plaque size, but still formed comets. **C)** Compounds that reduced plaque size and eliminated comets. **D)** Compounds that produced more plaques than untreated cells.

Figure 2: Compounds that modified actin morphology relative to untreated controls.

Cells were infected with vaccinia virus and compounds were added 1 hour post viral adsorption. Cells were fixed and stained for microscopy 16 hours post infection. **A)** No treatment control. **B)** Eph_wbz_203 had no effect on actin tail formation. **C)** STI-F eliminated actin tails. **D)** Apck19 eliminated actin tails. **E)** Apck20 modified overall actin morphology.

Table 1: Compound Classes and Structures

Compound Name	Structure
Apck101	
Eph_2wbz 105	
STI-F	 <p style="text-align: center;">STI_F_1 C₃₅H₃₄FN₇O Exact Mass: 587.28</p>
AS605240 (AS1)	

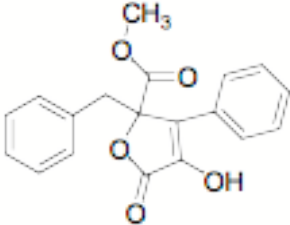
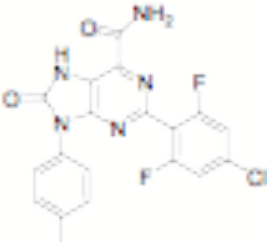
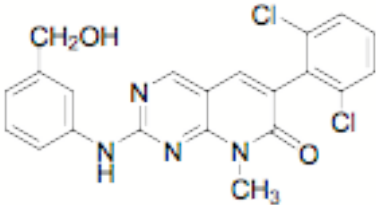
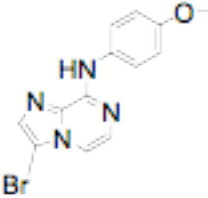
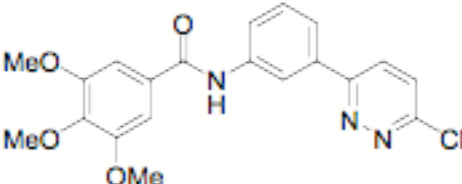
Butyrolactones-1	 <p>Chemical structure of Butyrolactones-1, a substituted butyrolactone. It features a five-membered lactone ring with a methyl group (CH₃) on the carbonyl oxygen, a hydroxyl group (OH) on the ring, and two phenyl rings attached to the ring carbons.</p>
dm-I-187	 <p>Chemical structure of dm-I-187, a complex heterocyclic molecule. It features a central pyrimidopyrimidinone core with various substituents, including an amide group (NH₂), a chlorine atom (Cl), and a fluorine atom (F).</p>
PD166326	 <p>Chemical structure of PD166326, a complex heterocyclic molecule. It features a central pyrimidopyrimidinone core with various substituents, including a hydroxymethyl group (CH₂OH), a chlorine atom (Cl), and a methyl group (CH₃).</p>
LG2-9	 <p>Chemical structure of LG2-9, a complex heterocyclic molecule. It features a central pyrimidopyrimidinone core with various substituents, including a bromine atom (Br) and a methoxy group (O).</p>
YYB20	 <p>Chemical structure of YYB20, a complex heterocyclic molecule. It features a central pyrimidopyrimidinone core with various substituents, including three methoxy groups (MeO) and a chlorine atom (Cl).</p>

Table 2: Compounds that Reduced Plaque Size

APCK48	AS605091 (AS3)
APCK44	AS605240 (AS1)
APCK40	LG2-9
Apck109	LG2-13
Apck108	LG2-55
Apck107	LG2-62
Apck106	LG2-71
Apck102	LG2-79
Eph_2wbz 105	LG2-85
Eph-2wbz 107	LG2-95
Eph_2wbz 110	LG2-98
Eph_2wbz 112	LG2-101
Eph_2wbz 203	LG2-111
Eph-2wbz 211	PD-Br
Eph2_wbz 216	YYA104
Eph2_wbz 217	YYA194
Eph_2wbz 105	dm-I-187
Eph-2wbz 107	dm-I-193
YYB32	dm-I-203
YYB41	WBZ4
YYB44	STLL3
YYB19	STI-OH
butyeolactones-1	STLF2
JaK2F	

Table 3: Compounds that Eliminated Plaques

Apck103
Apck105
APCK43
Eph_2wbz 106
Eph_2wbz 104
Eph2_wbz 102
Eph2_wbz 117
Eph2_wbz 103
LG2-91
LG2-102
LG2-96
YYA188
YYA195
StiAF3_Ue
AS604850 (AS2)

Table 4: Compounds that Increased Virion Release

APcK32
Apck34
APcK110
dm-I_180
YYB34
YYB31
JGAP-5
JGAP-11
JGAP-13

Table 5: Compounds that Eliminated Comet Tails

Apck26
Apck27
Apck35
Apck104
Apck111
dm-I-196
Sti-F

Table 6: Compounds that Damaged the Cell Monolayer

LG2-11
Apck101
Eph2_wbz 116
YYA26b
YYA103
YYA105
YYA187
YYA190
PD166326
YYB21
YYB23
dm-I-183
WBZ-6
CGP-2
CGP51148
StiAF3-iAR
AMN-107

Table 7: Compounds that did not change Plaque Size

Apck17	LG2-89
Apck18	dm-I 174
Apck19	dm-I 177
Apck20	dm-I 178
Apck21	dm-I-184
Apck22	dm-I 185
Apck23	dm-I 186
Apck24	dm-I 189
Apck25	dm-I 190
Apck28	dm-I 192
Apck29	dm-I 195
Apck30	dm-I 197
Apck31	dm-I 198
Apck33	dm-I 199
Apck36	dm-I 202
Apck37	YYB20
Apck38	YYB22
Apck39	YYB24
Apck41	YYB25
Apck42	YYB28
Apck45	YYB29
Apck47	YYB30
Apck49	YYB36
Apck50	YYB37
Apck51	YYB38
Apck53	YYB39
Apck54	YYB42
Apck55	YYA181
Apck56	Eph_2wbz 108
Apck58	Eph_2wbz 109
Apck112	Eph_2wbz101
Apck114	Eph_2wbz 111
Apck115	Eph_2wbz 115
Apck116	Eph_2wbz 204
LG2-7	Eph_2wbz 207
LG2-53	Eph_2wbz 208
LG2-60	Eph_2wbz 210
LG2-65	Eph_2wbz 212
LG2-73	Butyrolactones-Bio
LG2-75	Butyrolactones-2
LG2-77	Jazi-1
LG2-81	
LG2-87	

**Table 8: Compounds that
Reduced/Eliminated Actin
Tails**

Apck19
APcK37
APcK38
APCK41
Apck43
APCK49
APCK58
LG2-55
dm-I-203
dm-I-184
YYB19
YYB20
YYB21
YYb22
YYB23
YYB24
YYA181
STI3
StiAF3_Ue
WBZ-4
STI-F
butyeolactones-1
butyrolactones-2
Eph_2wbz 112
JGAP-5

Table 9: Compounds that Shortened Actin Tails

Eph2 wbz 103
APCK55
LG2-9
LG2-65
YYA103
PD-Br
YYB39
YYB40
YYB44
Jazj-1

Table 10: Compounds that Modified Actin Morphology

Eph_2wbz_202
Eph2_wbz_216
Eph2_wbz_217
Apck20
APck26
APck27
APcK29
APcK31
APcK35
APCK39
Apck102
Apck106
Apck107
APcK115
LG2-60
LG2-77
LG2-111
PD166326
YYA187
YYA190
YYA195
JGAP-13

**Table 11: Compounds
Exhibiting Cellular Toxicity by
Microscopy**

Apck23
APck24
APCK40
APCK42
APCK44
APCK47
APCK51
APCK53
APCK54
Apck111
Apck116
Eph_2wbz 104
Eph_2wbz 105
LG2-7
LG2-11
LG2-13
LG2-85
LG2-89
StiAF3-iAR

Table 12: Compounds that did not change Tail Morphology

Eph 2wbz 101	Apck110	LG2-53
Eph 2wbz 102	Apck112	LG2-62
Eph 2wbz 106	Apck114	LG2-73
Eph 2wbz 107	dm I 174	LG2-75
Eph 2wbz 108	dm I 177	LG2-81
Eph 2wbz 109	dm I 178	LG2-87
Eph 2wbz 110	dm I 180	LG2-96
Eph 2wbz 111	dm I 183	LG2-98
Eph 2wbz 115	dm I 185	LG2-101
Eph 2wbz 116	dm I 186	LG2-102
Eph 2wbz 117	dm I 187	YYB26b
Eph 2wbz 203	dm I 189	YYA104
Eph 2wbz 204	dm I 190	YYA105
Eph 2wbz 206	dm I 192	YYA188
Eph 2wbz 207	dm I 193	YYA194
Eph 2wbz 208	dm I 195	CGP51148
Eph 2wbz 210	dm I 196	STI-OH
Eph 2wbz 211	dm I 197	CGP-2
Eph 2wbz 212	dm I 198	STLF2
Apck17	dm I 199	WBZ-6
Apck18	dm I 202	WBZ-4
Apck21	AS605091 (AS3)	AMN107
Apck22	AS604850 (AS2)	JaK2F
Apck25	AS605240 (AS1)	JGAP-11
Apck28	YYB25	
Apck30	YYB28	
Apck32	YYB29	
Apck33	YYB30	
Apck34	YYB31	
Apck36	YYB32	
Apck45	YYB34	
Apck48	YYB36	
Apck50	YYB37	
Apck56	YYB38	
Apck101	YYB41	
Apck103	YYB42	
Apck104	YYB26b	
Apck105	Butyrolactones-Bio	
Apck108		
Apck109		

Table 13: Classification of Compound Mechanisms of Action

	Tails	Plaque Assay	Comet Tails	Primary Mechanism	Alternative Mechanism
Actin Tail Inhibitors	Short/no tails	Small plaques	No comet tails	Src/Abl-family tyrosine kinase inhibitor.	Inhibits virus upstream of EEV production.
Spread Inhibitors	No effect on tails	Small plaques	Reduced comet tails	Inhibits virion entry or release.	Inhibits virus upstream of EEV production.
Release Accelerators	No effect on tails	Large/WT plaques	Large Comet Tails	Inhibits an inhibitor of virion release.	

**Table 14: Putative
Src/Abl Kinase
Inhibitors**

LG2-9
LG2-55
Eph_2wbz112
Eph_2wbz103
Apck103
Apck43
PD-Br
dm-I-203
YYB44
YYB19
WBZ-4
STI-I3
StiAF3_Ue

**Table 15: Putative
Spread Inhibitors**

Eph_2wbz 102
Eph_2wbz 106
Eph_2wbz 107
Eph_2wbz 110
Eph_2wbz 117
Eph_2wbz 202
Eph_2wbz 203
Eph_2wbz 211
Apck48
Apck104
Apck105
Apck108
Apck109
AS605091 (AS3)
AS604850 (AS2)
AS605240 (AS1)
YYB32
YYB41
dm-I-187
dm-I-193
dm-I-196
LG2-62
LG2-71
LG2-79
LG2-95
LG2-98
LG2-91
LG2-101
LG2-102
Butyeolactones-1
YYA-104
YYA188
YYA-194
STI-OH
STLF2
LG1-96
Jak2F

**Table 16: Putative
Release Accelerators**

Apck32
Apck110
dm-l-180
YYB34
JGAP-11
JGAP-13

Figure 1

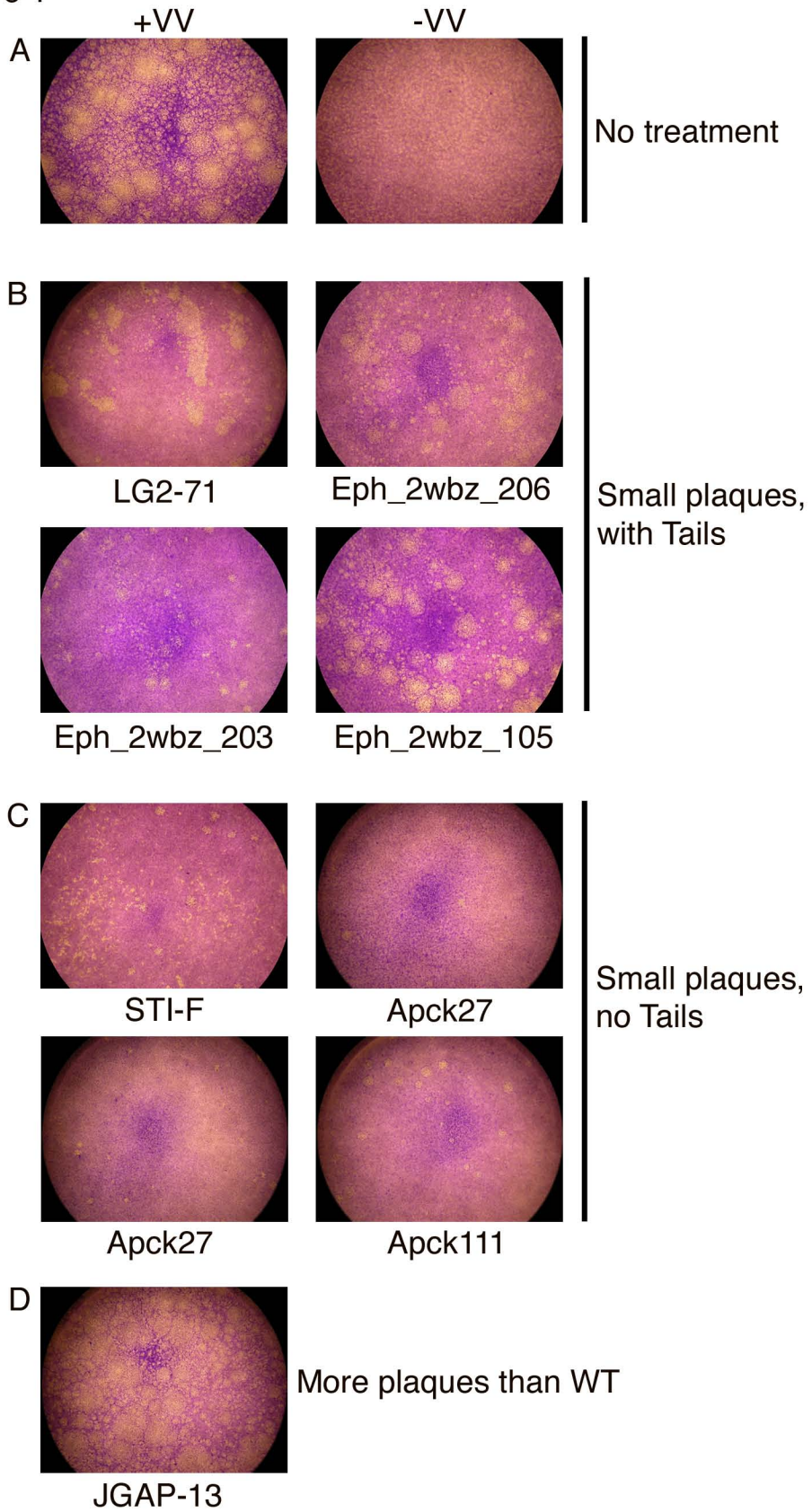
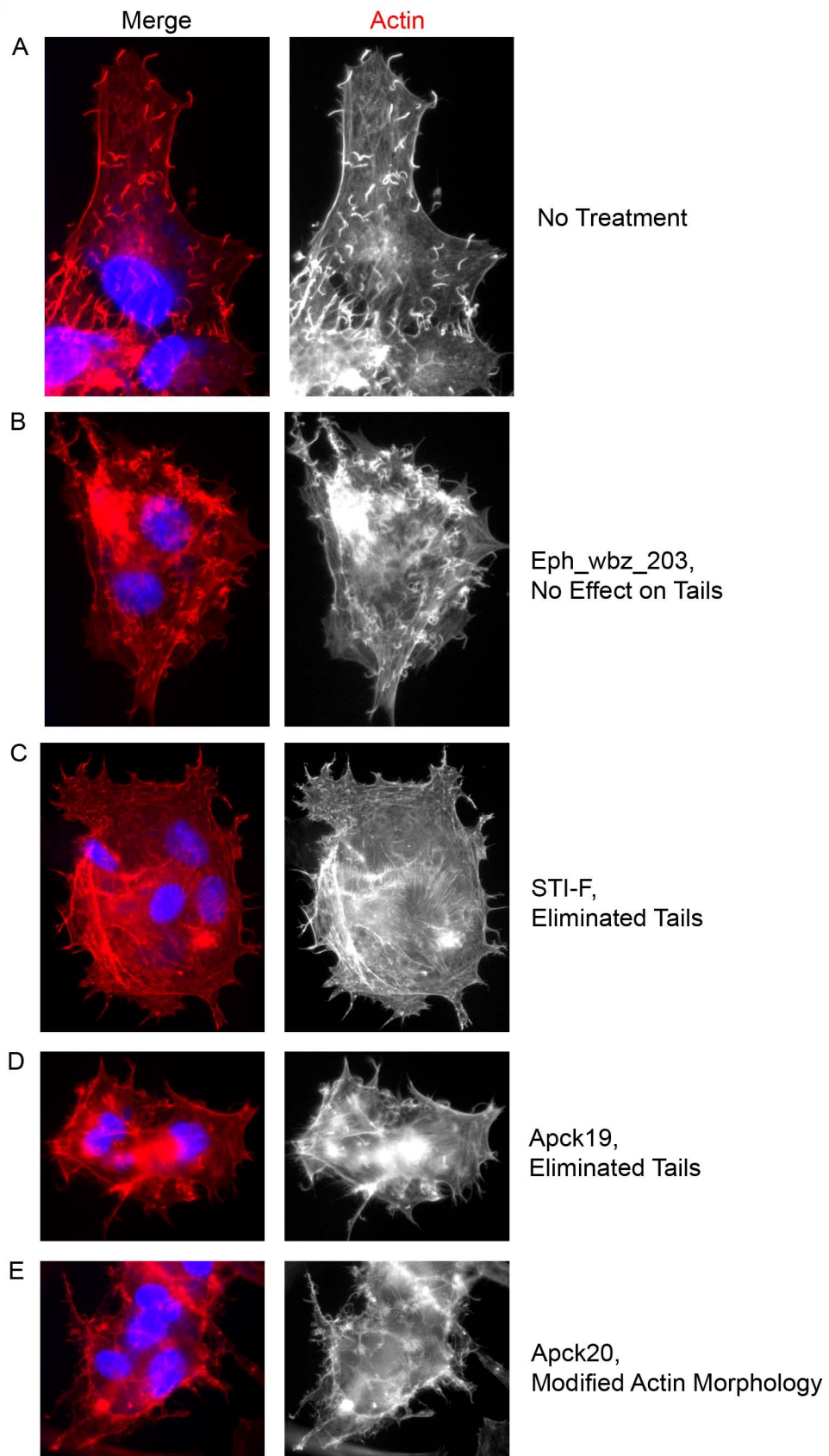


Figure 2



**CHAPTER III: MULTIPLE PHOSPHATIDYLINOSITOL 3-KINASES
REGULATE VACCINIA VIRUS MORPHOGENESIS**

Published as:

McNulty, S., Bornmann, W., Schriewer, J., Werner, C., Smith, S.K., Olson, V.A., Damon, I.K., Buller, R.M., Heuser, J., and Kalman, D. 2010. Multiple phosphatidylinositol 3-kinases regulate vaccinia virus morphogenesis. *PLoS ONE* 5(5): e10884.

Experiments were conceived by Shannon McNulty, Dan Kalman, Inger Damon, and Mark Buller. Experiments with Monkeypox were performed by Victoria Olson and Scott K. Smith. Ectromelia and MTS experiments were performed by Chas Werner and Jill Schriewer. Electron microscopy and supplementary movies were done by John Heuser. All other experiments were done by Shannon McNulty.

ABSTRACT

Poxvirus morphogenesis is a complex process that involves the successive wrapping of the virus in host cell membranes. We screened by plaque assay a focused library of kinase inhibitors for those that caused a reduction in viral growth and identified several compounds that selectively inhibit phosphatidylinositol 3-kinase (PI3K). Previous studies demonstrated that PI3Ks mediate poxviral entry. Using growth curves and electron microscopy in conjunction with inhibitors, we show that that PI3Ks additionally regulate morphogenesis at two distinct steps: immature to mature virion (IMV) transition, and IMV envelopment to form intracellular enveloped virions (IEV). Cells derived from animals lacking the p85 regulatory subunit of Type I PI3Ks ($p85\alpha^{-/-}\beta^{-/-}$) presented phenotypes similar to those observed with PI3K inhibitors. In addition, VV appear to redundantly use PI3Ks, as PI3K inhibitors further reduce plaque size and number in $p85\alpha^{-/-}\beta^{-/-}$ cells. Together, these data provide evidence for a novel regulatory mechanism for virion morphogenesis involving phosphatidylinositol dynamics and may represent a new therapeutic target to contain poxviruses.

INTRODUCTION

Orthopoxviruses, including vaccinia virus (VV), monkeypox (MPX), and variola (VarV), are large dsDNA viruses that cause characteristic umbilicated vesiculo-pustular skin lesions (“pox”). VarV is the causative agent of smallpox, and VV is used for vaccination against smallpox. Although smallpox has been eradicated, naturally occurring poxviruses are still of concern to humans. Molluscum contagiosum is prevalent in children and immunocompromised individuals [1,2], while MPX is endemic in Africa and has the potential for dissemination as evidenced by the 2003 outbreak in the United States [3,4].

Infection is initiated upon entry of either of two forms of the virus. The first, called the Intracellular Mature Virus (“IMV”, and also called Mature Virion “MV”), consists of a brick-shaped viral core surrounded by one or two lipid bilayers derived from an ER-golgi intermediate compartment (ERGIC) [5,6,7,8]. IMV enter the cell either through direct fusion with the plasma membrane or by internalization and fusion with an endocytic compartment [9,10,11,12]. A second infectious form of the virus, called the extracellular enveloped virus (“EEV”, and also called Enveloped Virus “EV”) [13], is released from the cell surface and consists of an IMV enveloped in additional host-cell derived membranes. Entry of EEV requires disruption of the outer viral membrane either at the plasma membrane or in endosomes [14,15,16]. After delivery of the viral core to the cytoplasm, early viral gene transcription and translation initiates replication and morphogenesis.

Morphogenesis is regulated at multiple steps [17], which have been characterized by electron microscopy in conjunction with mutant viruses containing deletions or

temperature-sensitive alleles of viral proteins. Morphogenesis ensues approximately four hours after entry with the appearance of viral crescents [18,19], which consist of semi-spherical membranes containing viral proteins apposed to the viroplasm. The crescent membrane extends to encase viroplasm, forming a spherical immature virion (IV). The transition from IV to IMV depends on several events, including proteolysis of core proteins such as A3 (P4b), A10 (P4a), and L4 (P25K), and formation of disulfide bonds within nascent viral proteins L1 and E10 [20,21,22,23]. IMV formation also depends on the viral kinase F10 [24], core proteins P4a, A10, P4b, A3, P25, and L4 [25], and on redox proteins G4 and E10 [26,27,28,29]. Mutations in these proteins result in slightly different phenotypic defects, including an inability to form complete crescents, misincorporation of the viroplasm with or without crescent resolution, malformed cores, or incomplete virion maturation.

Once formed, a subset of IMVs traffic along microtubules to a juxta-nuclear region where they are enveloped in host-cell membranes derived from endosomes or from the Golgi apparatus to form IEV (Intracellular Enveloped Virions) [30,31,32,33,34]. The mechanisms controlling envelopment are less well understood, but evidence suggests the involvement of F12 and A36, F13, A33, A34, A56 and B5 [13], which physically associate or facilitate localization of other proteins. For example, F13 and A34 have been shown to regulate the cellular trafficking of B5 and its incorporation into the IEV [35,36]. Ultimately, the interaction of these proteins allows the virus to utilize host membranes for envelopment.

While much information is available about the viral proteins that govern entry and maturation, much less is known about the host cell factors that contribute to trafficking

and membrane wrapping processes. In this paper, we provide evidence that maturation of several orthopoxviruses, including VV, MPX and ectromelia, is regulated by host phosphatidylinositol-3 family kinases (PI3K). PI3Ks catalyze addition of a phosphate group to the D3 hydroxyl of the inositol ring of phosphatidylinositol [37,38,39], and regulate many cellular processes including growth factor and hormonal signaling, autophagy, nutrient sensing, and endosomal trafficking [37,40,41,42].

PI3Ks are encoded by multiple genes and are categorized into three classes based on domain structure and substrate preference (reviewed by [38]). Kinases within each class are controlled by regulatory proteins. These proteins are encoded by multiply spliced genes, which can generate additional signaling complexity. Genes encoding PI3Ks are frequently mutated in human cancers, making this class of enzymes an important pharmaceutical target [43,44,45,46].

Many viruses, including VV and Cowpox, activate PI3Ks to inhibit cellular apoptosis [47,48,49]. Here we demonstrate that poxviruses additionally utilize PI3K at several distinct stages of morphogenesis, including early and late gene expression, late protein trafficking and envelopment, and maturation of virions, suggesting a much broader role for this class of host molecules than has been previously recognized.

MATERIALS AND METHODS

Cells, viruses and plaque assays. BSC40 cells (ATCC) were grown in DMEM or RPMI (Cellgro, MediaTech, Inc; Manassas, VA) supplemented with 10%FBS (Atlanta Biologicals; Norcross, GA) and 10 IU/mL Penicillin and 10 μ g/mL streptomycin (P/S; Cellgro, MediaTech, Inc.; Manassas, VA). BHK cells were grown in alpha-MEM

(Gibco; Carlsbad, CA) supplemented with 10%FBS and P/S; p85WT and p85 $\alpha^{-/-}$ cells were grown in DMEM with 10%FBS and P/S, while p85 $\alpha^{-/-}\beta^{-/-}$ cells were grown in DMEM with 15%FBS and P/S. All cells were grown at 37°C in a 5% CO₂ incubator. p85-deficient cells were provided by Lewis Cantley. Mouse embryonic fibroblasts were isolated from embryos that were heterozygous or homozygous for knockout of the PI3K-family related genes PIK3R1 and PIK3R2 [50,51]. Viral strains were grown and propagated as previously described [52]. All strains were titered on BSC40 cells.

PI3K Inhibitors: AS605240 and AS604850 were chemically synthesized as described [53] and are referred to in the text as AS1 and AS2, respectively. The PI3K-alpha Inhibitor 2 #B0304 or 3-(4-Morpholinothieno[3,2-d]pyrimidin-2-yl)phenol, referred to as B0304, was obtained from Echelon Biosciences, and LY294002 was obtained from Sigma-Aldrich (St. Louis, MO).

Plaque assays and calculation of IC₅₀ Values. To calculate IC₅₀ values, PI3K inhibitors were added post-viral adsorption to poxviral-infected monolayers. Experiments with vaccinia virus were conducted at Emory University under BSL-2 conditions. 100PFU of vaccinia virus strain WR was diluted in 500 μ L of 2% FBS/DMEM and added to monolayers of naïve BSC40, p85WT, p85 $\alpha^{-/-}$, or p85 $\alpha^{-/-}\beta^{-/-}$ cells in 12 well dishes. Virus was allowed to adsorb to and enter the cells for one hour at 37°C in 5% CO₂. After 1 hour, virus was removed and monolayers were washed twice with 1mL PBS. Media was then replaced with 10% FBS/DMEM containing PI3K inhibitors at different concentrations. Drugs were resuspended in 100% DMSO, and DMSO controls were performed in conjunction with assays using PI3K inhibitors. Two days after infection, monolayers were fixed and stained with crystal violet solution (0.1% crystal violet and

20% ethanol). The concentration of drug needed to reduce plaque numbers by half (IC_{50}) was calculated by fitting the data to a linear regression model using Prism software (GraphPad Prism Software, Inc., La Jolla, CA). Experiments with ectromelia virus were performed at the Saint Louis University School of Medicine. For these experiments, ECTV-Moscow strain p4 was used to infect BSC-1 cells at 50-75 plaques/well of a 12-well culture plate for one hour in DMEM (Lonza, Basel, Switzerland) supplemented with 2% Fetal Clone II (FCII, Hyclone, Thermo Scientific, Pittsburgh, PA). Serial dilutions of the compounds were made in DMEM-2% FCII and added to the infected cells along with DMEM-5% FCII-1% carboxymethylcellulose (Sigma-Aldrich; St. Louis, MO). The cultures were incubated 4-5 days and stained with crystal violet (0.13% crystal violet, 5% ethanol, 10% formaldehyde) to visualize plaque formation. IC_{50} values were calculated as described. Experiments with monkeypox were performed at the Centers for Disease Control and Prevention (CDC) in Atlanta, GA under BSL2+ conditions. For these experiments, 50PFU/mL of strain V79-1-005 in 2% FBS RPMI (Gibco; Carlsbad, CA) was added to BSC40 cells for one hour at 35.5°C in a 6% CO₂ incubator. After one hour virus was removed and monolayers were washed twice with 2% RPMI media. Media was replaced with 2%RPMI/1%DMSO containing PI3K inhibitors at different concentrations and cells were incubated at 35.5°C in 6% CO₂ for three days. After three days, monolayers were fixed and stained with 2X CV. IC_{50} and IC_{20} values were calculated as described.

Western analysis. BHK or p85 cells were grown in 10cm tissue culture dishes and infected at an MOI of five with vaccinia virus strain Western Reserve (WR). Briefly, virus was incubated in a minimal amount of 2% FBS/DMEM for one hour at 37°C to

allow virus to adsorb and enter monolayers. Monolayers were washed once with PBS and media was replaced with 10%FBS DMEM with or without PI3K inhibitors for an additional sixteen hours. Western analysis of P4b/4b was done in conjunction with infection periods of 6, 16 or 24 hours. Cells were lysed in RIPA buffer (Cell Signaling; Beverly, MA). The amount of protein was quantified using the Bio-Rad Dc Protein Assay Kit (Bio-Rad; Hercules, CA), and 50 μ g was separated by SDS-PAGE. For acid-bypass experiments p85WT and p85-deficient cells were grown in 10cm tissue culture dishes and infected and analyzed by the same protocol as Mercer and Townsley *et al.* [54,55]. Briefly, WR was added to cells at an MOI of 5 in 2mL of pre-cooled Opti-Pro SFM supplemented with P/S and 20mL 200 μ M L-Glutamine (Gibco; Carlsbad, CA) and virus was allowed to bind to cells at 4°C for one hour. Cells were treated with pre-warmed PBS and 1mM MES, pH of 5 for five minutes at 37°C in 5% CO₂. Media was then removed and the monolayers washed once with 5mL pre-warmed 10% FBS/DMEM, and media was replaced with 10% FBS/DMEM. After 2 hours, the infection was stopped by rinsing the cells with PBS and lysing the cells with RIPA Buffer (Cell Signaling; Beverly, MA). Proteins were quantified as above. To generate blots, proteins were then transferred to nitrocellulose, and the membranes were blocked with 3% BSA in Tris-buffered saline containing 0.5% Tween-20 (TBST) for one hour. Membranes were probed with antibodies in the blocking solution for an additional hour. For infections with B5-GFP [56] and F13-GFP VV [57], membranes were probed with GFP antibody (1:1000, Living Colors Full-length A.v. Polyclonal Antibody, Clontech; Mountain View, CA). Anti-L1 (10F5) was a gift from Jay Hooper at USAMRIID and was used at 1:1000 dilution for western blots and 1:50 for microscopy. Anti-P4b/4b was a gift from

Bernard Moss at NIH, and was used at 1:3500. Anti-E3 was a gift from Stuart Isaacs at University of Pennsylvania and was used at 1:1000. Bands were detected using anti-Mouse or anti-Rabbit HRP conjugated antibodies (GE Healthcare; UK) and blots were developed using Pierce ECL Western Blotting Substrate (Thermo Scientific; Waltham, MA). Independent experiments were performed in duplicate to confirm Western blot results. Fold change was calculated from a representative experiment by quantifying band intensity using Adobe Photoshop v10.0.1 and samples were normalized against Tubulin controls. Data is expressed as the fold change relative to untreated samples.

Microscopy. Deconvolution microscopy was carried out as previously described [52]. Spinning disk microscopy was performed at the Heuser lab on a Zeiss Axioplan 2 with Yokagawa CSU 10 confocal scanner unit.

Growth Curves. BHK or p85WT, p85 $\alpha^{-/-}$ or p85 $\alpha^{-/-}$ $\beta^{-/-}$ cells were grown to ~80% confluence in triplicate 12-well tissue culture dishes. Prior to infection cell numbers were quantified, and cells were infected at an MOI of 5, 1, 0.01, 0.001, or 0.0001 in 2%FBS/DMEM for one hour at 37°C with vaccinia virus strain WR. After adsorption, monolayers were washed twice with 1mL PBS and media was replaced with 10%FBS DMEM with or without PI3K inhibitors. AS1 and AS2 were used at 50 μ M, Rifampicin at 0.1mg/mL, and the carrier DMSO was maintained at 0.5%. At each time point, the supernatant was removed and the monolayers were scraped into 0.5mL 2%FBS/DMEM. Cell-associated virus was isolated by freezing and thawing cells three times, and then centrifuging at 500xg for three minutes to remove cell debris. Supernatants containing released virus or cell-associated virus were diluted in 2%FBS/DMEM and then added to naïve (uninfected) BSC40 monolayers.

Comet Assays. BSC40 cells were allowed to form confluent monolayers in 6-well dishes. Media was removed and replaced with 100PFU/well IHD-J vaccinia virus diluted in 500 μ L 2% FBS/DMEM. Virus adsorbed to the cells for one hour at 37°C. After adsorption virus was removed and monolayers were washed twice with 1mL PBS, and media was replaced with 10%FBS DMEM with or without PI3K inhibitors. AS1 and AS2 were added at 50 μ M, while B0304 and LY294002 were added at 20 μ M final concentrations. DMSO was added at a final concentration of 0.5%. Infections were stopped after 48 hours with the addition of crystal violet stain.

MTS Assay. Serial dilutions of PI3K compounds were made in DMEM (Lonza; Basel, Switzerland) supplemented with 2% Fetal Clone II (Hyclone, Thermo Scientific, Pittsburgh, PA). Compound dilutions were mixed with BSC-1 cells at 5000 cells per reaction in 100 μ l total volume. At the specified time point, 20 μ l of MTS [3-(4,5-dimethylthiazol-2-yl)-5-(3-carboxymethoxyphenyl)-2-(4-sulfophenyl)-2H-tetrazolium] solution (CellTiter 96 Aqueous One Solution Cell Proliferation Assay, Promega; Madison, WI) was added to each reaction and incubated 2-4 hours. The absorbance was measured at 490nm and used to determine percent cell viability for each reaction compared to untreated cells. Compound concentration was plotted versus percent cell viability to determine the concentration at which the cell viability was reduced by 50% (CC₅₀).

Trypan Blue Exclusion Assay. BHK cells were grown to ~80% confluency in 12-well tissue culture dishes and treated with 50 μ M AS1 or AS2 or treated with 0.5% DMSO in 10%FBS/DMEM. At each time point, cells were trypsinized with 0.5mL 0.25% Trypsin/EDTA (Cellgro, MediaTech, Inc.; Manassas, VA), and combined with removed

supernatant. Cells were spun down at 1500xg for five minutes. A supernatant volume of 800 μ l was removed and replaced with 0.4% (w/v) Trypan Blue in saline (Cellgro, MediaTech, Inc.; Manassas, VA) and cells were resuspended. Viable (clear) and nonviable (blue) cells were counted on a hemacytometer. Samples were scored from duplicate tissue culture wells.

TUNEL Assay. BHK or p85WT, p85 $\alpha^{-/-}$ or p85 $\alpha^{-/-}\beta^{-/-}$ cells were grown to near confluency on slides prepared for microscopy. Cells were treated with 50 μ M AS1 or AS2, and 20 μ M LY294002 or B0304 in 10%FBS/DMEM for sixteen hours. Apoptosis was detected using the ApoTag Fluorescein *in situ* Apoptosis Detection Kit (Chemicon International, Millipore; Billerica, MA). As a positive control cells were treated with 20U DNase1 (Epicentre; Madison, WI) for 10 minutes at room temperature post-fixation. Each experiment was carried out with duplicate microscope slides. Two images were taken per slide, and ~700 cells were counted per condition.

Electron Microscopy: Electron microscopy was performed by the Heuser lab at Washington University at St. Louis. Briefly, BHK, HeLa or p85WT or p85 $\alpha^{-/-}\beta^{-/-}$ cells were grown on Thermanox dishes (Nunc, Fisher Scientific), and infected with MVA or B5-GFP WR virus as previously described [58,59]. After a 17-hour infection period cells were fixed and processed for microscopy. For glutaraldehyde/KMnO₄ fixation and staining, cultures were fixed for 1 hour at room temperature with 2% glutaraldehyde in NaHCa Buffer (30mM HEPES, pH 7.4 with NaOH, 100mM NaCl, 2mM CaCl, and 10mM MgCl₂), washed 2 times with NaHCa buffer for 5 minutes, washed for 15 minutes with quenching solution (50mM glycine, 50mM lysine, 50mM NH₄Cl in NaHCa Buffer), followed by 5x washes with NaHCa buffer (5 minutes each wash) and 2 washes of 0.1M

NaCl (10 minutes each wash). Samples were stained with 0.5% KMnO₄ in 0.1M NaCl, washed twice with 0.1M NaCl and dehydrated with 25%, 50%, 75%, 95% and 100% ethanol over 20 minutes. Samples were embedded using the Protocol for Fast Embedding. Coverslips were dipped sequentially in: 100% ethanol, 100% ethanol, 100% propylene oxide, 100% propylene oxide, 50/50 (v/v) propylene oxide and epoxy resin, 50/50 (v/v) propylene oxide and epoxy resin, 100% epoxy resin, 100% epoxy resin, inverted over Beem capsules and allow to polymerize at 65°C. For glutaraldehyde/OsO₄ fixation and staining cultures were rinsed in Ringer's solution and fixed for 30-60 minutes at room temperature in 2% glutaraldehyde in NaHCA buffer. Post-fixation cells were rinsed twice in NaHCA buffer and stained with TA (1% tannic acid, 0.075% saponin in NaHCA Buffer) for 15 minutes at room temperature. Cells were then rinsed twice with NaHCA buffer, twice with 0.1M cacodylate buffer, pH 7.4, and postfixed with 0.5% OsO₄ in 0.1M cacodylate buffer, pH 7.4 for 15 minutes at room temperature. After OsO₄ samples were rinsed twice in 0.1M cacodylate buffer pH 7.4 (5 minutes each wash) and twice in 0.1M sodium acetate buffer, pH5.2 (20 minutes each wash). Samples were then stained with 4% uranyl acetate in 50mM sodium acetate buffer for 15 minutes in the dark at room temperature. Samples were then rinsed twice in 0.1M sodium acetate buffer (5 minutes each rinse) and dehydrated as above. Samples were embedded in resin as described above. Samples were prepped for EM as previously described [60].

RESULTS

PI3Ks regulate plaque morphology. To identify host kinases utilized by VV, we screened a small directed library, which included approximately 350 novel and

previously described inhibitors, for those that decreased the size of plaques. Monolayers were treated with compounds at a final concentration of 50-100 μ M. The construction and composition of the library is described elsewhere (S.M, D.K., and W.G.B. in preparation), but consisted of compounds that inhibited tyrosine kinases as well as other kinases. Here we focus on two inhibitors present in the library called AS1 (AS605240) and AS2 (AS604850), which decreased plaque size to pinpoints (Figure 1A).

AS1 and AS2 inhibit the p110-gamma subunit of the type 1 PI3K; but they also inhibit the other PI3K subtypes at higher concentrations (Table 1) [61]. To confirm that inhibition of PI3Ks by AS1 and AS2 could account for the pinpoint plaques, several well-characterized PI3K inhibitors were tested including wortmannin and LY294002, and a p110-alpha specific inhibitor B0304. Addition of LY294002 and B0304 after adsorption of the virus decreased plaque size relative to control-treated monolayers (Figure 1A). Wortmannin did not decrease plaque size up to 48 hours after infection, the longest time tested. However, this drug, in contrast to AS1, AS2 B0304 and LY294002, is a covalent inhibitor that reacts with tissue culture components and was not replenished during the experiment [61,62,63,64,65]. IC₅₀ values for AS1, AS2, B0304, and LY294002 were similar for several orthopoxviral species, including VV, MPX, and ectromelia (Table 1). Lighter crystal violet staining was apparent for MPX-infected monolayers. Therefore, IC₂₀ values for orthopoxviral infected cells are presented in Supplementary Table 1. Notably, fold differences in IC₅₀ and IC₂₀ values were similar for the different orthopoxviruses.

To ensure that PI3K inhibitors were targeting a host and not a viral kinase, we next assessed VV infection in fibroblast cells derived from wild type animals or from

animals with homozygous deletions in p85 α (p85 $\alpha^{-/-}$) or in both p85 α and p85 β (p85 $\alpha^{-/-}\beta^{-/-}$), the regulatory subunits of the Type 1 PI3Ks. Because the stability of the catalytic subunit depends on the regulatory subunit, p85 $\alpha^{-/-}$ and p85 $\alpha^{-/-}\beta^{-/-}$ cells are deficient in type 1 PI3K activity [50,66]. In accordance with results with PI3K inhibitors, the number of plaques appeared two-fold lower in the p85 $\alpha^{-/-}\beta^{-/-}$ cells compared to wild type cells (Figure 1B).

PI3K Regulation of early protein production. The PI3K inhibitor LY294002 can disrupt eIF4 complexes during VV infection, and reduces both late proteins and virion production [67]. We next determined the stage(s) viral morphogenesis is disrupted in cells treated with the PI3K inhibitors AS1 and AS2 (one hour after adsorption), or in p85-deficient cells. No significant difference in E3 levels, a measure of early protein synthesis, was evident in cells treated with AS1 or AS2 compared to untreated cells (Figure 1C). These data suggest that PI3Ks sensitive to AS1 or AS2 are not required for expression of early viral proteins, but exert their effects at later stages of maturation. In contrast, E3 levels were reduced by 62% and 93%, respectively, in the p85 $\alpha^{-/-}$ and p85 $\alpha^{-/-}\beta^{-/-}$ cells relative to the p85WT cells (Figure 1D). To confirm that this difference was a result of reduced protein levels, and not due to a defect in endocytic uptake in p85-deficient cells, we adsorbed virus to cells at 4°C and reduced the pH to catalyze entry [55]. Under these conditions, E3 levels were still reduced by 55% and 85%, respectively, in the p85 $\alpha^{-/-}$ and p85 $\alpha^{-/-}\beta^{-/-}$ cells relative to the p85WT cells (Figure 1E), suggesting that the observed reduction in E3 levels in p85-deficient cells (Figure 1D) resulted from a defect in early protein accumulation and not entry. We cannot rule out the possibility that an early p85-dependent transport or transcription step occurs before the addition of

inhibitors. This may account for the apparent differences in E3 levels between p85-deficient cells and the inhibitors.

PI3Ks mediate late protein production. We next investigated the role of PI3Ks in the production of IEV/EEV proteins using VV strains that express the B5 and F13 as GFP fusions under their own promoters (B5-GFP and F13-GFP). As shown in Figures 2A and 2B, treatment of infected cells post-adsorption with AS1 decreased F13 and B5 accumulation as measured by western analysis with GFP antibody. AS1 also reduced the levels of IMV-specific protein P4b/4b by 43.6% and 30.9% after 6 hours, and by 56% and 61.4% after 16 hours (Figure 2C). Notably, AS1 did not appear to affect the cleavage of the core protein P4b into 4b, a proteolytic step mediated by I7 during viral maturation [68]. In contrast, AS2 did not appear to cause significant decreases in F13, B5 or P4b levels, and did not affect proteolysis of P4b into 4b (Figure 2C). These results demonstrate that AS1 and AS2 appear to inhibit VV maturation through different mechanisms: AS1 inhibits late protein production, whereas AS2 does not.

In accordance with the results with AS1, p85 $\alpha^{-/-}$ and p85 $\alpha^{-/-}$ β $^{-/-}$ cells had reduced levels of F13, B5, and p4b and 4b (Figure 3A, 3B, 3C). In addition, the proteolysis of p4b into 4b does not appear to be significantly inhibited in the p85 $\alpha^{-/-}$ and p85 $\alpha^{-/-}$ β $^{-/-}$ cells (Figure 3C). Notably, the degree of reduction in late proteins appeared correlated with the genetic deficiency of the cell type used; thus, the p85 $\alpha^{-/-}$ β $^{-/-}$ cells express less late protein than the p85 $\alpha^{-/-}$ cells, which express less than control cells. As a control, neither the p85-deficient cells nor the inhibitor-treated cells showed increased TUNEL staining, suggesting that the reduction in late protein levels did not result from increased apoptosis (Supplementary Figures 1A and 1B). Collectively, these data suggest that PI3Ks may

regulate expression of late proteins in several ways: data with p85-deficient cells suggests that prior effects on early protein expression may contribute, whereas data with AS1 suggests that PI3Ks may affect a subsequent step(s). We cannot rule out the possibility that DNA replication may also be regulated by PI3Ks.

PI3Ks regulate localization of L1, F13 and B5. Previous studies demonstrate that F13 and B5 are required for envelopment of IMV [69,70,71,72,73], and that F13 regulates B5 movement from the Golgi to post-Golgi vesicles [35]. Because phosphoinositides are important regulators of endosome trafficking and Golgi structure, we hypothesized that PI3K inhibition or absence could disrupt IMV envelopment and, consequently, localization of B5 and F13. To test this, we assessed whether treatment with PI3K inhibitors altered the subcellular localization of F13, B5, and L1 in cells infected with VV F13-GFP, VV B5-GFP or WR.

AS1 reduced the percentage of infected cells expressing undetectable levels of F13-GFP by ~50% or B5-GFP by ~65% (Figure 4A and 4B). Similar effects were seen with the p110 α specific inhibitor B0304. In contrast, AS2 had no effect on the percentage of F13-GFP and B5-GFP positive cells (Figure 4A and 4B). In addition, AS1 or B0304 altered the subcellular localization of F13-GFP or B5-GFP fluorescence in individual cells (not shown and Figures 4C and 4D). Control cells typically exhibited multiple actin tails and numerous F13-GFP or B5-GFP positive virions in the cell periphery or on the tips of actin tails. AS1 or B0304 caused a reduction in the number of GFP-positive virions at the cell periphery, and a concomitant reduction in the number of actin tails (e.g. Figures 4C and 4D). Quantitation of actin tails from a representative experiment with AS1 on BSC40 cells is presented in Supplementary Figure 2.

Qualitatively, AS1 caused F13-GFP fluorescence to remain in a diffuse perinuclear compartment rather than puncta (Figure 4C), whereas B5-GFP fluorescence remained punctate (Figure 4D). AS2 was less effective than AS1, but also appeared to reduce both the number of F13-GFP and B5-GFP puncta at the cell periphery, and the number of actin tails relative to DMSO-treated cells (Figures 4C, 4D and S2). Compared to control or AS2-treated cells, the amount of the IMV protein L1 produced in AS1-treated cells was below the level of detection (Figure 5A).

We also performed spinning disk microscopy on HeLa cells treated with PI3K inhibitors and infected with B5-GFP to more clearly resolve membrane localization of late proteins. As seen in z-stack videos, B5-GFP fluorescence in untreated HeLa cells localized to both the plasma membrane and to punctate structures on the plasma membrane (Supplementary Movie 1). Treatment with AS1 caused B5-GFP to localize to a perinuclear location, albeit with some fluorescence evident in punctate structures (Supplementary Movie 2). Treatment with AS2 had a similar effect and caused B5 to localize to vacuoles and a small amount on the plasma membrane (Supplementary Movie 3).

Compared to wild type cells, $p85\alpha^{-/-}$ and $p85\alpha^{-/-}\beta^{-/-}$ cells had fewer actin tails (Figure 6A, 6B, 7A, and 7C), and fewer B5-GFP- or F13-GFP fluorescent puncta in the cellular periphery (e.g. Figure 6A and 7A, lower panels). When evident, B5-GFP and F13-GFP fluorescence localized in a perinuclear region (Figures 6A and 7A, S3, Supplementary Movie 4 and 5). However, the percentage of cells expressing detectable B5-GFP fluorescence was markedly reduced in $p85\alpha^{-/-}\beta^{-/-}$ cells (Figure 7B). No significant difference in the amount or localization of the L1 protein was evident (Figure

6B) as measured by cellular fluorescence. Collectively, these observations indicate that PI3Ks mediate the localization of F13 and B5, and levels of L1, though some differences between the inhibitors and the p85-deficient cells were evident.

PI3Ks regulate production of IMV and the amount of released virus. Based on the immunofluorescence microscopy, we hypothesized that PI3Ks may control formation of IMV and the wrapping of IEV/EEV. To assess viral production and released virus, we constructed growth curves at high and low MOI in the presence or absence of PI3K inhibitors. For all of these experiments, inhibitors were added one hour post adsorption to eliminate possible effects of PI3Ks on entry. At an MOI of 0.01 (Figure 8A), AS1 decreased the amount of cell-associated virus (CAV) relative to the DMSO controls by 20.8-fold. These effects appear similar to those observed with rifampicin (0.1mg/mL), which blocks the morphogenesis of IMV and reduced viral loads by 15.4-fold (Figure 8A, see also [74]). In addition to the inhibitory effects on CAV production, AS1 also reduced the amount of virus released from cells by 127.8-fold (Figure 8B). AS2 treatment moderately reduced the production of CAV by 5-Fold (Figure 8A) and the amount of released virus by 28.8-fold (Figure 8B). No significant difference was evident in the amount of cell-associated and released virus produced in the p85WT and p85 $\alpha^{-/-}$ cells at an MOI of 0.01 (Figure 8C and 8D). By contrast, p85 $\alpha^{-/-}\beta^{-/-}$ cells produced 19.3-fold less CAV, and released 20-fold less EEV (Figure 8C and 8D). For both the PI3K inhibitor-treated and p85-deficient cells, similar fold decreases were observed in virion production and release at MOIs ranging from 0.0001 to 5 (Supplementary Figures 4A-D and 5A-D), suggesting that the observed effects reflected a role for PI3Ks in

morphogenesis rather than cell-to-cell spread. Moreover, these data suggest that the block of virion morphogenesis by the PI3K inhibitors is incomplete, and it cannot be overcome simply by adding more virus to cells.

Another measure of released virus is the comet, an archipelago of small plaques that are evident adjacent to the main plaque (arrow in Figure 8E, DMSO) and have been attributed to the release of the EEV [69,75]. Comets are particularly apparent with the poxvirus strain IHD-J [76]. Upon infection of cells with IHD-J and treatment with 50 μ M AS2 or 20 μ M B0304, plaques still form but comets are not evident (Figure 8E and Supplementary Figure 6). By contrast, 50 μ M AS1 and 20 μ M LY294002 reduced the overall plaque size but comets are still visible, albeit smaller than those evident on control cells.

PI3K inhibitors have limited toxicity. We considered the possibility that the drugs may have deleterious effects on cells. Therefore, we conducted toxicity assays during the same time periods that were used for the growth curves. Specifically, we measured the effect of the PI3K inhibitors on cellular respiration using an MTS assay (Figure 8F) and on cell viability using a trypan blue exclusion assay (Figure 8G). The MTS assay was conducted on uninfected BSC-1 cells at different drug concentrations for 8, 12, and 24 hours to calculate the amount of drug needed to reduce formazan production by half (CC_{50}). Although the MTS assay indicated some cellular toxicity at high concentrations, we found that the cells remained impermeable to trypan blue dye (Figure 8G). Thus, although PI3K inhibitors may, at high concentrations disrupt mitochondrial enzymes, they do not appear to disrupt the cellular membrane. A TUNEL assay conducted at 16 hours post drug addition confirmed that the PI3K inhibitor treated cells and p85-deficient

cells did not have significantly increased the rates of apoptosis (Supplementary Figure 1A and 1B). Together, these data indicate that the compounds did not have significant toxic effects at the concentrations used to inhibit viral phenotypes and at exposure times relevant to this study. Moreover, the presence of plaques, albeit small ones, in the presence of drug suggests that inhibition of morphogenesis is not complete at the concentrations tested.

PI3K inhibitors regulate virion morphogenesis at two distinct stages. To test the possibility that PI3K are directly involved in virion morphogenesis, we next visualized viral maturation by electron microscopy (EM) (Figure 9). Ultrastructural analysis of cells infected with the poxviruses MVA (Figure 9A-C) and B5-GFP, strain WR (Figure 9D-F) revealed virions at different stages of morphogenesis, as reported [31,77]. These stages are annotated in Figure 9A and 9D and include 1) crescents; 2) immature virions (IV); 3) intracellular mature virions (IMV); 4) intracellular enveloped virions (IEV); 5) cell-associated enveloped virions (CEV); and 6) extracellular enveloped virions (EEV). Treatment of cells with AS1 for 16 hours post-viral entry resulted in an apparent increase in the number of immature virions compared to untreated cells (Figure 9B and 9E). In addition, we could find few IMV. In contrast, AS2-treated cells had large numbers of IMV and EEV are not evident on the plasma membrane (Figure 9C and 9F). Additional images are presented in Supplementary Information (Supplementary Figure 7A-D).

Similar to the untreated BHK cells, the p85WT cells exhibited virions in multiple stages of maturation (not shown). p85 $\alpha^{-/-}$ $\beta^{-/-}$ cells also had virions in multiple stages of maturation. These stages are annotated in Figure 10C and include 1) Crescents, 2) IV, and 3) IMV. However, in contrast to the p85WT cells, we were unable to find IEV in

sections, and EEV are not evident on the plasma membrane of $p85\alpha^{-/-}\beta^{-/-}$ cells (Figure 10A). Similar to the AS2-treated cells, we also observed large numbers of IMV (Figure 10B). Additional images are presented in Supplementary Information (Supplementary Figures 8A-C). Collectively these data suggest that PI3Ks regulate morphogenesis at two distinct transitions; IV to IMV transition (AS1-sensitive), and IMV envelopment to form IEV (AS2-sensitive, p85-dependent).

PI3K usage by vaccinia virus is functionally redundant. The observation that $p85\alpha^{-/-}\beta^{-/-}$ cells exhibited only a slight reduction in virion production relative to wild-type cells (Figure 1B) suggests that VV may utilize multiple PI3K in a redundant fashion. To test this hypothesis, we assessed plaque formation in wild type and $p85\alpha^{-/-}\beta^{-/-}$ cells in the presence or absence of PI3K inhibitors. In the $p85\alpha^{-/-}$ and $p85\alpha^{-/-}\beta^{-/-}$ cells a significant fraction of type 1 PI3K activity is reduced [50,66], however, the type 1b, type 2 and type 3 PI3Ks are still functional. We reasoned that a lower concentration of inhibitor would be required to block plaque formation in knockout cells compared to wild type cells. As shown in Figure 11A, the IC_{50} values, calculated on the basis of percent reduction in plaque number, were significantly higher for AS1 in p85WT cells (50.3 μ M) compared to $p85\alpha^{-/-}\beta^{-/-}$ cells (11.2 μ M). A similar result was obtained for AS2 (37.1 μ M) in p85WT cells compared to the $p85\alpha^{-/-}\beta^{-/-}$ cells (21.1 μ M). Together these data suggest that several PI-3 kinase isoforms, likely acting in a redundant fashion, regulate VV morphogenesis at multiple steps.

DISCUSSION

Herein we define the involvement of PI3Ks in orthopoxvirus morphogenesis using PI3K inhibitors and cell lines deficient in the regulatory subunit of Type I PI3Ks, p85. The inhibitors AS1 and AS2 were originally developed to inhibit the p110-gamma subunit of the Type Ib PI3K, but they also inhibit the other PI3K subtypes at higher concentrations [61], preventing assignment of a specific PI3K isoform to stages of orthopoxviral morphogenesis. Nevertheless, data with cell lines lacking p85 indicates that the PI3K inhibitors are likely targeting a host kinase and not a viral one. The inhibitors tested decrease plaque size for VV, ectromelia virus and monkeypox virus, implying that PI3K-dependent mechanisms are conserved among poxviruses. We hypothesize that differences in the IC_{50} and IC_{20} values for these viruses may be due to differential PI3K usage by the viruses, a topic that we are currently exploring. A summary of our results using the PI3K inhibitors and p85-deficient cells is presented in Figure 11B.

PI3K contribution to early protein expression. We found that the PI3K inhibitors AS1 and AS2 when added post adsorption did not affect levels of early protein E3 (Figure 1C), whereas E3 levels were decreased in the p85 deficient cells independent of entry (Figure 1D and 1E, Figure 11B #2). Without EM, we cannot rule out the possibility that p85 deficient cells also have an entry defect. However, this seems unlikely because such an effect is not recapitulated in our growth curves (Fig 8C and 8D, Supplementary Figure 5). Thus our data suggest that PI3Ks that depend on p85 regulate levels of early proteins, but not virion entry. The reduction in early protein levels in the p85-deficient cells is in agreement with those obtained by Hu *et al.*, demonstrating that early protein F4 levels are

reduced with VV and Canarypox, following pretreatment with PI3K inhibitor LY294002 and in cells transiently transfected with a p85 dominant negative construct [78]. Work by Soares *et al.* is in partial agreement with this result; they observed a decrease in CrmA/SPI-2 levels following pretreatment with LY294002 and infection with Cowpox, but not VV [48]. Because both Hu *et al.* and Soares *et al.* pretreated cells with LY294002, it is possible that the observed defects in early protein synthesis do not result from effects on early protein synthesis, but rather result from defects in virion entry, a result reported by Mercer *et al.* [54]. By adding our compounds post viral adsorption we avoided such artifacts, and showed that early protein levels are reduced in a p85-dependent, but AS1/AS2-independent manner. However, we cannot rule out the possibility that adding of AS1 or AS2 at one hour following adsorption and entry was too late to affect a p85-dependent PI3K step that regulates early protein expression.

Although Assarsson *et al.* demonstrated that E3 is expressed early during an infection, no data exists describing the location of E3 transcription inside or outside the virion [79]. Because VV carries the entire complement of enzymes required for early gene transcription within the viral core, and early protein translation occurs after core uncoating, we hypothesize that p85-dependent PI3Ks may function in some aspect of core uncoating [80,81,82,83]. Therefore, if viral uncoating is delayed, E3 transcription/translation may be delayed as well. Alternatively, Mallardo *et al.* have demonstrated that the sites of early protein synthesis are distinct from the sites of DNA replication [84]. Therefore, p85-dependent PI3Ks may also function to localize the early protein synthesis machinery.

PI3K contribute to late protein expression. The observed defects in early protein levels in the p85-deficient cells have raised the possibility that delays in late protein synthesis can be ascribed to upstream effects on early proteins. Moreover, we cannot rule out the possibility that DNA replication may be delayed or diminished in these cells. However, P4b was still proteolytically processed, implying that the I7 protease was functional in these cells. We also found that AS1, but not AS2, appeared to reduce late proteins F13, B5, and P4b/4b to a similar extent as in the p85-deficient cells (Figure 11B, #3). Notably, AS1 and p85-deficient cells did not appear to exert a complete block of morphogenesis as P4b was still proteolytically processed and infectious virus was still produced and released in these cells. Nevertheless, inhibitors AS1 and AS2 both reduce plaque size to a similar degree, and our results suggest that they may be doing so by different mechanisms.

Both inhibitors were developed to inhibit the p110-gamma isoform of the PI3Ks and structurally, they have the same chemical backbone, but differ in side group substitutions. Interestingly, Camps *et al.* demonstrate that AS1 and AS2 inhibit the similar classes of PI3K isoforms, albeit with different efficacy [61]. We hypothesize that the differences in drug structure and kinase specificity lead to the observed differences in late protein synthesis. We cannot rule out the possibility that differences between the p85-deficient cells and PI3K-inhibitor treated cells may be attributed to p85-dependent, catalytic subunit-independent signaling, a mechanism that has been described previously [50,85].

Zaborowska and Soares *et al.* also found that pretreatment of VV infected cells with LY294002 reduces late IMV protein production, a result consistent with our AS1 data [48,67]. Zaborowska *et al.* demonstrate that this decrease is due to disrupted eIF4F

complex following PI3K inhibition [67]. Furthermore, Hu *et al.* identified a similar reduction in late protein F4 mRNA levels following LY294002 pretreatment or in cells expressing a p85 dominant negative construct [78]. Our results with PI3K inhibitors and in p85 deficient cells are consistent with, but also expand and qualify these results. We demonstrate that AS1 not only reduces late IMV proteins, but also reduces late IEV/CEV/EEV-specific proteins as well (Figure 2). Furthermore, our data provides a context for the involvement of host PI3K in VV morphogenesis by tying these results to specific p85 isoforms.

PI3K regulate B5 and F13 trafficking. Husain *et al.* demonstrated that F13 regulates B5 movement from the Golgi to post-Golgi vesicles [35]. Specifically, upon expression of F13 with mutations in the palmylation site or with mutations in the phospholipase active site motif, both B5 and F13 remain in the cytoplasm or cis-Golgi (p115-positive) structures [35] and fail to localize to peripheral punctate structures. Roper and Sung further demonstrate that these same mutations in the phospholipase C motif reduce both plaque and IEV/CEV/EEV formation [72,73]. Furthermore, butanol-1 treatment, which inhibits phospholipase D activity, also decreases EEV production and redistributes F13 to the juxtannuclear Golgi region [86]. Moreover, Ward *et al.* also showed that mutations in a dileucine motif of a chimeric B5 protein could prevent plasma membrane retrieval, as measured by antibody uptake and staining, implying a mechanism for B5 retrograde trafficking [87]. Altogether, these results demonstrate that F13 and B5 localization depends on endosomal trafficking, and given the potential phospholipase activity of F13, may also depend on phospholipid turnover.

Consistent with this idea, we found that localization of F13 and B5 was dependent on PI3K activity. AS1 treatment caused F13 to localize to a cytoplasmic compartment, in a manner reminiscent of F13(C186S) palmitylation and F13(D319E) phospholipase D (PLD) active site mutants, which exhibited similar localization [35]. In contrast, AS2 treatment caused B5 and F13 to remain in a perinuclear compartment, although “breakthrough” wrapped virus and actin tails were observed. The phenotype seen in the p85-deficient cells appears to be closer to that seen with AS2 treatment and resembles the F13(C185S) and F13(K314R) mutants, which remain in a cis-Golgi (p115-positive) compartment [35]. The phenotypic similarities of PI3K absence/inhibition with the palmitylation and PLD active site mutants demonstrates that F13 and B5 trafficking is dependent on membrane association and lipid signaling.

PI3K mediate VV morphogenesis. Our data with PI3K inhibitors and p85-deficient cells suggest that morphogenesis is differentially regulated by multiple PI3Ks at different stages. Specifically, differences in virion production for both the PI3K inhibitors and the p85-deficient cells were evident in growth curves, by microscopy, and by electron microscopy, and indicate that PI3Ks regulate production of both IMVs (Figure 11B, #5) and IEV/EEVs (Figure 11B, #7). The AS1 inhibitor morphological block appeared reminiscent of morphological defects seen with the vaccinia redox proteins, A2.5, E10, G4, phosphoprotein A13 and LY294002 pretreatment [20,22,26,28,48]. In contrast, AS2-treated cells had large numbers of IMV (Figure 9C and 9F), reminiscent of morphological defects seen following IMCBH treatment [88,89]. Similar to AS2-treated cells, p85 deficient cells did not wrap IMV to form IEV and viral morphogenesis in these cells appears similar to the AS2-treated cells. Furthermore, we observed similar

morphological defects following PI3K inhibition/absence in both MVA and WR infected cells, suggesting that the involvement of host PI3K is conserved across multiple poxviral species. Overall, the similarity of viral morphological blocks seen in inhibitor treated cells and the p85-deficient cells demonstrates that PI3Ks function to correctly localize envelope-specific viral proteins to nascent envelopes, leading to the formation of the envelope membranes.

VV Uses PI3K in a redundant manner. Several observations suggest that VV uses PI3K redundantly. We define redundancy as the capacity to use PI3K at multiple steps of virion morphogenesis and the ability to use multiple PI3K at each morphological step. In contrast to previous reports with particular PI3K inhibitors (e.g. LY294002 and Wortmannin), our use of several PI3K inhibitors has allowed us to resolve several stages at which PI3K act, including the IV to IMV transition and, the IMV to IEV transition. Furthermore, we observed that the $p85\alpha^{-/-}\beta^{-/-}$ cells had delayed early protein synthesis and were deficient in IMV wrapping. These data suggest that p85-dependent PI3K and PI3K-inhibitor sensitive PI3K are used for multiple steps of virion morphogenesis.

Furthermore, we find that VV can use multiple PI3K at each morphological step, because plaque formation was only reduced by half in the $p85\alpha^{-/-}\beta^{-/-}$ cells compared to the $p85\alpha^{-/-}$ and $p85^{WT}$ cells (Figure 1B). This incomplete phenotype lead us to hypothesize that PI3K activity persisted in the p85-deficient cells because the p85 regulatory subunit is only used by the type 1a PI3K kinases, and the type 1b, type 2 and type 3 phosphatidylinositol 3-kinases are still functional in the $p85\alpha^{-/-}\beta^{-/-}$ cells. We found that addition of the PI3K inhibitors had an additive effect in reducing the number of plaques on the p85 deficient cells and could completely eliminate plaques at higher

concentrations. Together, these observations suggest that VV uses PI3K in a functionally redundant manner; that is, VV uses multiple PI3Ks at each of several steps in morphogenesis. Our use of PI3K inhibitors in conjunction with p85-deficient cells provides a significant advance in our understanding of how PI3Ks are utilized by poxviruses.

PI3K redundancy may help to extend both the host range and cell type specificity for the virus, as PI3K isoforms are differentially expressed through out the body [37]. Such redundancy is not without precedent. Viable mice can be generated from mice missing one splice variant of p85 α , but not from mice missing all p85 α splice variants, implying that the p85 α isoforms are functionally redundant [90]. Moreover, redundancy may also be a common feature of host-pathogen signaling. Swimm *et al.* and Reeves *et al.* demonstrate that EPEC and VV can use host tyrosine kinases redundantly to make actin protrusions [52,91,92]. Redundancy in PI3K signaling has also been reported for Ebola entry into p85-deficient cells [93], and insulin signaling in HepG2 cells [94].

Why would VV use PI3Ks for virion morphogenesis? Other viruses, including VV and cowpox, activate PI3K to inhibit cellular apoptosis [47,48,49]. However, other pathogens, like *Salmonella* and *M. tuberculosis*, disrupt PI3K signaling to inhibit endosome to lysosome fusion, thereby creating a novel pathogen-specific endosome [95,96,97]. PI3K signaling has been shown to act as a signaling molecule, creating phosphatidylinositol 3-phosphate (PI3P) microdomains on membranes [98]. The local PI3P concentration on endosomes can act as a “zipcode” within the host cells; for instance, PI3P is usually localized to multi-vesicular bodies, autophagosomes and early endosomes [99,100]. We demonstrate that VV uses PI3Ks to correctly target and localize

components required for morphogenesis. This may consist of both the protein components (e.g. B5 and F13) as well as lipid components, as the IMV form has been shown to be enriched in phosphoinositides [7,101,102]. PI3K interact with many of the rab proteins [103,104], and rab1 and rab2 are markers for the intermediate compartment [105] and have already been shown to co-localize with VV replication centers [7,106], perhaps suggesting a mechanism for PI3K-dependent acquisition of the IMV envelope acquisition.

PI3K may also regulate IMV wrapping to form IEV. Chen *et al.* provide evidence that F13 can interact with host proteins TIP47 and rab9 to nucleate the IMV wrapping complex [107]. Membranes derived from early endosomes can also envelope IMV particles, as Tooze *et al.* demonstrate that cells treated with Brefeldin A still envelope IMV, and that these IEV are positive for exogenously added HRP [30]. Mechanistically, PI3K inhibitors or deficient cells could disrupt IMV wrapping by interfering with Golgi and/or early endosome trafficking. Since other enveloped viruses need to acquire a lipid membrane, it is possible that PI3Ks and lipid dynamics may be utilized by other wrapped viruses to hijack host cell membranes. Overall, the small molecules that target PI3Ks or other host enzymes that regulate morphogenesis yield new insight into the mechanism of viral envelopment and may represent a new class of antiviral therapeutic drugs, a prospect that we are currently testing.

Acknowledgements

This work was supported by NIH R56A105896101A2 and R01A107246201A2 to DK. We thank Jay Hooper (USAMRIID), Bernard Moss (NIH) and Stuart Isaacs (University of Pennsylvania) for sharing antibodies and Lewis Cantley (Harvard) for sharing the p85-deficient cells. Many thanks to Victor Faundez (Emory University) for insightful comments and discussion. Statistical support was provided by Kirk Easley (Emory University).

Author Contributions

Conceived and designed experiments: SM, JS, CW, SKS, VAO, JH, DK. Performed the experiments: SM, JS, CW, SKS, VAO, JH. Contributed reagents/materials/analysis tools: WB, PR. Analyzed the data: SM, JS, CW, SKS, VAO, IKD, RMR, JH, DK. Wrote the paper: SM, DK.

Funding

This work was supported by NIH R56A105896101A2 and R01A107246201A2 to DK.

LITERATURE CITED

1. **Fenner FH, Donald Ainslie; Arita, Isao; Jezek, Zdenek; Ladnyi, Ivan Danilovich** (1988) Smallpox and its Eradication. Geneva.
2. **Gur I (2008)** The epidemiology of *Molluscum contagiosum* in HIV-seropositive patients: a unique entity or insignificant finding? *Int J STD AIDS* 19: 503-506.
3. **Reed KD, Melski JW, Graham MB, Regnery RL, Sotir MJ, et al.** (2004) The detection of monkeypox in humans in the Western Hemisphere. *N Engl J Med* 350: 342-350.
4. **Rimoin AW, Kisalu N, Kebela-Ilunga B, Mukaba T, Wright LL, et al.** (2007) Endemic human monkeypox, Democratic Republic of Congo, 2001-2004. *Emerg Infect Dis* 13: 934-937.
5. **Rodriguez JR, Risco C, Carrascosa JL, Esteban M, Rodriguez D** (1997) Characterization of early stages in vaccinia virus membrane biogenesis: implications of the 21-kilodalton protein and a newly identified 15-kilodalton envelope protein. *J Virol* 71: 1821-1833.
6. **Hollinshead M, Vanderplasschen A, Smith GL, Vaux DJ** (1999) Vaccinia virus intracellular mature virions contain only one lipid membrane. *J Virol* 73: 1503-1517.
7. **Sodeik B, Doms RW, Ericsson M, Hiller G, Machamer CE, et al.** (1993) Assembly of vaccinia virus: role of the intermediate compartment between the endoplasmic reticulum and the Golgi stacks. *J Cell Biol* 121: 521-541.
8. **Risco C, Rodriguez JR, Lopez-Iglesias C, Carrascosa JL, Esteban M, et al.** (2002) **Endoplasmic reticulum-Golgi intermediate compartment membranes and vimentin filaments participate in vaccinia virus assembly.** *J Virol* 76: 1839-1855.
9. **Armstrong JA, Metz DH, Young MR** (1973) The mode of entry of vaccinia virus into L cells. *J Gen Virol* 21: 533-537.
10. **Carter GC, Law M, Hollinshead M, Smith GL** (2005) Entry of the vaccinia virus intracellular mature virion and its interactions with glycosaminoglycans. *J Gen Virol* 86: 1279-1290.
11. **Chang A, Metz DH** (1976) Further investigations on the mode of entry of vaccinia virus into cells. *J Gen Virol* 32: 275-282.
12. **Dales S** (1963) The uptake and development of vaccinia virus in strain L cells followed with labeled viral deoxyribonucleic acid. *J Cell Biol* 18: 51-72.
13. **Smith GL, Vanderplasschen A, Law M** (2002) The formation and function of extracellular enveloped vaccinia virus. *J Gen Virol* 83: 2915-2931.
14. **Vanderplasschen A, Hollinshead M, Smith GL** (1998) Intracellular and extracellular vaccinia virions enter cells by different mechanisms. *J Gen Virol* 79 (Pt 4): 877-887.
15. **Ichihashi Y** (1996) Extracellular enveloped vaccinia virus escapes neutralization. *Virology* 217: 478-485.
16. **Law M, Carter GC, Roberts KL, Hollinshead M, Smith GL** (2006) Ligand-induced and nonfusogenic dissolution of a viral membrane. *Proc Natl Acad Sci U S A* 103: 5989-5994.

17. **Condit RC, Moussatche N, Traktman P** (2006) In a nutshell: structure and assembly of the vaccinia virion. *Adv Virus Res* 66: 31-124.
18. **Kajioka R, Siminovitch L, Dales S** (1964) The Cycle of Multiplication of Vaccinia Virus in Earle's Strain L Cells. Ii. Initiation of DNA Synthesis and Morphogenesis. *Virology* 24: 295-309.
19. **Dales S, Mosbach EH** (1968) Vaccinia as a model for membrane biogenesis. *Virology* 35: 564-583.
20. **Senkevich TG, Weisberg AS, Moss B** (2000) Vaccinia virus E10R protein is associated with the membranes of intracellular mature virions and has a role in morphogenesis. *Virology* 278: 244-252.
21. **Blouch RE, Byrd CM, Hruby DE** (2005) Importance of disulphide bonds for vaccinia virus L1R protein function. *Virol J* 2: 91.
22. **Unger B, Traktman P** (2004) Vaccinia virus morphogenesis: a13 phosphoprotein is required for assembly of mature virions. *J Virol* 78: 8885-8901.
23. **Betakova T, Wolffe EJ, Moss B** (1999) Regulation of vaccinia virus morphogenesis: phosphorylation of the A14L and A17L membrane proteins and C-terminal truncation of the A17L protein are dependent on the F10L kinase. *J Virol* 73: 3534-3543.
24. **Punjabi A, Traktman P** (2005) Cell biological and functional characterization of the vaccinia virus F10 kinase: implications for the mechanism of virion morphogenesis. *J Virol* 79: 2171-2190.
25. **Byrd CM, Hruby DE** (2006) Vaccinia virus proteolysis--a review. *Rev Med Virol* 16: 187-202.
26. **White CL, Weisberg AS, Moss B** (2000) A glutaredoxin, encoded by the G4L gene of vaccinia virus, is essential for virion morphogenesis. *J Virol* 74: 9175-9183.
27. **Senkevich TG, White CL, Koonin EV, Moss B** (2000) A viral member of the ERV1/ALR protein family participates in a cytoplasmic pathway of disulfide bond formation. *Proc Natl Acad Sci U S A* 97: 12068-12073.
28. **Senkevich TG, White CL, Weisberg A, Granek JA, Wolffe EJ, et al.** (2002) Expression of the vaccinia virus A2.5L redox protein is required for virion morphogenesis. *Virology* 300: 296-303.
29. **Senkevich TG, White CL, Koonin EV, Moss B** (2002) Complete pathway for protein disulfide bond formation encoded by poxviruses. *Proc Natl Acad Sci U S A* 99: 6667-6672.
30. **Tooze J, Hollinshead M, Reis B, Radsak K, Kern H** (1993) Progeny vaccinia and human cytomegalovirus particles utilize early endosomal cisternae for their envelopes. *Eur J Cell Biol* 60: 163-178.
31. **Schmelz M, Sodeik B, Ericsson M, Wolffe EJ, Shida H, et al.** (1994) Assembly of vaccinia virus: the second wrapping cisterna is derived from the trans Golgi network. *J Virol* 68: 130-147.
32. **Ploubidou A, Moreau V, Ashman K, Reckmann I, Gonzalez C, et al.** (2000) Vaccinia virus infection disrupts microtubule organization and centrosome function. *Embo J* 19: 3932-3944.
33. **Ward BM** (2005) Visualization and characterization of the intracellular movement of vaccinia virus intracellular mature virions. *J Virol* 79: 4755-4763.

34. **Sanderson CM, Hollinshead M, Smith GL** (2000) The vaccinia virus A27L protein is needed for the microtubule-dependent transport of intracellular mature virus particles. *J Gen Virol* 81: 47-58.
35. **Husain M, Moss B** (2001) Vaccinia virus F13L protein with a conserved phospholipase catalytic motif induces colocalization of the B5R envelope glycoprotein in post-Golgi vesicles. *J Virol* 75: 7528-7542.
36. **Earley AK, Chan WM, Ward BM** (2008) The vaccinia virus B5 protein requires A34 for efficient intracellular trafficking from the endoplasmic reticulum to the site of wrapping and incorporation into progeny virions. *J Virol* 82: 2161-2169.
37. **Hirsch E, Costa C, Ciruolo E** (2007) Phosphoinositide 3-kinases as a common platform for multi-hormone signaling. *J Endocrinol* 194: 243-256.
38. **Hawkins PT, Anderson KE, Davidson K, Stephens LR** (2006) Signalling through Class I PI3Ks in mammalian cells. *Biochem Soc Trans* 34: 647-662.
39. **Berridge MJ, Irvine RF** (1989) Inositol phosphates and cell signalling. *Nature* 341: 197-205.
40. **Vieira OV, Botelho RJ, Rameh L, Brachmann SM, Matsuo T, et al.** (2001) Distinct roles of class I and class III phosphatidylinositol 3-kinases in phagosome formation and maturation. *J Cell Biol* 155: 19-25.
41. **Backer JM** (2008) The regulation and function of Class III PI3Ks: novel roles for Vps34. *Biochem J* 410: 1-17.
42. **Franke TF** (2008) Intracellular signaling by Akt: bound to be specific. *Sci Signal* 1: pe29.
43. **Knight ZA, Shokat KM** (2007) Chemically targeting the PI3K family. *Biochem Soc Trans* 35: 245-249.
44. **Knight ZA, Gonzalez B, Feldman ME, Zunder ER, Goldenberg DD, et al.** (2006) A pharmacological map of the PI3-K family defines a role for p110alpha in insulin signaling. *Cell* 125: 733-747.
45. **Ruckle T, Schwarz MK, Rommel C** (2006) PI3Kgamma inhibition: towards an 'aspirin of the 21st century'? *Nat Rev Drug Discov* 5: 903-918.
46. **Jiang BH, Liu LZ** (2008) PI3K/PTEN signaling in tumorigenesis and angiogenesis. *Biochim Biophys Acta* 1784: 150-158.
47. **Buchkovich NJ, Yu Y, Zampieri CA, Alwine JC** (2008) The TORrid affairs of viruses: effects of mammalian DNA viruses on the PI3K-Akt-mTOR signalling pathway. *Nat Rev Microbiol* 6: 266-275.
48. **Soares JA, Leite FG, Andrade LG, Torres AA, De Sousa LP, et al.** (2009) Activation of the PI3K/Akt pathway early during vaccinia and cowpox virus infections is required for both host survival and viral replication. *J Virol* 83: 6883-6899.
49. **Cooray S** (2004) The pivotal role of phosphatidylinositol 3-kinase-Akt signal transduction in virus survival. *J Gen Virol* 85: 1065-1076.
50. **Ueki K, Fruman DA, Brachmann SM, Tseng YH, Cantley LC, et al.** (2002) Molecular balance between the regulatory and catalytic subunits of phosphoinositide 3-kinase regulates cell signaling and survival. *Mol Cell Biol* 22: 965-977.

51. **Brachmann SM, Yballe CM, Innocenti M, Deane JA, Fruman DA, et al.** (2005) Role of phosphoinositide 3-kinase regulatory isoforms in development and actin rearrangement. *Mol Cell Biol* 25: 2593-2606.
52. **Reeves PM, Bommarius B, Lebeis S, McNulty S, Christensen J, et al.** (2005) Disabling poxvirus pathogenesis by inhibition of Abl-family tyrosine kinases. *Nat Med* 11: 731-739.
53. **Rueckle TJ, Xuiliang; Gaillard, Pascale; Church, Dennis; Vallotton Tania.** (2005) Azolidinolone-vinyl Fused-Benzene Derivatives. In: WIPO, editor.
54. **Mercer J, Helenius A** (2008) Vaccinia virus uses macropinocytosis and apoptotic mimicry to enter host cells. *Science* 320: 531-535.
55. **Townsley AC, Weisberg AS, Wagenaar TR, Moss B** (2006) Vaccinia virus entry into cells via a low-pH-dependent endosomal pathway. *J Virol* 80: 8899-8908.
56. **Ward BM, Moss B** (2001) Vaccinia virus intracellular movement is associated with microtubules and independent of actin tails. *J Virol* 75: 11651-11663.
57. **Geada MM, Galindo I, Lorenzo MM, Perdiguero B, Blasco R** (2001) Movements of vaccinia virus intracellular enveloped virions with GFP tagged to the F13L envelope protein. *J Gen Virol* 82: 2747-2760.
58. **Szajner P, Weisberg AS, Lebowitz J, Heuser J, Moss B** (2005) External scaffold of spherical immature poxvirus particles is made of protein trimers, forming a honeycomb lattice. *J Cell Biol* 170: 971-981.
59. **Heuser J** (2005) Deep-etch EM reveals that the early poxvirus envelope is a single membrane bilayer stabilized by a geodetic "honeycomb" surface coat. *J Cell Biol* 169: 269-283.
60. **Huang RH, Wang Y, Roth R, Yu X, Purvis AR, et al.** (2008) Assembly of Weibel-Palade body-like tubules from N-terminal domains of von Willebrand factor. *Proc Natl Acad Sci U S A* 105: 482-487.
61. **Camps M, Ruckle T, Ji H, Ardisson V, Rintelen F, et al.** (2005) Blockade of PI3Kgamma suppresses joint inflammation and damage in mouse models of rheumatoid arthritis. *Nat Med* 11: 936-943.
62. **Yuan H, Barnes KR, Weissleder R, Cantley L, Josephson L** (2007) Covalent reactions of wortmannin under physiological conditions. *Chem Biol* 14: 321-328.
63. **Woscholski R, Kodaki T, McKinnon M, Waterfield MD, Parker PJ** (1994) A comparison of demethoxyviridin and wortmannin as inhibitors of phosphatidylinositol 3-kinase. *FEBS Lett* 342: 109-114.
64. **Powis G, Bonjouklian R, Berggren MM, Gallegos A, Abraham R, et al.** (1994) Wortmannin, a potent and selective inhibitor of phosphatidylinositol-3-kinase. *Cancer Res* 54: 2419-2423.
65. **Stein RC, Waterfield MD** (2000) PI3-kinase inhibition: a target for drug development? *Mol Med Today* 6: 347-357.
66. **Yu J, Zhang Y, McIlroy J, Rordorf-Nikolic T, Orr GA, et al.** (1998) Regulation of the p85/p110 phosphatidylinositol 3'-kinase: stabilization and inhibition of the p110alpha catalytic subunit by the p85 regulatory subunit. *Mol Cell Biol* 18: 1379-1387.
67. **Zaborowska I, Walsh D** (2009) PI3K signaling regulates rapamycin-insensitive translation initiation complex formation in Vaccinia Virus-infected cells. *J Virol*.

68. **Ericsson M, Cudmore S, Shuman S, Condit RC, Griffiths G, et al.** (1995) Characterization of ts 16, a temperature-sensitive mutant of vaccinia virus. *J Virol* 69: 7072-7086.
69. **Blasco R, Moss B** (1991) Extracellular vaccinia virus formation and cell-to-cell virus transmission are prevented by deletion of the gene encoding the 37,000-Dalton outer envelope protein. *J Virol* 65: 5910-5920.
70. **Engelstad M, Smith GL** (1993) The vaccinia virus 42-kDa envelope protein is required for the envelopment and egress of extracellular virus and for virus virulence. *Virology* 194: 627-637.
71. **Wolffe EJ, Isaacs SN, Moss B** (1993) Deletion of the vaccinia virus B5R gene encoding a 42-kilodalton membrane glycoprotein inhibits extracellular virus envelope formation and dissemination. *J Virol* 67: 4732-4741.
72. **Sung TC, Roper RL, Zhang Y, Rudge SA, Temel R, et al.** (1997) Mutagenesis of phospholipase D defines a superfamily including a trans-Golgi viral protein required for poxvirus pathogenicity. *EMBO J* 16: 4519-4530.
73. **Roper RL, Moss B** (1999) Envelope formation is blocked by mutation of a sequence related to the HKD phospholipid metabolism motif in the vaccinia virus F13L protein. *J Virol* 73: 1108-1117.
74. **Moss B, Rosenblum EN, Katz E, Grimley PM** (1969) Rifampicin: a specific inhibitor of vaccinia virus assembly. *Nature* 224: 1280-1284.
75. **Herrera E, Lorenzo MM, Blasco R, Isaacs SN** (1998) Functional analysis of vaccinia virus B5R protein: essential role in virus envelopment is independent of a large portion of the extracellular domain. *J Virol* 72: 294-302.
76. **Blasco R, Sisler JR, Moss B** (1993) Dissociation of progeny vaccinia virus from the cell membrane is regulated by a viral envelope glycoprotein: effect of a point mutation in the lectin homology domain of the A34R gene. *J Virol* 67: 3319-3325.
77. **Dales S** (1965) Replication of Animal Viruses as Studied by Electron Microscopy. *Am J Med* 38: 699-715.
78. **Hu N, Yu R, Shikuma C, Shiramizu B, Ostrowski MA, et al.** (2009) Role of cell signaling in poxvirus-mediated foreign gene expression in mammalian cells. *Vaccine* 27: 2994-3006.
79. **Assarsson E, Greenbaum JA, Sundstrom M, Schaffer L, Hammond JA, et al.** (2008) Kinetic analysis of a complete poxvirus transcriptome reveals an immediate-early class of genes. *Proc Natl Acad Sci U S A* 105: 2140-2145.
80. **Condit RC, Niles EG** (2002) Regulation of viral transcription elongation and termination during vaccinia virus infection. *Biochim Biophys Acta* 1577: 325-336.
81. **Pedersen K, Snijder EJ, Schleich S, Roos N, Griffiths G, et al.** (2000) Characterization of vaccinia virus intracellular cores: implications for viral uncoating and core structure. *J Virol* 74: 3525-3536.
82. **Holowczak JA** (1972) Uncoating of poxviruses. I. Detection and characterization of subviral particles in the uncoating process. *Virology* 50: 216-232.
83. **Joklik WK** (1964) The Intracellular Uncoating of Poxvirus DNA. Ii. The Molecular Basis of the Uncoating Process. *J Mol Biol* 8: 277-288.

- 84. Mallardo M, Leithe E, Schleich S, Roos N, Doglio L, et al.** (2002) Relationship between vaccinia virus intracellular cores, early mRNAs, and DNA replication sites. *J Virol* 76: 5167-5183.
- 85. Mauvais-Jarvis F, Ueki K, Fruman DA, Hirshman MF, Sakamoto K, et al.** (2002) Reduced expression of the murine p85 α subunit of phosphoinositide 3-kinase improves insulin signaling and ameliorates diabetes. *J Clin Invest* 109: 141-149.
- 86. Husain M, Moss B** (2002) Similarities in the induction of post-Golgi vesicles by the vaccinia virus F13L protein and phospholipase D. *J Virol* 76: 7777-7789.
- 87. Ward BM, Moss B** (2000) Golgi network targeting and plasma membrane internalization signals in vaccinia virus B5R envelope protein. *J Virol* 74: 3771-3780.
- 88. Hiller G, Eibl H, Weber K** (1981) Characterization of intracellular and extracellular vaccinia virus variants: N1-isonicotinoyl-N2-3-methyl-4-chlorobenzoylhydrazine interferes with cytoplasmic virus dissemination and release. *J Virol* 39: 903-913.
- 89. Payne LG, Kristenson K** (1979) Mechanism of vaccinia virus release and its specific inhibition by N1-isonicotinoyl-N2-3-methyl-4-chlorobenzoylhydrazine. *J Virol* 32: 614-622.
- 90. Vanhaesebroeck B, Ali K, Bilancio A, Geering B, Foukas LC** (2005) Signalling by PI3K isoforms: insights from gene-targeted mice. *Trends Biochem Sci* 30: 194-204.
- 91. Swimm A, Bommarius B, Li Y, Cheng D, Reeves P, et al.** (2004) Enteropathogenic *Escherichia coli* use redundant tyrosine kinases to form actin pedestals. *Mol Biol Cell* 15: 3520-3529.
- 92. Bommarius B, Maxwell D, Swimm A, Leung S, Corbett A, et al.** (2007) Enteropathogenic *Escherichia coli* Tir is an SH2/3 ligand that recruits and activates tyrosine kinases required for pedestal formation. *Mol Microbiol* 63: 1748-1768.
- 93. Saeed MF, Kolokoltsov AA, Freiberg AN, Holbrook MR, Davey RA** (2008) Phosphoinositide-3 kinase-Akt pathway controls cellular entry of Ebola virus. *PLoS Pathog* 4: e1000141.
- 94. Chaussade C, Rewcastle GW, Kendall JD, Denny WA, Cho K, et al.** (2007) Evidence for functional redundancy of class IA PI3K isoforms in insulin signalling. *Biochem J* 404: 449-458.
- 95. Scott CC, Cuellar-Mata P, Matsuo T, Davidson HW, Grinstein S** (2002) Role of 3-phosphoinositides in the maturation of *Salmonella*-containing vacuoles within host cells. *J Biol Chem* 277: 12770-12776.
- 96. Mallo GV, Espina M, Smith AC, Terebiznik MR, Aleman A, et al.** (2008) SopB promotes phosphatidylinositol 3-phosphate formation on *Salmonella* vacuoles by recruiting Rab5 and Vps34. *J Cell Biol* 182: 741-752.
- 97. Fratti RA, Backer JM, Gruenberg J, Corvera S, Deretic V** (2001) Role of phosphatidylinositol 3-kinase and Rab5 effectors in phagosomal biogenesis and mycobacterial phagosome maturation arrest. *J Cell Biol* 154: 631-644.
- 98. Weiner OD, Neilsen PO, Prestwich GD, Kirschner MW, Cantley LC, et al.** (2002) A PtdInsP(3)- and Rho GTPase-mediated positive feedback loop regulates neutrophil polarity. *Nat Cell Biol* 4: 509-513.

99. **Lindmo K, Stenmark H** (2006) Regulation of membrane traffic by phosphoinositide 3-kinases. *J Cell Sci* 119: 605-614.
100. **Stenmark H, Gillooly DJ** (2001) Intracellular trafficking and turnover of phosphatidylinositol 3-phosphate. *Semin Cell Dev Biol* 12: 193-199.
101. **Cluett EB, Kuismanen E, Machamer CE** (1997) Heterogeneous distribution of the unusual phospholipid semilysoisophosphatidic acid through the Golgi complex. *Mol Biol Cell* 8: 2233-2240.
102. **Cluett EB, Machamer CE** (1996) The envelope of vaccinia virus reveals an unusual phospholipid in Golgi complex membranes. *J Cell Sci* 109 (Pt 8): 2121-2131.
103. **Chamberlain MD, Berry TR, Pastor MC, Anderson DH** (2004) The p85alpha subunit of phosphatidylinositol 3'-kinase binds to and stimulates the GTPase activity of Rab proteins. *J Biol Chem* 279: 48607-48614.
104. **Shin HW, Hayashi M, Christoforidis S, Lacas-Gervais S, Hoepfner S, et al.** (2005) An enzymatic cascade of Rab5 effectors regulates phosphoinositide turnover in the endocytic pathway. *J Cell Biol* 170: 607-618.
105. **Martinez O, Goud B** (1998) Rab proteins. *Biochim Biophys Acta* 1404: 101-112.
106. **Krijnse-Locker J, Schleich S, Rodriguez D, Goud B, Snijder EJ, et al.** (1996) The role of a 21-kDa viral membrane protein in the assembly of vaccinia virus from the intermediate compartment. *J Biol Chem* 271: 14950-14958.
107. **Chen Y, Honeychurch KM, Yang G, Byrd CM, Harver C, et al.** (2009) Vaccinia virus p37 interacts with host proteins associated with LE-derived transport vesicle biogenesis. *Virology* 6: 44.
108. **Hayakawa M, Kaizawa H, Moritomo H, Koizumi T, Ohishi T, et al.** (2006) Synthesis and biological evaluation of 4-morpholino-2-phenylquinazolines and related derivatives as novel PI3 kinase p110alpha inhibitors. *Bioorg Med Chem* 14: 6847-6858.

FIGURE LEGENDS

Table 1. 50% Inhibitory Concentration (IC₅₀) of PI3K inhibitors added post-adsorption to poxvirus-infected monolayers. ¹[61] ²[108] ³[65]

Figure 1. A. PI3K inhibitors reduce plaque size in BSC40 cells. Cells were infected with 100 PFU of vaccinia virus (VV), strain WR. Inhibitors were added one hour post viral entry. First row: LY294002, 20μM; B0304, 20μM; AS1, 50μM; AS2, 50μM (LY294002 and B0304 are in 0.2% DMSO and AS1 and AS2 are in 0.5% DMSO); 0.5% DMSO alone. Insets show representative plaques from 50μM AS1 and 0.5% DMSO treated wells. Second row: 10μM Wortmannin in 0.1% DMSO did not appear to reduce VV plaque size; 0.1% DMSO control. Results are from three independent trials. **B.** p85WT and p85α^{-/-} cells form two times more plaques than p85α^{-/-}β^{-/-} cells. Cells were infected with equal amounts of virus and monolayers were stained with crystal violet 48 hours post infection. Results are from eight independent trials. **C.** PI3K inhibitors do not decrease early viral protein expression. BSC40 cells were infected at pH 7.4 and MOI=5 with VV and PI3K inhibitors were added 1 hour post-viral entry and allowed to infect for an additional 2 hours. Proteins were subjected to western analysis by anti-E3 mAb and anti-Tubulin mAb. For quantification (right) bands were normalized to tubulin loading control and data is expressed as the fold change relative to DMSO-treated samples. **D.** Early protein expression is reduced in p85-deficient cells. Cells were infected at an MOI=5 with VV at pH=7.4 and analyzed as in C. **E.** Early protein expression is reduced in p85-deficient cells. Cells were infected at an MOI=5 with VV. Virus was bound to cells at 4°C, after which cells were moved to 37°C with PBS, pH=5. Following a 2 hour

infection, equal amounts of protein were subjected to western analysis with anti-E3 mAb or anti-Tubulin, and quantitated as in C.

Figure 2. PI3K inhibitors reduce late viral protein expression. BHK cells were infected with VV at an MOI of 5, and PI3K inhibitors were added following entry. After 16 hours proteins were subjected to western analysis with various antibodies, including anti-Tubulin to ensure equal loading. Quantitation (right) is described in Methods. Data are expressed as the fold change relative to DMSO-treated samples. **A.** Cells were infected with VV strain WR expressing B5-GFP under its own promoter, and subjected to western analysis with GFP (top) or tubulin (bottom) antibodies. **B.** Cells were infected with VV strain WR expressing F13-GFP, and analyzed as in A. **C.** Cells were infected with VV strain WR for 6 or 16 hours. Filters were probed with P4b/4b or tubulin antibodies. Results are from two or three independent trials.

Figure 3. Late viral protein synthesis is reduced in p85-deficient cells. p85-deficient cells were infected with VV at an MOI of 5 for 16 hours and subjected to western analysis with various antibodies. **A.** Cells were infected with VV strain WR expressing B5-GFP under its own promoter. Filters were probed with GFP (top) or tubulin (bottom) antibodies. **B.** Cells were infected with VV strain WR expressing F13-GFP. Filters were probed with GFP (top) or tubulin antibodies. **C.** Cells were infected with VV strain WR for 6 or 16 hours. Filters were probed with P4b/4b or tubulin antibodies. Results are from two or three independent trials.

Figure 4. PI3K inhibitors alter the distribution of F13 and B5 in infected cells. **A.** BHK cells were infected with VV F13-GFP, and treated with AS1 (50 μ M) or AS2 (50 μ M) post-adsorption for 16 hours. Cells were fixed and stained with phalloidin to visualize actin (red) and DAPI to visualize DNA (blue). Approximately 600 cells were counted per condition and cells were scored positive if a FITC (GFP) signal could be detected. **B.** BHK cells were infected with VV B5-GFP, and treated with PI3K inhibitors post adsorption for 16 hours, and stained as in A. Approximately 400 cells were counted per condition. **C.** PI3K inhibitors alter the distribution of F13-GFP in infected cells. Cells were infected and stained as in A. Note that AS1 and AS2 cause a reduction of punctate FITC fluorescence at the cell periphery, which represents virions, as well as a reduction in the number of actin tails. AS1 also caused F13-GFP to localize to the cytoplasm instead of on punctate virions. **D.** PI3K inhibitors alter the distribution of B5-GFP in infected cells. Cells were infected and stained as in B. Note that AS1 and AS2 had similar effects on localization of B5 and F13, namely a reduction in peripheral punctate virions and reduced numbers of actin tails. Results are from three independent trials.

Figure 5. PI3K inhibitors alter the levels of L1 in infected cells. **A.** BHK cells were infected with VV WR, and treated with AS1 (50 μ M) or AS2 (50 μ M) post-adsorption for 16 hours. Cells were fixed and stained with phalloidin to visualize actin (red), DAPI to visualize DNA (blue), and stained with L1 antibodies to visualize IMV. Note that AS1 causes a reduction of punctate FITC fluorescence in the cells, as well as a reduction in the number of actin tails. AS2 also causes a modest reduction in the number of actin tails relative to DMSO controls. Results are from two independent trials.

Figure 6. Localization of F13-GFP and L1 in p85-deficient cells. **A.** p85-deficient cells were infected with VV F13-GFP for 16 hours. Cells were fixed and stained with phalloidin to visualize actin (red) and DAPI to visualize DNA (blue). Note that in the $p85\alpha^{-/-}$ and $p85\alpha^{-/-}\beta^{-/-}$ cells there is a reduction of punctate FITC fluorescence at the cell periphery, which represents virions, as well as a reduction in the number of actin tails. F13 remains in a peri-nuclear location in p85-deficient cells. **B.** L1 production and localization in p85-deficient cells. p85-deficient cells were infected with VV, strain WR for 16 hours. Cells were fixed and stained with phalloidin to visualize actin (red), DAPI to visualize DNA (blue), and L1 antibody, followed by FITC conjugated anti-Mouse antibody. No difference in L1 localization the p85-deficient cells compared to wild type cells was apparent. Results are from three independent trials.

Figure 7. Localization of B5-GFP in p85-deficient cells. **A.** p85-deficient cells were infected with VV B5-GFP for 16 hours. Cells were fixed and stained with phalloidin to visualize actin (red) and DAPI to visualize DNA (blue). Note that in the $p85\alpha^{-/-}$ and $p85\alpha^{-/-}\beta^{-/-}$ cells there is a reduction of punctate FITC fluorescence at the cell periphery, which represents virions, as well as a reduction in the number of actin tails. B5 remains in a peri-nuclear location in p85-deficient cells. **B.** p85-deficient cells were infected as in **A** and percent B5-GFP cells were quantified. Approximately 400 cells were counted per condition and cells were scored positive if a FITC (GFP) signal could be detected. $p85\alpha^{-/-}\beta^{-/-}$ cells had significantly reduced rates of B5-GFP positive cells. Results are from three independent trials. **C.** p85-deficient cells form fewer actin tails than p85WT cells. Actin

tails were counted for ~10 cells per condition. Data is from one representative experiment.

Figure 8. PI3K absence or inhibition reduces IHD-J virion production and release. **A-B.** Multistep growth curves of cell-associated (A) or released virus (B) conducted at an MOI of 0.01. AS1 and AS2 were used at 50 μ M, Rifampicin 0.1mg/mL, and the carrier DMSO at 0.5%. **A.** Multistep growth curves of cell-associated infectious virions, MOI of 0.01. AS1 and rifampicin reduce the amount of virus produced over time relative to DMSO control cells, (20.8-fold and 15.4-fold reduction at 36 hours). AS2 caused a modest reduction in the amount of virus produced over time relative to DMSO controls (5-fold reduction at 36 hours). **B.** Multistep growth curves of released infectious virions, MOI of 0.01. Note that AS1, AS2, and rifampicin reduce the amount of virus released into the supernatant (Fold reduction at 36 hours: AS1- 127.8-fold, AS2- 28.8-fold, Rifampicin- 55.6-fold). **C-D.** Multistep growth curves of cell-associated or released virus conducted at an MOI of 0.01 in p85-deficient cells. **C.** Multistep growth curves of cell-associated infectious virions, MOI of 0.01. From 8 to 36 hours, a reduction in the amount of virus produced was apparent in p85 $\alpha^{-/-}\beta^{-/-}$ cells compared to the p85WT and p85 $\alpha^{-/-}$ cells (19.3-fold reduction at 36 hours). **D.** Multistep growth curves of released infectious virions, MOI of 0.01. A reduction in the amount of virus released from the p85 $\alpha^{-/-}\beta^{-/-}$ cells compared to the p85WT and p85 $\alpha^{-/-}$ cells was apparent (20-fold reduction at 36 hours). Results are from one trial conducted in triplicate, and match growth curves conducted using WR. **E.** PI3K inhibitors reduce comet tails formed by VV, strain IHD-J. Monolayers were infected with 100PFU of virus, and plaques were visualized 48 hours

later with crystal violet stain. Experiments were conducted in three independent trials. **F,G.** Toxicity assays of PI3K inhibitors on uninfected cells. **F.** MTS assay on BSC-1 cells treated with PI3K inhibitors for different periods of time. MTS production is a measure of mitochondrial metabolism. Values represent the concentration of drug (in μM) required to reduce formazan production by half. Experiments were conducted in two independent trials. **G.** Trypan blue exclusion assays of BHK cells treated with PI3K inhibitors (AS1 and AS2, $50\mu\text{M}$) for different time periods.

Figure 9. PI3K inhibitors disrupt vaccinia virus maturation. **A.** BHK cells were infected with MVA for 17 hours plus or minus PI3K inhibitors. Untreated samples exhibit characteristic virion morphogenesis (4100x, Glut/ KMnO_4 fixative). **A'**: 1) Crescents; 2) Immature virions; 3) Mature virion, IMV; **A''**: 4) IEV; 5) CEV; 6) EEV. **B.** In cells treated with $50\mu\text{M}$ AS1, virions at the immature to IMV transition, but not at later stages, are evident (10,000x, Glut/ OsO_4 fixative). a) Replication center and crescents; b) Immature virion; c) Immature virion with nucleoid. **C.** In cells treated with $50\mu\text{M}$ AS2, virions at the IMV wrapping step but not at later stages are evident (6800x, Glut/ KMnO_4 Fix). a') Immature virion; b') IMV. Note the lack of virions associated with the plasma membrane, characteristic of IEV inhibition. **D.** HeLa cells were infected with B5-GFP WR for 17 hours plus or minus PI3K inhibitors. Untreated samples exhibit characteristic virion morphogenesis (10,000x, Glut/ KMnO_4 Fix). **D'**: 1) Crescents; 2) Immature virions; **D''**: 3) Mature virion, IMV; 4) IEV. **E.** In cells treated with $50\mu\text{M}$ AS1, virions at the immature to IMV transition, but not at later stages, are evident (10,000x, Glut/ OsO_4 Fix). a) Viral crescents; b) Immature virion; c) Immature virion with nucleoid. **F.**

Samples treated with 50 μ M AS2 are stuck at the IMV wrapping step (7000x, Glut/KMn₄). a') Crescents; b') Immature virion; c') IMV. Note the lack of virions associated with the plasma membrane, a characteristic of IEV inhibition.

Figure 10. VV morphogenesis is disrupted in the p85-deficient cells. p85 $\alpha^{-/-}$ $\beta^{-/-}$ cells were infected with B5-GFP WR for 17 hours. **A,B,C.** p85 $\alpha^{-/-}$ $\beta^{-/-}$ cells exhibit characteristic virion morphogenesis (A,B. 4,100X, OsO₄ Fix; C. 14,000X OsO₄ fix), but are stuck at the IMV wrapping step. **1)** Crescents; **2)** Immature virions; **3)** Mature virion, IMV (4,100X, OsO₄ Fix). Note the lack of virus associated with the plasma membrane.

Figure 11. PI3K usage by VV is functionally redundant. **A.** PI3K inhibitors reduce plaque numbers in p85-deficient cells. Drugs were added to p85-deficient cells post viral adsorption at different concentrations. The concentration of drug needed to reduce plaque numbers by half (IC₅₀) was calculated by fitting the data to a linear regression model using Prism software (GraphPad Prism Software, Inc., La Jolla, CA). IC₅₀ values are lower for p85-deficient cells. Results are from three independent trials. **B.** Summary of vaccinia virus morphogenesis in p85-deficient cells or following PI3K inhibitor treatment. After VV entry (1) virion uncoating and early protein synthesis occurs (2). These steps are followed by late protein production (3), formation of viral replication centers and viral crescents (4). Crescents envelope viroplasm to form immature virions (IV, 5). The cores of IV condense to form mature virions (IMV, 6). A subset of the IMV traffic to the Golgi Complex where they are enveloped in a host cell derived membrane to form IEV (7). IEV fuse with the plasma membrane, releasing virus to the extracellular

milieu, (CEV, 8). CEV form actin tails beneath the virus and ultimately, release to form extracellular enveloped virions (EEV, 9). Our results suggest that involvement of PI3Ks at steps 2,3,5, and 7. Steps 2 and 7 are disrupted in the p85-deficient cells, AS1 treatment disrupts steps 3 and 5, and AS2 disrupts steps 7. Thus, PI3K usage by VV is redundant; multiple PI3Ks acting at each of several steps regulate VV morphogenesis.

Supplementary Figures:

Supplementary Table 1. 20% Inhibitory Concentration (IC₂₀) of PI3K inhibitors added post-adsorption to poxvirus-infected monolayers. ¹[61] ²[108] ³[65]

S1A. TUNEL assay for PI3K inhibitor treated BHK cells. PI3K inhibitors were added to uninfected BHK cells on glass coverslips for 16 hours. Media was removed and the cells were fixed and processed for the TUNEL assay. AS1 and AS2 were added at 50µM and were in 0.5% DMSO. B0304 and LY294002 were at 20µM and were in 0.2% DMSO. DNase1 was used as a positive control. Approximately 700 cells were counted per condition. PI3K inhibitors did not increase the levels of apoptosis in the BHK cells following 16 hour treatment. **S1B.** TUNEL assay for p85-deficient cells. Uninfected p85WT or -deficient cells were added to glass coverslips for 16 hours, and then fixed and processed for the TUNEL assay. DNase1 was used as a positive control. Approximately 700 cells were counted per condition. The rates of apoptosis are not increased in the p85-deficient cells.

S2. PI3K Inhibitors Reduce the Number of Actin Tails/Cell. BSC40 Cells were infected with WR and treated with 100 μ M AS1 and AS2 post-adsorption, and the cells were fixed and stained with FITC-phalloidin 16 hours later. The number of actin tails was counted on ten cells per condition.

S3. Screen shots from z-stack of spinning disk microscopy of p85WT or p85 $\alpha^{-/-}$ $\beta^{-/-}$ cells infected with F13-GFP. Note the punctate virions in the p85WT cells, and the lack of these structures in the p85 $\alpha^{-/-}$ $\beta^{-/-}$ cells. Instead, the F13 protein localizes to a peri-nuclear structure.

S4. A-B Single step growth curves conducted at MOI=5 in PI3K inhibitor-treated cells. VV, strain IHD-J was allowed to bind and enter BHK cells for 1 hour, monolayers were washed with PBS twice, and media was added containing PI3K inhibitors (50 μ M), DMSO (0.5%) or Rifampicin (0.1mg/mL). **C-D.** Multistep growth curves conducted in PI3K inhibitor-treated cells. Cells were infected at different MOIs with Vaccinia virus, strain IHD-J. Virus was allowed to bind and enter BHK cells for 1 hour, monolayers were washed with PBS twice, and media was added containing PI3K inhibitors (50 μ M), DMSO (0.5%) or Rifampicin (0.1mg/mL). Supernatants and monolayers were collected at 24 hours post infection.

S5. A-B Single step growth curves conducted at MOI=5 in p85-deficient cells. VV strain IHD-J was allowed to bind and enter cells for 1 hour, monolayers were washed with PBS

twice, and fresh media was added. **C-D.** Multistep growth curves conducted in p85-deficient cells. Cells were infected at different MOIs with VV strain IHD-J as in A and B.

S6. PI3K inhibitors reduce comet tails formed by VV, strain IHD-J. Insets show enlarged image of plaques boxed in top panels. Insets are at the same scale.

S7A-D. PI3K inhibitors disrupt vaccinia virus maturation. **A-B.** BHK cells were infected with MVA for 17 hours and treated with 50 μ M AS1 (A. 8,200X, KMnO₄ fix. B. 8,200X OsO₄ Fix). **C-D.** HeLa cells were infected with B5-GFP for 17 hours and treated with 50 μ M AS2 (C,D. 8,200X, KMnO₄ fix).

S8A-C. VV morphogenesis is disrupted in the p85-deficient cells. p85 $\alpha^{-/-}$ $\beta^{-/-}$ cells were infected with B5-GFP WR for 17 hours. (A. 2,700X, OsO₄ Fix; B. 4,100X, OsO₄ C. 8,200X OsO₄ fix).

Supplementary Movie 1: Spinning disk microscopy of untreated HeLa cells infected with VV B5-GFP strain WR for 17 hours.

Supplementary Movie 2: Spinning disk microscopy of HeLa cells infected with VV B5-GFP strain WR and treated with AS1 50 μ M for 17 hours.

Supplementary Movie 3: Spinning disk microscopy of HeLa cells infected with VV B5-GFP strain WR and treated with AS2 50 μ M for 17 hours.

Supplementary Movie 4: Spinning disk microscopy of p85WT cells infected with VV

F13-GFP for 17 hours.

Supplementary Movie 5: Spinning disk microscopy of p85 $\alpha^{-/-}\beta^{-/-}$ cells infected with VV

F13-GFP for 17 hours.

Table 1:

	Inhibits:	Vaccinia IC₅₀	Ectromelia IC₅₀	Monkeypox IC₅₀	Other Targets:
AS1	p110- gamma	37.4 ±1.1µM	13.0 ±1.3µM	12.1 ±3.9µM	p110-alpha, p110-beta, p110-delta, PKCβII ¹
AS2	p110- gamma	44.6 ±2.1µM	44.7 ±14.2µM	9.3 ±4.3µM	p110-alpha, p110-beta, p110-delta ¹
B0304	p110-alpha	9.8 ±0.3µM	1.8 ±0µM	6.1 ±4.8µM	p110-beta, p110-delta, p110gamma ²
LY294002	Broad- Spectrum PI3K Inhibitor ³	44.1 ±6.9µM	14.4 ±4.2µM	20.3 ±10.7µM	

Supplementary Table 1:

	Inhibits:	Vaccinia IC₂₀	Ectromelia IC₂₀	Monkeypox IC₂₀	Other Targets:
AS1	p110- gamma	16.32 ±1.9µM	6.87 ±1.5µM	4.56 ±4.7µM	p110-alpha, p110- beta, p110-delta, PKCβII ¹
AS2	p110- gamma	21.79 ±3.1µM	27.00 ±3.4µM	3.58 ±1.4µM	p110-alpha, p110- beta, p110-delta ¹
B0304	p110- alpha	4.00 ±0.3µM	3.25 ±0.2µM	0.8 ±0.6µM	p110-beta, p110- delta, p110gamma ²
LY294002	Broad- Spectrum PI3K Inhibitor ³	19.76 ±6.4µM	1.05 ±0.0µM	2.83 ±3.0µM	

Figure 1

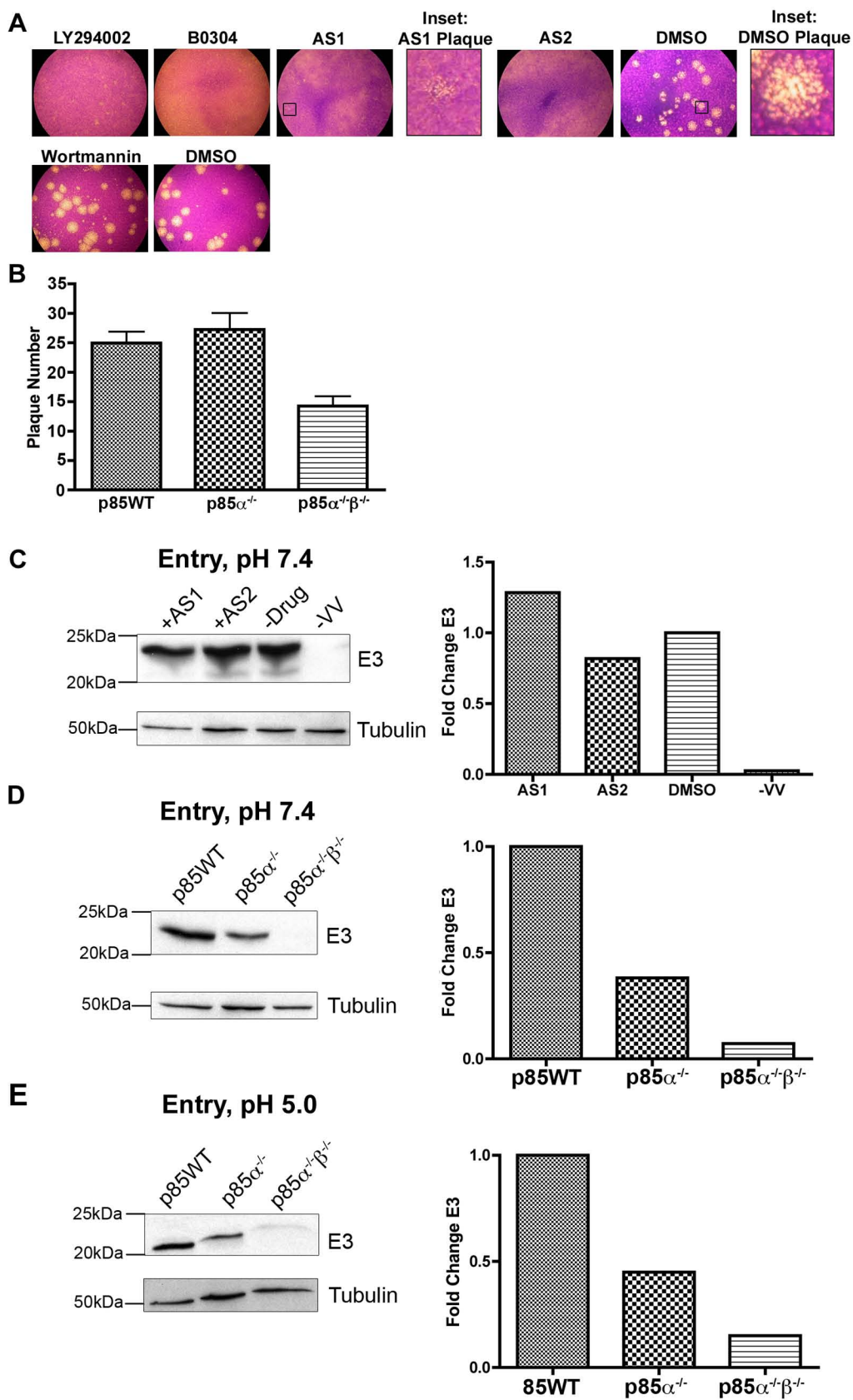


Figure 2

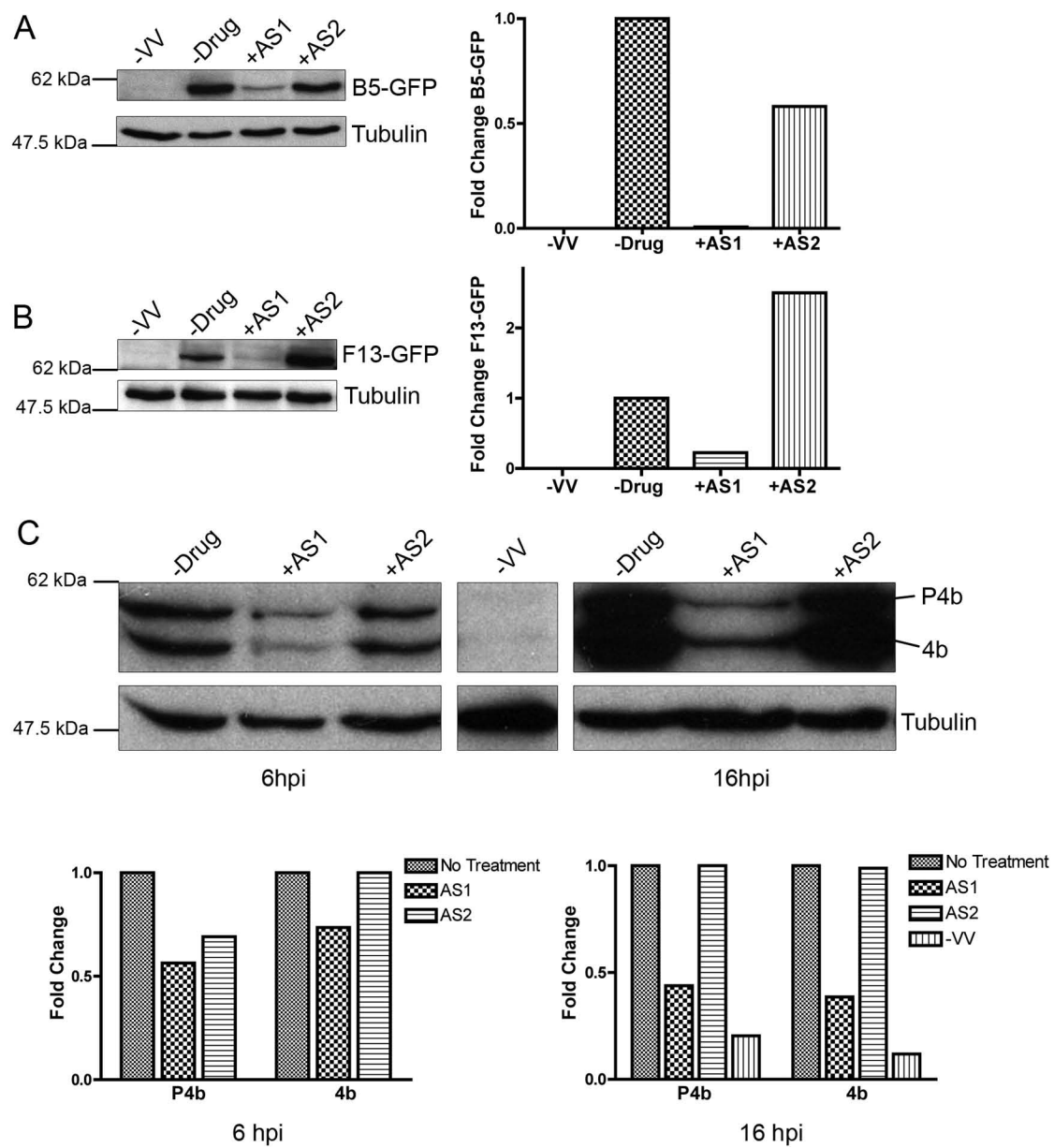


Figure 3

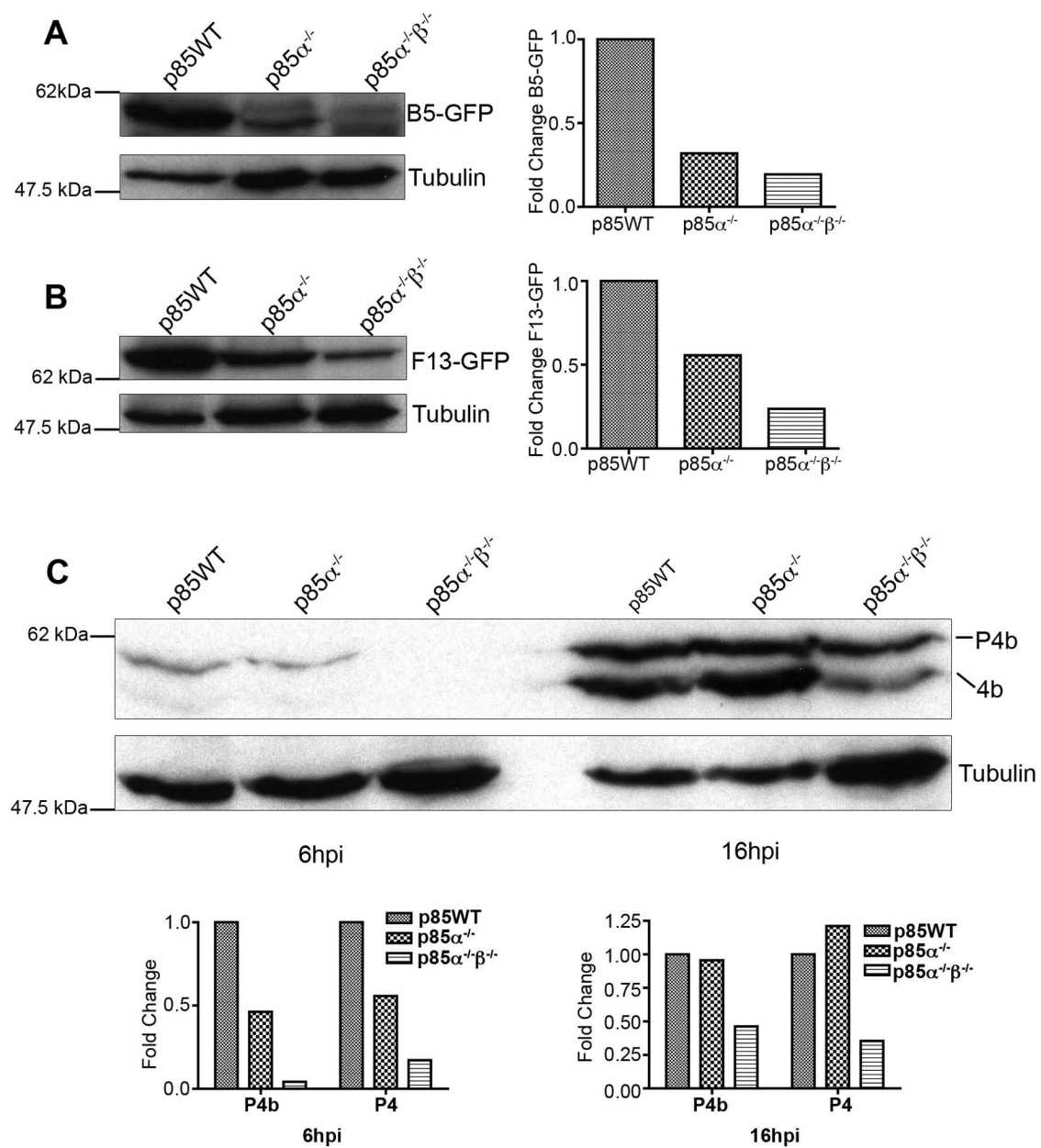


Figure 4

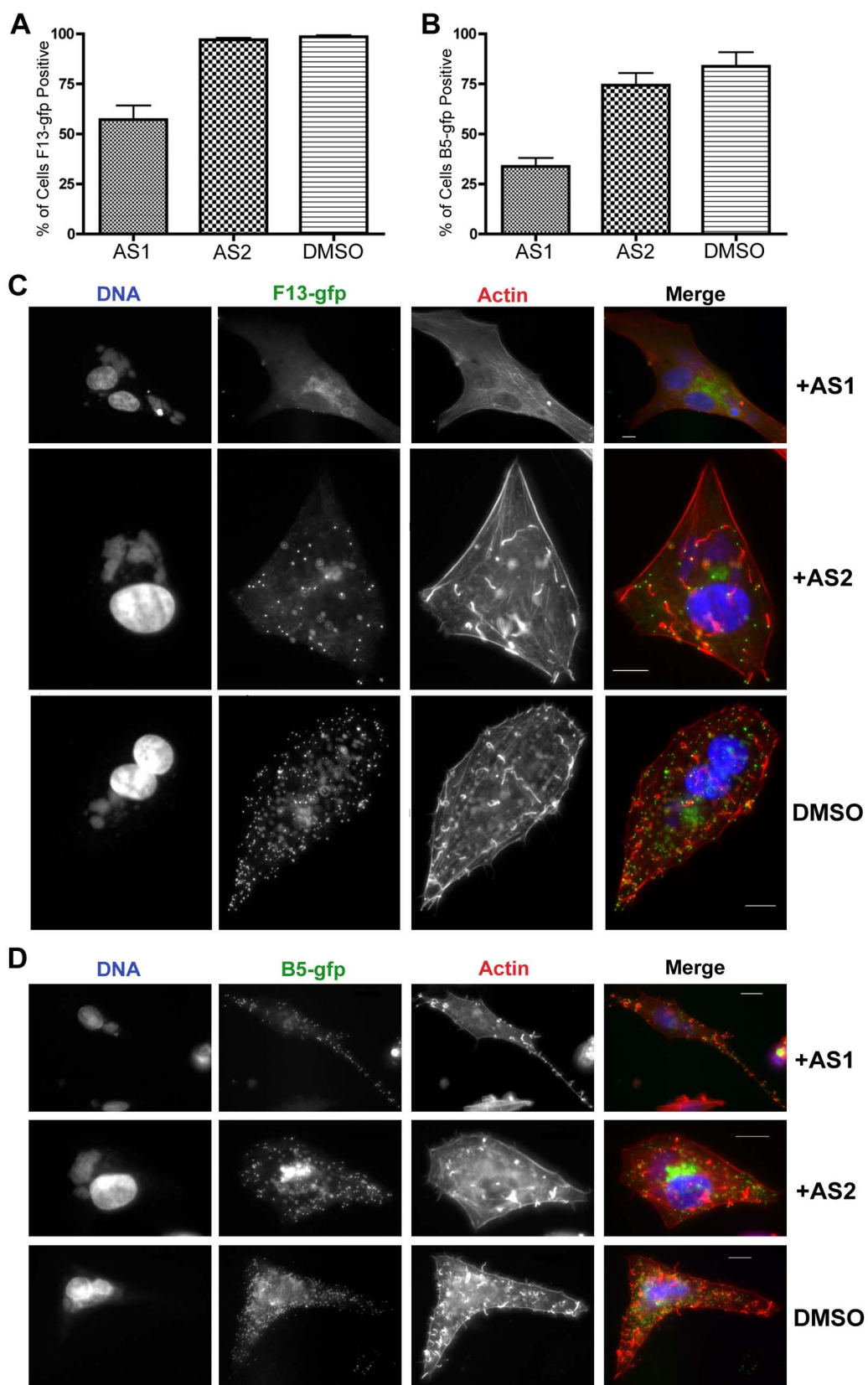


Figure 5

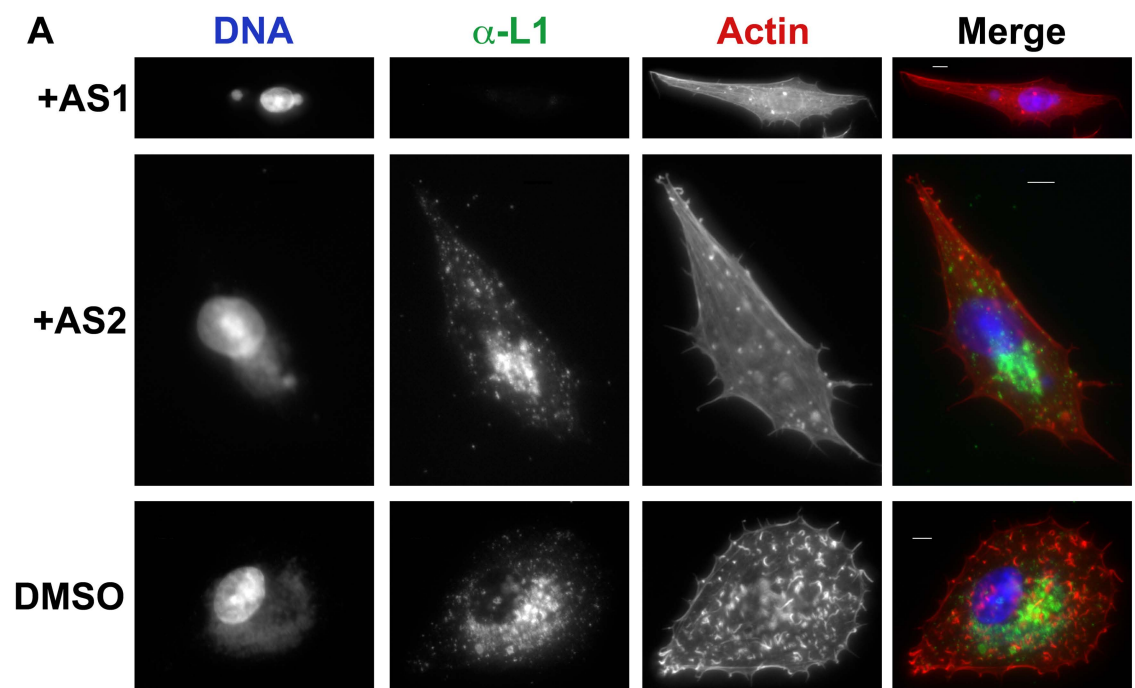


Figure 6

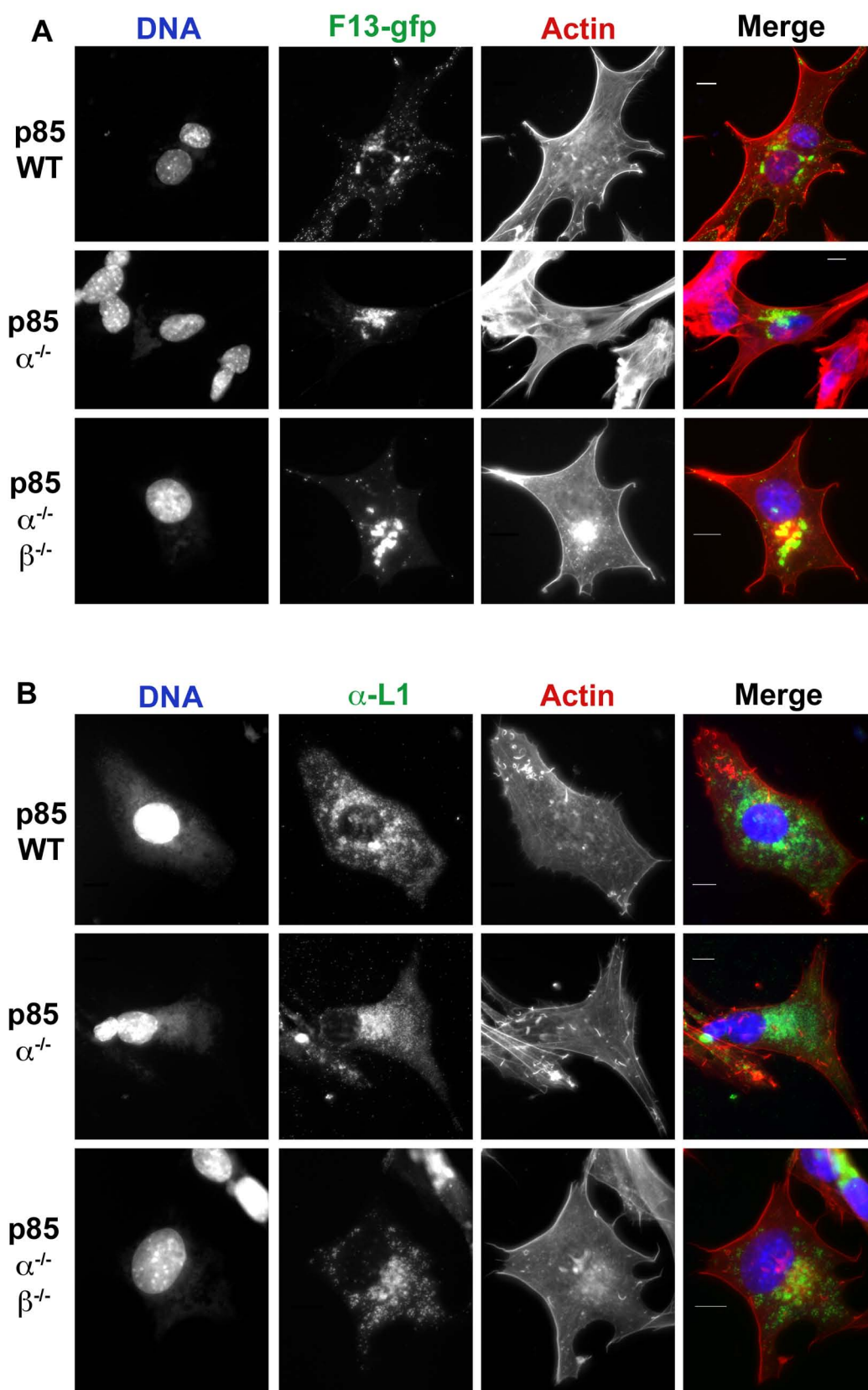


Figure 7

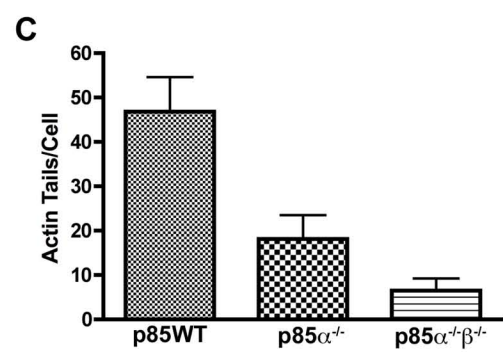
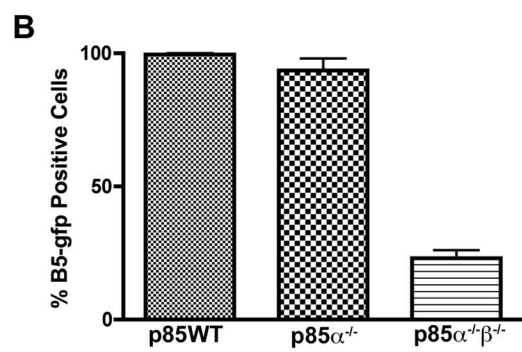
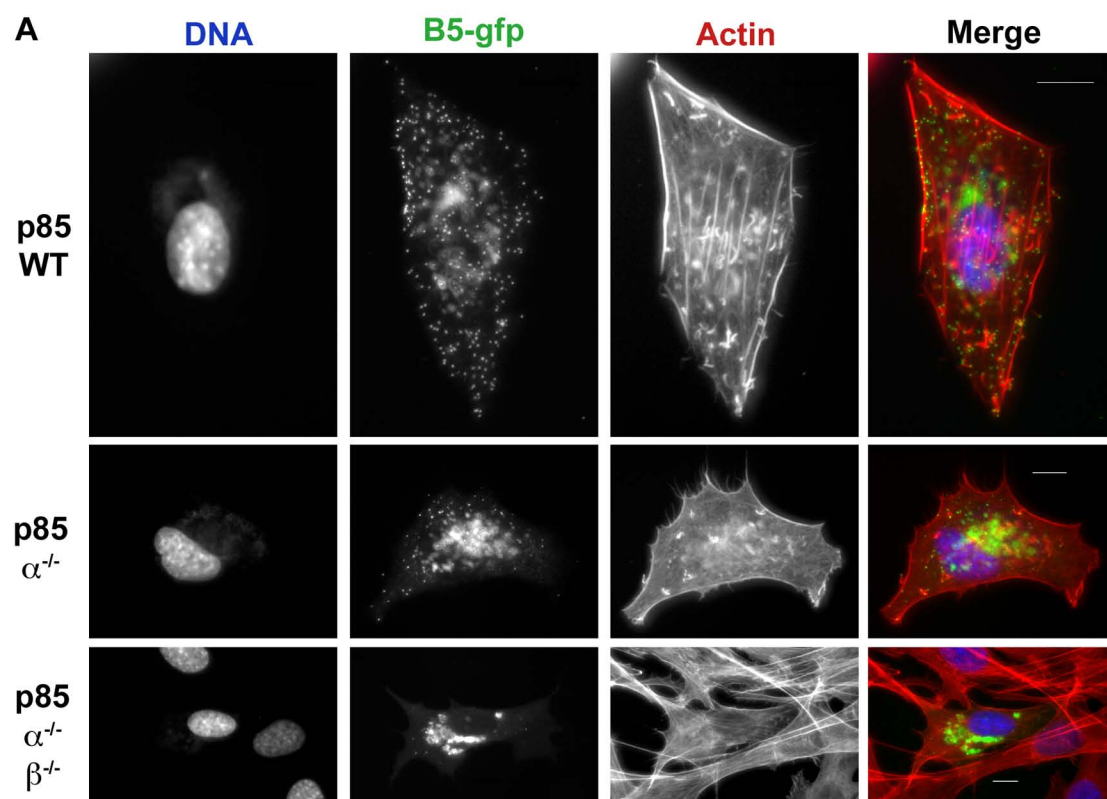


Figure 8

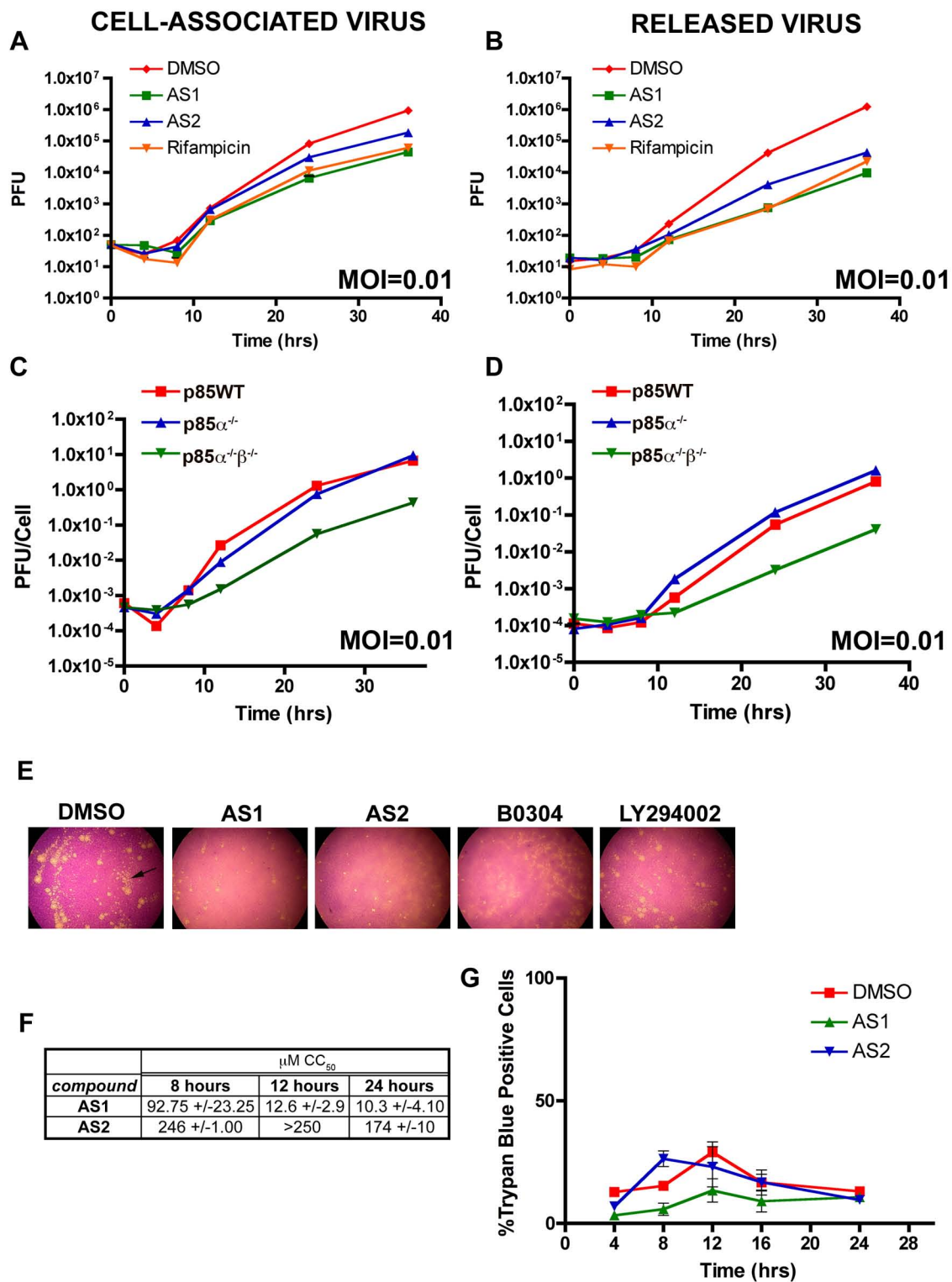
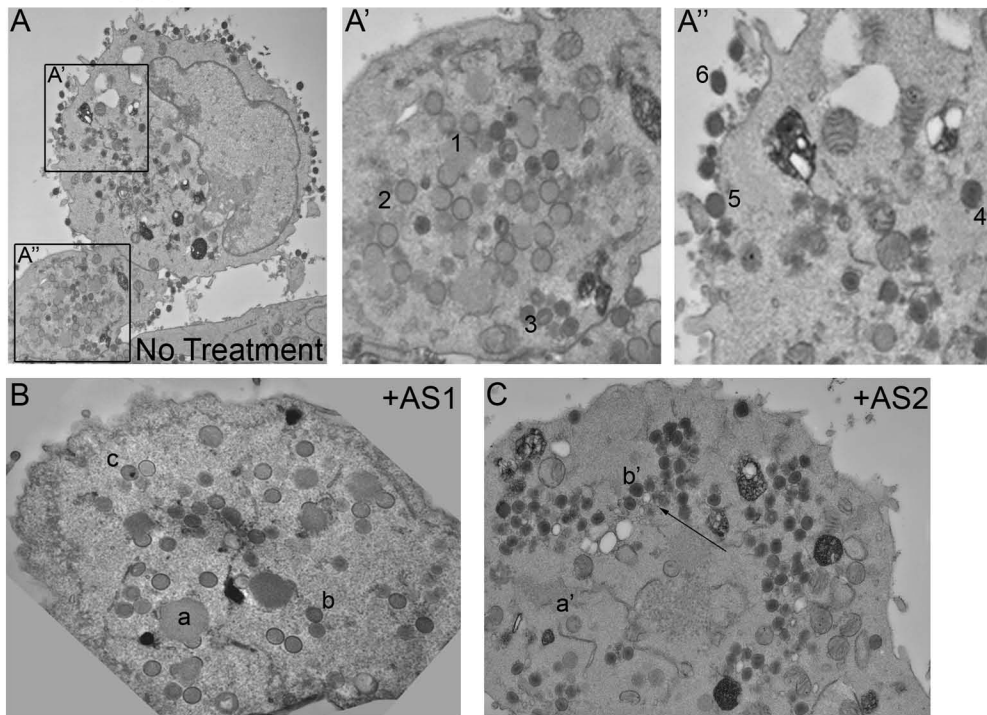


Figure 9

MVA Infection:



B5-GFP, WR Infection:

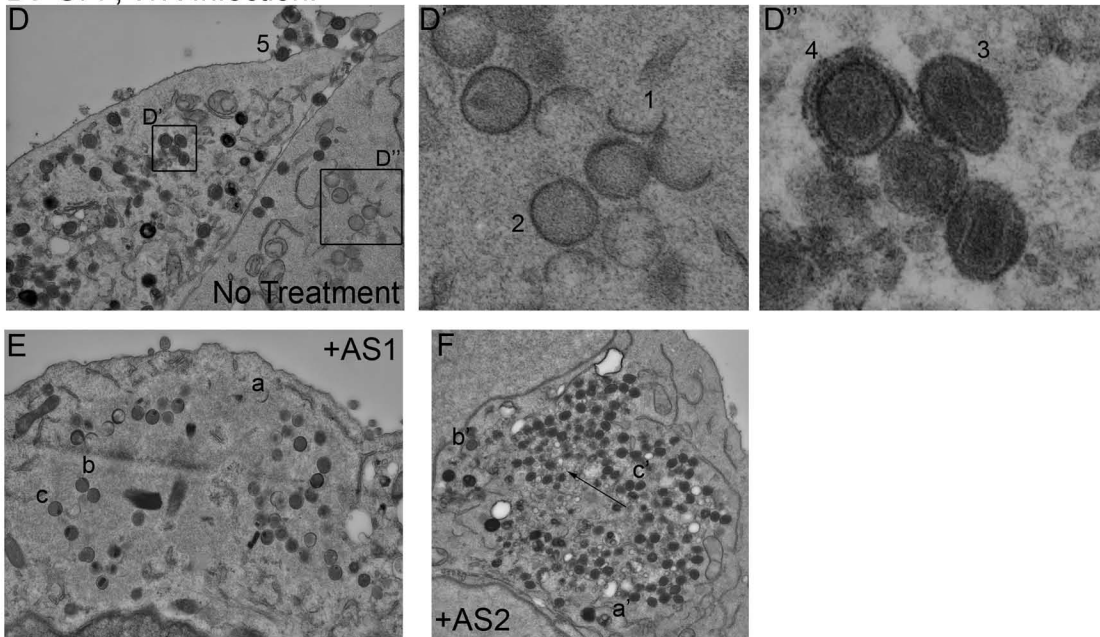


Figure 10

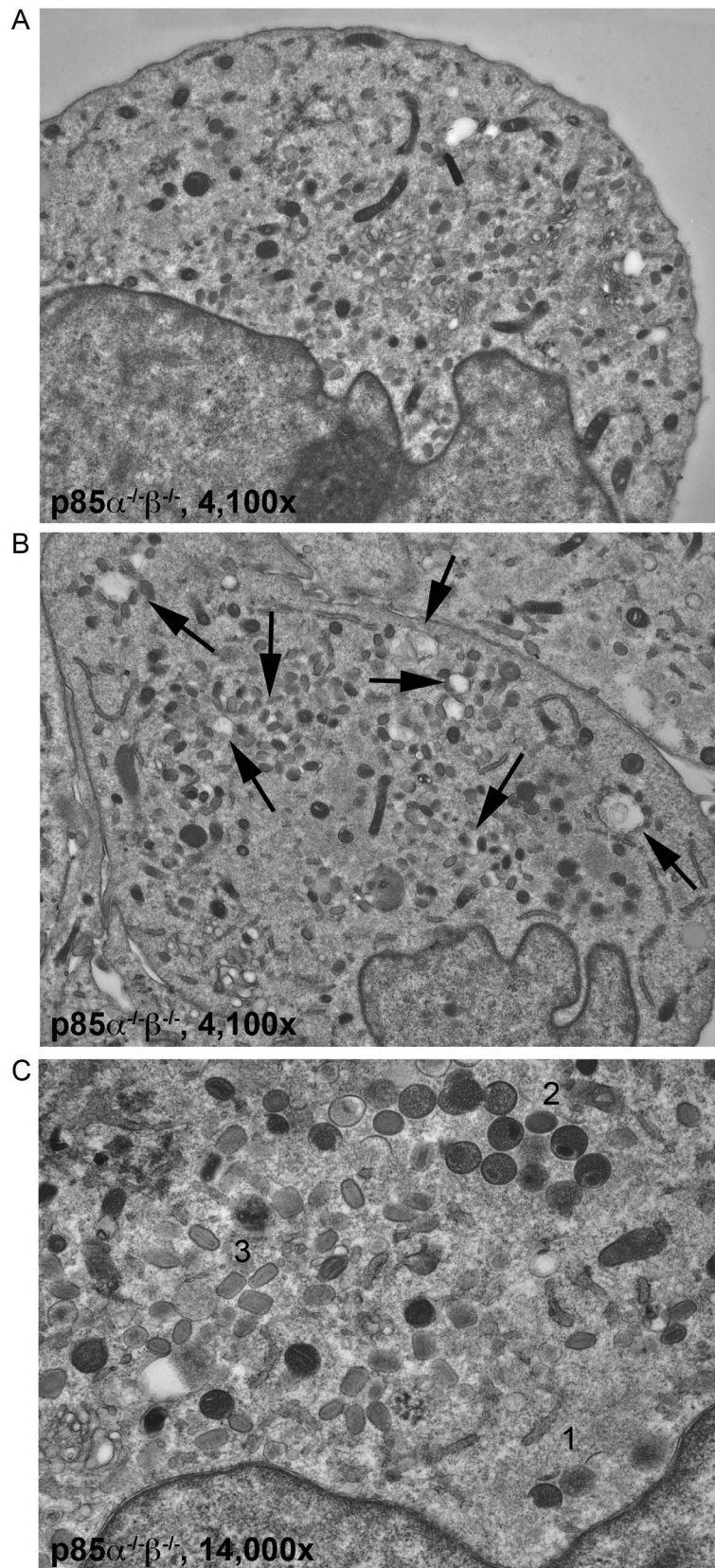
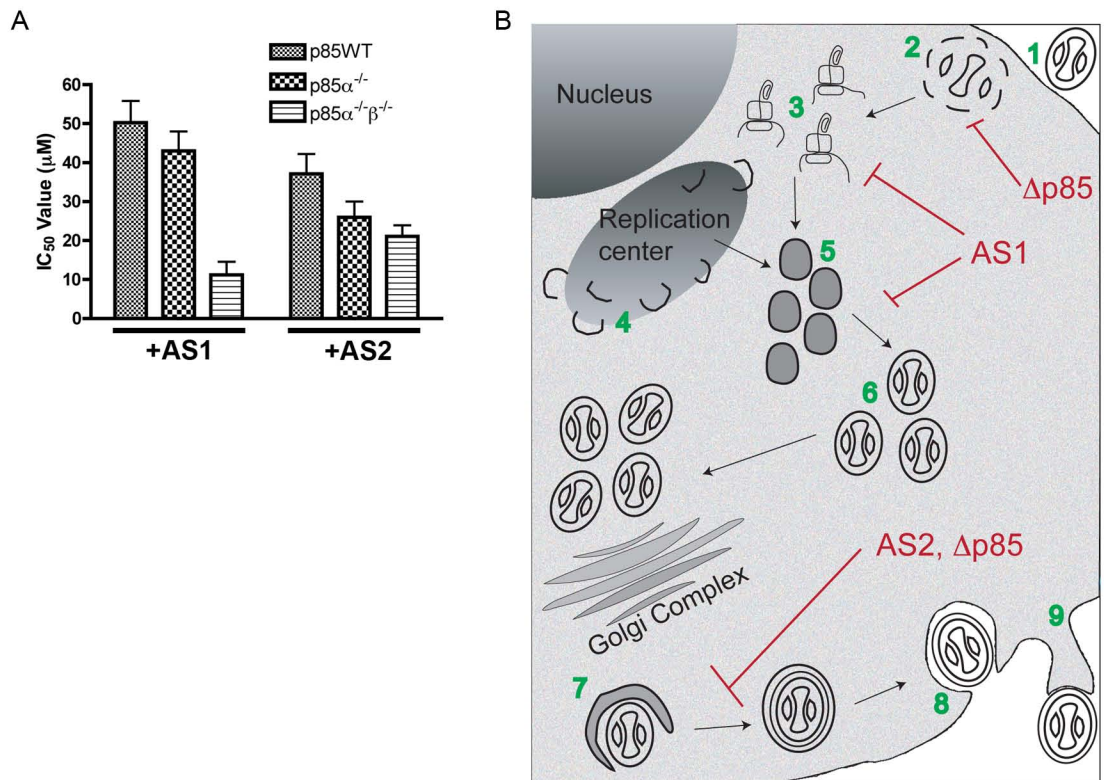
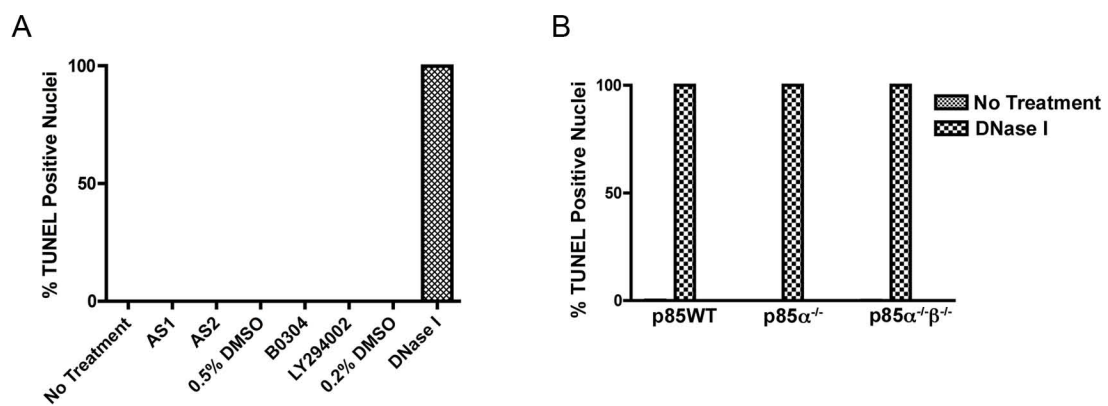


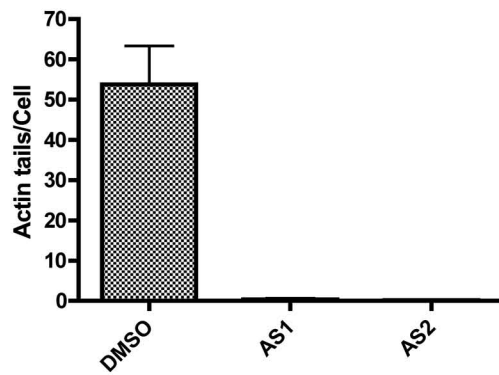
Figure 11



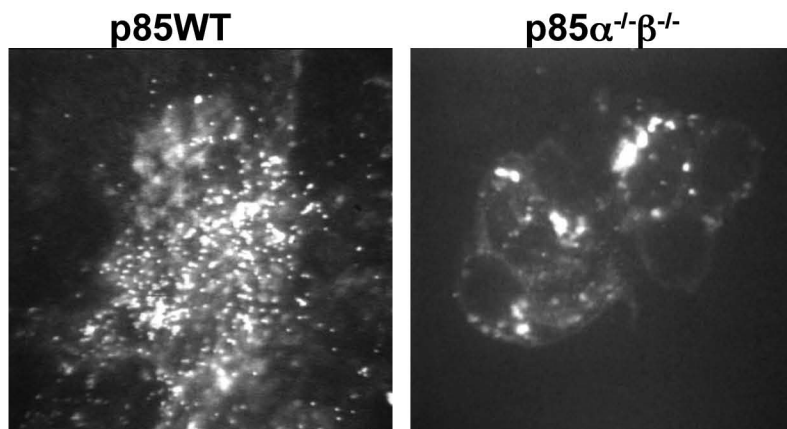
Supplementary Figure 1



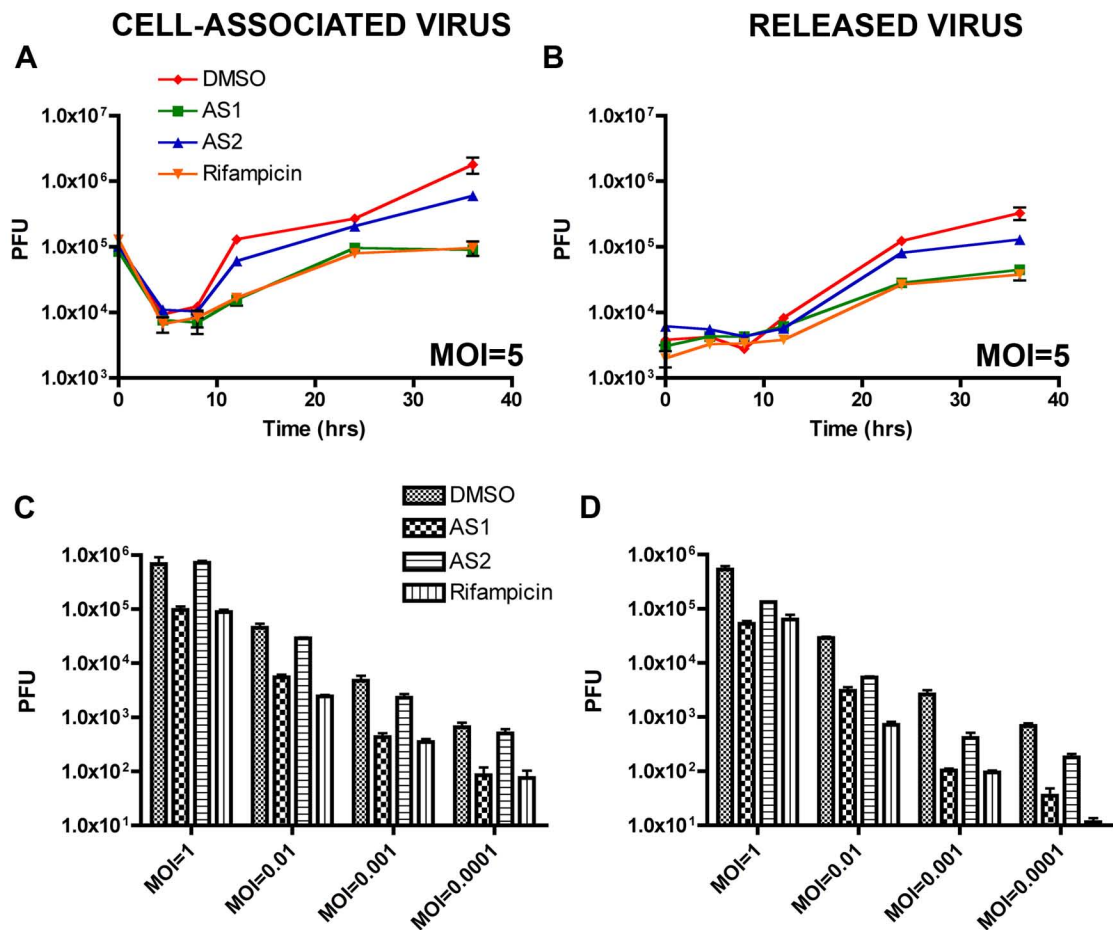
Supplementary Figure 2



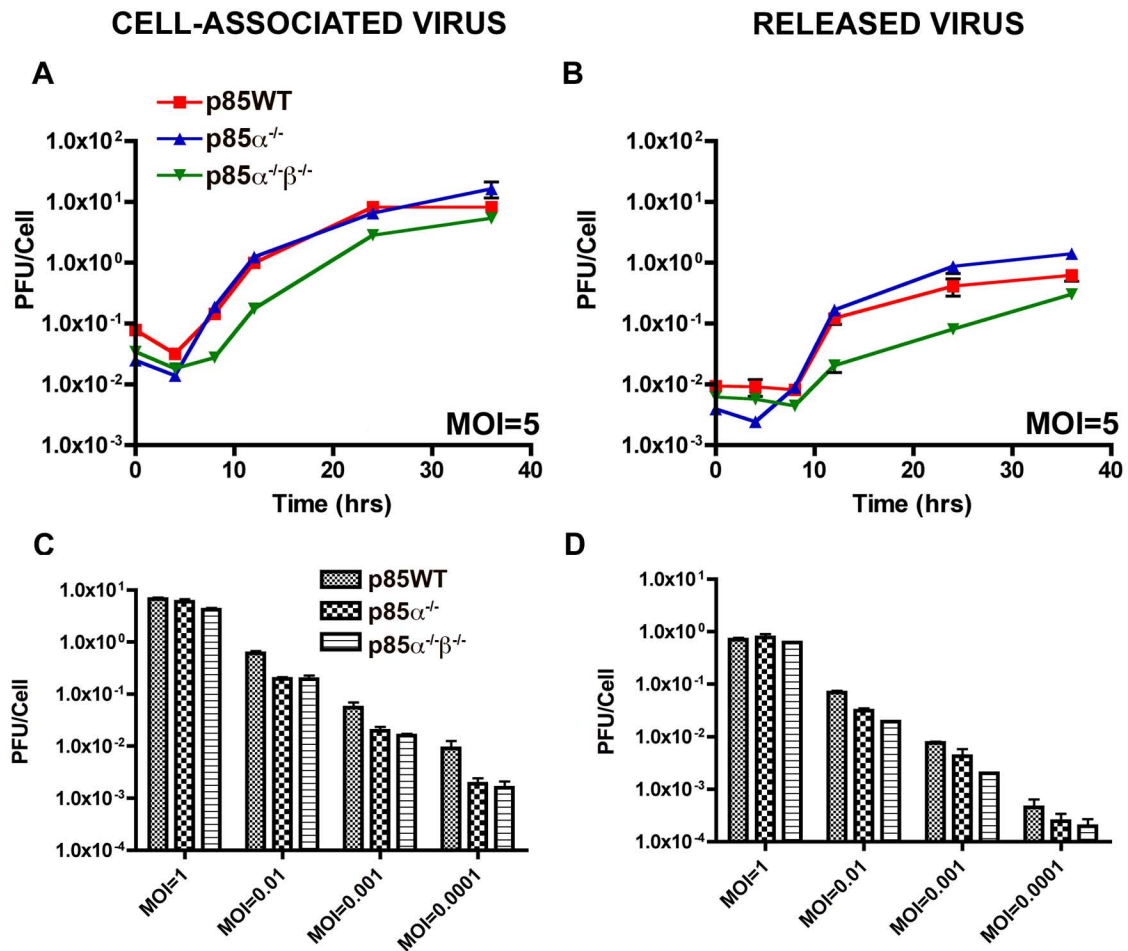
Supplementary Figure 3



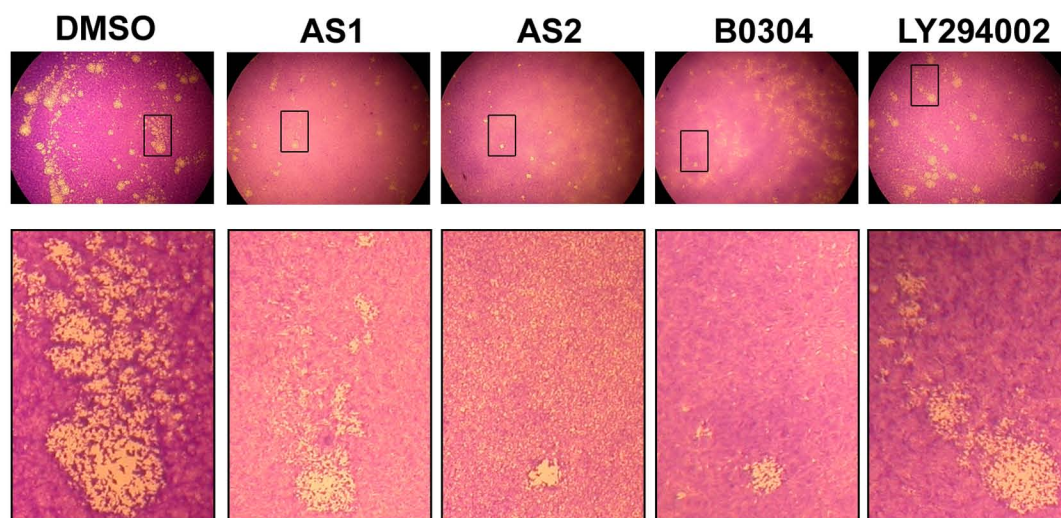
Supplementary Figure 4



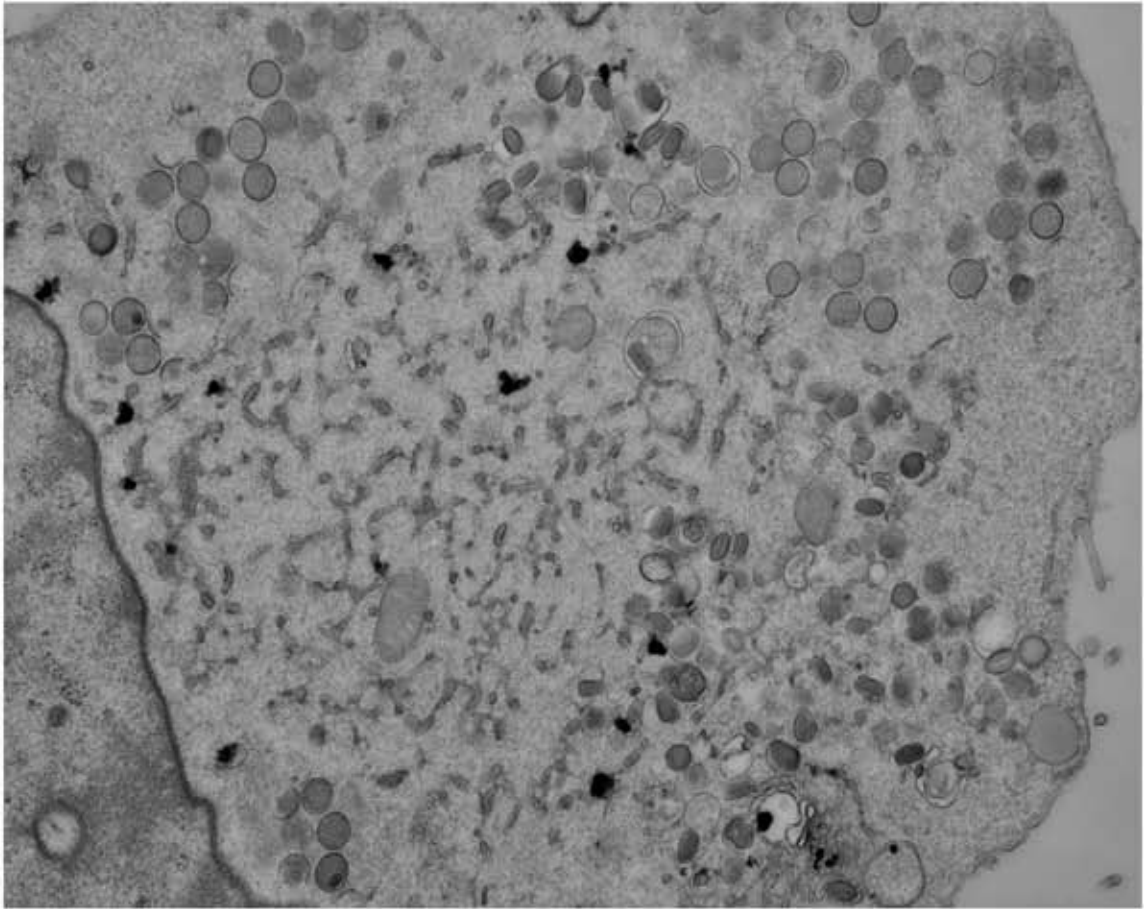
Supplementary Figure 5



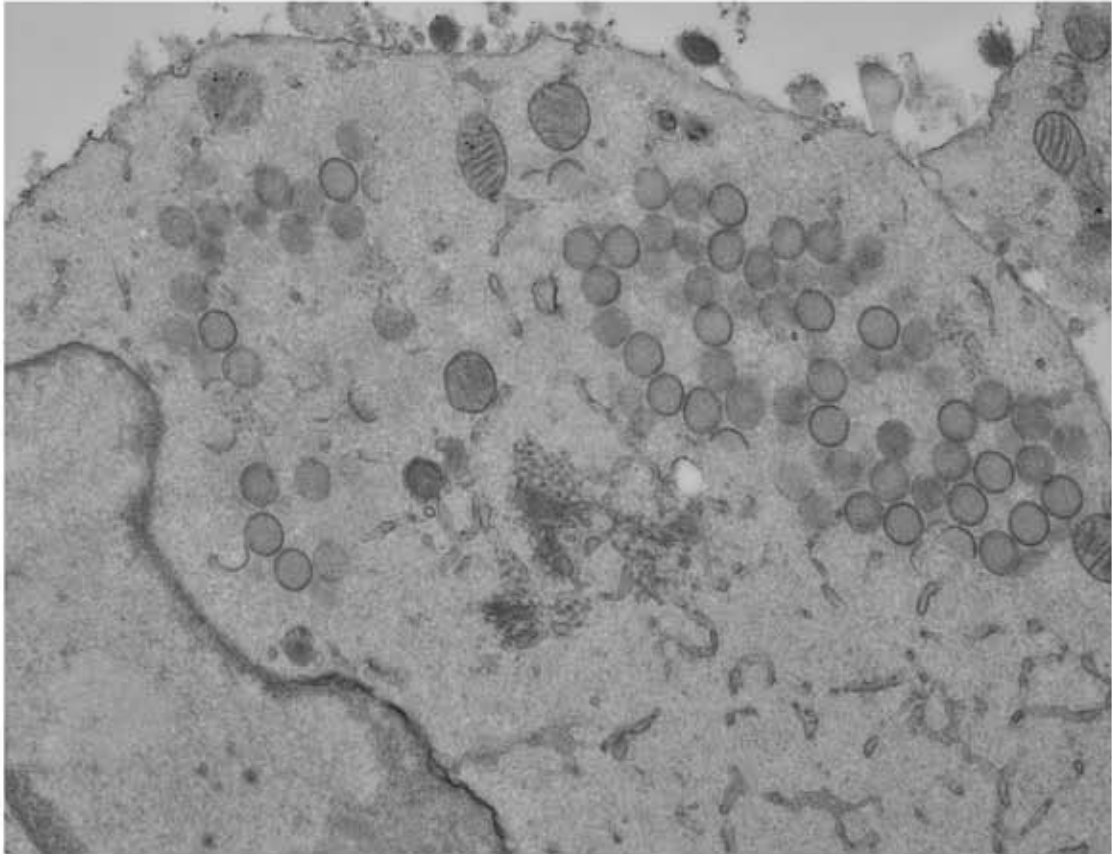
Supplementary Figure 6



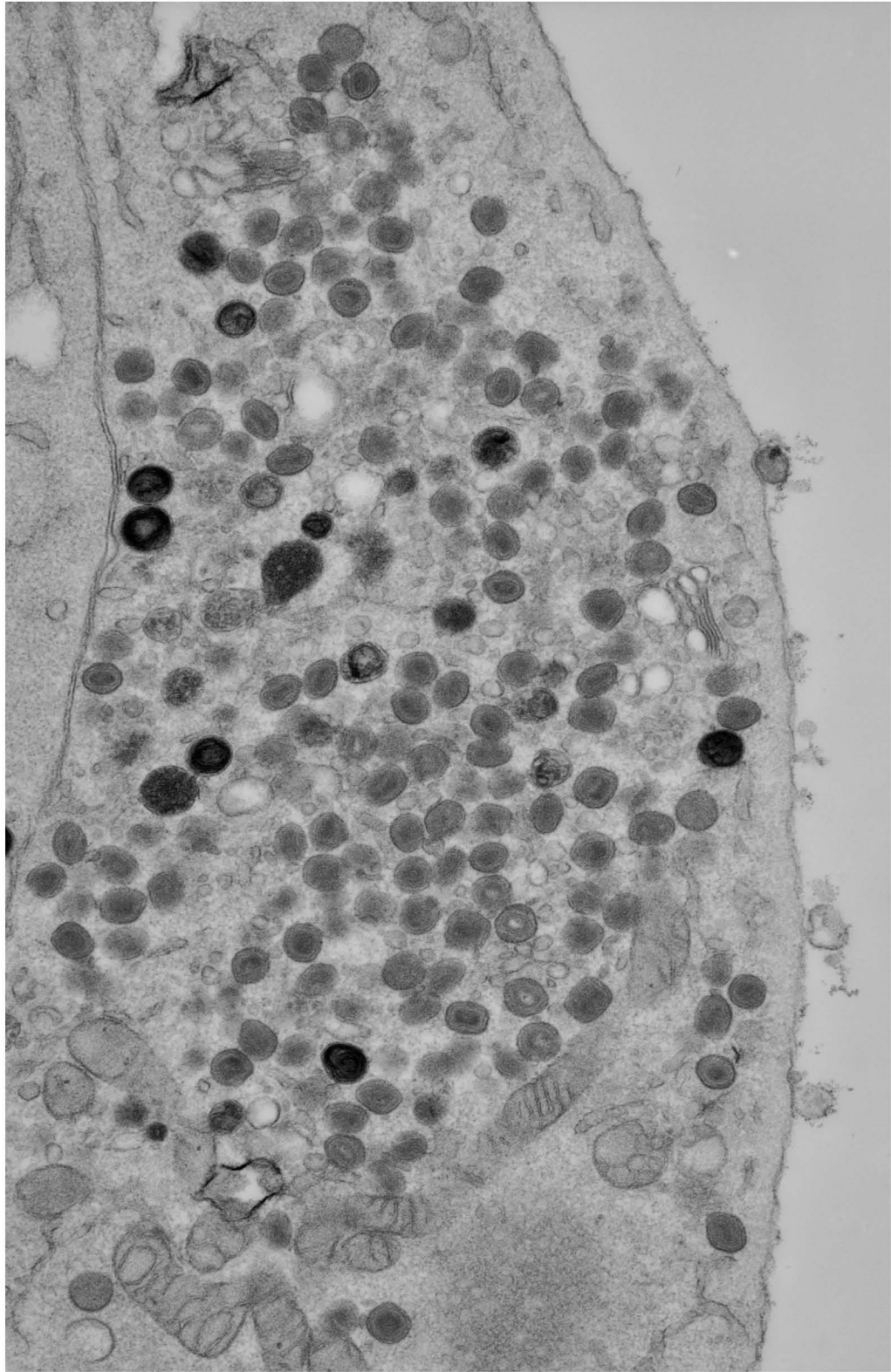
S7A



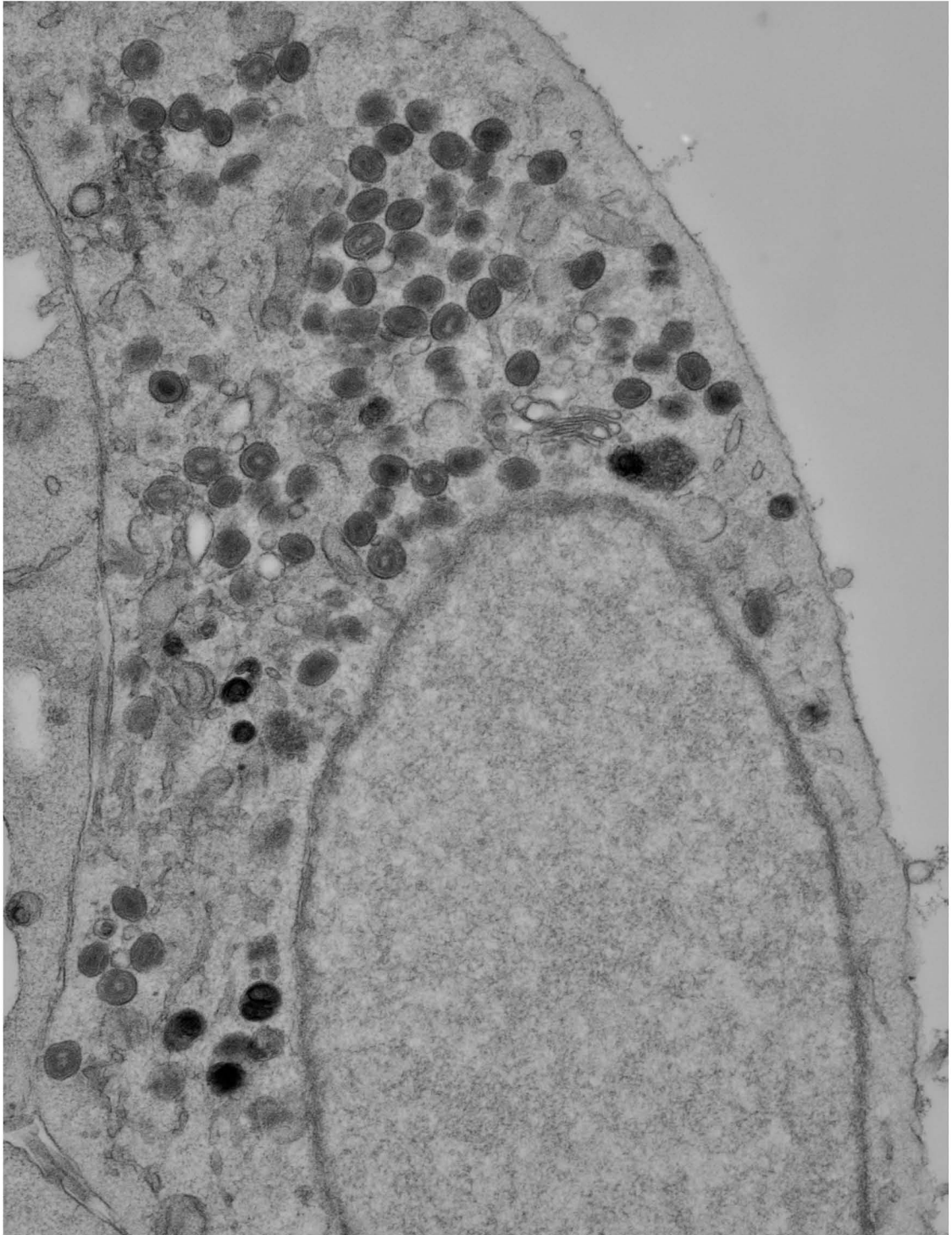
S7B



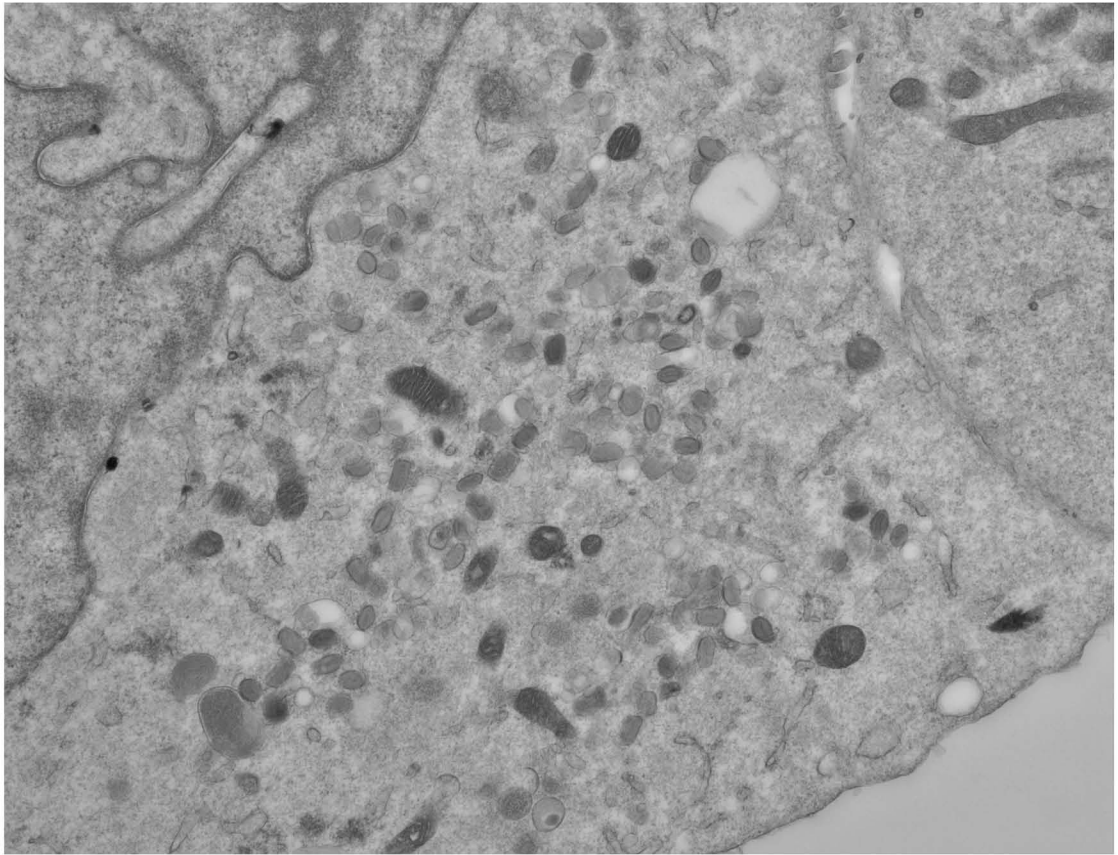
S7C



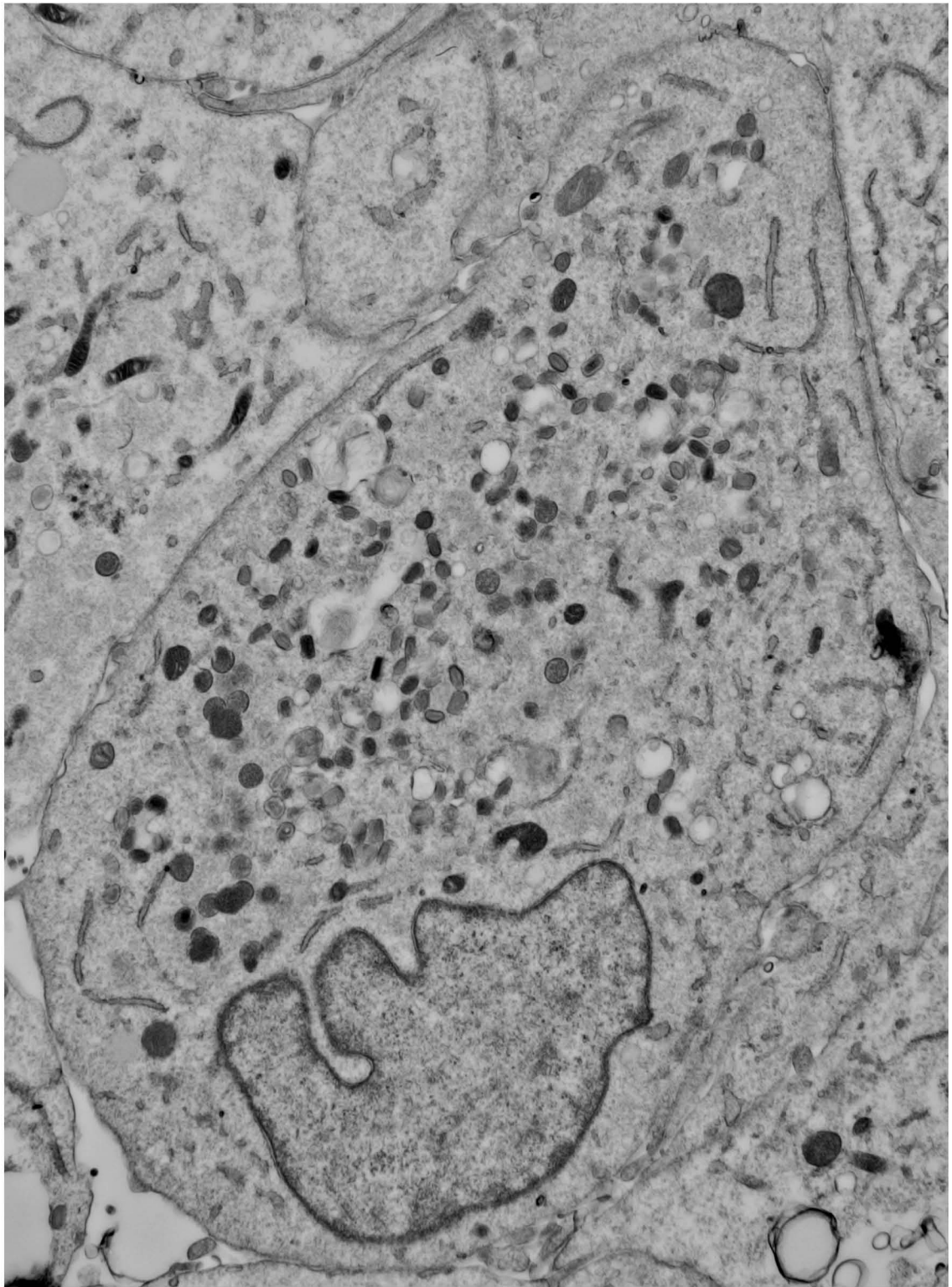
S7D



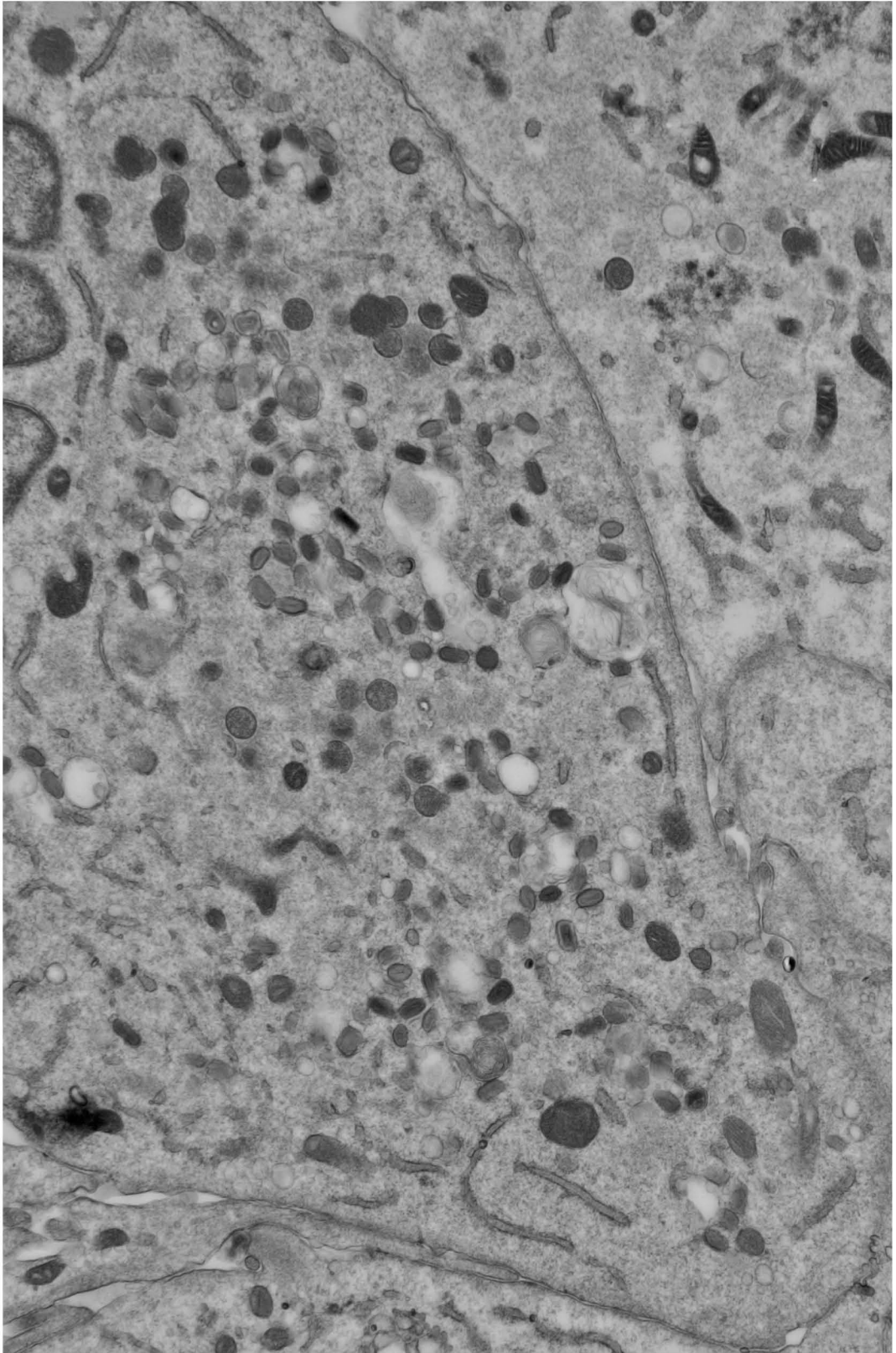
S8A



S8B



S8C



**CHAPTER IV: THE HOST PHOSPHOINOSITIDE 5-PHOSPHATASE SHIP2
REGULATES DISSEMINATION OF VACCINIA VIRUS**

Shannon McNulty¹, Christophe Erneux², and Daniel Kalman³

¹Microbiology and Molecular Genetics Graduate Program, Emory University School of Medicine, Atlanta, GA 30322, USA.

²Institut de Recherche Interdisciplinaire en Biologie Humaine et Moléculaire, Free University of Brussels, Campus Erasme, Brussels, Belgium.

³ Department of Pathology and Laboratory Medicine, Emory University School of Medicine, Atlanta, Georgia 30322, USA.

Submitted to The Journal of Virology November 16, 2010.

All experiments were conceived by Shannon McNulty, Christophe Erneux, and Daniel Kalman. Reagents were provided by Christophe Erneux. All experiments were performed by Shannon McNulty.

SUMMARY

After fusing with the plasma membrane enveloped poxvirus virions form actin-filled membranous protrusions, called tails, beneath themselves and move towards adjacent uninfected cells. While much is known about the host and viral proteins that mediate formation of actin tails, much less is known about the factors controlling release. We found that the phosphoinositide 5-phosphatase SHIP2 localizes to actin tails. Localization requires phosphotyrosine, Abl- and Src-family tyrosine kinases and N-WASP, but not the Arp2/3 complex, nor actin. Cells lacking SHIP2 have normal actin tails, but release more virus. Moreover, cells infected with viral strains with mutations in the release inhibitor A34, release more virus but recruit less SHIP2 to tails. Thus, the inhibitory effects of A34 on viral release are mediated by SHIP2. Together, these data suggest that SHIP2 is an intrinsic antiviral factor that regulates dissemination of poxviruses from infected cells.

INTRODUCTION

Orthopoxviruses, including vaccinia virus (VV), monkeypox (MPX), and variola (VarV), are large dsDNA viruses that cause characteristic umbilicated vesiculo-pustular skin lesions (“pox”). VarV is the causative agent of smallpox, and VV is used for vaccination against smallpox. Although smallpox has been eradicated, naturally occurring poxviruses are still of concern to humans. In particular, MPX is endemic in Africa (55) and has the potential for spread to humans from bushmeat and squirrels (27, 28, 51, 55, 56), and recent outbreaks in the Democratic Republic of Congo have raised the possibility of human-to-human transmission (56). Efforts to understand the capacity for human-to-human transmission amongst poxviruses have focused on how the virus spreads from cell to cell.

Infection by poxviruses is initiated upon entry of either of two different forms of the virus. The first, called the intracellular mature virus (IMV; also called mature virion (MV)), consists of a viral core surrounded by one or two lipid bilayers derived from an ER-golgi intermediate compartment (ERGIC) (20, 57, 59, 69). A second infectious form of the virus, called the extracellular enveloped virus (EEV; also called enveloped virus “EV”) (65), consists of an IMV enveloped in additional membranes derived from the host cell. IMV are released following lysis of host cells (58), whereas the precursor of EEV traffic along microtubules to the cell periphery (14, 19, 54, 73). Upon fusion with the plasma membrane, the doubly-enveloped virion stimulates formation of actin-filled membranous protrusions called “tails,” and then disengages from the host cell.

Formation of actin tails occurs by a mechanism conserved amongst VV, MPX and VarV (53). EV recruit host Abl- and Src- family tyrosine kinases (38, 39, 52), which

phosphorylate viral protein A36 at residues 112 and 132, thereby facilitating recruitment of Nck, Grb2, WIP and N-WASP (12, 13, 36, 61, 74). Interactions with PI(4,5)P₂ in the plasma membrane induce conformational changes in N-WASP, which allow the protein to bind to and activate Arp2/3 complex, a nucleator for actin polymerization (36, 60). The rate of actin tail formation and length appear to be a function of the turnover rate and interactions amongst viral factors and recruited host proteins (8, 74).

While much information is available about the viral and host factors that initiate actin polymerization, much less is known about the viral and host factors that contribute to virion release. Based on mutation experiments, several viral factors (including F12, F13, A33, A34, B5, and A36) have been implicated in viral release (65), although in many cases, such mutations also affect actin tail formation or specific infectivity thereby precluding unequivocal determination of the role these proteins play in release. That virus release also depends on cell type (35, 42), indicates that host factors also participate. Reeves *et al.* separated actin motility from release by demonstrating that redundant Src- and Abl-family tyrosine kinases mediate tail formation, whereas only Abl-family kinases mediate release (52).

Previous work from our lab and others has implicated PI 3-kinase activities at several distinct steps of viral maturation, though not in formation of actin tails nor in release (34, 68, 79). Nevertheless, the observation that host proteins involved with vesicular trafficking, such as Alix, Tsg101 and eps15, also affect poxviral spread (21) suggest lipid signaling may regulate viral dissemination. In this regard, we considered the possibility that other lipid and phosphoinositide (PI) signaling molecules, such as phosphatases, might also participate in virion release.

SHIP2 and its related isoform SHIP1 are SH2 domain-containing inositol polyphosphate 5-phosphatases (7, 26, 30, 31, 45). Whereas SHIP1 is expressed in hematopoietic cells, SHIP2 is expressed ubiquitously (17, 63). Both isoforms exhibit PI 5-phosphatase activity with respect to PI(3,4,5)P₃ and PI(4,5)P₂ as substrates (5, 15, 17, 37, 47, 70, 75) Originally identified as a negative regulator of insulin signaling (6), SHIP2 mutations have also been linked to metabolic disorders, including, type II diabetes (22-24, 32, 64). In addition, SHIP2 has also been implicated in regulating cytoskeletal organization and endocytosis (37, 49, 66, 78). Furthermore, Smith *et al.* demonstrated that SHIP2 localizes to actin protrusions, called pedestals, which form beneath enteropathogenic *E. coli* (EPEC), and that reduction of SHIP2 levels causes an aberrant pedestal structure (66).

Here we demonstrate that SHIP2 localizes beneath VV during actin tail formation in a manner that depends on both tyrosine kinases and N-WASP, but not actin. We also show that SHIP2 negatively regulates release of virions, and may act as a host defense molecule that limits poxvirus dissemination.

RESULTS

The inositol phosphatase SHIP2 localizes to VV actin tails. To explore a role for PI signaling in actin tail formation and virion release, we first assessed whether PI kinases or phosphatases localized beneath virions. We could not detect localization of Type I PI 3-kinases with several antisera (data not shown). However, an endogenous protein recognized by an antibody to the phosphoinositide phosphatase SHIP2 was enriched relative to the cytoplasm at the tips of actin tails and directly apposed to the virion

(Figure 1A, A'). Localization of SHIP2 was apparent in the majority of actin tails in BSC40 cells. The localization appeared specific, as antisera that detects SHIP1 but not SHIP2, did not recognize epitopes in actin tails (Figure 1B). Western analysis confirmed that SHIP1 was not expressed at detectable levels in BSC40 cells in contrast to SHIP2 (Figure S1A,B). However, exogenously expressed SHIP1 did localize to tails in BSC40 cells (Figure S1C).

To identify the domains of SHIP2 necessary for recruitment to actin tails, we transiently transfected vectors expressing SHIP2-WT or SHIP2 variants containing point mutations or deletions of particular domains into BSC40 cells (Figure 1C). Overexpressed SHIP2-WT (Figure 1D) localized to the tops of tails, as did a phosphatase dead mutant (D607A) (Figure 1E), and a SAM domain deletion mutant (SHIP2- Δ SAM; Figure 1F). The localization of SHIP2- Δ SAM to actin tails appeared consistent with the localization of exogenous SHIP1, which lacks a SAM domain (Figure S1C). By contrast, SHIP2 lacking the SH2 domain (SHIP2- Δ SH2) did not localize to actin tails (Figure 1G). Together, these data suggest that the SH2 domain is required for localization of SHIP2 to actin tails; however, neither phosphatase activity nor the SAM domain appear to be required for localization.

Localization of SHIP2 requires Abl- and Src family tyrosine kinases and N-WASP, but not actin. Observations with SHIP2- Δ SH2 indicated that tyrosine phosphorylation might be required for localization of SHIP2 to actin tails. We next assessed whether localization of SHIP2 was evident in cell lines lacking particular tyrosine kinases, or in cells treated with tyrosine kinase inhibitors. SHIP2 remained localized to actin tails formed on Abl1^{-/-}Abl2^{-/-} cells, Src^{-/-}Fyn^{-/-}Yes^{-/-} cells, and on cells treated with 10 μ M

imatinib mesylate (STI-571 or Gleevec), an inhibitor of Abl-family kinases (Figure 2A) (62). However, in cells treated with dasitinib (BMS-354825 or Sprycel), an inhibitor of both Abl- and Src-family kinases and actin tails (53), no localization of SHIP2 was evident apposed to virions (Figure 2B).

To determine whether localization of SHIP2 requires other components of VV actin tails, we next assessed SHIP2 localization in fibroblast cell lines derived from N-WASP^{fl/fl} or N-WASP^{-/-} mice, and infected with VV. Cell lines deficient in N-WASP fail to form tails (67); therefore, we measured the colocalization of SHIP2 with phosphotyrosine and α -B5, components of cell-associated virions. In N-WASP^{fl/fl} cells, 25% of virions colocalized with both SHIP2 and phosphotyrosine (Figure 2C,D and Figure S2). In contrast, only 1.9% of virions lacking a phosphotyrosine signal colocalized with SHIP2. In N-WASP^{-/-} cells, the percentage of virions colocalizing with SHIP2 was similar whether phosphotyrosine was present or not (1.8-2.7%), and similar to that observed in N-WASP^{fl/fl} cells for virions lacking phosphotyrosine. This data suggests that N-WASP and phosphotyrosine together are required for localization of SHIP2. To rule out the possibility that localization of SHIP2 required the Arp2/3 complex or actin, we assessed localization of SHIP2 in BSC40 cells expressing N-WASP- Δ CA, which fails to recruit the Arp2/3 complex and thereby precludes formation of actin tails (25). As shown in Figure 2E, SHIP2, N-WASP- Δ CA, and the virion (detected with α -B5 mAb) colocalized. Collectively, these data suggest that: (i) activity of Abl- or Src-family kinases, perhaps acting redundantly (52), is required for localization of SHIP2; and (ii) localization depends on N-WASP but not the Arp2/3 complex nor actin. The interaction between SHIP2 and N-WASP appears to be indirect as we were unable to detect a direct

association of SHIP2 with N-WASP in immunoprecipitation experiments (data not shown).

SHIP2 does not regulate formation of actin tails. Localization of SHIP2 beneath virions on actin tails raised the possibility that the protein might regulate either actin tails or virion release or both. To test these possibilities, we first assessed actin tails in embryonic fibroblasts derived from SHIP2^{+/+} and SHIP2^{-/-} mice. As shown in Figure 3A, the number and size of actin tails appeared similar in the two cell types, as did the velocities of virions on tails (data not shown). We confirmed that SHIP2 was not expressed in the SHIP2^{-/-} cells by Western blot analysis, and that SHIP2 was evident only on the tops of actin tails found in SHIP2^{+/+} but not in SHIP2^{-/-} cells (Figure S3). Previous work by Smith *et al.* identified two interactors of SHIP2, SHC and LPD that localize to EPEC pedestals (66) and Krause *et al.* identified LPD as localizing to VV actin tails (29). We confirmed that LPD, as well as SHC localized to the tips of VV tails (Figure S4A,B). However, SHC and LPD were recruited to tails in both SHIP2^{+/+} cells and SHIP2^{-/-} cells. Together, these data suggest that SHIP2 is neither required for formation of actin tails, nor for the recruitment of LPD or SHC.

SHIP2 Regulates Virion Dissemination by Inhibiting Release of EEV. We next investigated the effects of SHIP2 on plaque formation. To do this, SHIP2^{+/+} or SHIP2^{-/-} cells were infected with VV strain, IHD-J, which releases large numbers of EEV (3). Plaques formed by IHD-J are similar in size to those seen with other strains (e.g. WR), and are evident 32 hrs post infection (e.g. Figure 3B, upper panel). However, unlike WR, IHD-J plaques are associated with an archipelago of smaller plaques, termed “comets,” which are evident 48 hours after infection, and indicative of enhanced EEV release in this

strain (1, 18). Characteristic plaques formed by IHD-J were evident on SHIP2^{+/+} and SHIP2^{-/-} cells by 32 hours (Figure 3B, upper panel), though plaques were slightly larger on SHIP2^{-/-} cells. Comets visualized at 48 hours post infection were significantly larger in SHIP2^{-/-} cells compared to those on SHIP2^{+/+} cells, often merging with adjacent comets and extending across the plate (Figure 3B, lower panel). We next measured the amount of EEV released by SHIP2^{+/+} or SHIP2^{-/-} cells into the supernatant. In accordance with the plaque assays, ~3-fold more EEV and CAV grew in SHIP2^{-/-} cells compared to SHIP2^{+/+} cells at low MOI (0.01) (Figure 3C), consistent with increased viral spread in the monolayer. We did not observe a difference in the ratio of EEV:CAV between both cell types, and viral replication was similar at MOI of 5 suggesting that the SHIP2 does not affect viral replication (data not shown). To corroborate data from SHIP2^{-/-} cells, we next knocked down SHIP2 in BSC40 cells. BSC40 cells treated with either of three siRNAs specific to SHIP2 (sequences 2, 3, 4) exhibited larger comets than those seen with Negative siRNA, the transfection reagent (RNAiMAX), or untreated cells (Figure 3D). Knockdown of SHIP2 was confirmed by Western analysis (Figure 3E).

To confirm that the large comets formed on the SHIP2^{-/-} cells were specifically due to increased release of EEV, we carried out two additional experiments. Reeves *et al.* found that release of EEV required activity of Abl-family tyrosine kinases (52). In accordance with the idea that more EEV are released from SHIP2^{-/-} cells than SHIP2^{+/+} cells, we found that the Abl-family tyrosine kinase inhibitor imatinib mesylate blocked comets in SHIP2^{+/+} cells and reduced the size and extent of comets in SHIP2^{-/-} cells (Figure 4A). Second, we infected both cells types with WR vRB12, a virus lacking F13L (2), a gene required to form EEV and comets. As shown in Figure 4B, vRB12 formed

similar sized plaques on both SHIP2^{+/+} and SHIP2^{-/-} cells, but did not form comets on either cell type. We could find no evidence to support the possibility that differences in infectivity or rates of cellular migration could account for the apparent increase in size of comets in SHIP2^{-/-} cells. Specific infectivity of VV produced in SHIP2^{-/-} and SHIP2^{+/+} cells was similar, as was the numbers of plaques formed on both cell types, and no differences in rates of movement of SHIP2^{+/+} and SHIP2^{-/-} cells were evident (data not shown). Collectively, these data suggest that SHIP2 inhibits release of EEV.

VV Protein A34 mediates the effects of SHIP2 on inhibition of EEV release. The observation that deletion of A34 in VV enhances release of virus (33), suggests that A34, a component of EEV, acts as an inhibitor of release. In accordance with this idea, the VV strain IHD-J, which contains a mutation in A34, releases more EEV and forms larger comets than strain WR, and a WR strain containing A34 derived from IHD-J (called WI) forms larger comets than WR (3). The large comets evident in SHIP2^{-/-} cells compared to SHIP2^{+/+} cells led us to hypothesize that A34 may act via SHIP2. To test this possibility, we assessed the effects of WR and WI comets formed on SHIP2^{-/-} and SHIP2^{+/+} cells. As shown in Figure 4C, WR was unable to form comets on SHIP2^{+/+} cells, but did form comets on SHIP2^{-/-} cells (Figure 4C). WI produced small comets on SHIP2^{+/+} cells, but large comets on SHIP2^{-/-} cells (Figure 4D), reminiscent of those seen with IHD-J in these cells (Figure 3B). We hypothesized that the capacity of IHD-J and WI to form larger comets than WR was due to differences in the recruitment of SHIP2 to actin tails in these strains. As shown in Figure 4E, an inverse correlation exists between EEV release and the efficacy of SHIP2 recruitment to actin tails. Thus, whereas strain WR recruited SHIP2 to 69% of actin tails, strains IHD-J and WI recruited SHIP2 to 54% and 49% of tails,

respectively, a statistically significant difference compared to WR ($p < 0.0003$, and $p < 0.0001$; Figure 4E). Collectively, these data suggest that (i) recruitment of SHIP2, via its SH2 domain, requires NWASP and Abl- and Src-family tyrosine kinases, but these proteins alone are not sufficient; ii) viral protein A34 recruits SHIP2 to actin tails; and (iii) that SHIP2 at least in part mediates inhibition of release by A34.

DISCUSSION

Here we explore the role of the phosphoinositide 5-phosphatase SHIP2 in release of VV from infected cells. We found that SHIP2 localizes to actin tails in an SH2-dependent manner, suggesting that phosphorylated tyrosines on cellular or viral proteins within the tail mediate recruitment. Host Src- and Abl-family kinases localize to and redundantly form tails (13, 52), and we find that these kinases are also required for recruitment of SHIP2 (Figure 2). Abl- but not Src-family kinases also appear to play a role in enhancing release of EEV (52). In this regard, comets formed on SHIP2^{+/+} and SHIP2^{-/-} cells are blocked by imatinib mesylate, a specific inhibitor of Abl-family kinases (52). Thus, Abl-family kinases play dual but antagonistic roles in EEV release, by both facilitating recruitment of a release inhibitor (SHIP2) and promoting virion release (Figure 5).

Src- and Abl-family tyrosine kinases phosphorylate the viral protein A36 at two sites suggesting that phosphorylated A36 may directly recruit SHIP2 (39). However, this seems unlikely because phospho-A36 recruits NWASP via Nck and WIP (13, 36), and SHIP2 recruitment also depends on NWASP. We cannot rule out the possibility that factors distal to NWASP may recruit SHIP2. Whereas Grb2 is one such candidate (61),

the Arp2/3 complex and actin do not appear to be involved as SHIP2 does not affect actin tails and NWASP- Δ CA, which does not recruit the Arp2/3 complex, still recruits SHIP2. In this regard, Smith *et al.* found that SHIP2 appears to regulate host lipids and actin polymerization in EPEC pedestals (66), which resemble actin tails formed by vaccinia (16). However, our data do not recapitulate the EPEC phenotype, suggesting that VV utilizes SHIP2 in a manner distinct from EPEC.

Still unresolved is whether SHIP2 inhibits virion release via its catalytic activity or, alternatively, serves as a scaffold to recruit effectors. Two known SHIP2 binding partners, SHC and LPD, are recruited to VV actin tails, though by a mechanism that appears to be independent of SHIP2 (Figure S3). Nevertheless, other SHIP2 effectors have been described including EGFR, filamin, p130Cas, Cbl, Vinexin, Arap3, APS, JIP-1, and Intersectin (11, 37, 40, 41, 46, 48, 50, 71, 76, 77).

Another possibility is that SHIP2 phosphatase activity is required to inhibit release of EEV. In this regard, we have attempted to localize PH domains that specifically recognize various PIPs on actin tails. Although some PH domains do appear to localize, point mutants that abolish binding to lipid moieties *in vitro* also localize, suggesting that recruitment is nonspecific (S.L.M. and D.K. unpublished). Furthermore, we have been unable to detect Akt-PH, Akt, or Akt-(P)S473 at the tops of tails (S.L.M. and D.K. unpublished). Notably, we cannot rule out the possibility that expression of the PH-domain alone does not compete effectively with intact proteins that utilize multiple binding sites, a phenomenon we observed previously with localization of proline rich regions and SH2 domains from tyrosine kinases in EPEC pedestals (4).

Do viral proteins participate with SHIP2 to regulate release of EEV? The observation that deletion of A34 or point mutations within A34 (K151E) enhance release of EEV (3) raises the possibility that the normal function of A34 is to suppress EEV release. Our data suggest that A34 mediates recruitment of SHIP2, and that SHIP2 at least in part mediates inhibition of release by A34 (Figure 4). A34 exists in a complex with viral proteins A33, A36, B5, and F13 (43, 44); therefore, it remains possible that SHIP2 tethers a complex of host and viral proteins that regulate viral release. Other intrinsic host defense molecules have been recently described including tetherin and viperin, which are induced in an interferon-dependent manner. Tetherin is antagonized by the HIV proteins VPU, and viperin by a cellular protein FPPS, which facilitates virion release (9) (72). By contrast, VV regulation of release through SHIP2 appears distinct. Rather than antagonizing release, A34 cooperates with SHIP2 to inhibit release. A34 is a transmembrane glycoprotein with homology to c-type lectins (10), and may detect the presence of leukocytes, cell adhesion molecules or endocytic receptors. In so doing, A34 may play a gatekeeper role so as to limit release except when environmental conditions are conducive to dissemination.

EXPERIMENTAL PROCEDURES

Cells, Viruses, and Reagents. BSC40, 3T3, Abl1^{-/-}Abl2^{-/-}, NWASP^{flf}, and NWASP^{-/-} cells (ATCC) were grown in DMEM (Cellgro, MediaTech, Inc; Manassas, VA) supplemented with 10%FBS (Atlanta Biologicals; Norcross, GA) and 10 IU/mL Penicillin and 10 µg/mL streptomycin (P/S; Cellgro, MediaTech, Inc.; Manassas, VA). Src^{-/-}Fyn^{-/-}Yes^{-/-} cells were grown in DMEM (Gibco; Carlsbad, CA) supplemented with

10% FBS and P/S. SHIP2^{+/+} and SHIP2^{-/-} cells were grown in DMEM (Gibco; Carlsbad, CA) supplemented with 10% FBS, P/S, and 1% of 50mM β -Mercaptoethanol in DPBS. All cells were grown at 37°C in a 5% CO₂ incubator. Mouse embryonic fibroblasts were isolated from embryos that were homozygous for a knockout of the SHIP2 (INPPL1) gene (6) and were prepared as reported in Zhang *et al.* (80) Viral strains were grown and propagated as previously described (52). All strains were titered on BSC40 cells.

Microscopy. Various cell lines used for microscopy were plated onto PDL/Collagen coated glass coverslips and infected with $\sim 10^6$ PFU WR or F13-gfp virus for 16 hours. After 16 hours, cells were fixed as previously described (52) and processed for microscopy. To detect DNA, cells were stained with 17 μ g/mL DAPI. Actin was visualized using Phalloidin-564 (Molecular Probes, Invitrogen; Carlsbad, CA). Antibodies for microscopy were used at the following dilutions: Anti-SHIP1 (Cell Signaling Technology; Beverly, MA), anti-SHIP2 (α -INPPL1, Novus Biologicals, Littleton, CO), anti-LPD (α -RAPH, Sigma; St. Louis, MO), and anti-SHC (BD Transduction Labs) were used at 1:50 dilution, anti-Xpress (Invitrogen; Carlsbad, CA) was used at 1:200, anti-PY (4G10, Millipore; Billerica, MA) and anti-Myc (9E10, Millipore; Billerica, MA) were used at 1:250, and anti-B5 was used at 1:5000 (a gift from Jay Hooper, USAMRIID). Tyrosine kinase inhibitors, imatinib mesylate and dasitinib, were added to cells at 10 μ M for 30 minutes after a 15.5 hour infection. For transfections, cells were transfected with various SHIP2 constructs (47, 80) or Myc-SHIP1 using FuGene 6 (Roche, Indianapolis, IN) for 48 hours.

Comet Assays. Experiments with vaccinia virus were conducted under BSL-2 conditions. 100PFU or 10PFU of vaccinia virus strain WR, IHD-J, vRB12 (WR Δ F13),

or WI was diluted in 500 μ L of 2% FBS/DMEM and added to monolayers of naïve BSC40, SHIP2^{+/+}, or SHIP2^{-/-} cells in 6 well dishes. Virus was allowed to adsorb to and enter the cells for one hour at 37°C in 5% CO₂. Unbound virus was then removed by washing monolayers with one mL PBS. Media was then replaced with 10% FBS/DMEM. Two days after infection, monolayers were fixed and stained with crystal violet solution (0.1% crystal violet and 20% ethanol).

EEV and CAV measurements. To quantify the amount of EEV and CAV produced SHIP2^{+/+} and SHIP2^{-/-} cells were grown in 6-well dishes in triplicate wells. Cell numbers were quantified and cells were infected at a multiplicity of infection (MOI) of 5 or 0.01 with strain IHD-J. Virus was diluted in 500 μ L of 2% FBS in DMEM and allowed to adsorb to cells for one hour. Unbound virus was then removed by washing cells three times with PBS, and then adding 1.5 mL of 10% FBS in DMEM. To quantify EEV, supernatant was removed at 24 or 48 hours later, spun at 400xg for 10 minutes to remove cells. IMV were neutralized with 1:1000 10F5 (anti-L1) antibody (a gift from Jay Hooper, USAMRIID) for one hour at 37°C; the supernatant was then diluted and added to naïve BSC40 cells monolayers, and plaques enumerated after two days. To quantify CAV, monolayers were scraped into one mL 2%FBS in DMEM, and virus was released through three freeze/thaw cycles. CAV were diluted and added to naïve BSC40 monolayers.

RNAi. To knockdown SHIP2 protein, BSC40 cells in duplicate 6-wells were transfected with 50nM RNA complementary to SHIP2 (INPPL1 ON-TARGET plus siRNA Human sequences 1, 2, 3, 4, Dharmacon) using RNAiMAX lipofectamine reagent (Invitrogen; Carlsbad, CA). After 3 days cells were infected with 100PFU VV, strain IHDJ, for 48

hours. After this time plaques were fixed and stained with crystal violet. To confirm protein knockdown BSC40 cells in duplicate 6-wells were transfected with 50nM RNA complementary to SHIP2 for three days and protein knockdown was confirmed by Western blot with anti-SHIP2 (α -INPPL1, 1:500, Novus Biologicals, Littleton, CO) and anti-Tubulin (1:5000, Abcam; Cambridge, MA).

Specific Infectivity. To determine specific infectivity, SHIP2^{+/+} and SHIP2^{-/-} cells were grown in three 150cm² tissue culture dishes, and infected with $\sim 10^8$ PFU/mL IHD-J for three days. To liberate virus, flasks were subjected to three freeze/thaw cycles. Media and cell debris was purified from media by spinning samples at 10,000 RPM in a JA-10 rotor for 1.25 hrs. Cell debris and virus was resuspended in two mL 2% FBS in DMEM. To remove cell debris, samples were spun at 400xg for 10 minutes. Virus was further purified through a 36% sucrose cushion, followed by two 25-40% sucrose gradients. Viral particles were quantified with OD₂₆₀, where one OD₂₆₀ = 1.2×10^{10} particles. To calculate infectious particles, purified virus was diluted in 2% FBS in DMEM and added to naïve monolayers, and the plaques enumerated two days later. Specific infectivity was calculated as 136.3 ± 46.5 particles/PFU for SHIP2^{+/+} cells and 80.0 ± 18.0 particles/PFU for SHIP2^{-/-} cells.

Western Blot Analysis. BSC40 or J774A.1 cells were grown in 10 cm tissue culture dishes. Cells were lysed in RIPA buffer (Cell Signaling; Beverly, MA), and the protein concentration determined using the Bio-Rad Dc Protein Assay Kit (Bio-Rad; Hercules, CA). 50 μ g of protein was separated by SDS-PAGE; proteins were then transferred to nitrocellulose membranes. Those were blocked with 3% BSA in Tris-buffered saline containing 0.5% Tween-20 (TBST) for one hour. Membranes were probed with anti-

SHIP1 (1:1000), anti-SHIP2 (1:500), or anti-Tubulin (1:5000, Abcam; Cambridge, MA) in blocking solution for an additional hour. Bands were detected using anti-Mouse or anti-Rabbit HRP conjugated antibodies (GE Healthcare; UK) and blots were developed using Pierce ECL Western Blotting Substrate (Thermo Scientific; Waltham, MA).

ACKNOWLEDGEMENTS

We thank Jay Hooper (USAMRIID) for sharing antibodies and Bernard Moss (NIH) for sharing the WI virus. We also thank Jack Taunton (UCSF) for sharing the NWAP^{f/f} and NWASP^{-/-} cells. Many thanks to Sam Speck, Eric Hunter, Victor Faundez, Aron Lukacher and Alyson Swimm (Emory University) for insightful comments and discussion. This work was supported by National Institutes of Health R56A105896101A2 and R01A107246201A2 to DK and by a grant from the Fonds de la Recherche Scientifique Médicale (FRSM) to CE.

REFERENCES

1. **Blasco, R., and B. Moss.** 1991. Extracellular vaccinia virus formation and cell-to-cell virus transmission are prevented by deletion of the gene encoding the 37,000-Dalton outer envelope protein. *J Virol* **65**:5910-20.
2. **Blasco, R., and B. Moss.** 1992. Role of cell-associated enveloped vaccinia virus in cell-to-cell spread. *J Virol* **66**:4170-9.
3. **Blasco, R., J. R. Sisler, and B. Moss.** 1993. Dissociation of progeny vaccinia virus from the cell membrane is regulated by a viral envelope glycoprotein: effect of a point mutation in the lectin homology domain of the A34R gene. *J Virol* **67**:3319-25.
4. **Bommarius, B., D. Maxwell, A. Swimm, S. Leung, A. Corbett, W. Bornmann, and D. Kalman.** 2007. Enteropathogenic *Escherichia coli* Tir is an SH2/3 ligand that recruits and activates tyrosine kinases required for pedestal formation. *Mol Microbiol* **63**:1748-68.
5. **Chi, Y., B. Zhou, W. Q. Wang, S. K. Chung, Y. U. Kwon, Y. H. Ahn, Y. T. Chang, Y. Tsujishita, J. H. Hurley, and Z. Y. Zhang.** 2004. Comparative mechanistic and substrate specificity study of inositol polyphosphate 5-phosphatase *Schizosaccharomyces pombe* Synaptojanin and SHIP2. *J Biol Chem* **279**:44987-95.
6. **Clement, S., U. Krause, F. Desmedt, J. F. Tanti, J. Behrends, X. Pesesse, T. Sasaki, J. Penninger, M. Doherty, W. Malaisse, J. E. Dumont, Y. Le Marchand-Brustel, C. Erneux, L. Hue, and S. Schurmans.** 2001. The lipid phosphatase SHIP2 controls insulin sensitivity. *Nature* **409**:92-7.
7. **Damen, J. E., L. Liu, P. Rosten, R. K. Humphries, A. B. Jefferson, P. W. Majerus, and G. Krystal.** 1996. The 145-kDa protein induced to associate with Shc by multiple cytokines is an inositol tetrakisphosphate and phosphatidylinositol 3,4,5-triphosphate 5-phosphatase. *Proc Natl Acad Sci U S A* **93**:1689-93.
8. **Dodding, M. P., and M. Way.** 2009. Nck- and N-WASP-dependent actin-based motility is conserved in divergent vertebrate poxviruses. *Cell Host Microbe* **6**:536-50.
9. **Douglas, J. L., J. K. Gustin, K. Viswanathan, M. Mansouri, A. V. Moses, and K. Fruh.** 2010. The great escape: viral strategies to counter BST-2/tetherin. *PLoS Pathog* **6**:e1000913.
10. **Duncan, S. A., and G. L. Smith.** 1992. Identification and characterization of an extracellular envelope glycoprotein affecting vaccinia virus egress. *J Virol* **66**:1610-21.
11. **Dyson, J. M., C. J. O'Malley, J. Becanovic, A. D. Munday, M. C. Berndt, I. D. Coghill, H. H. Nandurkar, L. M. Ooms, and C. A. Mitchell.** 2001. The SH2-containing inositol polyphosphate 5-phosphatase, SHIP-2, binds filamin and regulates submembraneous actin. *J Cell Biol* **155**:1065-79.
12. **Frischknecht, F., S. Cudmore, V. Moreau, I. Reckmann, S. Rottger, and M. Way.** 1999. Tyrosine phosphorylation is required for actin-based motility of vaccinia but not *Listeria* or *Shigella*. *Curr Biol* **9**:89-92.

13. **Frischknecht, F., V. Moreau, S. Rottger, S. Gonfloni, I. Reckmann, G. Superti-Furga, and M. Way.** 1999. Actin-based motility of vaccinia virus mimics receptor tyrosine kinase signalling. *Nature* **401**:926-9.
14. **Geda, M. M., I. Galindo, M. M. Lorenzo, B. Perdiguero, and R. Blasco.** 2001. Movements of vaccinia virus intracellular enveloped virions with GFP tagged to the F13L envelope protein. *J Gen Virol* **82**:2747-60.
15. **Giuriato, S., D. Blero, B. Robaye, C. Bruyns, B. Payraastre, and C. Erneux.** 2002. SHIP2 overexpression strongly reduces the proliferation rate of K562 erythroleukemia cell line. *Biochem Biophys Res Commun* **296**:106-10.
16. **Gouin, E., M. D. Welch, and P. Cossart.** 2005. Actin-based motility of intracellular pathogens. *Curr Opin Microbiol* **8**:35-45.
17. **Habib, T., J. A. Hejna, R. E. Moses, and S. J. Decker.** 1998. Growth factors and insulin stimulate tyrosine phosphorylation of the 51C/SHIP2 protein. *J Biol Chem* **273**:18605-9.
18. **Herrera, E., M. M. Lorenzo, R. Blasco, and S. N. Isaacs.** 1998. Functional analysis of vaccinia virus B5R protein: essential role in virus envelopment is independent of a large portion of the extracellular domain. *J Virol* **72**:294-302.
19. **Hollinshead, M., G. Rodger, H. Van Eijl, M. Law, R. Hollinshead, D. J. Vaux, and G. L. Smith.** 2001. Vaccinia virus utilizes microtubules for movement to the cell surface. *J Cell Biol* **154**:389-402.
20. **Hollinshead, M., A. Vanderplassen, G. L. Smith, and D. J. Vaux.** 1999. Vaccinia virus intracellular mature virions contain only one lipid membrane. *J Virol* **73**:1503-17.
21. **Honeychurch, K. M., G. Yang, R. Jordan, and D. E. Hrubby.** 2007. The vaccinia virus F13L YPPL motif is required for efficient release of extracellular enveloped virus. *J Virol* **81**:7310-5.
22. **Ishida, S., A. Funakoshi, K. Miyasaka, H. Shimokata, F. Ando, and S. Takiguchi.** 2006. Association of SH-2 containing inositol 5'-phosphatase 2 gene polymorphisms and hyperglycemia. *Pancreas* **33**:63-7.
23. **Kagawa, S., T. Sasaoka, S. Yaguchi, H. Ishihara, H. Tsuneki, S. Murakami, K. Fukui, T. Wada, S. Kobayashi, I. Kimura, and M. Kobayashi.** 2005. Impact of SRC homology 2-containing inositol 5'-phosphatase 2 gene polymorphisms detected in a Japanese population on insulin signaling. *J Clin Endocrinol Metab* **90**:2911-9.
24. **Kaisaki, P. J., M. Delepine, P. Y. Woon, L. Sebag-Montefiore, S. P. Wilder, S. Menzel, N. Vionnet, E. Marion, J. P. Riveline, G. Charpentier, S. Schurmans, J. C. Levy, M. Lathrop, M. Farrall, and D. Gauguier.** 2004. Polymorphisms in type II SH2 domain-containing inositol 5-phosphatase (INPPL1, SHIP2) are associated with physiological abnormalities of the metabolic syndrome. *Diabetes* **53**:1900-4.
25. **Kalman, D., O. D. Weiner, D. L. Goosney, J. W. Sedat, B. B. Finlay, A. Abo, and J. M. Bishop.** 1999. Enteropathogenic *E. coli* acts through WASP and Arp2/3 complex to form actin pedestals. *Nat Cell Biol* **1**:389-91.
26. **Kavanaugh, W. M., D. A. Pot, S. M. Chin, M. Deuter-Reinhard, A. B. Jefferson, F. A. Norris, F. R. Masiarz, L. S. Cousens, P. W. Majerus, and L.**

- T. Williams.** 1996. Multiple forms of an inositol polyphosphate 5-phosphatase form signaling complexes with Shc and Grb2. *Curr Biol* **6**:438-45.
27. **Khodakevich, L., Z. Jezek, and D. Messinger.** 1988. Monkeypox virus: ecology and public health significance. *Bull World Health Organ* **66**:747-52.
28. **Khodakevich, L., M. Szczeniowski, D. Manbu ma, Z. Jezek, S. Marennikova, J. Nakano, and D. Messinger.** 1987. The role of squirrels in sustaining monkeypox virus transmission. *Trop Geogr Med* **39**:115-22.
29. **Krause, M., J. D. Leslie, M. Stewart, E. M. Lafuente, F. Valderrama, R. Jagannathan, G. A. Strasser, D. A. Rubinson, H. Liu, M. Way, M. B. Yaffe, V. A. Boussiotis, and F. B. Gertler.** 2004. Lamellipodin, an Ena/VASP ligand, is implicated in the regulation of lamellipodial dynamics. *Dev Cell* **7**:571-83.
30. **Liubin, M. N., P. A. Algate, S. Tsai, K. Carlberg, A. Aebersold, and L. R. Rohrschneider.** 1996. p150Ship, a signal transduction molecule with inositol polyphosphate-5-phosphatase activity. *Genes Dev* **10**:1084-95.
31. **Liu, Y., and V. A. Bankaitis.** 2010. Phosphoinositide phosphatases in cell biology and disease. *Prog Lipid Res* **49**:201-17.
32. **Marion, E., P. J. Kaisaki, V. Pouillon, C. Gueydan, J. C. Levy, A. Bodson, G. Krzentowski, J. C. Daubresse, J. Mockel, J. Behrends, G. Servais, C. Szpirer, V. Kruys, D. Gauguier, and S. Schurmans.** 2002. The gene INPPL1, encoding the lipid phosphatase SHIP2, is a candidate for type 2 diabetes in rat and man. *Diabetes* **51**:2012-7.
33. **McIntosh, A. A., and G. L. Smith.** 1996. Vaccinia virus glycoprotein A34R is required for infectivity of extracellular enveloped virus. *J Virol* **70**:272-81.
34. **McNulty, S., W. Bornmann, J. Schriewer, C. Werner, S. K. Smith, V. A. Olson, I. K. Damon, R. M. Buller, J. Heuser, and D. Kalman.** 2010. Multiple phosphatidylinositol 3-kinases regulate vaccinia virus morphogenesis. *PLoS One* **5**:e10884.
35. **Meiser, A., D. Boulanger, G. Sutter, and J. Krijnse Locker.** 2003. Comparison of virus production in chicken embryo fibroblasts infected with the WR, IHD-J and MVA strains of vaccinia virus: IHD-J is most efficient in trans-Golgi network wrapping and extracellular enveloped virus release. *J Gen Virol* **84**:1383-92.
36. **Moreau, V., F. Frischknecht, I. Reckmann, R. Vincentelli, G. Rabut, D. Stewart, and M. Way.** 2000. A complex of N-WASP and WIP integrates signalling cascades that lead to actin polymerization. *Nat Cell Biol* **2**:441-8.
37. **Nakatsu, F., R. M. Perera, L. Lucast, R. Zoncu, J. Domin, F. B. Gertler, D. Toomre, and P. De Camilli.** 2010. The inositol 5-phosphatase SHIP2 regulates endocytic clathrin-coated pit dynamics. *J Cell Biol* **190**:307-15.
38. **Newsome, T. P., N. Scaplehorn, and M. Way.** 2004. SRC mediates a switch from microtubule- to actin-based motility of vaccinia virus. *Science* **306**:124-9.
39. **Newsome, T. P., I. Weisswange, F. Frischknecht, and M. Way.** 2006. Abl collaborates with Src family kinases to stimulate actin-based motility of vaccinia virus. *Cell Microbiol* **8**:233-41.

40. **Onnockx, S., J. De Schutter, M. Blockmans, J. Xie, C. Jacobs, J. M. Vanderwinden, C. Erneux, and I. Pirson.** 2008. The association between the SH2-containing inositol polyphosphate 5-Phosphatase 2 (SHIP2) and the adaptor protein APS has an impact on biochemical properties of both partners. *J Cell Physiol* **214**:260-72.
41. **Paternotte, N., J. Zhang, I. Vandenbroere, K. Backers, D. Blero, N. Kioka, J. M. Vanderwinden, I. Pirson, and C. Erneux.** 2005. SHIP2 interaction with the cytoskeletal protein Vinexin. *Febs J* **272**:6052-66.
42. **Payne, L. G.** 1979. Identification of the vaccinia hemagglutinin polypeptide from a cell system yielding large amounts of extracellular enveloped virus. *J Virol* **31**:147-55.
43. **Perdiguero, B., and R. Blasco.** 2006. Interaction between vaccinia virus extracellular virus envelope A33 and B5 glycoproteins. *J Virol* **80**:8763-77.
44. **Perdiguero, B., M. M. Lorenzo, and R. Blasco.** 2008. Vaccinia virus A34 glycoprotein determines the protein composition of the extracellular virus envelope. *J Virol* **82**:2150-60.
45. **Pesesse, X., S. Deleu, F. De Smedt, L. Drayer, and C. Erneux.** 1997. Identification of a second SH2-domain-containing protein closely related to the phosphatidylinositol polyphosphate 5-phosphatase SHIP. *Biochem Biophys Res Commun* **239**:697-700.
46. **Pesesse, X., V. Dewaste, F. De Smedt, M. Laffargue, S. Giuriato, C. Moreau, B. Payrastre, and C. Erneux.** 2001. The Src homology 2 domain containing inositol 5-phosphatase SHIP2 is recruited to the epidermal growth factor (EGF) receptor and dephosphorylates phosphatidylinositol 3,4,5-trisphosphate in EGF-stimulated COS-7 cells. *J Biol Chem* **276**:28348-55.
47. **Pesesse, X., C. Moreau, A. L. Drayer, R. Woscholski, P. Parker, and C. Erneux.** 1998. The SH2 domain containing inositol 5-phosphatase SHIP2 displays phosphatidylinositol 3,4,5-trisphosphate and inositol 1,3,4,5-tetrakisphosphate 5-phosphatase activity. *FEBS Lett* **437**:301-3.
48. **Prasad, N., R. S. Topping, and S. J. Decker.** 2001. SH2-containing inositol 5'-phosphatase SHIP2 associates with the p130(Cas) adapter protein and regulates cellular adhesion and spreading. *Mol Cell Biol* **21**:1416-28.
49. **Prasad, N. K., and S. J. Decker.** 2005. SH2-containing 5'-inositol phosphatase, SHIP2, regulates cytoskeleton organization and ligand-dependent down-regulation of the epidermal growth factor receptor. *J Biol Chem* **280**:13129-36.
50. **Raaijmakers, J. H., L. Deneubourg, H. Rehmann, J. de Koning, Z. Zhang, S. Krugmann, C. Erneux, and J. L. Bos.** 2007. The PI3K effector Arap3 interacts with the PI(3,4,5)P3 phosphatase SHIP2 in a SAM domain-dependent manner. *Cell Signal* **19**:1249-57.
51. **Reed, K. D., J. W. Melski, M. B. Graham, R. L. Regnery, M. J. Sotir, M. V. Wegner, J. J. Kazmierczak, E. J. Stratman, Y. Li, J. A. Fairley, G. R. Swain, V. A. Olson, E. K. Sargent, S. C. Kehl, M. A. Frace, R. Kline, S. L. Foldy, J. P. Davis, and I. K. Damon.** 2004. The detection of monkeypox in humans in the Western Hemisphere. *N Engl J Med* **350**:342-50.

52. **Reeves, P. M., B. Bommarius, S. Lebeis, S. McNulty, J. Christensen, A. Swimm, A. Chahroudi, R. Chavan, M. B. Feinberg, D. Veach, W. Bornmann, M. Sherman, and D. Kalman.** 2005. Disabling poxvirus pathogenesis by inhibition of Abl-family tyrosine kinases. *Nat Med* **11**:731-9.
53. **Reeves, P. M., S. K. Smith, V. A. Olson, S. H. Thorne, W. Bornmann, I. K. Damon, and D. Kalman.** 2011. Variola and monkeypox utilize conserved mechanisms of virion motility and release that depend on Abl- and Src-family tyrosine kinases. *Journal of Virology* **85**.
54. **Rietdorf, J., A. Ploubidou, I. Reckmann, A. Holmstrom, F. Frischknecht, M. Zettl, T. Zimmermann, and M. Way.** 2001. Kinesin-dependent movement on microtubules precedes actin-based motility of vaccinia virus. *Nat Cell Biol* **3**:992-1000.
55. **Rimoin, A. W., N. Kisalu, B. Kebela-Ilunga, T. Mukaba, L. L. Wright, P. Formenty, N. D. Wolfe, R. L. Shongo, F. Tshioko, E. Okitolonda, J. J. Muyembe, R. W. Ryder, and H. Meyer.** 2007. Endemic human monkeypox, Democratic Republic of Congo, 2001-2004. *Emerg Infect Dis* **13**:934-7.
56. **Rimoin, A. W., P. M. Mulembakani, S. C. Johnston, J. O. Smith, N. K. Kisalu, T. L. Kinkela, S. Blumberg, H. A. Thomassen, B. L. Pike, J. N. Fair, N. D. Wolfe, R. L. Shongo, B. S. Graham, P. Formenty, E. Okitolonda, L. E. Hensley, H. Meyer, L. L. Wright, and J. J. Muyembe.** 2010. Major increase in human monkeypox incidence 30 years after smallpox vaccination campaigns cease in the Democratic Republic of Congo. *Proc Natl Acad Sci U S A*.
57. **Risco, C., J. R. Rodriguez, C. Lopez-Iglesias, J. L. Carrascosa, M. Esteban, and D. Rodriguez.** 2002. Endoplasmic reticulum-Golgi intermediate compartment membranes and vimentin filaments participate in vaccinia virus assembly. *J Virol* **76**:1839-55.
58. **Roberts, K. L., and G. L. Smith.** 2008. Vaccinia virus morphogenesis and dissemination. *Trends Microbiol* **16**:472-9.
59. **Rodriguez, J. R., C. Risco, J. L. Carrascosa, M. Esteban, and D. Rodriguez.** 1997. Characterization of early stages in vaccinia virus membrane biogenesis: implications of the 21-kilodalton protein and a newly identified 15-kilodalton envelope protein. *J Virol* **71**:1821-33.
60. **Rohatgi, R., H. Y. Ho, and M. W. Kirschner.** 2000. Mechanism of N-WASP activation by CDC42 and phosphatidylinositol 4, 5-bisphosphate. *J Cell Biol* **150**:1299-310.
61. **Scaplehorn, N., A. Holmstrom, V. Moreau, F. Frischknecht, I. Reckmann, and M. Way.** 2002. Grb2 and Nck act cooperatively to promote actin-based motility of vaccinia virus. *Curr Biol* **12**:740-5.
62. **Schindler, T., W. Bornmann, P. Pellicena, W. T. Miller, B. Clarkson, and J. Kuriyan.** 2000. Structural mechanism for STI-571 inhibition of abelson tyrosine kinase. *Science* **289**:1938-42.
63. **Schurmans, S., R. Carrio, J. Behrends, V. Pouillon, J. Merino, and S. Clement.** 1999. The mouse SHIP2 (Inpp1) gene: complementary DNA, genomic structure, promoter analysis, and gene expression in the embryo and adult mouse. *Genomics* **62**:260-71.

64. **Sleeman, M. W., K. E. Wortley, K. M. Lai, L. C. Gowen, J. Kintner, W. O. Kline, K. Garcia, T. N. Stitt, G. D. Yancopoulos, S. J. Wiegand, and D. J. Glass.** 2005. Absence of the lipid phosphatase SHIP2 confers resistance to dietary obesity. *Nat Med* **11**:199-205.
65. **Smith, G. L., A. Vanderplassen, and M. Law.** 2002. The formation and function of extracellular enveloped vaccinia virus. *J Gen Virol* **83**:2915-31.
66. **Smith, K., D. Humphreys, P. J. Hume, and V. Koronakis.** 2010. Enteropathogenic *Escherichia coli* recruits the cellular inositol phosphatase SHIP2 to regulate actin-pedestal formation. *Cell Host Microbe* **7**:13-24.
67. **Snapper, S. B., F. Takeshima, I. Anton, C. H. Liu, S. M. Thomas, D. Nguyen, D. Dudley, H. Fraser, D. Purich, M. Lopez-Illasaca, C. Klein, L. Davidson, R. Bronson, R. C. Mulligan, F. Southwick, R. Geha, M. B. Goldberg, F. S. Rosen, J. H. Hartwig, and F. W. Alt.** 2001. N-WASP deficiency reveals distinct pathways for cell surface projections and microbial actin-based motility. *Nat Cell Biol* **3**:897-904.
68. **Soares, J. A., F. G. Leite, L. G. Andrade, A. A. Torres, L. P. De Sousa, L. S. Barcelos, M. M. Teixeira, P. C. Ferreira, E. G. Kroon, T. Souto-Padron, and C. A. Bonjardim.** 2009. Activation of the PI3K/Akt pathway early during vaccinia and cowpox virus infections is required for both host survival and viral replication. *J Virol* **83**:6883-99.
69. **Sodeik, B., R. W. Doms, M. Ericsson, G. Hiller, C. E. Machamer, W. van 't Hof, G. van Meer, B. Moss, and G. Griffiths.** 1993. Assembly of vaccinia virus: role of the intermediate compartment between the endoplasmic reticulum and the Golgi stacks. *J Cell Biol* **121**:521-41.
70. **Taylor, V., M. Wong, C. Brandts, L. Reilly, N. M. Dean, L. M. Cowser, S. Moodie, and D. Stokoe.** 2000. 5' phospholipid phosphatase SHIP-2 causes protein kinase B inactivation and cell cycle arrest in glioblastoma cells. *Mol Cell Biol* **20**:6860-71.
71. **Vandenbroere, I., N. Paternotte, J. E. Dumont, C. Erneux, and I. Pirson.** 2003. The c-Cbl-associated protein and c-Cbl are two new partners of the SH2-containing inositol polyphosphate 5-phosphatase SHIP2. *Biochem Biophys Res Commun* **300**:494-500.
72. **Wang, X., E. R. Hinson, and P. Cresswell.** 2007. The interferon-inducible protein viperin inhibits influenza virus release by perturbing lipid rafts. *Cell Host Microbe* **2**:96-105.
73. **Ward, B. M., and B. Moss.** 2001. Vaccinia virus intracellular movement is associated with microtubules and independent of actin tails. *J Virol* **75**:11651-63.
74. **Weisswange, I., T. P. Newsome, S. Schleich, and M. Way.** 2009. The rate of N-WASP exchange limits the extent of ARP2/3-complex-dependent actin-based motility. *Nature* **458**:87-91.
75. **Wisniewski, D., A. Strife, S. Swendeman, H. Erdjument-Bromage, S. Geromanos, W. M. Kavanaugh, P. Tempst, and B. Clarkson.** 1999. A novel SH2-containing phosphatidylinositol 3,4,5-trisphosphate 5-phosphatase (SHIP2) is constitutively tyrosine phosphorylated and associated with src

- homologous and collagen gene (SHC) in chronic myelogenous leukemia progenitor cells. *Blood* **93**:2707-20.
76. **Xie, J., S. Onnockx, I. Vandenbroere, C. Degraef, C. Erneux, and I. Pirson.** 2008. The docking properties of SHIP2 influence both JIP1 tyrosine phosphorylation and JNK activity. *Cell Signal* **20**:1432-41.
 77. **Xie, J., I. Vandenbroere, and I. Pirson.** 2008. SHIP2 associates with intersectin and recruits it to the plasma membrane in response to EGF. *FEBS Lett* **582**:3011-7.
 78. **Yu, J., H. Peng, Q. Ruan, A. Fatima, S. Getsios, and R. M. Lavker.** 2010. MicroRNA-205 promotes keratinocyte migration via the lipid phosphatase SHIP2. *FASEB J.*
 79. **Zaborowska, I., and D. Walsh.** 2009. PI3K signaling regulates rapamycin-insensitive translation initiation complex formation in vaccinia virus-infected cells. *J Virol* **83**:3988-92.
 80. **Zhang, J., Z. Liu, J. Rasschaert, D. Blero, L. Deneubourg, S. Schurmans, C. Erneux, and X. Pesesse.** 2007. SHIP2 controls PtdIns(3,4,5)P(3) levels and PKB activity in response to oxidative stress. *Cell Signal* **19**:2194-200.

FIGURE LEGENDS

Figure 1. SHIP2 is recruited to VV actin tails via its SH2 domain.

(A) Images of BSC40 cells were infected with VV and stained with antibodies recognizing endogenous SHIP2. Inset in A' shows magnification of boxed region in (A).

(B) Images of BSC40 cells infected with VV and stained with antibodies recognizing endogenous SHIP1. See also Figure S1.

(C) Domain organization of SHIP2 and SHIP2 mutants.

(D-G) Images of BSC40 cells expressing Xpress-SHIP2WT (D), or SHIP2 mutants Xpress-SHIP2D607A (E), Xpress-SHIP2 Δ SAM (F), or Xpress-SHIP2 Δ SH2 (G). Note that deletion of the SH2 domain prevents localization to actin tails. Insets below each image show magnification of boxed region. Scale bars represent 10 μ m.

Figure 2. Localization of SHIP2 requires Abl- and Src family tyrosine kinases and N-WASP, but not actin.

(A) Images of endogenous SHIP2 in actin tails on 3T3 cells. 3T3 cells treated with 10 μ M imatinib mesylate, which inhibits Abl1 and Abl2, Abl1^{-/-} Abl2^{-/-} cells or Src^{-/-}Fyn^{-/-} Yes^{-/-} cells. Scale bars represent 2 μ m.

(B) Endogenous SHIP2 does not appear localized on F13-GFP positive virions following dasatinib treatment, which inhibits both Src- and Abl-family kinases and blocks actin tails. Scale bars represent 2 μ m.

(C) Images of colocalization of SHIP2 with vaccinia virus protein B5 and phosphotyrosine (PY) in NWASP^{f/f} or NWASP^{-/-} cells. Arrows indicate colocalization of

all three proteins, and inset is a magnification of the indicated virion. Scale bars represent 5 μm . See also Figure S2.

(D) Quantification of colocalization of B5 fluorescence, SHIP2, and PY in images such as in (C). Data are expressed as percent of total virions on which SHIP2 was colocalized with B5 with or without PY staining in NWASP^{fl/fl} cells (n=1244 virions) and NWASP^{-/-} cells (n=1133 virions).

(E) Localization of SHIP2 to virions does not require actin. BSC40 cells were transfected with pNWASP-WT-HA or pNWASP- Δ CA-HA and infected with VV. Colocalization of SHIP2 with B5 was evident in cells transfected with either NWASP-WT-HA or NWASP- Δ CA-HA. Scale bars represent 2 μm .

Figure 3. SHIP2 regulates virion dissemination independent of actin tail formation.

(A) VV forms actin tails on SHIP2^{+/+} cells and SHIP2^{-/-} cells. Cells were stained for actin (red) and DNA (blue). Scale bars represent 10 μm . See also Figures S3 and S4.

(B) VV strain IHD-J forms larger comet tails in SHIP2^{-/-} cells than SHIP2^{+/+} cells. Cells were infected for 32 hours (upper panels, 60X) or 48 hours (lower panels, 10X), and stained with crystal violet to visualize plaques.

(C) Quantification of extracellular enveloped virions (EEV) and cell-associated virions (CAV) from SHIP2^{+/+} and SHIP2^{-/-} cells at 24 and 48 hours post infection.

(D) SHIP2 knockdown with siRNA enhances virion release relative to control cells. BSC40 cells were left untreated, or treated with lipofectamine reagent (RNAiMAX), Negative siRNA, or either of three siRNAs that target SHIP2 (#2, #3, or #4) for 3 days,

and infected with VV strain IHD-J for 2 days and stained and visualized at 16X magnification.

(E) Upper Panel: western analysis with SHIP2 antisera of lysates of BSC40 cells left untreated or treated as in (D). Lower panel: western analysis of lysates with tubulin antisera to confirm equivalent loading of samples.

Figure 4. A34 and SHIP2 negatively regulate virion dissemination.

(A) Release of virions from SHIP2^{+/+} and SHIP2^{-/-} cells is sensitive to imatinib mesylate. Cells were infected with VV IHD-J for 48 hours post infection and stained with crystal violet. Plaques were visualized by microscopy at 16X magnification. Imatinib mesylate (10 μ M) was added to cells at 1 hour post infection.

(B) Comets formed on SHIP2^{+/+} and SHIP2^{-/-} cells are specifically due to EEV. Cells were infected for 72 hours with WR vRB12, a virus lacking the F13L gene, and unable to form EEV. Although plaques formed on the two cell types were of similar size, no comets were evident. Plaques were visualized at 60X magnification.

(C) Plaques formed by VV strain WR on SHIP2^{+/+} and SHIP2^{-/-} cells 48 hours post infection (10X).

(D) Plaques formed by VV strain WI on SHIP2^{+/+} and SHIP2^{-/-} cells 48 hours post infection (10X).

(E) Quantification of SHIP2 recruitment to actin tails in cells infected with VV strains WR, IHD-J or WI. WR (n=2597 tails, 45 cells) recruits more SHIP2 to tails than IHD-J (n=2046 tails, 58 cells) (p=0.0003) or WI (n=2763 tails, 32 cells) (p=0.0001).

Supplementary Figure 1. SHIP1/2 Expression and Myc-SHIP1 Localization in BSC40 Cells, related to Figure 1.

(A) Endogenous SHIP2 expression in BSC40 cells. 50µg total cellular protein was separated by SDS-PAGE, transferred to nitrocellulose and probed with antibodies specific to SHIP2.

(B) Endogenous SHIP1 expression in BSC40 and J774A.1 cells. 50µg total cellular protein was separated by SDS-PAGE, transferred to nitrocellulose and probed with antibodies specific to SHIP1.

(C) Exogenously expressed SHIP1 localizes to VV actin tails. Cells were transfected with pMyc-SHIP1 for 32 hours and infected with VV for 16 hours. Cells were stained with DAPI (DNA), cy3-phalloidin (actin), and anti-myc. Scale bars represent 10 µm.

Supplementary Figure 2: Images of SHIP2 with vaccinia virus protein B5 and phosphotyrosine (PY) colocalization in NWASP^{fl/fl} or NWASP^{-/-} cells, related to Figure 2. Arrows indicate colocalization of all three proteins. Scale bars represent 5 µm.

Supplementary Figure 3. Endogenous SHIP2 localization in SHIP2^{+/+} and SHIP2^{-/-} cells, related to Figure 3.

(A) Cells were infected with VV strain WR for 16 hours, fixed and stained with antibodies recognizing endogenous SHIP2. Scale bars represent 10 µm and inset scale bar represents 5 µm.

(B) Uninfected SHIP2^{+/+} and SHIP2^{-/-} cells fixed and stained with antibodies recognizing endogenous SHIP2. Scale bars represent 10 μm .

Supplementary Figure 4. Localization of putative SHIP2 effectors LPD and SHC to VV actin tails appears independent of SHIP2, related to Figure 3.

(A-B) SHIP2^{+/+} or SHIP2^{-/-} cells were infected with VV strain WR for 16 hours, then fixed and stained with antibodies recognizing endogenous LPD (A) or endogenous SHC (B). Scale bars represent 5 μm .

Figure 1

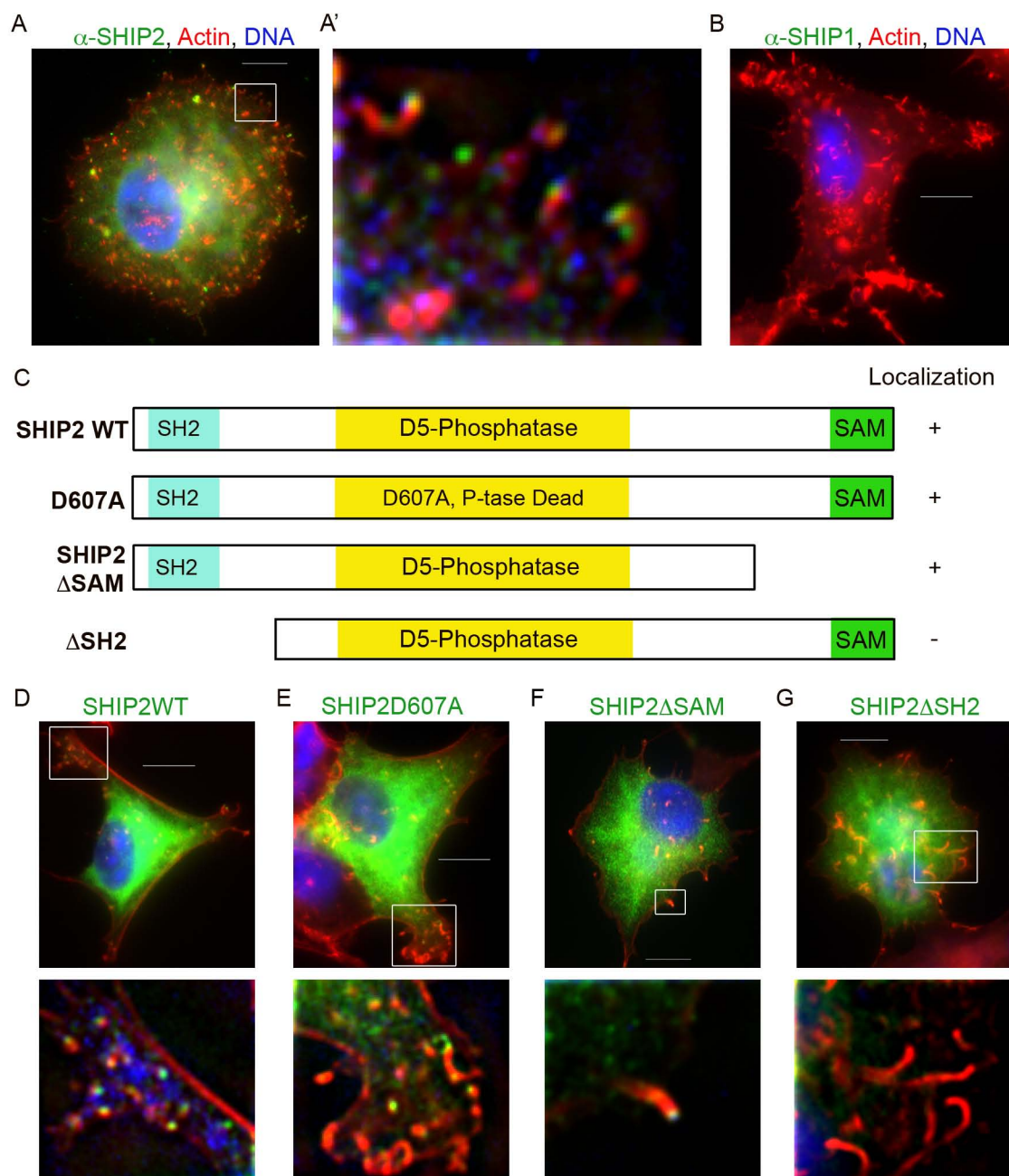


Figure 2

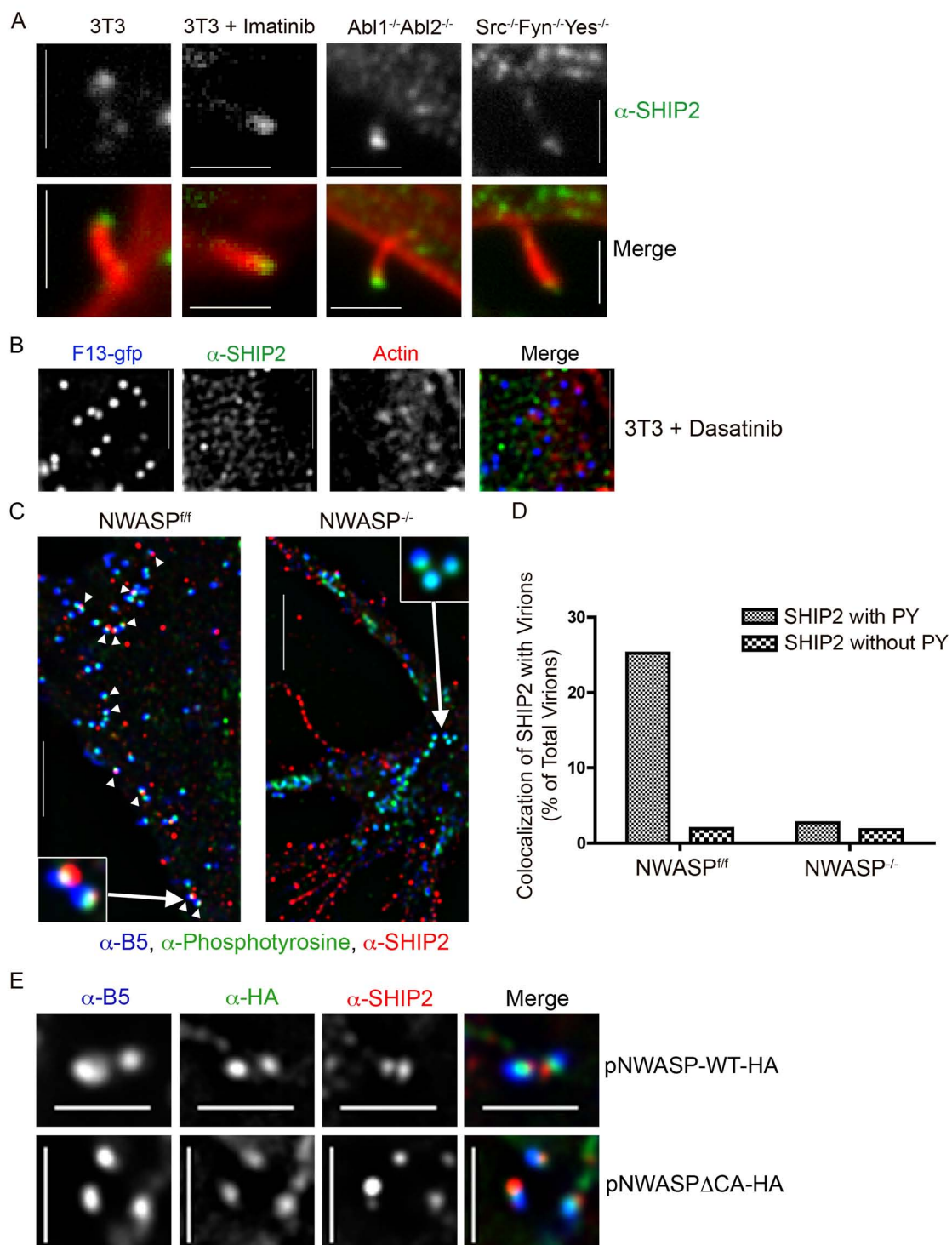


Figure 3

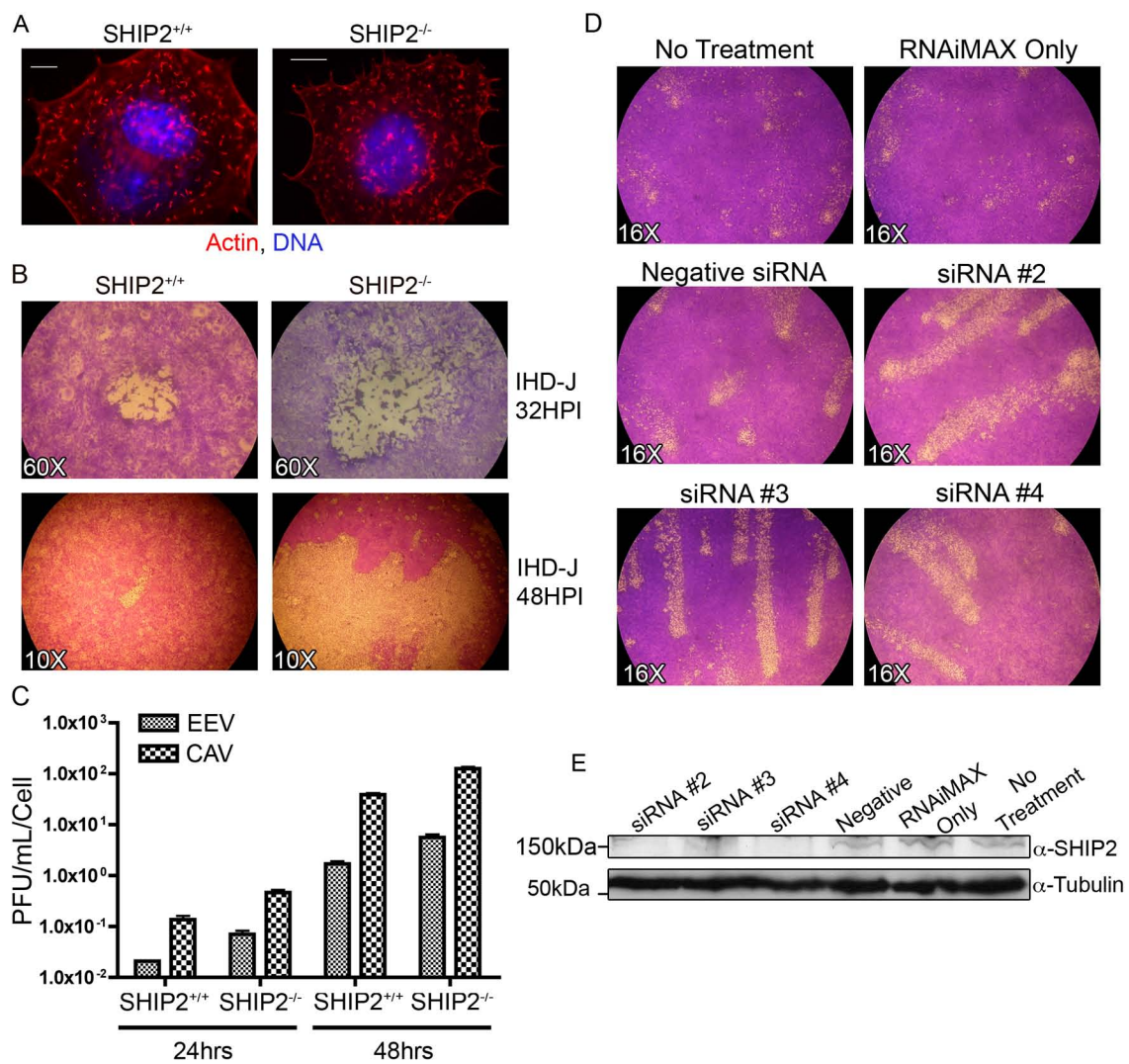


Figure 4

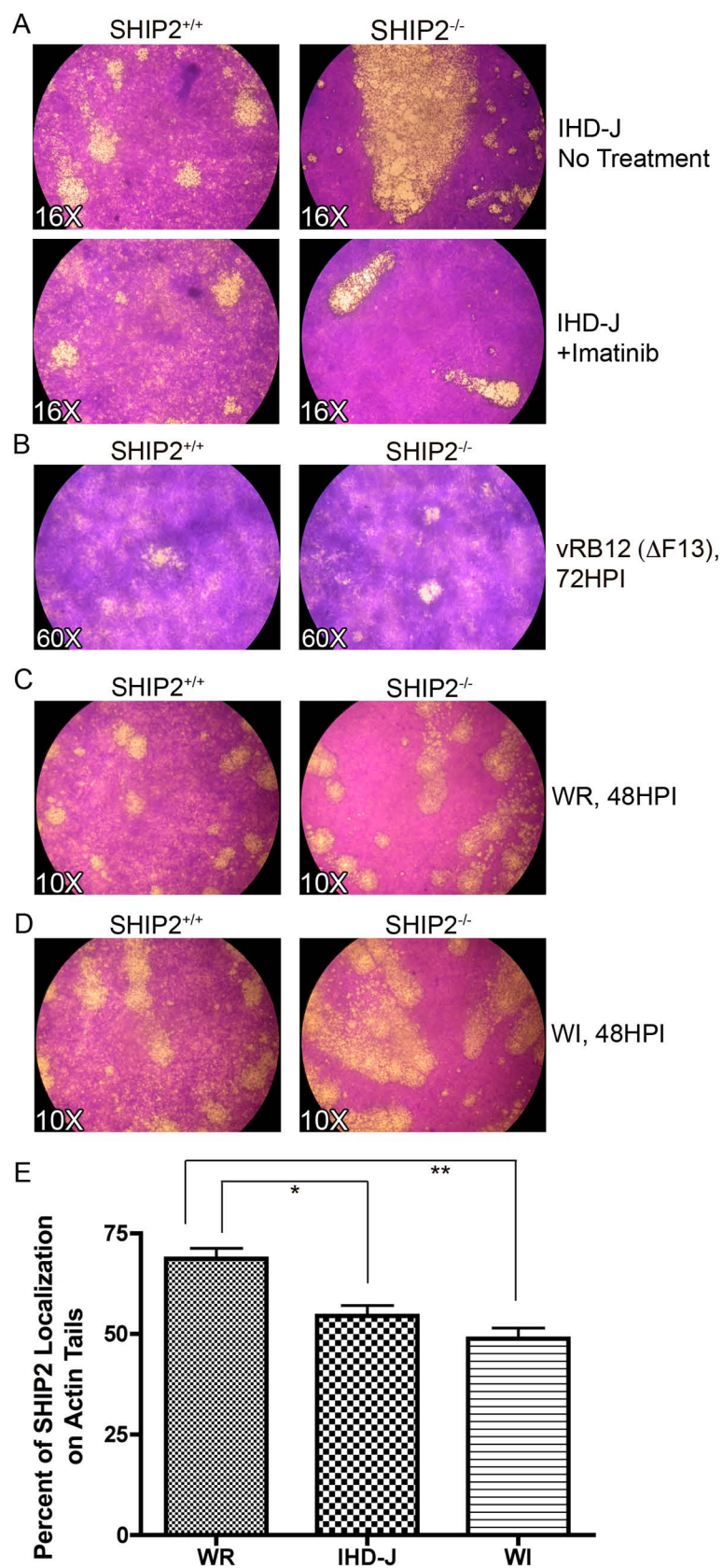
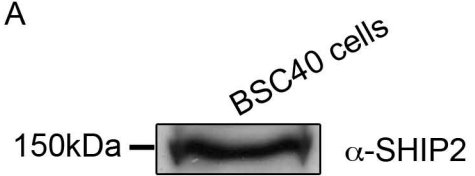


Figure 5

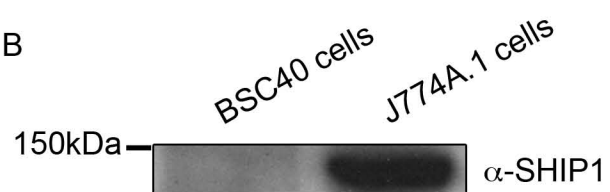


Supplementary Figure 1

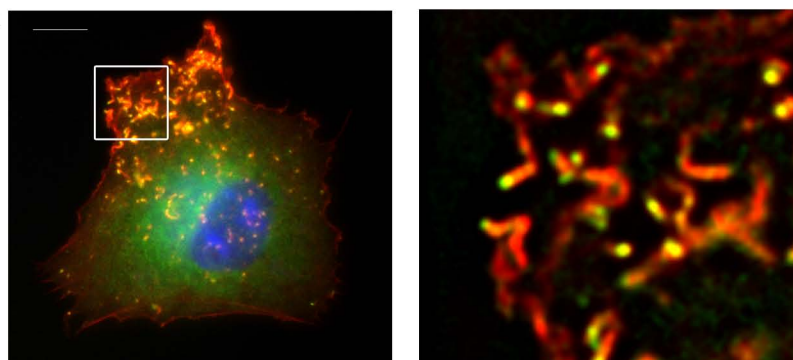
A



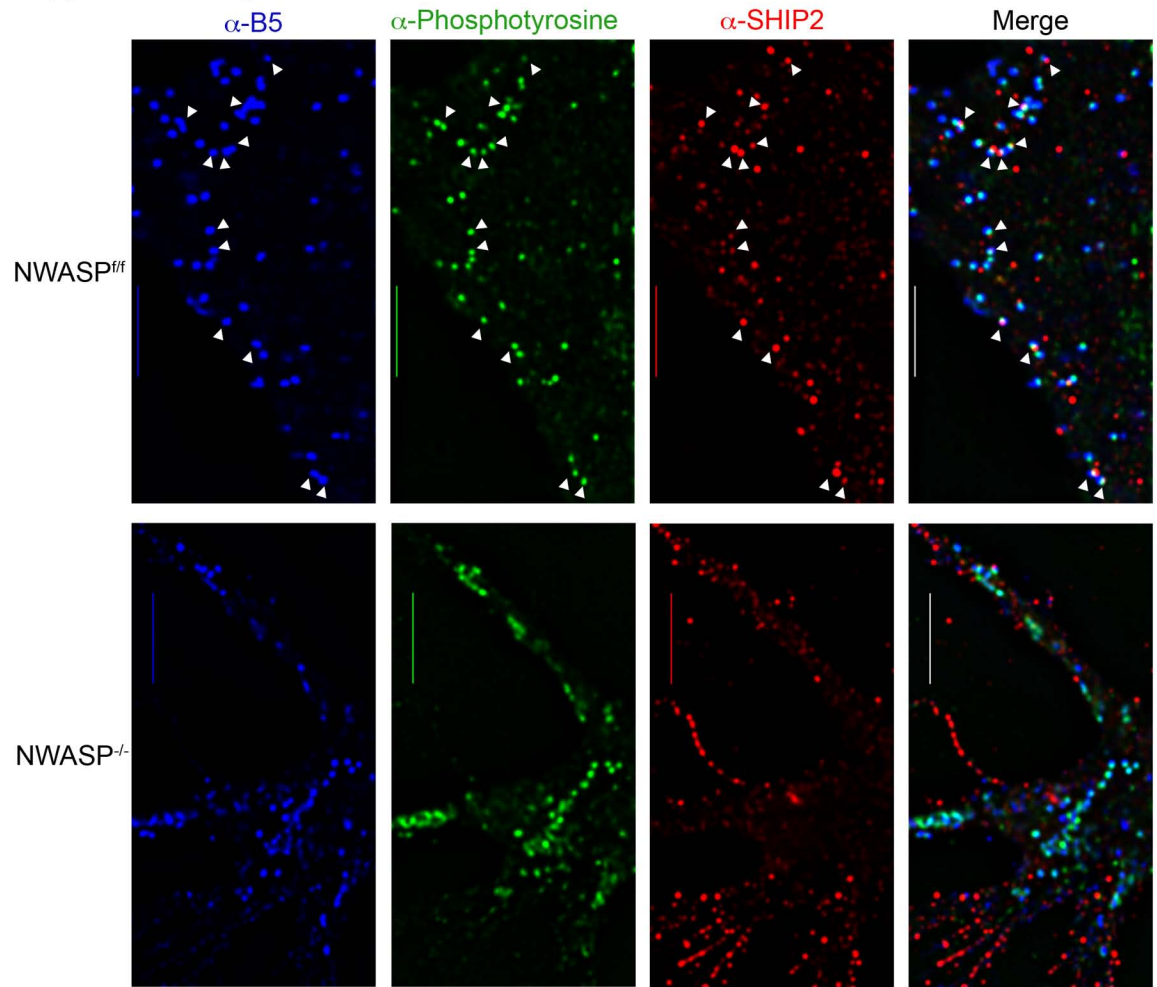
B



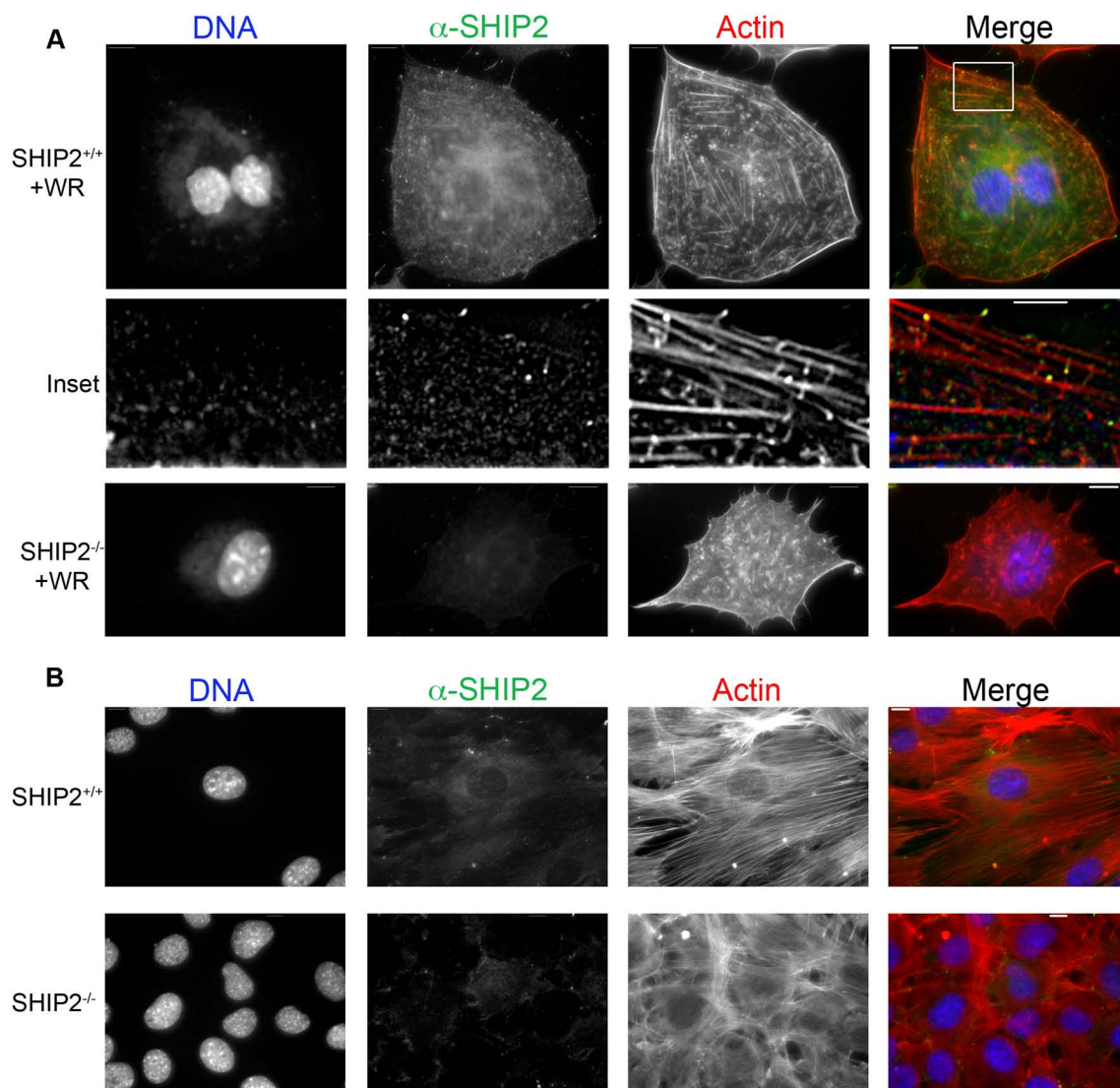
C

 α -Myc-SHIP1, Actin, DNA

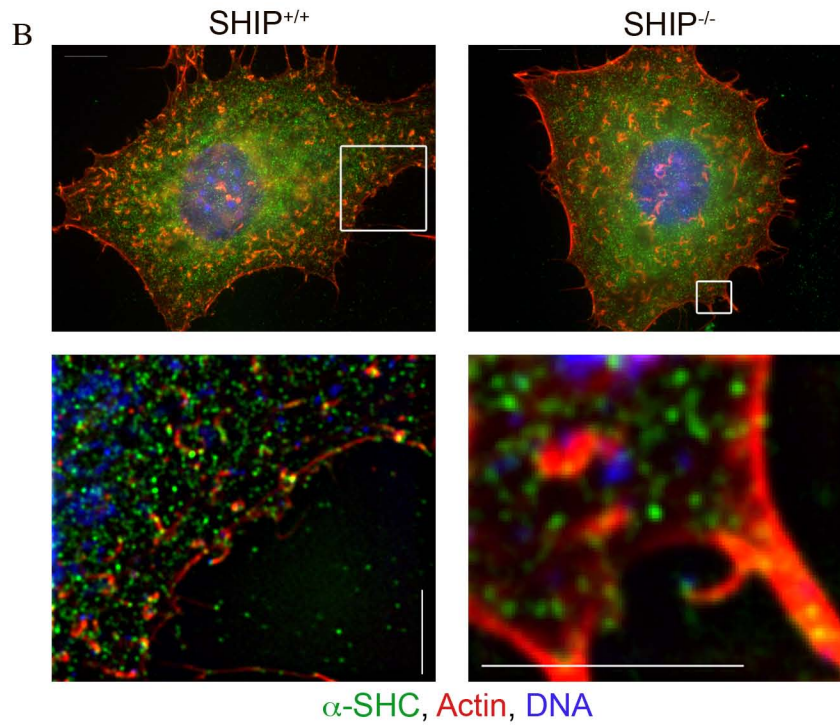
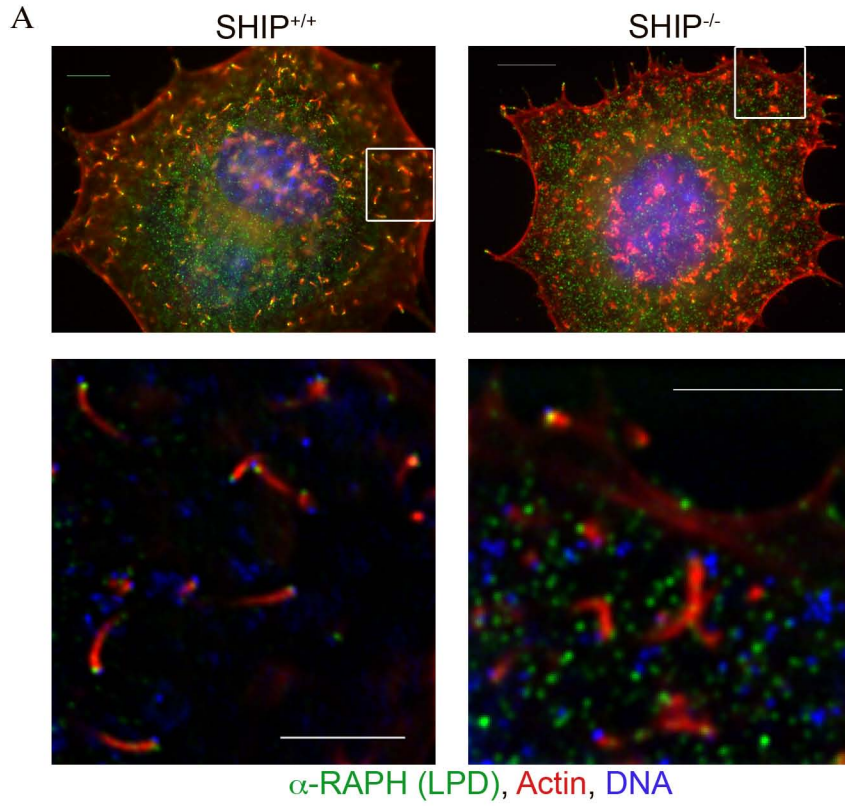
Supplemental Figure 2



Supplementary Figure 3



Supplementary Figure 4



CHAPTER V:
ADDITIONAL OBSERVATIONS

All experiments were performed by Shannon McNulty. Reagents were provided by Eric Hunter, Victor Faundez, and Jonathan Backer.

CHAPTER V: ADDITIONAL OBSERVATIONS

In the course of completing Chapters I, II, and III several additional observations arose which did not fit into these chapters. These observations yield new insight into the mechanisms of poxviral pathogenesis, however their stories are incomplete. With additional experimentation these investigations may produce exciting avenues further elaborating poxviral replication and spread.

5.1 Identification of Src- and Abl-family Tyrosine Kinase Substrates Facilitating Vaccinia Virus Actin Tail Motility and Infectious Virion Release

5.1.1 INTRODUCTION

Previous research by Frischknecht *et al.* and Reeves *et al.* identified that tyrosine kinases localize to the tops of VV actin tails (4, 17) and that inhibition of Src- and Abl-family kinases can abolish tail formation, whereas inhibition of Abl-family tyrosine kinases abolishes virion release (17, 18). These data imply that tyrosine phosphorylated substrates control different aspects of viral dissemination. While several proteins have been identified as participating in actin tail formation and infectious virions release, the contribution of tyrosine kinase substrates remain unidentified. Therefore, we were interested identifying the Src- and Abl-family kinases substrates that contribute to VV actin tail motility and EEV release.

To identify tyrosine kinase substrates, we investigated two different proteomic approaches. To identify both cellular and host substrates, we isolated proteins from infected/uninfected and tyrosine kinase inhibitor treated/untreated cells and identified proteins by Mass Spectrometry (MS). To identify only viral substrates, we performed *in*

vitro kinase reactions using purified viral proteins. By uncovering these novel substrates we hoped to shed new light on the mechanisms of viral pathogenesis and dissemination.

5.1.2 RESULTS

iTraq Mass Spectrometry

To identify both host and viral tyrosine kinase substrates, proteins were isolated from cells treated with tyrosine kinase inhibitors with or without VV infection. These proteins were initially separated by 2D gel electrophoresis and proteins/phosphoproteins were visualized with phosphor-specific stains. Overall protein spot differences were significantly different between gels, complicating the identification of treatment- and viral-specific differences. Therefore, we designed a similar approach that removed 2D gels from the procedure and applied the proteins directly to mass spectrometry.

iTraq is a quantitative mass spectrometry approach that differentially labels proteins from separate experimental conditions, and quantifies the relative abundances of peptides from each experimental sample. This procedure is outlined in Figure 1. Cell lysates from differentially treated samples (+/-tyrosine kinase inhibitor, and +/-VV) are digested with trypsin (Figure 1, Step 1). To ensure complete digestion pre- and post-digestion aliquots are analyzed by SDS-PAGE. Peptides derived from the samples are covalently labeled on amide residues (Figure 1, Step 2), each with a different isobaric reactive group consisting of a label with a mass-to-charge ratio (m/z) of 114, 115, 116, 117 (“reporters,” red box in Figure 1, Step 6) and a spacer (blue box, Figure 1, Step 6). Following collision of the labeled peptide with the noble gasses in the MS, the reporter, spacer, and peptide dissociate, allowing quantitation of the amount of reporter and the

peptide sequence (the spacer is not detected in the spectra). iTraQ labeling was confirmed by removing a 2% fraction from each labeled sample, spotting them on a plate, and analyzing them by MALDI-TOF (note the tag in red, Figure 1, Step 2). The labeled peptides of the four conditions were then combined (Figure 1, Step 3). A 5% fraction from the combined sample was reserved for the analysis of housekeeping proteins by Q-TOF (QSTAR-XL, Applied Biosystems). The values obtained were then used to correct for differences in protein concentration between samples. Phosphotyrosine peptides from the combined fraction were immunoprecipitated with two anti-phosphotyrosine (pY) antibodies (PT-66 (Sigma), and PY100 (Cell Signaling)) attached to protein G beads (Figure 1, Step 4). The phosphopeptides were eluted from the antibody in 100 mM glycine, pH2.5.

To verify phosphoprotein enrichment in the eluate, dot blots were performed using a rabbit a-pY antibody (Figure 1, Step 4). Dot blot data indicated that PT-66 and PY-100 were sufficient to precipitate all detectable phosphorylated peptides. Phosphopeptides were further enriched by immobilized metal affinity chromatography (IMAC) columns charged with TiO_2 or Fe^{3+} (Figure 1, Step 5). Labeled peptides recovered from the IMAC column were purified by HPLC and then subjected to tandem MS using Q-TOF (Figure 1, Step 6). Spectra were acquired in realtime, in 6s MS/MS cycles; MS^1 spectra are acquired in 1s intervals, followed by MS^2 spectra acquired for 5s intervals. Approximately three peptides with the highest intensity per each 6s cycle were chosen for tandem MS. Only peaks with charge states between two and five, with m/z values of 360-1200 and over the intensity threshold greater than 35 counts were used for MS^2 . Identical peptides identified in MS^1 were eliminated from MS^2 by defining a

temporary exclusion parameter of 120s. The minimal intensity threshold was chosen based on the signal-to-noise of the MS.

During MS², the labels, spacer, and peptide fragmented. The labels have different peak mass-to-charge (m/z) ratios (114, 115, 116 and 117), which are easily identifiable and do not overlap with m/z peaks of amino acids. For a given label, assessment of the peak area at the corresponding m/z peak (e.g. 114) represents the amount of that peptide in the sample. By measuring the peak areas of each of the four labels for that peptide, the peptide levels between experimental samples were quantitatively compared. Moreover, the sequence of the peptide was readily determined by analysis of the rest of the spectrum. Data acquisition and spectra processing were performed using the Analyst QS software package (Applied Biosystems).

To quantitatively compare phosphoprotein samples, data within each sample was normalized based on three considerations. First, iTraq spectra from each isobaric label (e.g. 116) was adjusted to account for contamination from other iTraq channels (e.g. 114, 115, 117). This was accomplished using the Certificate of Analysis supplied by the manufacturer (Applied Biosystems), which is unique to each iTraq kit. Second, each sample contains slightly different amounts of protein, so the data was normalized based on the initial weight of the lyophilized lysate. Third, to account for nonspecific changes in proteins due to the procedure (e.g. sample degradation) we normalized samples against “housekeeping proteins.” Such proteins would be expected to exhibit a 1:1 ratio relative to the uninfected and untreated sample. To do this, an aliquot representing 5% of the labeled sample before IP was used to identify “housekeeping” proteins. Once twenty of these proteins were identified, the levels of three peptides from each protein was

assessed, and the mean iTraQ values was used to normalize the channels of the immunoprecipitated peptides.

iTraQ data quantification and peptide analysis was performed using the ProQuant script in the Analyst QS software. Additional peptide analysis was performed using ProGroup, which generates protein ID confidence values, and consolidates redundant and similar peptides into protein groups. We also used Protein Pilot, a software program that uses a slightly different peptide identification algorithm, and additionally allows identification of residues modified by phosphorylation or the attachment of an iTraQ group.

While the iTraQ Mass Spectrometry approach appeared promising, we ultimately decided not to further pursue this line of investigation. Despite careful experimentation, we were unable to identify the viral protein A36, which has already been identified as a Src- and Abl-family tyrosine kinase substrate necessary for actin tail formation and virion release (12, 36). These data indicate that our MS procedure was not sensitive enough to detect known viral tyrosine kinase substrates. Further experimentation established that the sensitivity of our MS was significantly lower than that of our collaborator, Forest White.

***In vitro* kinase reactions identify Abl viral substrates**

In collaboration with Phil Felgner's group at UC Irvine, we carried out kinase assays with Abl on the entire vaccinia proteome (tagged with HA and 6-His epitopes), produced by *in vitro* transcription and translation (IVTT). To do *in vitro* kinase assays, purified kinases together with ATP were incubated with the transcription/translation mix

alone, or with the mix containing each transcribed and translated vaccinia protein. We separated proteins by SDS-PAGE or tris-tricine gels, transferred proteins to Immobilon-FL, and probed with rat α -HA mAb 3F10 and mouse α -phosphotyrosine mAb 4G10 followed by appropriate fluorescent secondary antibodies (Cy5 and Cy7). The membranes were then imaged with an Odyssey Infrared Imaging System (Licor). The proteome in its entirety was analyzed with 17 gels in about a week. Some proteins on gels ran as multiple bands possibly corresponding to internal transcriptional initiations, truncations, or degradation products, and not all proteins were produced at detectable levels. The negative control was the IVTT mix without DNA, and the positive control was a known Abl substrate, Abl-tide. Using this methodology, we have identified 60 proteins phosphorylated by Abl. These putative substrates are listed in Table 1.

5.1.3 FUTURE DIRECTIONS

To discover putative Src- and Abl-family kinase substrates that contribute to poxviral pathogenesis we performed quantitative mass spectrometry and *in vitro* kinase reactions. We were unable to identify kinase substrates by mass spectrometry due to sensitivity limitations of this approach. However, we were able to identify many putative viral substrates by the *in vitro* kinase assay.

There are multiple improvements that can be made to improve iTraq mass spectrometry sensitivity. Forest White's group at MIT loads their peptide samples directly onto hand-made electrospray ionization (ESI) tips that are downstream of the liquid chromatography machine. In contrast, we loaded our peptide samples upstream of the liquid chromatography machine and could have lost peptides in the machine, before

they even entered the ESI tip. To improve MS sensitivity we could load our samples similar to Forest White, and/or start with a larger sample size. Additionally, an eight channel iTraQ labeling approach was recently developed, extending the number of samples that can be incorporated and compared for each experiment.

Many putative viral Abl kinase substrates were identified by the *in vitro* kinase approach. However, there are several drawbacks to this approach which may produce many false positive hits. Since the proteins were produced using an *in vitro* transcription/translation reaction in the absence of a cellular environment and chaperones the possibility exists that many phosphorylations are not biologically relevant. We are unable to confirm whether the proteins exist in their native conformation using this approach. Additionally, the putative substrates identified may not normally interact with Abl kinases during a viral infection due to their location in the cell. To verify positive substrates from this screen one could make Y->F mutations within the predicted substrate and verify a change in phosphorylation during a viral infection by Western blot using wild-type and Abl1^{-/-}Abl2^{-/-} cells. Alternatively, one could screen for a phenotype with the Y->F mutant, and/or verify phosphorylation sites by Mass Spectrometry. Overall, the proteomic approach to identify putative Src- and Abl-family kinase substrates was very useful, but any substrates identified by these approaches should be further verified for biological relevancy.

5.2 vps34/15

5.2.1 INTRODUCTION

In Chapter II we identified that Vaccinia virus uses host PI3K during viral morphogenesis, and that kinase usage is redundant. By adding PI3K inhibitors to p85-deficient cells we were unable to completely inhibit viral production. This data imply that additional host kinases may be utilized during viral replication. Therefore, we set out to identify these kinases and their mechanism of involvement within the viral lifecycle.

The mammalian PI3K family is divided into three different classes based on kinase substrate preference and domain structure. Class I kinases phosphorylate PI(4,5)P₂ into PI(3,4,5)P₃ and consist of heterodimers of regulatory (p85) and catalytic subunits (p110) (8). Class II kinases have recently been identified, and though not fully characterized, are hypothesized to phosphorylate PI(4)P and PI into PI(3,4)P₂ and PI(3,4,5)P₃, respectively. Class II kinases do not exist as heterodimers (8). Their activity may be regulated through membrane binding, as PI3K-c2 α has a PX domain capable of binding lipids (31). Class III kinases phosphorylate PI into PI(3)P and consist of a heterodimer of regulatory (vps15) and catalytic subunit (vps34) (8). Vps34/15 is the sole PI3K in yeast, and was originally identified in a screen for mutants defective in Vacuolar Protein Sorting of proteins from the Golgi apparatus to the vacuole (13).

In yeast vps34/15 exists as a heterodimer capable of directing vacuolar transport (13). The mammalian homologue of yeast vps34 shares 37% identity and 58% similarity (32) and has been demonstrated to be similarly regulated by vps15 (37). Vps15 contains an N-terminal myristylation site, and shares sequence similarity with serine/threonine kinases (13). In yeast and mammals, vps15 regulates the activity of vps34 and an intact kinase domain of vps15 is required for activity of vps34(37). However, the specifics of

protein phosphorylation and their contribution to vps34/15 activity have not been clearly resolved (13).

By producing PI(3)P on target membranes, vps34/15 creates a spacial and temporal signal that drives vesicular trafficking. This lipid signal recruits proteins with specific PI(3)P domains (such as FYVE, and PX) to target membranes. These target membranes include early and late autophagosomes, early and late endosomes, and the multivesicular body (MVB) (25). Vps34/15 specificity in signaling is determined through its interaction with additional accessory molecules, like Beclin 1, UVRAG, atg14L, rab5, and rab7 (25).

While much is known about the cellular endocytic events controlled by vps34/15, much less is known about how pathogens disrupt and hijack vps34/15-regulated signaling. During maturation a subset of Vaccinia virus (VV) virions become enveloped in additional host cell-derived membranes. The origin on these membranes is not well understood, but they are hypothesized to be derived from endosomes or Golgi apparatus (16, 20, 22, 30, 33). Since the vps34/15 complex is a central component of endocytic signaling, we investigated the contribution of the Class III PI3K to the VV lifecycle.

5.2.2 RESULTS

Vps34/15 localize to VV actin tails

To investigate if vps34/15 contributes to poxviral pathogenesis, we infected BSC40 cells with 3uL of $\sim 10^8$ PFU WR for 16 hours, fixed and stained cells with antibodies recognizing endogenous vps34 (923B, rabbit, 1:50). Surprisingly, we found that vps34 localized to the tops of actin tails (Figure 2). To confirm that localization was

specific we also stained cells with a second vps34 antibody (243, rabbit, 1:50), which also localized to the tops of actin tails (Figure 3). To confirm that vps34 existed as a heterodimer at the top of tails, we also stained cells with antibodies recognizing endogenous vps15 (rabbit, 1:50). This antibody also localized to the top of VV actin tails (Figure 4).

To confirm that these antibodies were recognizing cellular and not viral epitopes, we transiently transfected BSC40 cells with plasmids expressing epitope-tagged vps34/15. When expressed in uninfected cells vps34 exhibited diffuse cytoplasmic staining (Figure 5A). By contrast, when expressed individually vps15 exhibited a punctuate localization (Figure 5B). When vps15 and vps34 were expressed from a bicistronic plasmid, vps34 exhibited a more punctuate localization (Figure 5C). These data demonstrate that vps15 directs the localization of vps34, in agreement with data from Yan *et al.* suggesting that vps15 regulates the activity of vps34 (37). In virally infected cells, we could localize ectopically expressed vps15 on tails (although it was not on every tail) (Figure 6), however, when expressed alone we were unable to clearly identify vps34 on tails (Figure 7). Co-expression of vps34/15 from the bicistronic plasmid localized to a minority of tails, although staining was very faint (Figure 8).

Vps34/15 inhibitors reduce plaque size

Since vps34/15 localized to the tops of VV actin tails, we investigated whether a vps34 inhibitor, 3-methyladenine (3-MA) could inhibit or reduce VV plaque size. 3-MA is not a specific inhibitor and can inhibit both Type I and Type III kinases. However, *in vitro* experiments demonstrate that 3-MA has a lower IC_{50} for vps34 (25 μ M) than for Class I

PI3Ks (60-245 μ M) (11). When added 1 hour post viral adsorption 3-MA completely inhibited VV plaques formed on BSC40 cells at 48 hours post infection in a range of 10-25mM (Figure 9). In collaboration with Jonathan Backer at Albert Einstein College of Medicine we also test vps34 activity during a vaccinia infection. Preliminary experiments indicate that overall protein levels were significantly lower in virally-infected cells than uninfected cells. While we found that vps34 activity was lower in infected cells, we hypothesize that this difference was due to reduced vps34 recovery in these cells, as a consequence of overall reduced protein levels. When normalized to a housekeeping protein, preliminary experiments suggest that vps34 specific activity may be higher in virally infected cells than uninfected cells (data not shown).

Rab Proteins 4a, 5, 7, and 11 Do Not Localize to VV Actin Tails

Rab proteins are a major component of the eukaryotic endomembrane system and regulate vesicle budding, uncoating, motility, and fusion (29). These proteins are GTPases that exist in an “ON” GTP-bound state, and “OFF” GDP-bound state and interconversion between these states results in major conformational changes (29). These conformational changes subsequently regulate effector interactions, and membrane association. Humans have over 60 different rab proteins capable of regulating membrane transport (29).

Because we observed vps34/15 localizing to the top of VV actin tails, we were interested in understanding whether additional vps34/15 effectors also localized to this region. Vps34/15 can form multi-protein complexes capable of regulating cellular signaling. A key component of many of these complexes, Beclin I (6), was previously

identified as unnecessary during a poxviral infection (38). Therefore, we investigated the localization of other known vps34/15 effectors to the tops of tails, such as rab7 and rab5, which have previously been identified as vps34/15 interactors (23, 28). *Salmonella* and *Mycobacterium tuberculosis* have both been found to disrupt vps34-rab5 signaling to maintain a pathogen-specific endosome within cells (3, 10). These data demonstrate that multiple pathogens may disrupt vps34/15 signaling to enhance replication and spread.

To identify whether Vaccinia virus and vps34/15 colocalize with rab proteins, cells were transfected with various rab-gfp constructs (rab4a, rab5, rab7 and rab11) for ~32 hours, and then infected with vaccinia virus for 16 hours. Cells were fixed and stained for actin or a component of the IMV virion, L1. We were unable to identify colocalization of any rab proteins to the top of VV tails or colocalizing with VV protein L1 (data not shown). However, cellular trafficking can be disrupted with a constitutively active rab5 construct, which produces enlarged endosomes (Figure 10). In virally infected cells EEV-specific protein B5 did not colocalize with rab5 (Figure 11A). However, when cells were transfected with constitutively active rab5 and virally infected, a subset of B5 was mislocalized to the enlarged vesicles, and infectious B5-positive virions were still produced (Figure 11B). These data suggest that viral protein B5 depends on a functional endosomal system for correct localization.

5.2.3 FUTURE DIRECTIONS

The observation that components of endocytic trafficking are important during a vaccinia infection is intriguing, but further research is needed to complete the story. Localization of vps34/15 to the tops of VV actin tails suggests that VV hijacks these

kinases for a specific mechanism. Therefore, a logical extension of this work would be to try to uncover how the virus uses these kinases. Cells deficient in these kinases do not currently exist. However, one could knockdown vps34/15 by siRNA, and observe whether this disrupts vaccinia replication, spread, or both. In addition, one could add exogenous PI(3)P to cells to determine whether the product of vps34/15 also disrupts the vaccinia replication cycle. Furthermore, determining whether vps34/15 interacts with known actin tail components/regulators, such as NWASP, Abl- and Src-family tyrosine kinases, Nck, Grb2, WIP, SHIP2, A34, and A36 would greatly contribute to the story.

5.3 Phosphatidylinositol 5-Kinases

5.3.1 INTRODUCTION

In Chapter IV we identified that the host lipid phosphatase, SHIP2, localizes to VV actin tails, and while not necessary for tail formation, regulates virion release. SHIP2 is a specific 5'-phosphatase, and preferentially catalyzes hydrolysis of $\text{Ins}(1,2,3,4,5)\text{P}_5 > \text{Ins}(1,3,4,5)\text{P}_4 > \text{PtdIns}(3,4,5)\text{P}_3 \approx \text{PtdIns}(3,5)\text{P}_2 \approx \text{Ins}(1,4,5,6)\text{P}_4$ at the 5' position (1, 15). This data led us to hypothesize that lipids phosphorylated at the 5' position may regulate virion release. Interestingly, Rivera *et al.* found that overexpression of PIP5K can induce actin tail formation beneath endosomes in uninfected cells (19). Therefore, we investigated the localization of phosphatidylinositol 5-kinases (PIP5K) to the tops of VV actin tails.

PIP5K's are divided into different families based on their enzymatic activity and homology. These include Type I kinases, which phosphorylate various substrates (PI, PI(3)P, PI(4)P, and PI(3,4)P) at the D5 position (14). In contrast, the Type II kinases,

while classified as PI5K, are actually PI4K, and phosphorylate PI(3)P and PI(5)P at the D4 position (14). A third class of PIP5K, “PIKfyve” was recently identified by Shisheva *et al.* that exhibits sequence similarity to yeast Fab1p and produces PI(5)P and PI(3,5)P (21, 24). With the exception of the Type III kinases, the other Type I and Type II kinases exist as multiple isoforms, and multiple splice variants (14). Such complexity may contribute to specificity in cellular signaling.

5.3.2 RESULTS

An unidentified PIP5K localizes to VV actin tails.

To investigate the localization of PIP5K's to the top of VV actin tails, we infected BSC40 cells for 16 hours with VV strain WR, fixed and stained cells with an antibody specific to PIP5K-pan (1:50, Santa Cruz, P11K 1, H-300), which recognizes PIP5K I α , β , and γ isoforms (Figure 12). We found that this antibody localized to the tops of VV actin tails, and that this localization was specific, as secondary antibodies alone did not stain tails (data not shown). The PIP5K-pan antibody also localized to the tops of tails formed on SHIP2^{+/+} and SHIP2^{-/-} cells, suggesting that localization does not depend on the SHIP2 5-phosphatase (Figure 13). To further identify the specific PIP5K protein that localizes to tails, we infected BSC40 cells with WR for 16 hours, fixed and stained with antibodies from Pietro de Camilli's lab that are specific to PIP5K γ -pan (recognizes isoforms 87/90) and PIP5K γ -90 (“ZOLA”) (35). We were unable to observe localization of proteins detected by these antibodies on the tops of tails (data not shown). Ishihara *et al.* demonstrated that the PIP5K- γ isoforms are preferentially expressed in the brain, lung and kidney (9), therefore the possibility exists that this isoform is not expressed in BSC40

cells. Furthermore, we transfected cells with a vector from Gonzala Rivera that expresses PIP5K- α and observed that PIP5K- α did not localize to VV actin tails, nor induce actin tails in uninfected cells (data not shown).

Previous work from our lab identified that SHIP2 and vps34/15 localize to the tops of VV actin tails. Therefore, as a natural extension of this work we wondered whether PI(3,5)P may be produced at the tops of tails, and hypothesized that we could localize the Type III kinase, PIKfyve to this region. PIKfyve was identified by Shisheva *et al.* and specifically phosphorylates PI and PI(3)P to produce PI(5)P and PI(3,5)P₂ (21, 24). BSC40 cells were infected with VV, strain WR for 16 hours, fixed and stained with anti-PIKfyve at 1:50. We were unable to observe a PIKfyve signal on uninfected or infected cells. Furthermore, we were unable to identify cells transfected with a vector expressing PIKfyve. These data suggest that PIKfyve does not localize to VV actin tails.

5.3.3 FUTURE DIRECTIONS

In Chapter IV we identified that the host 5' lipid phosphatase localizes to VV actin tails, and inhibits virion release. This data suggest that lipid signaling, specifically through the D5 position on the inositol headgroup, may regulate VV actin tail formation and/or virion release. Therefore, we investigated the localization of PIP5K to the tops of VV actin tails and observed staining with a promiscuous PIP5K antibody on the tops of tails. We were unable to observe localization of PIP5K- α , PIP5K- γ , and PIKfyve on the tops of tails, suggesting that PIP5K- β , or other PIP5K splice variants may localize to tails.

To test this hypothesis, one could infect cells and stain with antibodies specific to PIP5K- β . If this kinase localizes to tails, then cell lines deficient in PIP5K- β (either knockouts, or siRNA-treated) should be infected with VV to investigate the contribution of these kinases to the viral lifecycle. Intriguingly, River *et al.* found that cells deficient in Nck suppress actin comet tail formation due to overexpression of PIP5K (19). These data suggest that Nck may couple phosphotyrosine and phosphoinositide levels. Since Nck, phosphotyrosine, and phosphoinositide kinases/phosphatases localize to the tops of VV actin tails, this may provide an avenue of further research to elucidate the contribution of lipid signaling to VV pathogenesis.

5.4 SHIP2 is not recruited to EPEC pedestals, and does *not* alter pedestal morphology

In a study published in *Cell Host and Microbe*, Smith *et al.* investigate the role of the host lipid phosphatase SHIP2 in formation of actin-filled membranous protrusions, called “pedestals,” that form beneath wild type enteropathogenic *E. coli* (26). These pedestals can also be formed upon “prime and challenge”, a procedure where a cell is primed with a non-adherent EPEC strain ($\Delta tir-eae$ pTir^{EPEC}), which inserts virulence factors such as Tir into the host cell, and then challenged with a strain containing the adhesive Tir ligand, intimin (e.g. K-12 intimin). Smith *et al.* report that EPEC, but not EHEC, recruits SHIP2 to pedestals, and that recruitment depends on Tir residues Y482 and Y551 (27). When Y/F mutants are constructed (e.g. EPEC pTir^{Y482F Y511F}), “medusa-like” pedestals form, and SHIP2 is not recruited. Moreover, though no quantitation was provided, Smith *et al.* present immunofluorescence images suggesting that knockdown of SHIP2 induces “medusa-like” pedestals upon EPEC infection or following EPEC prime

and challenge, though the significance of these disrupted pedestals for host defense or pathogenicity remains unclear.

Concurrent with the publication by Smith *et al.*, we had been investigating the contribution of SHIP2 to actin tails formed by Vaccinia virus (VV). SHIP2 is recruited to VV-induced actin tails (Chapter IV), but is not required for the formation of VV actin tails. Accordingly, tails formed normally in cells derived from animals lacking SHIP2 (SHIP2^{-/-}) compared to control cells derived from age-matched animals (SHIP2^{+/+}). Given the similarity in signaling between EPEC pedestals and VV-induced actin tails (5, 7), the results reported by Smith *et al.* seemed surprising. In accordance with Smith *et al.*, we found that neither SHIP2, nor SHIP1 localized to EPEC pedestals (Figure 14A). Additionally, we could identify no difference in EPEC pedestal morphology between SHIP2^{+/+} and SHIP2^{-/-} cells (Figure 14B). Similar results were obtained using a modified prime and challenge protocol (Figure 14C). Thus, SHIP2^{+/+} or SHIP2^{-/-} cells were primed for three hours with EPEC Δ *eae* (Δ intimin), and extracellular bacteria were removed by washing cells and incubating with 100 μ g/mL gentamicin for one hour. Primed cells were then challenged with EPEC Δ *tir* for one additional hour to induce actin pedestals. Again, pedestals were indistinguishable in SHIP^{+/+} and SHIP^{-/-} cells, and we were unable to detect medusa-like pedestals reported by Smith *et al.* We considered the possibility that pedestal morphology was altered as a consequence of SHIP2 knockdown (the procedure used by Smith *et al.*) rather than its absence. After knockdown of SHIP2 expression (Figure 14F) using either of three siRNA's specific to mouse SHIP2 (Dharmacon), we infected cells with wild-type EPEC, or used the modified prime and challenge protocol. Again, pedestals were unchanged relative to controls. Quantitation of actin pedestals

indicated that morphologies reported by Smith *et al.*, were not apparent in cells infected with EPEC. In a minority of cells infected by the prime and challenge protocol we could find short, noncontinuous pedestals (data not shown). However, we observed this phenotype in both SHIP2^{+/+}, SHIP2^{-/-}, siRNA-treated and control siRNA cells.

Since our investigations were unable to repeat the observations of Smith *et al.*, we questioned what could lead to such dramatically different results. Although our prime and challenge method differed slightly (Smith *et al.* primed with EPEC $\Delta tir-eae$ pTir^{EPEC} and challenged with K12 expressing intimin, whereas we used EPEC Δeae and EPEC Δtir , respectively), this seems an unlikely explanation. We cannot, however, rule out two additional possibilities. First, it is possible that the medusa-like phenotype resulted from an off-target effect of the siRNA used by Smith *et al.*, despite the report of a similar morphology with the EPEC Tir^{Y482F Y511F} mutant. A second possibility is that there exist cell-type specific on-off rates of proteins participating in actin polymerization that may subtly alter pedestal morphology. A recent report indicates a difference in morphology of VV actin tails when the Tir-like viral protein A36 was substituted with a divergent poxviral protein (which contained a different tyrosine spacing than A36) (2). Dodding *et al.* and Weisswange *et al.* effectively demonstrated that tail shape and speed can be modified by differences in the recruitment of cellular proteins (2, 34). Thus, it remains possible that differences in the levels or interactions of actin polymerizing proteins in cell lines used in our study and Smith *et al.* (they used HeLa, whereas we used MEFs and BSC40 cells) may account for the observed disparity. Resolution of this conundrum would require measurement of the on/off rates of actin pedestal components as per Dodding *et al.* and Weisswange *et al.* in different cell types and under different

conditions. Without additional data, the role of SHIP2 in pedestal morphology appears indeterminate at present. Further experiments are needed to clarify the contribution of SHIP2 and the medusa pedestal phenotype to the mechanisms of EPEC pathogenesis.

LITERATURE CITED

1. **Chi, Y., B. Zhou, W. Q. Wang, S. K. Chung, Y. U. Kwon, Y. H. Ahn, Y. T. Chang, Y. Tsujishita, J. H. Hurley, and Z. Y. Zhang.** 2004. Comparative mechanistic and substrate specificity study of inositol polyphosphate 5-phosphatase *Schizosaccharomyces pombe* Synaptojanin and SHIP2. *J Biol Chem* **279**:44987-95.
2. **Dodding, M. P., and M. Way.** 2009. Nck- and N-WASP-dependent actin-based motility is conserved in divergent vertebrate poxviruses. *Cell Host Microbe* **6**:536-50.
3. **Fratti, R. A., J. M. Backer, J. Gruenberg, S. Corvera, and V. Deretic.** 2001. Role of phosphatidylinositol 3-kinase and Rab5 effectors in phagosomal biogenesis and mycobacterial phagosome maturation arrest. *J Cell Biol* **154**:631-44.
4. **Frischknecht, F., V. Moreau, S. Rottger, S. Gonfloni, I. Reckmann, G. Superti-Furga, and M. Way.** 1999. Actin-based motility of vaccinia virus mimics receptor tyrosine kinase signalling. *Nature* **401**:926-9.
5. **Frischknecht, F., and M. Way.** 2001. Surfing pathogens and the lessons learned for actin polymerization. *Trends Cell Biol* **11**:30-38.
6. **Funderburk, S. F., Q. J. Wang, and Z. Yue.** The Beclin 1-VPS34 complex--at the crossroads of autophagy and beyond. *Trends Cell Biol* **20**:355-62.
7. **Gouin, E., M. D. Welch, and P. Cossart.** 2005. Actin-based motility of intracellular pathogens. *Curr Opin Microbiol* **8**:35-45.
8. **Hawkins, P. T., K. E. Anderson, K. Davidson, and L. R. Stephens.** 2006. Signalling through Class I PI3Ks in mammalian cells. *Biochem Soc Trans* **34**:647-62.
9. **Ishihara, H., Y. Shibasaki, N. Kizuki, T. Wada, Y. Yazaki, T. Asano, and Y. Oka.** 1998. Type I phosphatidylinositol-4-phosphate 5-kinases. Cloning of the third isoform and deletion/substitution analysis of members of this novel lipid kinase family. *J Biol Chem* **273**:8741-8.
10. **Mallo, G. V., M. Espina, A. C. Smith, M. R. Terebiznik, A. Aleman, B. B. Finlay, L. E. Rameh, S. Grinstein, and J. H. Brumell.** 2008. SopB promotes phosphatidylinositol 3-phosphate formation on *Salmonella* vacuoles by recruiting Rab5 and Vps34. *J Cell Biol* **182**:741-52.
11. **Miller, S., B. Tavshanjian, A. Oleksy, O. Perisic, B. T. Houseman, K. M. Shokat, and R. L. Williams.** Shaping development of autophagy inhibitors with the structure of the lipid kinase Vps34. *Science* **327**:1638-42.
12. **Newsome, T. P., I. Weisswange, F. Frischknecht, and M. Way.** 2006. Abl collaborates with Src family kinases to stimulate actin-based motility of vaccinia virus. *Cell Microbiol* **8**:233-41.
13. **Odorizzi, G., M. Babst, and S. D. Emr.** 2000. Phosphoinositide signaling and the regulation of membrane trafficking in yeast. *Trends Biochem Sci* **25**:229-35.
14. **Oude Weernink, P. A., M. Schmidt, and K. H. Jakobs.** 2004. Regulation and cellular roles of phosphoinositide 5-kinases. *Eur J Pharmacol* **500**:87-99.
15. **Pesesse, X., C. Moreau, A. L. Drayer, R. Woscholski, P. Parker, and C. Erneux.** 1998. The SH2 domain containing inositol 5-phosphatase SHIP2

- displays phosphatidylinositol 3,4,5-trisphosphate and inositol 1,3,4,5-tetrakisphosphate 5-phosphatase activity. *FEBS Lett* **437**:301-3.
16. **Ploubidou, A., V. Moreau, K. Ashman, I. Reckmann, C. Gonzalez, and M. Way.** 2000. Vaccinia virus infection disrupts microtubule organization and centrosome function. *Embo J* **19**:3932-44.
 17. **Reeves, P. M., B. Bommarius, S. Lebeis, S. McNulty, J. Christensen, A. Swimm, A. Chahroudi, R. Chavan, M. B. Feinberg, D. Veach, W. Bornmann, M. Sherman, and D. Kalman.** 2005. Disabling poxvirus pathogenesis by inhibition of Abl-family tyrosine kinases. *Nat Med* **11**:731-9.
 18. **Reeves, P. M., S. K. Smith, V. A. Olson, S. H. Thorne, W. Bornmann, I. K. Damon, and D. Kalman.** 2011. Variola and monkeypox utilize conserved mechanisms of virion motility and release that depend on Abl- and Src-family tyrosine kinases. *Journal of Virology* **85**.
 19. **Rivera, G. M., D. Vasilescu, V. Papayannopoulos, W. A. Lim, and B. J. Mayer.** 2009. A reciprocal interdependence between Nck and PI(4,5)P(2) promotes localized N-WASp-mediated actin polymerization in living cells. *Mol Cell* **36**:525-35.
 20. **Sanderson, C. M., M. Hollinshead, and G. L. Smith.** 2000. The vaccinia virus A27L protein is needed for the microtubule-dependent transport of intracellular mature virus particles. *J Gen Virol* **81**:47-58.
 21. **Sbrissa, D., O. C. Ikononov, and A. Shisheva.** 1999. PIKfyve, a mammalian ortholog of yeast Fab1p lipid kinase, synthesizes 5-phosphoinositides. Effect of insulin. *J Biol Chem* **274**:21589-97.
 22. **Schmelz, M., B. Sodeik, M. Ericsson, E. J. Wolffe, H. Shida, G. Hiller, and G. Griffiths.** 1994. Assembly of vaccinia virus: the second wrapping cisterna is derived from the trans Golgi network. *J Virol* **68**:130-47.
 23. **Shin, H. W., M. Hayashi, S. Christoforidis, S. Lacas-Gervais, S. Hoepfner, M. R. Wenk, J. Modregger, S. Uttenweiler-Joseph, M. Wilm, A. Nystuen, W. N. Frankel, M. Solimena, P. De Camilli, and M. Zerial.** 2005. An enzymatic cascade of Rab5 effectors regulates phosphoinositide turnover in the endocytic pathway. *J Cell Biol* **170**:607-18.
 24. **Shisheva, A., D. Sbrissa, and O. Ikononov.** 1999. Cloning, characterization, and expression of a novel Zn²⁺-binding FYVE finger-containing phosphoinositide kinase in insulin-sensitive cells. *Mol Cell Biol* **19**:623-34.
 25. **Simonsen, A., and S. A. Tooze.** 2009. Coordination of membrane events during autophagy by multiple class III PI3-kinase complexes. *J Cell Biol* **186**:773-82.
 26. **Smith, K., D. Humphreys, P. J. Hume, and V. Koronakis.** 2010. Enteropathogenic *Escherichia coli* recruits the cellular inositol phosphatase SHIP2 to regulate actin-pedestal formation. *Cell Host Microbe* **7**:13-24.
 27. **Smith, K., D. Humphreys, P. J. Hume, and V. Koronakis.** Enteropathogenic *Escherichia coli* recruits the cellular inositol phosphatase SHIP2 to regulate actin-pedestal formation. *Cell Host Microbe* **7**:13-24.
 28. **Stein, M. P., Y. Feng, K. L. Cooper, A. M. Welford, and A. Wandinger-Ness.** 2003. Human VPS34 and p150 are Rab7 interacting partners. *Traffic* **4**:754-71.
 29. **Stenmark, H.** 2009. Rab GTPases as coordinators of vesicle traffic. *Nat Rev Mol Cell Biol* **10**:513-25.

30. **Tooze, J., M. Hollinshead, B. Reis, K. Radsak, and H. Kern.** 1993. Progeny vaccinia and human cytomegalovirus particles utilize early endosomal cisternae for their envelopes. *Eur J Cell Biol* **60**:163-78.
31. **Vanhaesebroeck, B., J. Guillermet-Guibert, M. Graupera, and B. Bilanges.** 2010. The emerging mechanisms of isoform-specific PI3K signalling. *Nat Rev Mol Cell Biol* **11**:329-41.
32. **Volinia, S., R. Dhand, B. Vanhaesebroeck, L. K. MacDougall, R. Stein, M. J. Zvelebil, J. Domin, C. Panaretou, and M. D. Waterfield.** 1995. A human phosphatidylinositol 3-kinase complex related to the yeast Vps34p-Vps15p protein sorting system. *Embo J* **14**:3339-48.
33. **Ward, B. M.** 2005. Visualization and characterization of the intracellular movement of vaccinia virus intracellular mature virions. *J Virol* **79**:4755-63.
34. **Weisswange, I., T. P. Newsome, S. Schleich, and M. Way.** 2009. The rate of N-WASP exchange limits the extent of ARP2/3-complex-dependent actin-based motility. *Nature* **458**:87-91.
35. **Wenk, M. R., L. Pellegrini, V. A. Klenchin, G. Di Paolo, S. Chang, L. Daniell, M. Arioka, T. F. Martin, and P. De Camilli.** 2001. PIP kinase Igamma is the major PI(4,5)P(2) synthesizing enzyme at the synapse. *Neuron* **32**:79-88.
36. **Wolffe, E. J., A. S. Weisberg, and B. Moss.** 1998. Role for the vaccinia virus A36R outer envelope protein in the formation of virus-tipped actin-containing microvilli and cell-to-cell virus spread. *Virology* **244**:20-6.
37. **Yan, Y., R. J. Flinn, H. Wu, R. S. Schnur, and J. M. Backer.** 2009. hVps15, but not Ca²⁺/CaM, is required for the activity and regulation of hVps34 in mammalian cells. *Biochem J* **417**:747-55.
38. **Zhang, H., C. E. Monken, Y. Zhang, J. Lenard, N. Mizushima, E. C. Lattime, and S. Jin.** 2006. Cellular autophagy machinery is not required for vaccinia virus replication and maturation. *Autophagy* **2**:91-5.

FIGURE LEGENDS

Figure 1: Overview of iTraq Mass Spectrometry approach.

Figure 2: vps34 localizes to the tops of VV actin tails. BSC40 cells were infected with VV strain WR for 16 hours, fixed and stained with anti-vps34 (923B, 1:50, rabbit) recognizing endogenous protein.

Figure 3: vps34 localizes to the tops of VV actin tails. BSC40 cells were infected with VV strain WR for 16 hours, fixed and stained with anti-vps34 (243, 1:50, rabbit) recognizing endogenous protein.

Figure 4: vps15/p150 localizes to the tops of VV actin tails. BSC40 cells were infected with VV strain WR for 16 hours, fixed and stained with anti-vps15 (rabbit, 1:50) recognizing endogenous protein. **A)** Cells infected with WR. **B)** Uninfected cells. **C)** Cells infected with WR, and stained with FitC conjugated secondary antibody only.

Figure 5: Vps15 regulates vps34 localization. **A)** BSC40 cells were transfected with mRFP-vps34. Note the diffuse cytoplasmic localization of vps34 distinct from endogenous localization in Figures 2, and 3. **B)** BSC40 cells were transfected with V5-vps15. Note the punctuate localization of vps15. **C)** BSC40 cells were transfected with a bicistronic vector expressing V5-vps15 and myc-vps34. Note the punctuate localization of both vps34 and vps15.

Figure 6: Vps15 overexpression in virally-infected BSC40 cells. Cells were infected with VV strain WR for 16 hours, fixed and stained with antibodies recognizing v5 epitope-tagged vps15. Note localization of vps15 to the tops of tails.

Figure 7: Vps34-mRFP overexpression in virally-infected BSC40 cells. Cells were infected with VV strain WR for 16 hours, fixed and stained. Note that vps34, when overexpressed alone, did not localize to the tops of tails.

Figure 8: Vps34/15 bicistronic overexpression in virally-infected BSC40 cells. Cells were infected with VV strain WR for 16 hours, fixed and stained with antibodies recognizing V5-vps15 and myc-vps34. Both vps34/15 localize to tails, but localization is very faint.

Figure 9: 3-Methyladenine (3-MA) inhibits VV plaque size between 10-25mM. Compounds were added 1 hour post viral adsorption. 3-MA inhibitory activity is sensitive to freeze/thaw cycles.

Figure 10: Rab5 and Rab5(Q79L) constitutively active localization in uninfected cells. **A)** BSC40 cells were transfected with Rab5-gfp for 48 hours. Note the punctate perinuclear localization. **B)** BSC40 cells were transfected with Rab5(Q79L)-gfp for 48 hours. Note enlarged perinuclear endosomes.

Figure 11: Rab5 and Rab5(Q79L) localization in WR-infected cells. BSC40 cells were transfected with constructs for 32 hours, and infected with VV strain WR for 16 hours.

A) Cells transfected with rab5-gfp. Rab5-positive endosomes do not colocalize with viral protein B5, nor does overexpression disrupt VV actin tails. **B)** Cells transfected with rab5(Q79L)-gfp. Viral protein B5 is mislocalized into rab5(Q79L)-positive enlarged endosomes. Inset shows B5 in the lumen of enlarged endosome.

Figure 12: PIP5K localizes to VV actin tails. BSC40 cells were infected with viral strain WR for 16 hours, fixed and stained with antibodies recognizing endogenous PIP5K-pan (1:50, Santa Cruz, recognizes PIP5K α , β , and γ isoforms).

Figure 13: PIP5K localization to VV actin tails does not depend on SHIP2. Cells were infected with viral strain WR for 16 hours, fixed and stained with antibodies recognizing endogenous PIP5K-pan (1:50, Santa Cruz, recognizes PIP5K α , β , and γ isoforms). **A)** SHIP2^{+/+} cells. **B)** SHIP2^{-/-} cells.

Figure 14: SHIP2 is not recruited to EPEC pedestals, and does *not* alter pedestal morphology. **A)** Endogenous SHIP2 and SHIP1 staining in EPEC pedestals and VV actin tails. BSC40 cells were infected with EPEC for 5 hours, fixed and stained with antibodies recognizing SHIP2 or SHIP1. For VV infections, cells were infected 16 hours with VV strain WR, fixed and stained with antibodies recognizing endogenous SHIP2. Cells were stained with DAPI (DNA, blue), Cy3-phalloidin (actin, red), and secondary antibodies conjugated to FitC (green). **B)** SHIP2^{+/+} or SHIP2^{-/-} cells were infected with

EPEC for 5 hours and stained with DAPI (DNA, blue) and Cy3-phalloidin (actin, red).

C) SHIP2^{+/+} and SHIP2^{-/-} cells were primed with EPEC Δ eae (intimin) for 3 hours, washed and gentamicin was added for 1 hour. EPEC Δ Tir was added to cells for 2 hours and cells were fixed and stained with Cy3-phalloidin (red, actin), DAPI (DNA, blue) and α -Tir (green). **D)** SHIP2^{+/+} were transfected with siRNA against SHIP2 for 3 days, and infected with EPEC for 5 hours, fixed and stained with Cy3-Phalloidin (red, actin) and DAPI (DNA, blue). **E)** SHIP2^{+/+} cells were transfected with siRNA against SHIP2 for 3 days, and infected by Prime and Challenge. **F)** Western blot for SHIP2 in SHIP2^{+/+} cells treated with siRNA targeting SHIP2.

Table 1: Identification of Viral Abl Tyrosine Kinase Substrates

Entry and Release:	
A16L	Soluble myristylprotein; component of viral entry ; decrease A16L production causes decrease in specific infectivity.
A36R	IEV transmembrane phosphoprotein interacts with A33R and used in actin tail formation
F11L	Interacts with rhoA; prevents cell migration.
A27L	IMV surface protein; roles in IMV-cell attachment, fusion, and microtubule transport
A34R	EEV glycoprotein involved in CEV cell adherence and actin tail formation
Virion Maturation:	
A32L	Putative ATPase involved in DNA packaging
F13L	Palmytilated EEV membrane protein; phospholipase motif, required for IEV formation
A17L	IMV membrane protein required for morphogenesis
H3L	IMV heparin binding surface protein involved in IMV maturation
F10L	Ser/thr/Tyr kinase. Fills membrane crescents with viral proteins; encapsidated in virions.
A11R	Phosphorylated independent of F10 kinase. Decrease A11 leads to a block in virion assembly. Causes membrane formation and recruitment for MV's. Interacts with A32.
Core Protein 4a/b:	
A3L	p4b precursor of core protein 4b
A4L	39kDa core protein complexes with core protein p4a/4a
H3L	IMV surface heparin binding protein
A10L	Precursor p4a of core protein 4a, complexes with A4L
Unknown Functions:	
E2L	unknown
A51R	unknown
C8L	unknown
A31R	unknown
A49	unknown
A19L	unknown
WR201	unknown
F1L	unknown
B15	unknown

Table 1: continued...

Transcription:	
D7R	DNA-dependent RNA polymerase subunit
A24L	DNA-dependent RNA polymerase subunit
A29L	DNA-dependent RNA polymerase subunit
D11L	Transcription termination and elongation factor
D12L	Capping enzyme, transcription termination factor.
E4L	DNA-dependent RNA polymerase subunit
J4R	DNA-dependent RNA polymerase subunit
G2R	Late transcription termination factor.
H4L	Associates with DNA-dependent RNA polymerase
DNA Replication:	
A18R	DNA Helicase/ATPase
A20R	DNA polymerase
B1R	Serine/threonine kinase needed for DNA replication.
D4R	Interacts with A20, DNA polymerase processivity factor.
A22R	Concatomer resolution, RuvC-like
I3L	Putative ssDNA binding protein
Immunomodulatory:	
A44L	Hydroxysteroid dehydrogenase
B13	Inhibits caspases and apoptosis
A52R	TIR-dependent suppressor, host defense modulator
N1L	Virokine, host defense modulator
E3L	dsRNA binding protein, host defense modulator
M2L	NFkB inhibitor
Miscellaneous	
A2L	SS bond formation, links SH oxidase E10R and G4L
B18	Ankyrin-like protein
C12L	Serpin-like protein
K1L	Host range
L4R	ssDNA/RNA binding protein involved in early mRNA regulation
WR148	Gene fragment, cowpox Type-A inclusion protein
A57R	Guanylate Kinase, pseudogene
A45R	Inactive Cu-Zn superoxide dismutase
H1L	Tyrosine/serine phosphatase
WR208	Gene fragment, host defense modulator
A39R	Gene fragment, semaphorin-like
G4L	SS-bond formation, thioredoxin-like
WR011	Gene fragment, host defense modulator
H2R	Component of Entry/fusion complex
I4L	Ribonucleotide reductase large subunit

Figure 1

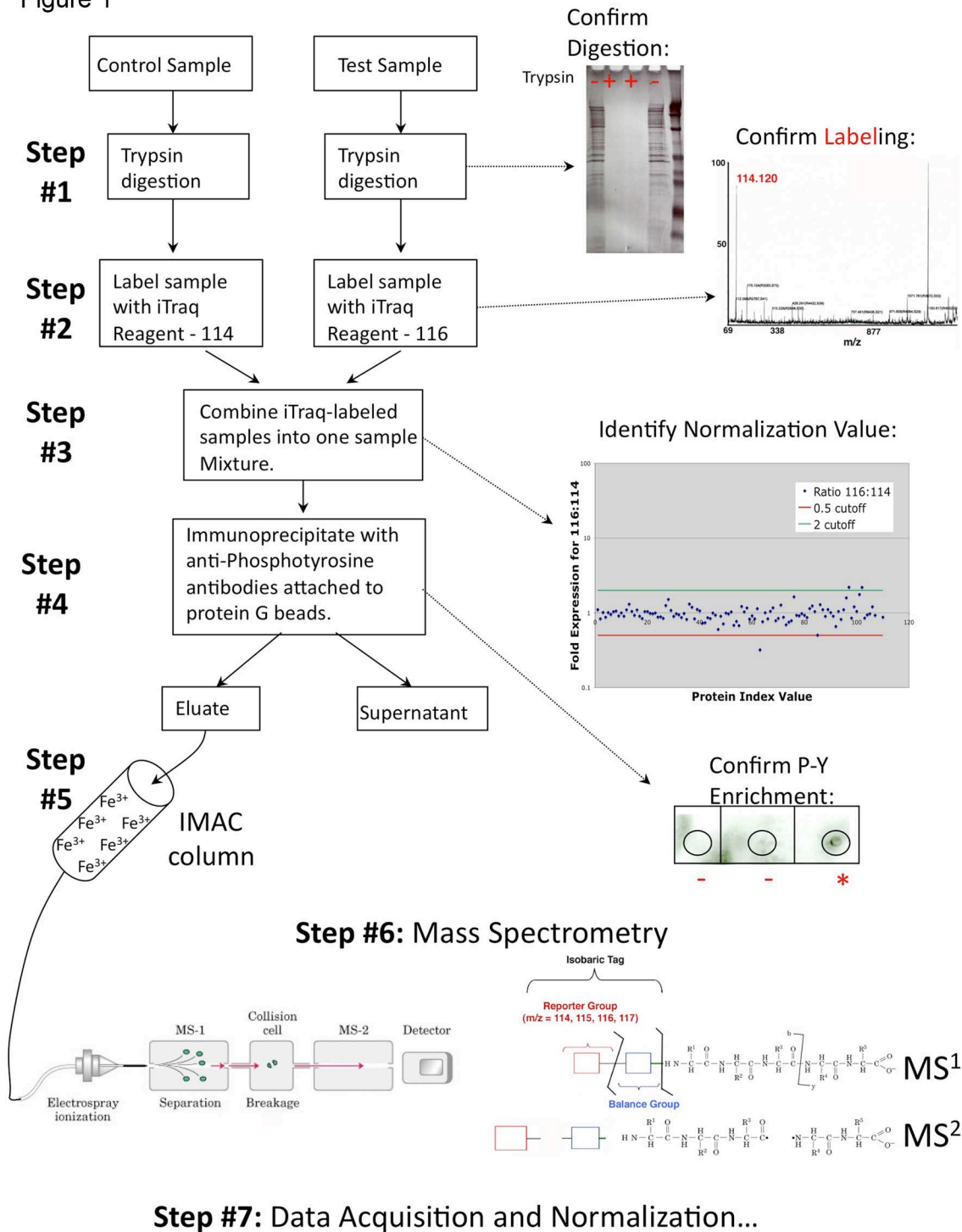


Figure 2

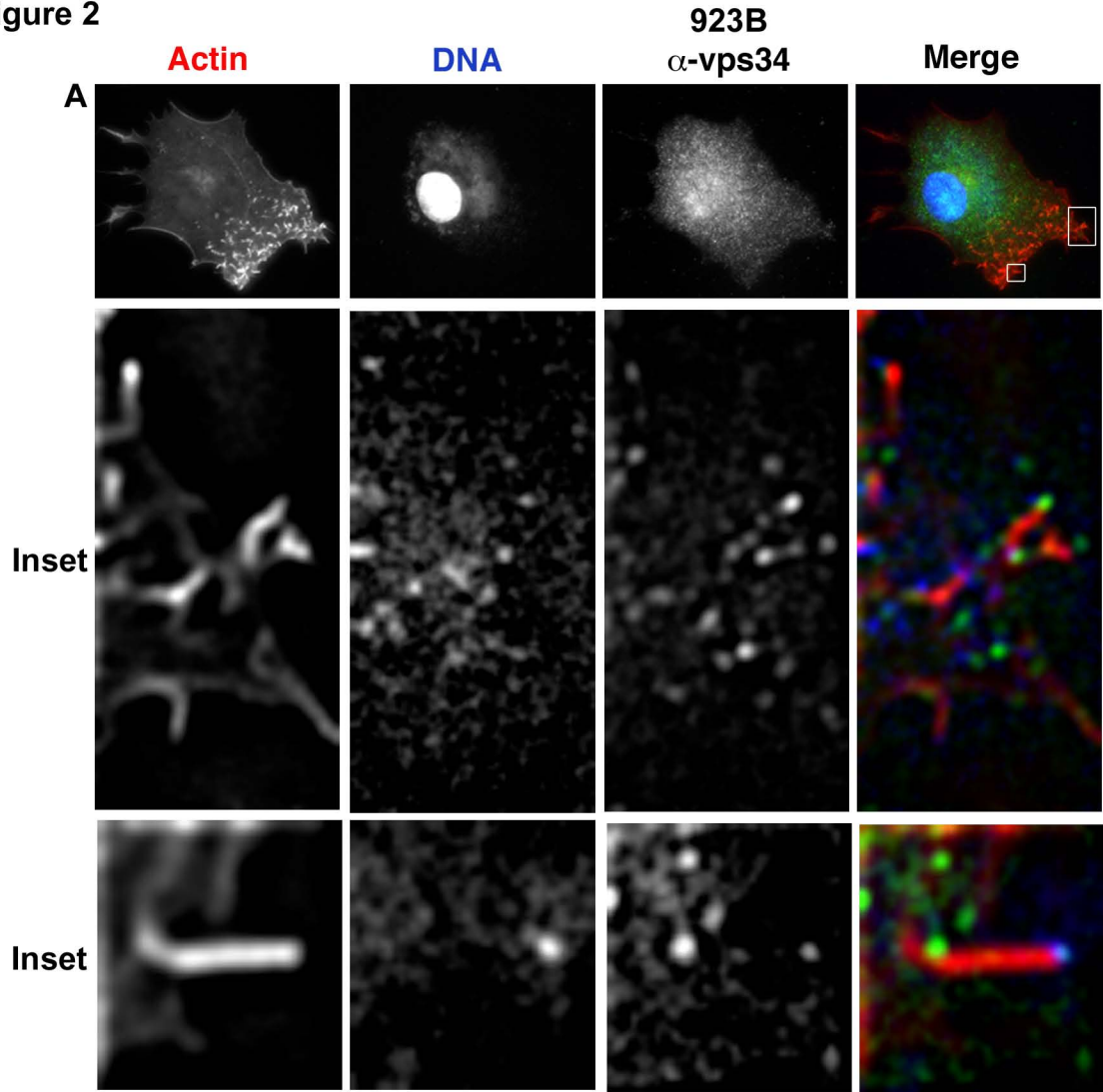


Figure 3

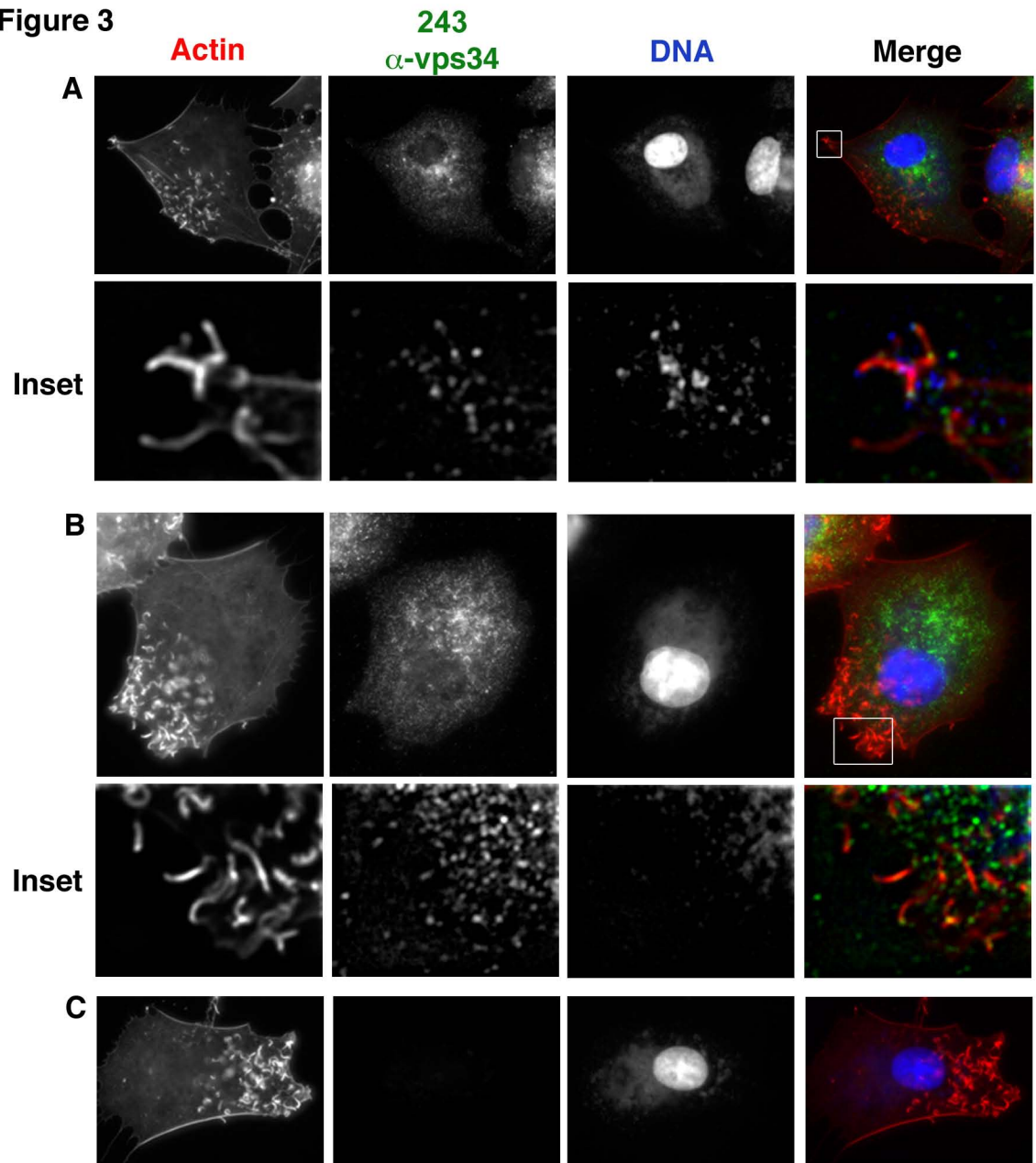


Figure 4

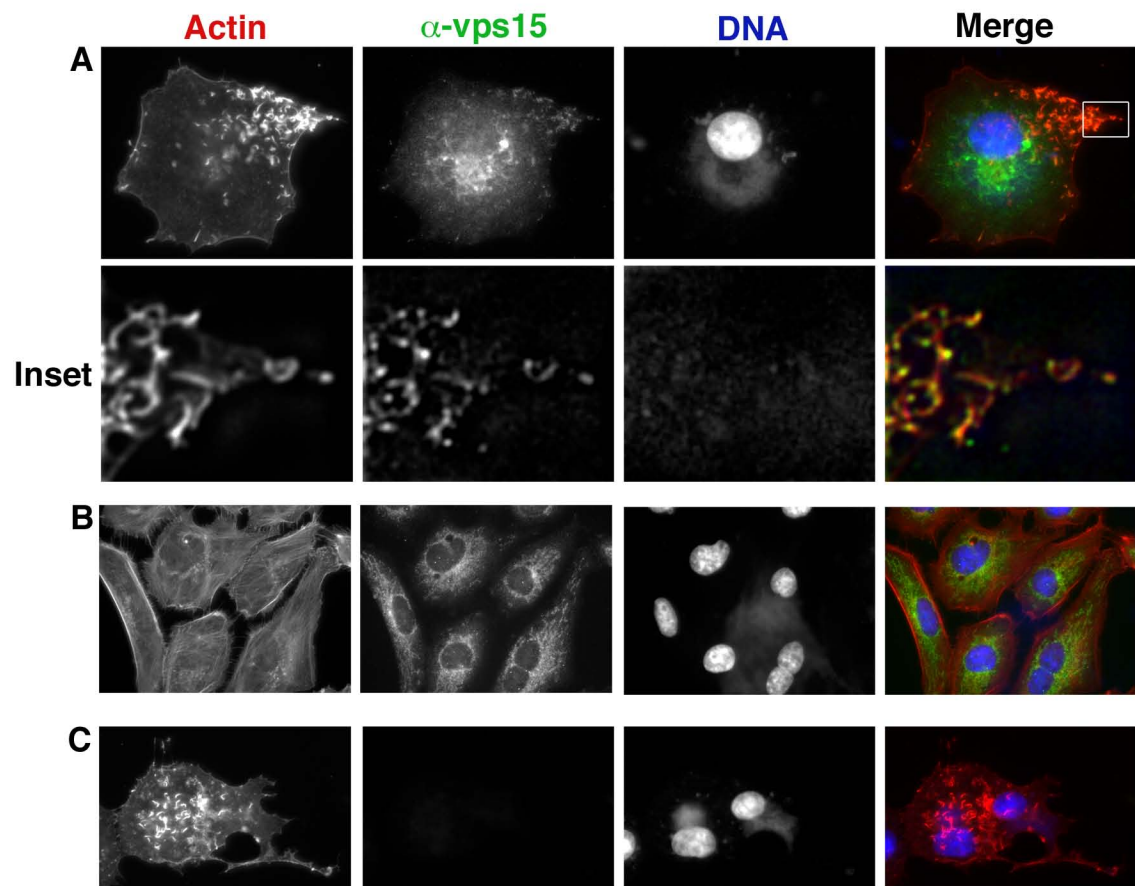


Figure 5

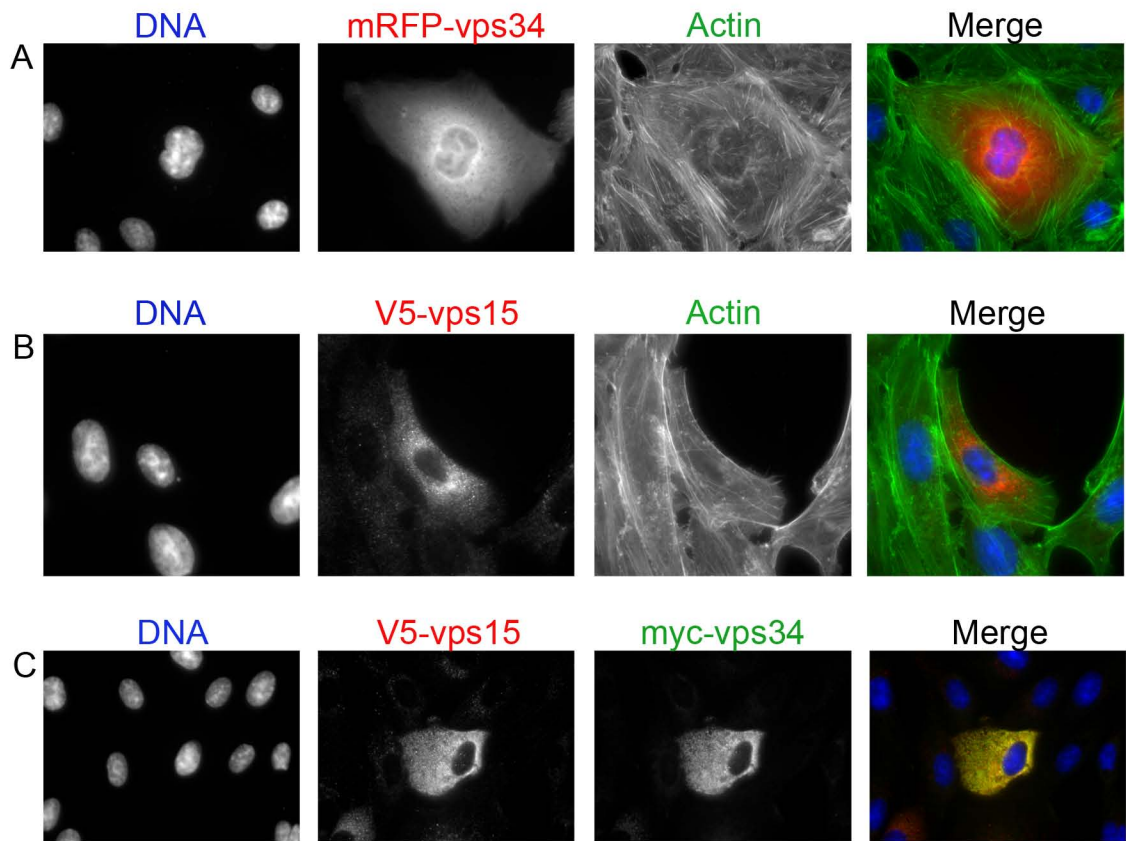


Figure 6

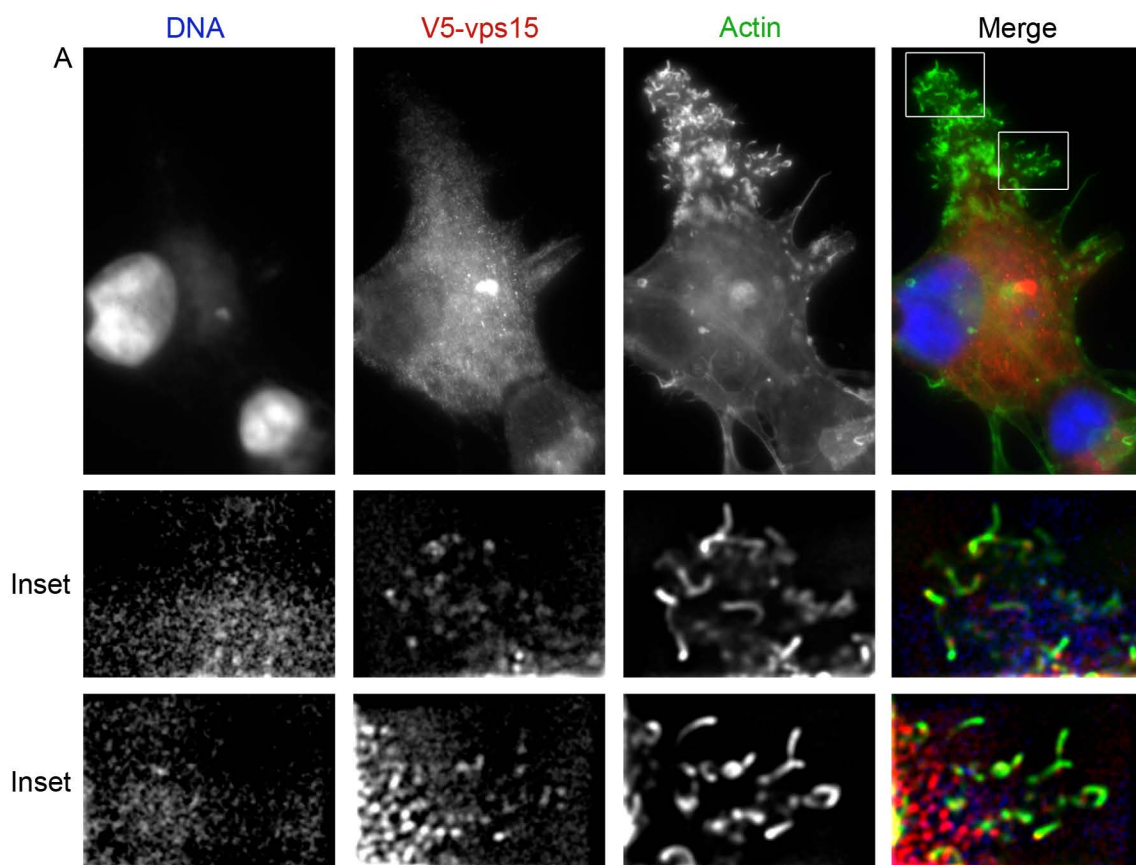


Figure 7

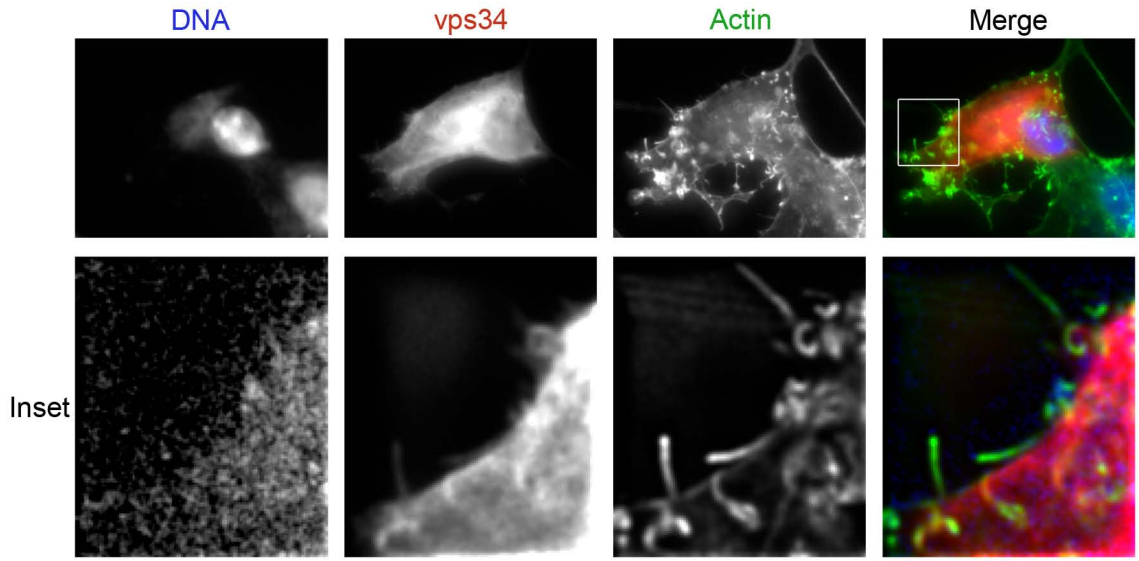


Figure 8

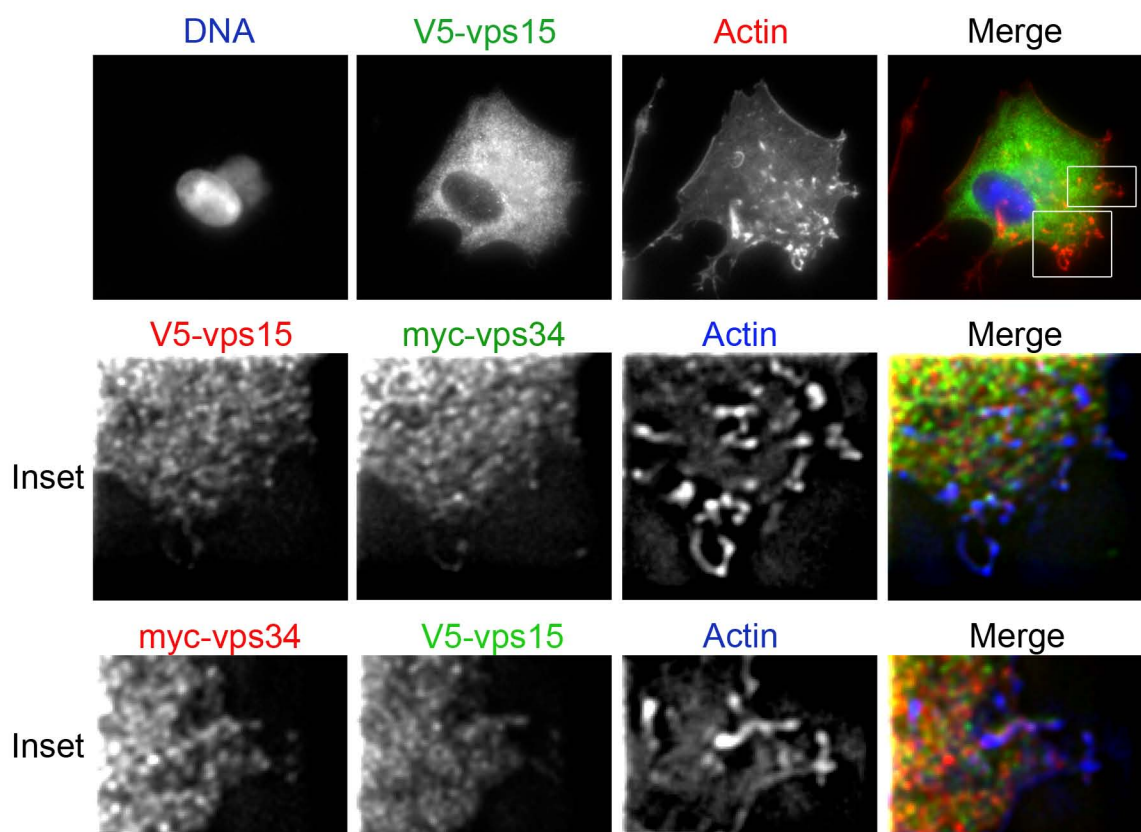


Figure 9

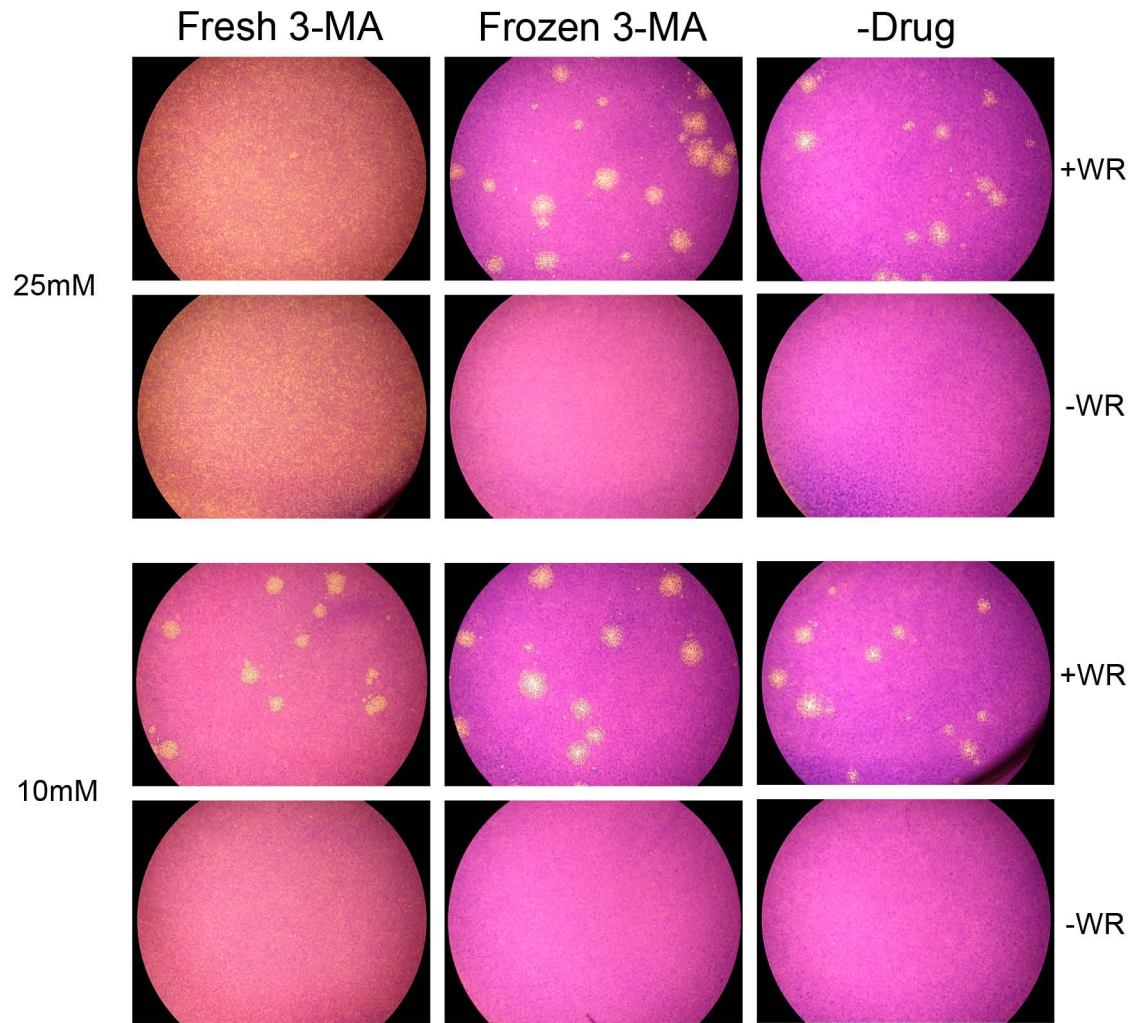


Figure 10

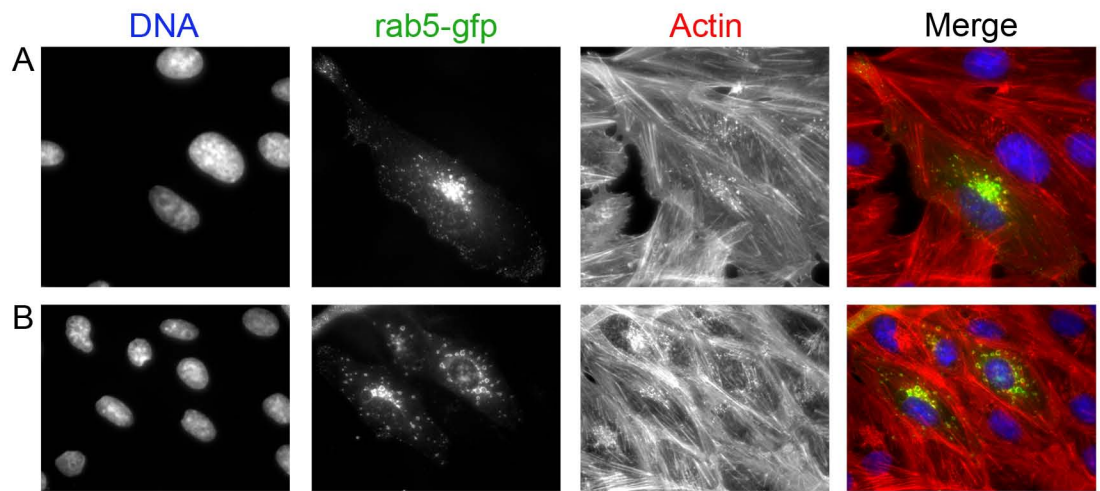


Figure 11

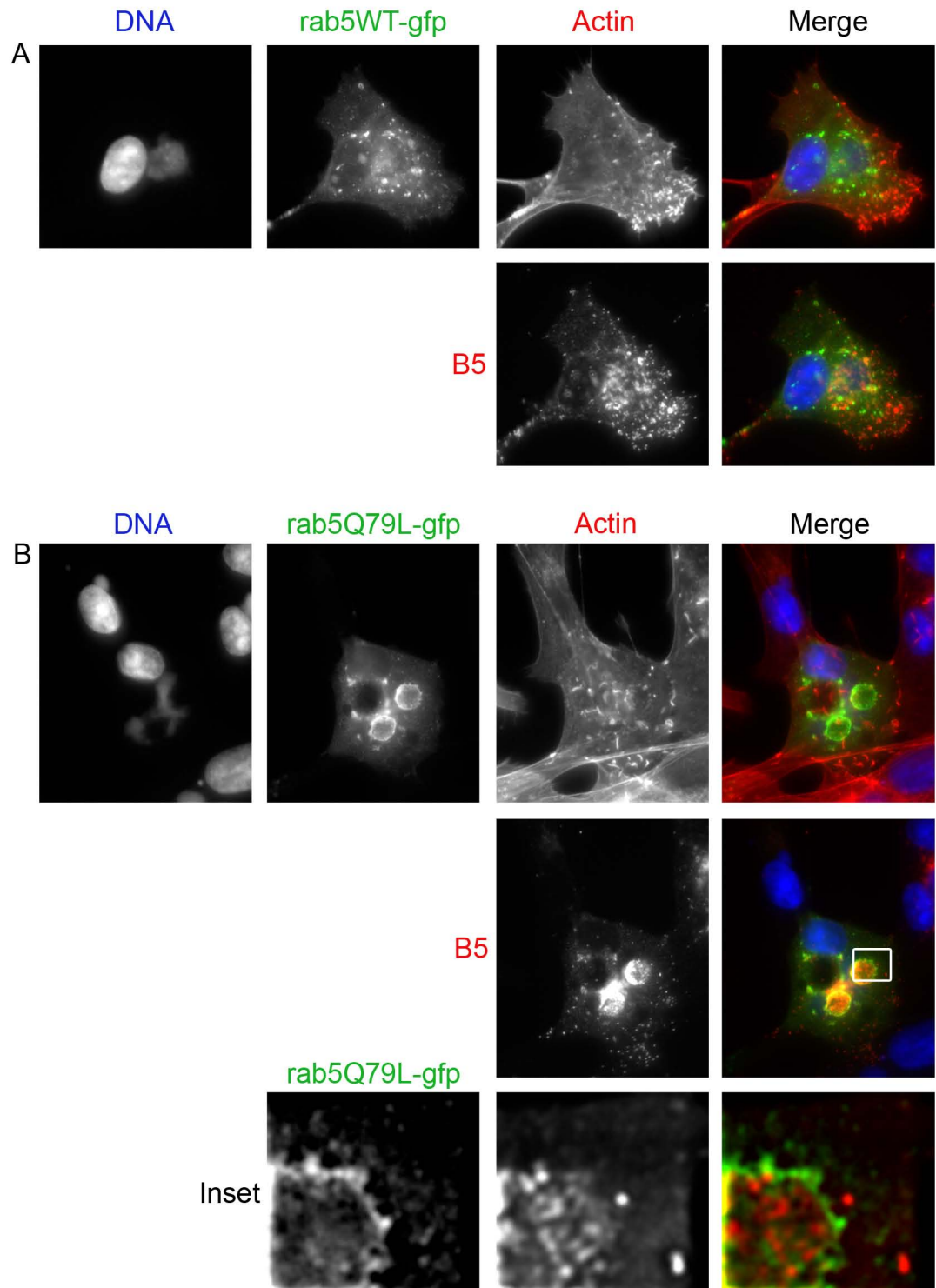


Figure 12

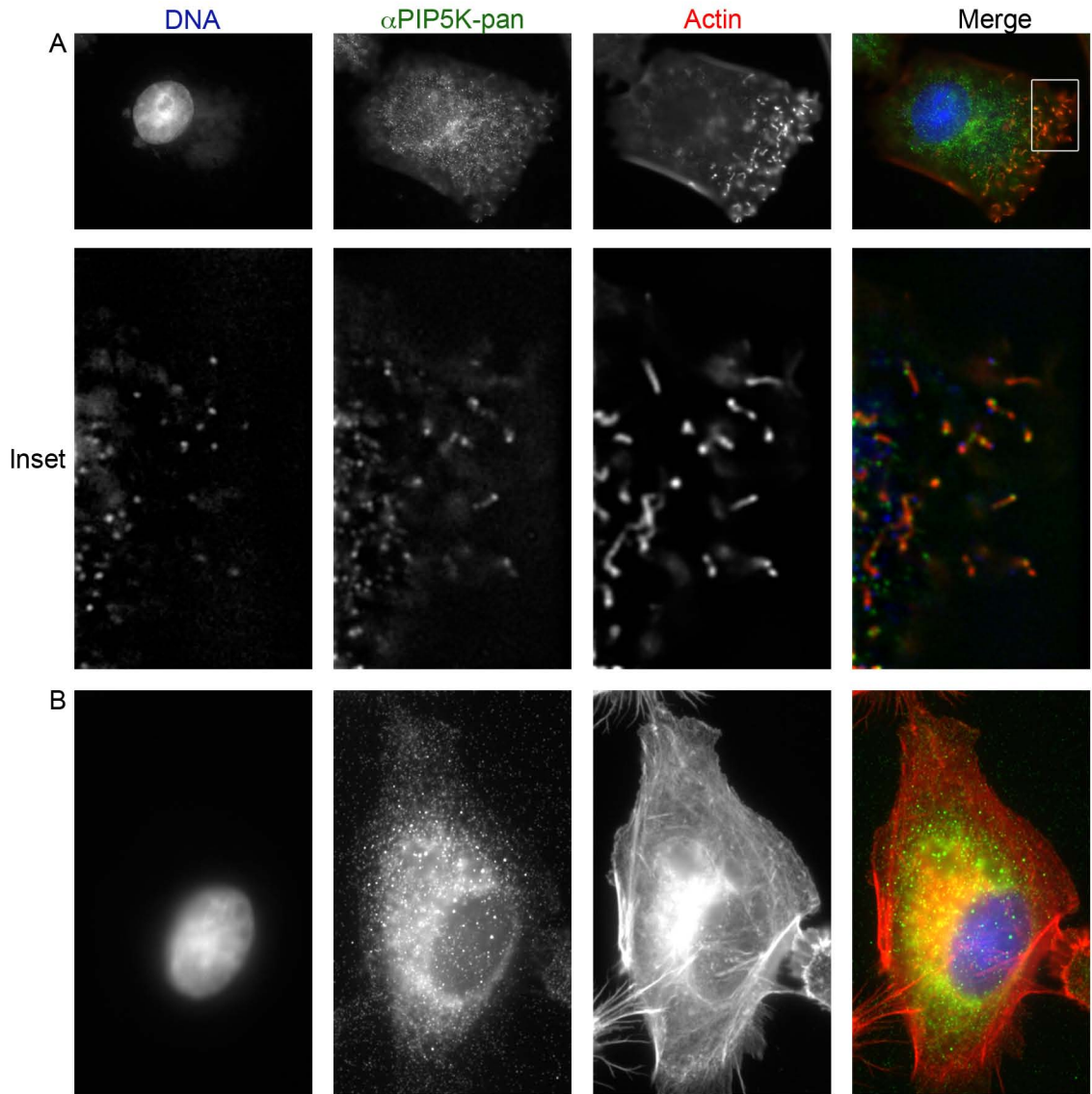


Figure 13

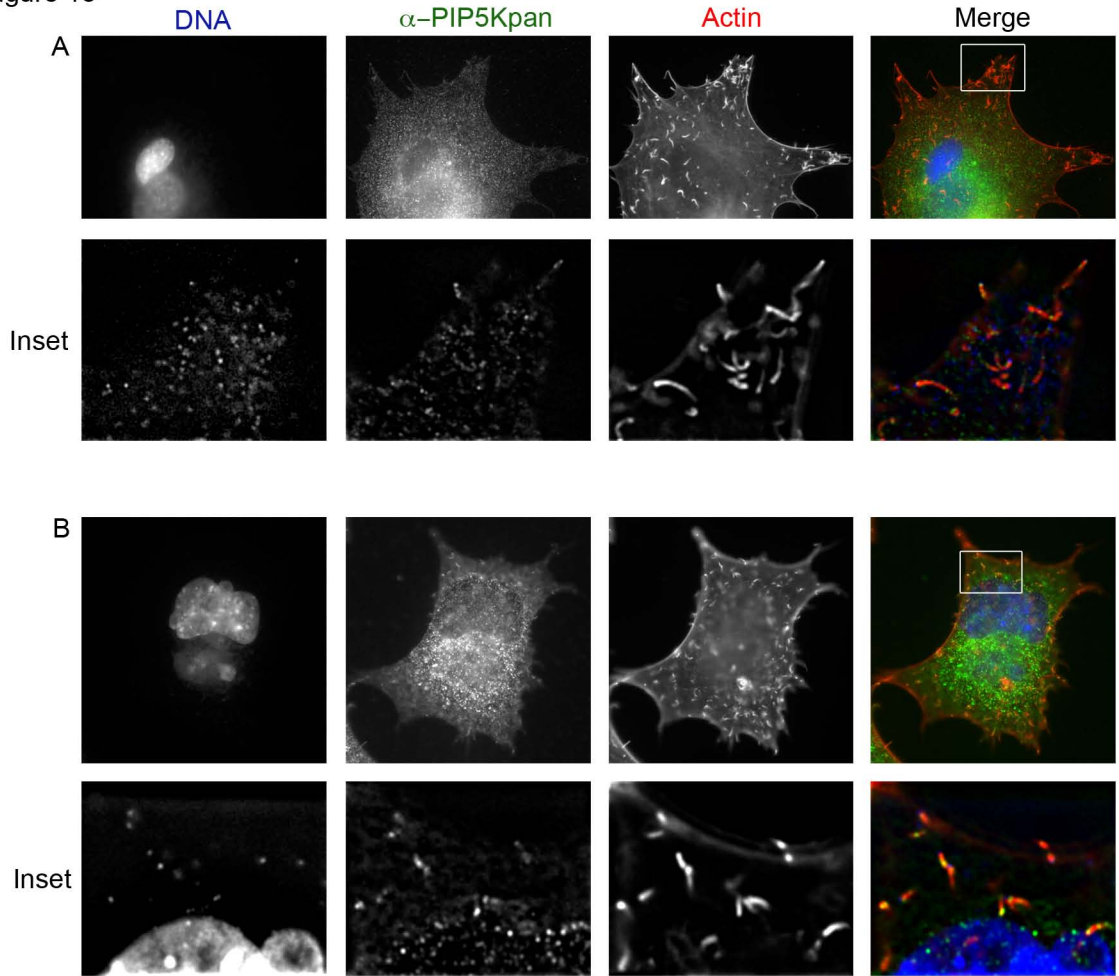
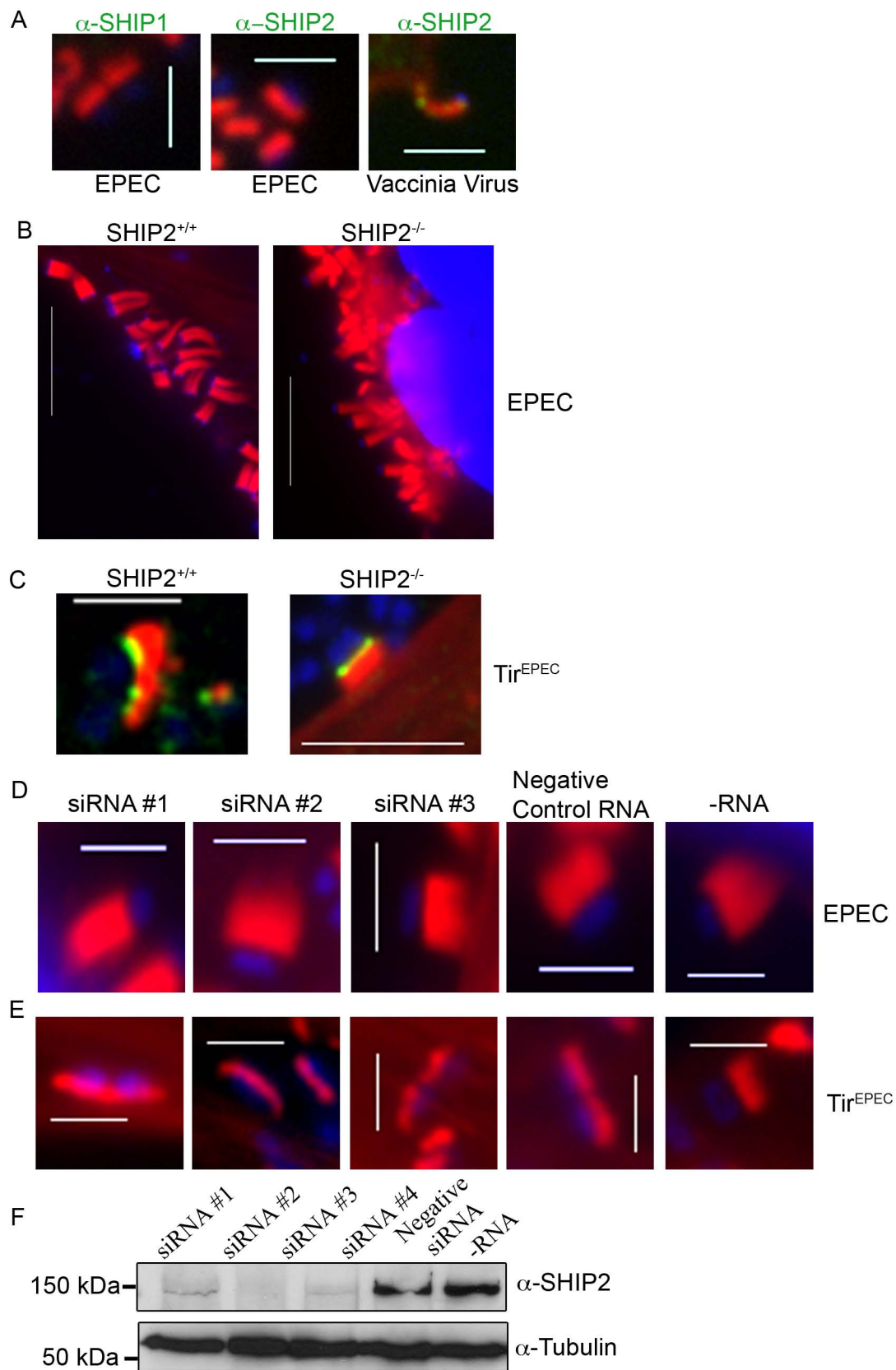


Figure 14



**CHAPTER VI: FUTURE DIRECTIONS
AND CONCLUSIONS**

6.1 FUTURE DIRECTIONS AND CONCLUSIONS

6.1.1 Phosphatidylinositol 3-Kinases and Vaccinia Virus

In Chapter II we found that PI3K inhibitors and p85-deficient cell lines disrupt virion morphogenesis at two distinct stages: intracellular to mature virus transition, and mature virus envelopment to form enveloped virions. Still unresolved is the exact mechanism whereby PI3Ks contribute to morphogenesis. Future directions should address how PI3K are involved in this process. Circumstantial evidence from similar papers and deletion mutant viral strains suggests that PI3K may regulate morphogenesis through both indirect and direct mechanisms.

In Chapter II, we found that both early and late viral protein synthesis are disrupted in cell lines treated with PI3K inhibitors, and in p85-deficient cells suggesting that PI3K absence/inhibition may indirectly decrease protein translation. The canonical PI3K pathway, described in Chapter I, is activation of PI3K signaling in response to pro-growth signals, which activate mTOR signaling, ultimately increasing protein translation through mTOR-mediated phosphorylation of ribosomal kinases and eukaryotic initiation factors. Zaborowska *et al.* demonstrated that eIF4 complexes are disrupted following PI3K inhibitor treatment during a vaccinia infection (43). A possible extension of the work described in Chapter II is to identify whether vaccinia signals through PI3K to activate the mTOR complex and initiate protein synthesis. Alternatively, one could investigate the mechanism whereby VV stimulates PI3K. Data from Zaborowska *et al.* and Soares *et al.* demonstrate that VV induces Akt activation through phosphorylation (33, 43). Following growth factor stimulation, Type I PI3K are recruited to the

membrane, producing PI(3,4,5)P₃, which recruits Akt and PDK1 to the membrane (8). VV may have a mechanism to induce PDK1 and mTOR activation. Intriguingly, poxviruses encode mRNA capping and decapping enzymes (17), suggesting that the virus controls protein translation at multiple steps, and in a manner that is interdependent on host proteins.

How could PI3K directly regulate virion morphogenesis? As previously discussed in Chapter I, lipid phosphorylations create zipcodes, or lipid microdomains on membranes leading to the recruitment of proteins in a spatial and temporal manner. Thus, VV could use lipid signaling on viral or host membranes to recruit proteins necessary for the viral lifecycle. For instance, we found that treatment with inhibitor AS1 (similar to LY294002 treatment (33)), inhibited virion morphogenesis prior to virion maturation. This block in morphogenesis appeared similar to the block observed with viral strains missing components of the vaccinia redox complex, A2.5, E10, G4, and phosphoprotein A13 (29, 30, 35, 39). Therefore, an extension of this work would be to investigate whether these proteins have any putative lipid binding domains. Cells deficient in p85 proteins did not exhibit a block in virion maturation, suggesting that p85-independent kinases mediate this step. Therefore, p85-independent kinases, such as Type II or Type III kinases, may localize to viral structures earlier in the infection period, and could colocalize with structures containing proteins A2.5, E10, G4 and A13. PI3K absence/inhibition could disrupt protein localization, producing a phenotype similar to A2.5, E10, G4, or A13 deletions.

Using p85-deficient cell lines, and following AS2 inhibitor treatment, we were also able to disrupt virion envelopment, a step that is downstream from virion maturation.

These data suggest that AS2 targets a p85-dependent kinase. We were unable to observe colocalization of p85 with a viral structure at 16 hours post infection (data not shown). However, this could be due to a p85 signal below the limit of detection, or we could have looked at a time point that was post viral wrapping. Future experiments should address the localization of p85 during viral replication. Also, since F13 localization is disrupted in PI3K-inhibitor and p85-deficient cells these data suggest that F13 may interact with PI3K or PI3K products. Intriguingly, F13 is predicted to have homology to phospholipase D, and mutations within the putative catalytic site disrupt F13 trafficking (9). Therefore, an extension of this work is to co-localize F13 with PI3K or fluorescent lipids, or colocalize PI3K with F13 binding proteins, such as TIP47, and rab9 (1).

The work described in Chapter III defines the involvement of host PI3K during vaccinia virus morphogenesis. This work, while informative, opens further avenues of research into enveloped virus replication and spread. Future directions should address the mechanism for PI3K involvement during virion morphogenesis, and possibly extend these observations to other viruses. For instance, Tooze *et al.* demonstrates that Herpesviruses and poxviruses acquire their envelopes from a similar endocytic compartment (34). These data suggest that Herpesviruses and other viruses may also utilize host PI3K during viral replication and dissemination.

6.1.2 SHIP2 and Vaccinia Virus

In Chapter IV we found that the host lipid 5-phosphatase, SHIP2, inhibits enveloped virus release, but is not necessary for actin tail formation. We also found that SHIP2 localizes to the tops of VV actin tails, identified the mechanism of SHIP2

localization, and found that SHIP2 may mediate inhibitory effects through the viral protein A34. Still unresolved is the exact mechanism whereby SHIP2 limits viral release.

An important question that arises from Chapter IV, is how does SHIP2 specifically inhibit virion release? Is SHIP2 modifying the phospholipids, or does SHIP2 function as merely a scaffolding protein? We attempted to answer these questions by creating stable complemented cell lines expressing SHIP2WT or SHIP2D607A (phosphatase dead). Unfortunately, SHIP2KO cells complemented with SHIP2WT and SHIP2D607A did not revert into a small comet phenotype observed with SHIP2WT cells. Microscopy confirmed that SHIP2 localized to tails in SHIP2KO cells overexpressing wild-type protein, however localization to tails was very faint. Conversations with our collaborator, Christophe Erneux yielded important clues that could explain the lack of complementation. Erneux provided the retroviral constructs and had earlier confirmed phosphatase activity of these constructs in Zhang *et al.* (45). However, he found that SHIP2 localization (when expressed from a retroviral construct) did not fully overlap with endogenous SHIP2 (data not published). This data suggests that retrovirally expressed epitope-tagged SHIP may not fully interact with the same subset of effector proteins as endogenous SHIP2. Furthermore, we hoped to observe a reduction in virion release by plaque assay – a phenotype that could be easily missed if other cells in the same well are missing SHIP2 (or SHIP2 is not expressed at a high enough level) and these cells continue to release lots of virions.

To separate whether SHIP2 inhibits virion release by catalytic or scaffolding activity, I propose the following experiments. I hypothesize that epitope-tagged retroviral constructs may interfere with protein-protein interactions, thus an untagged

SHIP2 construct should complement virion release in the SHIP2-deficient cells. I hypothesize that complemented SHIP2-deficient cells should release virions at a similar levels as wild-type SHIP2 cells. However, a drawback to this approach is that reduced virion release may be masked by cells in the same well that continue to release large amounts of virus. To overcome this limitation, I also propose knocking down SHIP2 in SHIP2WT or similar cell lines. Efforts to knockdown SHIP2 by siRNA in SHIP2WT and 3T3 cells was unsuccessful at increasing virion release. However, while SHIP2 was knocked down, it may not have been eliminated enough to increase virion release. Knockdown of SHIP2 in BSC40 cells did result in increased virion release. SHIP2 localizes to a majority of tails in BSC40 cells, but a reduced percentage of tails in SHIP2WT and 3T3 cells. These data suggest that unsuccessful results with SHIP2 knockdown in the SHIP2WT and 3T3 cells may result from a reduced percentage of SHIP2 localizing to actin tails in these cells.

Our initial hypothesis was that SHIP2 localizes to the tops of VV actin tails and modifies the lipids beneath the virions, ultimately contributing to retention of the virion on the cell surface. If modified lipids are being produced on tails, then we predict that we would be able to localize PIP-specific probes to this region. SHIP2^{-/-} and SHIP2^{+/+} cells were transfected with various PIP-specific probes (PH-Akt: PI(3,4)P₂ and PI(3,4,5)P₃; 2X-FYVE: PI(3)P; PX: PI(3)P; PLC-gamma: PI(4,5)P₂), however, we were unable to identify localization of any of these probes to the tops of VV actin tails. I hypothesize that there maybe spatial restrictions at the top of tails that occludes the interaction of these probes with their cognate lipids. Alternatively, these constructs could localize to tails, but at levels that are below the limit of detection.

Alternative approaches to define lipid-regulated virion release were also tested. Purified lipids were loaded onto histone carriers and added to cells for 30 minutes at the end of a 16 hour infection. Cells were then fixed and stained for actin and DNA. We hypothesized that PI(3,4,5)P₃ and uncleavable 5PT-PI(3,4,5)P₃ may increase virion release and/or disrupt actin tail formation. Unfortunately, we were unable to observe any of these changes. We also added PI(3,4,5)P₃, and uncleavable lipids 5MP-PI(3,4,5)P₃ and 3,4,5-PT-PI(3,4,5)P₃ to cells 8 hours post infection and found that exogenous lipids did not modify plaque morphology. Treating uninfected cells with fluorescent lipids at the same concentration for 30 minutes confirmed lipid delivery into the host plasma membrane. Therefore we hypothesize that exogenous lipid concentrations were insufficient to induce virion release. Also Zhang *et al.* demonstrated that metabolically stable lipids have low specificity towards SHIP2 (44). Alternatively SHIP2 may not modify lipids at the top of tails, and could function primarily as a scaffolding molecule. To further investigate lipid-mediated virion release, cells could be “loaded” with various fluorescent lipids post infection and visualized by microscopy. My hypothesis is that the virion may specifically cluster these lipids, resulting in a strong fluorescent signal beneath the virion. However, this approach is also limited by the magnitude of lipid fluorescence beneath the virions.

Our data demonstrates that SHIP2 associates with components of the actin tail and virion release machinery located beneath the virion. Our lab and Michael Way’s lab have identified several components of this complex, however not all of the components have been elucidated. Therefore, a natural extension of Chapter IV would be to define the proteins that bind to SHIP2 during a viral infection. This could be accomplished by

immunoprecipitating SHIP2, removing bands from SDS-PAGE and identifying SHIP2 effectors by mass spectrometry. Several SHIP2 effectors have been described including EGFR, filamin, p130Cas, Cbl, Vinexin, Arap3, APS, JIP-1, SHC, LPD and Intersectin (4, 13, 16, 18-20, 23, 32, 36, 40, 41). We were able to localize SHC and LPD to the tops of tails, however their localization did not change in SHIP2^{+/+} and SHIP2^{-/-} cells. These data suggest that SHC and LPD localization is not dependent on the presence or absence of SHIP2, but rather other proteins in the VV actin tail complex. SHC and LPD do not have defined catalytic activity, therefore we hypothesize that their function on actin tails may be similar to scaffolding proteins already localized on the tops of tails (WIP, Grb2 and NCK) (5, 12, 27).

In addition to using mass spectrometry to identify other SHIP2 interactors important for viral release, we can also investigate the contribution of known SHIP2 interactors to viral release. Nakatsu *et al.* recently identified that SHIP2 localizes to clathrin-coated pits via interactions with the scaffolding protein, intersectin (13). Intersectin is predicted to be a scaffolding protein that regulates the assembly of multi-protein complexes (22). It has two eps15 homology domains, five consecutive SH3 domains, and DH, PH and C2 domains (6, 10, 42). Interestingly, intersectin indirectly associates with NWASP (28), and directly associates with SHIP2 (13), SNAP-23 and SNAP-25 (15). Based on its direct interactions with the SNAP proteins, intersectin is predicted to couple endocytosis to exocytosis (15). The domain structure of intersectin suggests that it could interact with proteins that have already been localized to the tops of actin tails.

A proposed mechanism for actin tail formation and virion release is that viral protein A36, phosphorylated by Abl or Src kinases recruits Nck, WIP, Grb2 and NWASP to the virion (5, 12, 14, 24). NWASP may recruit SHIP2 and intersectin, and intersectin could recruit the SNAP lipid fusion proteins. The SNAPs could fuse the IEV membrane with the plasma membrane, exposing the virus to the extracellular environment. Exposing the virus to the outside of the membrane could change the curvature of the IEV membrane from a concave to a convex shape, a change that could be detected through BAR-domain containing proteins. The topological change in the IEV membrane could activate phosphoinositide 5-kinases, producing PI(4,5)P, which activates NWASP (26), producing actin polymerization only when the virus has been exposed to the extracellular environment. Work by Reeves *et al.* demonstrates that continual tyrosine kinase activity is necessary for actin tail formation (24, 25), as preformed tails can be eliminated through the addition of tyrosine kinase inhibitors. These data suggest that turnover of tyrosine phosphorylation maintains active actin polymerization. Work by Weisswange *et al.* demonstrates that NWASP turnover through the WH2 domain also enhances actin polymerization (38).

After formation of actin tails, an unknown signal induces virion release. We hypothesize that the viral protein A34, which has homology to c-type lectins (3), may detect the presence of leukocytes, cell adhesion molecules or endocytic receptors. In so doing, A34 may play a gatekeeper role so as to limit release except when environmental conditions are conducive to dissemination. A conformational change in A34 may disrupt the association with SHIP2, reducing SHIP2 activity and leading to virion release. This conformational change in A34 could be tyrosine phosphorylation by Abl-family kinases,

because we found that A34 could be phosphorylated by Abl-family kinases in our *in vitro* kinase reactions (Chapter V). I hypothesize that producing Y->F mutations within A34 may enhance virion release and restore specific activity, two phenotypes observed in an A34 deletion virus (11). Prasad *et al.* demonstrated that the SH2 domain of SHIP2 autoinhibits phosphatase activity through interactions with the carboxy-terminus (21). Therefore, A34 could reduce SHIP2 activity by removing an SH2 interaction, causing SHIP2 to become autoinhibited. Honeychurch *et al.* demonstrate that host proteins Eps15, Alix, and TSG101 may also participate in virion release (7). SHIP2 signaling could converge with the Eps15, Alix, and TSG101 proteins through intersectin. Furthermore, preliminary work from our lab suggests that Y->F mutations within viral protein F13 can also regulate virion release (data not shown). Since A34 indirectly associates with F13 through components of the EEV (31), we hypothesize that any changes that modify interactions of this complex could also modify virion release. Altogether these data suggest that virion release from actin tails is a complex process controlled by both cellular and viral factors.

Other cellular proteins have been identified that function as intrinsic viral release inhibitors. Tetherin/BST-2 is a cell surface marker that restricts the egress of HIV and other viruses by tethering mature virions to the cell surface (2). To overcome this restriction viruses such as HIV and Kaposi's Sarcoma-Associated Herpesvirus (KSHV) have viral proteins (VPU and K5) that antagonize the tetherin block, leading to viral release (2). A similar cellular antiviral protein, "viperin" was identified that inhibited Influenza A release from cells (37). Viperin disrupts the formation of lipid rafts, disrupting membrane microdomains utilized for virus budding (37). Interestingly,

expression of a cellular, rather than a viral, protein antagonizes viperin activity, leading to virion release (37). I hypothesize that SHIP2 is regulated in a manner that is distinct from tetherin and viperin. Instead of antagonizing host proteins to induce virion release, SHIP2 participates with the viral protein A34 to inhibit virion release. Additionally, tetherin and viperin are regulated in an interferon-dependent manner (2, 37); however, there is no evidence to suggest that SHIP2 is similarly regulated. Therefore, while SHIP2 can be classified as an intrinsic viral inhibitor, it does so in a manner that is distinct from other host antiviral release proteins.

6.1.3 Conclusions

Herein we provide evidence that host lipid signaling regulates poxviral pathogenesis. Using a combination of lipid kinase inhibitors and lipid kinase/phosphatase-deficient cell lines we demonstrate that poxviruses hijack host lipid modifying enzymes during viral replication and spread. Cellular lipid signaling is an essential component of eukaryotic cells. Disruption of specific components of this pathway, either through lipid/phosphatase inhibitors and/or deficient cell lines reverberates throughout the endosomal pathway. For instance, treating cells with PI3K inhibitors disrupts not only Type I kinases, and regulation of Akt signaling, but also disrupts endosomal trafficking. That pathogens, such as vaccinia virus, have evolved to hijack lipid signaling without overly disrupting cellular signaling (and producing apoptosis) suggests a highly specialized host-pathogen interaction. Since poxviruses have the ability to infect multiple cell types, this demonstrates a conservation in lipid signaling for both the virus and the eukaryotic host cell.

Viruses are obligate intracellular parasites dependent upon their host cells for replication and subsequent spread. As such, viral infections represent a balance between dependency upon an intact cell for replication, and disruption of the host cell for viral spread. Different viral families exhibit gradations along the replication/spread spectrum. However, all viruses are dependent upon the host cell for replication, suggesting that all viral families, both enveloped and non-enveloped, must hijack or circumvent cellular lipid signaling during replication. Just as lipid signaling regulates growth, endosomal trafficking, vesicle fusion, fission, and organelle identity, so do viruses hijack growth signals, vesicle trafficking, fusion, fission, and organelle regulation. Therefore, inhibitors of cellular lipid signaling may represent a novel class of antiviral agents. However, care must be taken to inhibit viral lipid signaling without significantly disrupting the cellular host. Overall, these observations provide new insight into viral usurpation of cellular lipid signaling and opens further avenues of research elucidating the mechanisms of viral replication and dissemination.

LITERATURE CITED

1. **Chen, Y., K. M. Honeychurch, G. Yang, C. M. Byrd, C. Harver, D. E. Hruby, and R. Jordan.** 2009. Vaccinia virus p37 interacts with host proteins associated with LE-derived transport vesicle biogenesis. *Virology* **6**:44.
2. **Douglas, J. L., J. K. Gustin, K. Viswanathan, M. Mansouri, A. V. Moses, and K. Fruh.** The great escape: viral strategies to counter BST-2/tetherin. *PLoS Pathog* **6**:e1000913.
3. **Duncan, S. A., and G. L. Smith.** 1992. Identification and characterization of an extracellular envelope glycoprotein affecting vaccinia virus egress. *J Virol* **66**:1610-21.
4. **Dyson, J. M., C. J. O'Malley, J. Becanovic, A. D. Munday, M. C. Berndt, I. D. Coghill, H. H. Nandurkar, L. M. Ooms, and C. A. Mitchell.** 2001. The SH2-containing inositol polyphosphate 5-phosphatase, SHIP-2, binds filamin and regulates submembraneous actin. *J Cell Biol* **155**:1065-79.
5. **Frischknecht, F., V. Moreau, S. Rottger, S. Gonfloni, I. Reckmann, G. Superti-Furga, and M. Way.** 1999. Actin-based motility of vaccinia virus mimics receptor tyrosine kinase signalling. *Nature* **401**:926-9.
6. **Guipponi, M., H. S. Scott, H. Chen, A. Schebesta, C. Rossier, and S. E. Antonarakis.** 1998. Two isoforms of a human intersectin (ITSN) protein are produced by brain-specific alternative splicing in a stop codon. *Genomics* **53**:369-76.
7. **Honeychurch, K. M., G. Yang, R. Jordan, and D. E. Hruby.** 2007. The vaccinia virus F13L YPPL motif is required for efficient release of extracellular enveloped virus. *J Virol* **81**:7310-5.
8. **Huang, J., and B. D. Manning.** 2009. A complex interplay between Akt, TSC2 and the two mTOR complexes. *Biochem Soc Trans* **37**:217-22.
9. **Husain, M., and B. Moss.** 2001. Vaccinia virus F13L protein with a conserved phospholipase catalytic motif induces colocalization of the B5R envelope glycoprotein in post-Golgi vesicles. *J Virol* **75**:7528-42.
10. **Hussain, N. K., M. Yamabhai, A. R. Ramjaun, A. M. Guy, D. Baranes, J. P. O'Bryan, C. J. Der, B. K. Kay, and P. S. McPherson.** 1999. Splice variants of intersectin are components of the endocytic machinery in neurons and nonneuronal cells. *J Biol Chem* **274**:15671-7.
11. **McIntosh, A. A., and G. L. Smith.** 1996. Vaccinia virus glycoprotein A34R is required for infectivity of extracellular enveloped virus. *J Virol* **70**:272-81.
12. **Moreau, V., F. Frischknecht, I. Reckmann, R. Vincentelli, G. Rabut, D. Stewart, and M. Way.** 2000. A complex of N-WASP and WIP integrates signalling cascades that lead to actin polymerization. *Nat Cell Biol* **2**:441-8.
13. **Nakatsu, F., R. M. Perera, L. Lucast, R. Zoncu, J. Domin, F. B. Gertler, D. Toomre, and P. De Camilli.** 2010. The inositol 5-phosphatase SHIP2 regulates endocytic clathrin-coated pit dynamics. *J Cell Biol* **190**:307-15.
14. **Newsome, T. P., I. Weisswange, F. Frischknecht, and M. Way.** 2006. Abl collaborates with Src family kinases to stimulate actin-based motility of vaccinia virus. *Cell Microbiol* **8**:233-41.

15. **Okamoto, M., S. Schoch, and T. C. Sudhof.** 1999. ESH1/intersectin, a protein that contains EH and SH3 domains and binds to dynamin and SNAP-25. A protein connection between exocytosis and endocytosis? *J Biol Chem* **274**:18446-54.
16. **Onnockx, S., J. De Schutter, M. Blockmans, J. Xie, C. Jacobs, J. M. Vanderwinden, C. Erneux, and I. Pirson.** 2008. The association between the SH2-containing inositol polyphosphate 5-Phosphatase 2 (SHIP2) and the adaptor protein APS has an impact on biochemical properties of both partners. *J Cell Physiol* **214**:260-72.
17. **Parrish, S., W. Resch, and B. Moss.** 2007. Vaccinia virus D10 protein has mRNA decapping activity, providing a mechanism for control of host and viral gene expression. *Proc Natl Acad Sci U S A* **104**:2139-44.
18. **Paternotte, N., J. Zhang, I. Vandenbroere, K. Backers, D. Blero, N. Kioka, J. M. Vanderwinden, I. Pirson, and C. Erneux.** 2005. SHIP2 interaction with the cytoskeletal protein Vinexin. *Febs J* **272**:6052-66.
19. **Pesesse, X., V. Dewaste, F. De Smedt, M. Laffargue, S. Giuriato, C. Moreau, B. Payrastre, and C. Erneux.** 2001. The Src homology 2 domain containing inositol 5-phosphatase SHIP2 is recruited to the epidermal growth factor (EGF) receptor and dephosphorylates phosphatidylinositol 3,4,5-trisphosphate in EGF-stimulated COS-7 cells. *J Biol Chem* **276**:28348-55.
20. **Prasad, N., R. S. Topping, and S. J. Decker.** 2001. SH2-containing inositol 5'-phosphatase SHIP2 associates with the p130(Cas) adapter protein and regulates cellular adhesion and spreading. *Mol Cell Biol* **21**:1416-28.
21. **Prasad, N. K., M. E. Werner, and S. J. Decker.** 2009. Specific tyrosine phosphorylations mediate signal-dependent stimulation of SHIP2 inositol phosphatase activity, while the SH2 domain confers an inhibitory effect to maintain the basal activity. *Biochemistry* **48**:6285-7.
22. **Predescu, S. A., D. N. Predescu, B. K. Timblin, R. V. Stan, and A. B. Malik.** 2003. Intersectin regulates fission and internalization of caveolae in endothelial cells. *Mol Biol Cell* **14**:4997-5010.
23. **Raaijmakers, J. H., L. Deneubourg, H. Rehmann, J. de Koning, Z. Zhang, S. Krugmann, C. Erneux, and J. L. Bos.** 2007. The PI3K effector Arap3 interacts with the PI(3,4,5)P3 phosphatase SHIP2 in a SAM domain-dependent manner. *Cell Signal* **19**:1249-57.
24. **Reeves, P. M., B. Bommarius, S. Lebeis, S. McNulty, J. Christensen, A. Swimm, A. Chahroudi, R. Chavan, M. B. Feinberg, D. Veach, W. Bornmann, M. Sherman, and D. Kalman.** 2005. Disabling poxvirus pathogenesis by inhibition of Abl-family tyrosine kinases. *Nat Med* **11**:731-9.
25. **Reeves, P. M., S. K. Smith, V. A. Olson, S. H. Thorne, W. Bornmann, I. K. Damon, and D. Kalman.** 2011. Variola and monkeypox utilize conserved mechanisms of virion motility and release that depend on Abl- and Src-family tyrosine kinases. *Journal of Virology* **85**.
26. **Rohatgi, R., H. Y. Ho, and M. W. Kirschner.** 2000. Mechanism of N-WASP activation by CDC42 and phosphatidylinositol 4, 5-bisphosphate. *J Cell Biol* **150**:1299-310.

27. **Scaplehorn, N., A. Holmstrom, V. Moreau, F. Frischknecht, I. Reckmann, and M. Way.** 2002. Grb2 and Nck act cooperatively to promote actin-based motility of vaccinia virus. *Curr Biol* **12**:740-5.
28. **Schafer, D. A.** 2002. Coupling actin dynamics and membrane dynamics during endocytosis. *Curr Opin Cell Biol* **14**:76-81.
29. **Senkevich, T. G., A. S. Weisberg, and B. Moss.** 2000. Vaccinia virus E10R protein is associated with the membranes of intracellular mature virions and has a role in morphogenesis. *Virology* **278**:244-52.
30. **Senkevich, T. G., C. L. White, A. Weisberg, J. A. Granek, E. J. Wolffe, E. V. Koonin, and B. Moss.** 2002. Expression of the vaccinia virus A2.5L redox protein is required for virion morphogenesis. *Virology* **300**:296-303.
31. **Smith, G. L., A. Vanderplasschen, and M. Law.** 2002. The formation and function of extracellular enveloped vaccinia virus. *J Gen Virol* **83**:2915-31.
32. **Smith, K., D. Humphreys, P. J. Hume, and V. Koronakis.** 2010. Enteropathogenic *Escherichia coli* recruits the cellular inositol phosphatase SHIP2 to regulate actin-pedestal formation. *Cell Host Microbe* **7**:13-24.
33. **Soares, J. A., F. G. Leite, L. G. Andrade, A. A. Torres, L. P. De Sousa, L. S. Barcelos, M. M. Teixeira, P. C. Ferreira, E. G. Kroon, T. Souto-Padron, and C. A. Bonjardim.** 2009. Activation of the PI3K/Akt pathway early during vaccinia and cowpox virus infections is required for both host survival and viral replication. *J Virol* **83**:6883-99.
34. **Tooze, J., M. Hollinshead, B. Reis, K. Radsak, and H. Kern.** 1993. Progeny vaccinia and human cytomegalovirus particles utilize early endosomal cisternae for their envelopes. *Eur J Cell Biol* **60**:163-78.
35. **Unger, B., and P. Traktman.** 2004. Vaccinia virus morphogenesis: a13 phosphoprotein is required for assembly of mature virions. *J Virol* **78**:8885-901.
36. **Vandenbroere, I., N. Paternotte, J. E. Dumont, C. Erneux, and I. Pirson.** 2003. The c-Cbl-associated protein and c-Cbl are two new partners of the SH2-containing inositol polyphosphate 5-phosphatase SHIP2. *Biochem Biophys Res Commun* **300**:494-500.
37. **Wang, X., E. R. Hinson, and P. Cresswell.** 2007. The interferon-inducible protein viperin inhibits influenza virus release by perturbing lipid rafts. *Cell Host Microbe* **2**:96-105.
38. **Weisswange, I., T. P. Newsome, S. Schleich, and M. Way.** 2009. The rate of N-WASP exchange limits the extent of ARP2/3-complex-dependent actin-based motility. *Nature* **458**:87-91.
39. **White, C. L., A. S. Weisberg, and B. Moss.** 2000. A glutaredoxin, encoded by the G4L gene of vaccinia virus, is essential for virion morphogenesis. *J Virol* **74**:9175-83.
40. **Wisniewski, D., A. Strife, S. Swendeman, H. Erdjument-Bromage, S. Geromanos, W. M. Kavanaugh, P. Tempst, and B. Clarkson.** 1999. A novel SH2-containing phosphatidylinositol 3,4,5-trisphosphate 5-phosphatase (SHIP2) is constitutively tyrosine phosphorylated and associated with src homologous and collagen gene (SHC) in chronic myelogenous leukemia progenitor cells. *Blood* **93**:2707-20.

41. **Xie, J., S. Onnockx, I. Vandenbroere, C. Degraef, C. Erneux, and I. Pirson.** 2008. The docking properties of SHIP2 influence both JIP1 tyrosine phosphorylation and JNK activity. *Cell Signal* **20**:1432-41.
42. **Yamabhai, M., N. G. Hoffman, N. L. Hardison, P. S. McPherson, L. Castagnoli, G. Cesareni, and B. K. Kay.** 1998. Intersectin, a novel adaptor protein with two Eps15 homology and five Src homology 3 domains. *J Biol Chem* **273**:31401-7.
43. **Zaborowska, I., and D. Walsh.** 2009. PI3K signaling regulates rapamycin-insensitive translation initiation complex formation in Vaccinia Virus-infected cells. *J Virol*.
44. **Zhang, H., J. He, T. G. Kutateladze, T. Sakai, T. Sasaki, N. Markadieu, C. Erneux, and G. D. Prestwich.** 5-Stabilized phosphatidylinositol 3,4,5-trisphosphate analogues bind Grp1 PH, inhibit phosphoinositide phosphatases, and block neutrophil migration. *Chembiochem* **11**:388-95.
45. **Zhang, J., Z. Liu, J. Rasschaert, D. Blero, L. Deneubourg, S. Schurmans, C. Erneux, and X. Pesesse.** 2007. SHIP2 controls PtdIns(3,4,5)P(3) levels and PKB activity in response to oxidative stress. *Cell Signal* **19**:2194-200.

